

Rochester Institute of Technology

**RIT Digital Institutional Repository**

---

Theses

---

8-7-2017

## **The Influence of a Metallic Substrate on the Post Impact Structural Characteristics of a Composite Shaft**

Charles R. Eastwood  
cre6328@rit.edu

Follow this and additional works at: <https://repository.rit.edu/theses>

---

### **Recommended Citation**

Eastwood, Charles R., "The Influence of a Metallic Substrate on the Post Impact Structural Characteristics of a Composite Shaft" (2017). Thesis. Rochester Institute of Technology. Accessed from

This Thesis is brought to you for free and open access by the RIT Libraries. For more information, please contact [repository@rit.edu](mailto:repository@rit.edu).

**The Influence of a Metallic Substrate on the Post Impact Structural  
Characteristics of a Composite Shaft**

by

Charles R. Eastwood

A Thesis Submitted in Partial Fulfillment of the Requirements for the Degree of Master of  
Science in Manufacturing and Mechanical Systems Integration

Department of Manufacturing and Mechanical Engineering Technology

College of Applied Science and Technology

Rochester Institute of Technology

Rochester, NY

August 7, 2017

# Table of Contents

<b>Committee Approval .....</b>	<b>IV</b>
<b>Abstract.....</b>	<b>1</b>
<b>1 Background.....</b>	<b>3</b>
<b>1.1 History.....</b>	<b>4</b>
<b>1.2 Applications .....</b>	<b>4</b>
<b>1.3 Properties .....</b>	<b>5</b>
<b>2 Problem.....</b>	<b>5</b>
<b>2.1 Theoretical Perspective.....</b>	<b>7</b>
<b>3 Purpose .....</b>	<b>8</b>
<b>4 Hypotheses.....</b>	<b>8</b>
<b>5 Significance.....</b>	<b>11</b>
<b>6 Literature Review .....</b>	<b>12</b>
<b>6.1 Applications .....</b>	<b>12</b>
<b>6.2 Composite Metal Interface .....</b>	<b>13</b>
<b>6.3 Composite Impact .....</b>	<b>13</b>
<b>7 Methodology.....</b>	<b>14</b>
<b>7.1 Independent Variables.....</b>	<b>15</b>
<b>7.2 Dependent Variable.....</b>	<b>17</b>
<b>7.3 Control Variables .....</b>	<b>18</b>
<b>7.4 Manufacturing Procedure .....</b>	<b>21</b>
7.4.1 Machining .....	21
7.4.2 Aluminum Sleeve Assembly.....	26
7.4.3 Composite Sleeve Layup .....	27
7.4.4 Composite Sleeve Assembly.....	31
7.4.5 Test Preparation .....	31
<b>7.5 Test Procedure.....</b>	<b>32</b>
7.5.1 Pre and Post Impact Torsion Procedure.....	34
7.5.2 Pre and Post Impact Tension Procedure .....	36
7.5.3 Impact Procedure .....	37
<b>7.6 Data Collection .....</b>	<b>42</b>
<b>7.7 Data Analysis .....</b>	<b>43</b>
7.7.1 Pre Impact Torsion Data Analysis .....	45
7.7.2 Composite Layer Data Analysis .....	56
7.7.3 Pre Impact Tension Data Analysis.....	61
7.7.4 Impact Data Analysis.....	68
7.7.5 Post Impact Torsion Data Analysis.....	73
7.7.6 Post Impact Tension Data Analysis .....	78
7.7.7 Post Impact Torsion Change Data Analysis .....	83

7.7.8	Post Impact Tension Change Data Analysis.....	88
<b>7.8</b>	<b>Observations .....</b>	<b>94</b>
7.8.1	Pre Impact Torsion Observations.....	94
7.8.2	Composite Layer Observations.....	96
7.8.3	Pre Impact Tension Observations .....	98
7.8.4	Impact Observations .....	101
7.8.5	Post Impact Torsion Observations.....	104
7.8.6	Post Impact Tension Observations.....	106
7.8.7	Post Impact Torsion Change Observations.....	108
7.8.8	Post Impact Tension Change Observations .....	110
7.8.9	Torsion Effective Modulus vs. Density Comparison.....	112
<b>8</b>	<b>Limitations .....</b>	<b>115</b>
<b>9</b>	<b>Future Work .....</b>	<b>118</b>
<b>10</b>	<b>Conclusion .....</b>	<b>119</b>
<b>11</b>	<b>Bibliography .....</b>	<b>122</b>
<b>12</b>	<b>Appendix.....</b>	<b>129</b>
12.1	Machining.....	129
12.2	Pre Impact Torsion Data Analysis.....	131
12.3	Composite Layer Data Analysis .....	142
12.4	Pre Impact Tension Data Analysis.....	153
12.5	Impact Data Analysis .....	164
12.6	Post Impact Torsion Data Analysis.....	175
12.7	Post Impact Tension Data Analysis .....	186
12.8	Post Impact Torsion Change Data Analysis .....	197
12.9	Post Impact Tension Change Data Analysis .....	208
12.10	Observations .....	219

## Committee Approval

---

Mark Olles, Ph. D.

Date

Thesis Advisor. Assistant Professor: Manufacturing and Mechanical Engineering Technology.

---

Christopher Lewis, Ph. D.

Date

Committee Member. Assistant Professor: Manufacturing and Mechanical Engineering Technology.

---

Robert Garrick, Ph. D., PE

Date

Department Chair: Manufacturing and Mechanical Engineering Technology.

## **Abstract**

The objective was to develop and characterize a potential method to alleviate the issues regarding post impact effective modulus of composites in a tubular geometry. The hypothesis was that the use of a metallic substrate may increase post impact stiffness characteristics of the sample geometry, compared to a traditional fiber reinforced composite tube, in the torsion and tensile loading scenarios. This required the manufacture of non substrate fiber reinforced composite samples and aluminum substrate composite samples, and testing under torsion and tension loading scenarios. Main sample testing was carried out below the sample yield point, and therefore tests were nondestructive in nature.

This research has concluded with statistical significance that an aluminum substrate decreases loss in torsional effective modulus following impact compared to a composite shaft only composed of carbon fiber reinforced epoxy. Samples with both aluminum sleeve factor levels produced significantly lower post impact effective modulus change compared to traditional composite counterparts. This appears to be correlated with the elimination of visible fiber and matrix rupture during the impact event. Therefore, torsional effective modulus decrease of the aluminum sleeve tubes appears to be dictated by tube geometry change. This is in contrast to traditional composite tubes, where a decrease in effective modulus was primarily dictated by the decrease in fiber cross sectional area.

This research has concluded that the aluminum substrate decreases post impact tensile effective modulus change compared to traditional composite tubes, but statistical significance could not be attained due to the high degree of variance within each of the sleeve thickness factor levels. Samples with aluminum sleeves produced lower post impact effective modulus change compared

to the traditional composite counterparts, but each sample sleeve thickness factor level variance was relatively high compared to the difference in mean values.

# 1 Background

Composite materials are by definition any material that is composed of two or more substances: typically, a matrix and a reinforcement. The matrix, otherwise known as a binder, is used to encompass the reinforcement to hold it in place. For structural applications, the reinforcement is typically fiber based. They are used due to their relative ease of manufacturability, as well as their structural properties and surface area for matrix contact. Examples of composites can range from concrete to advanced fiber reinforced composites containing carbon or aramid fiber in a plastic matrix. (Strong, 2008, p. 1-2)

Carbon fiber is typically manufactured using polyacrylonitrile (PAN) and pitch precursors. PAN precursors are the most commercially available and was the material used in the creation of carbon fiber for this experiment. The material was oxidized, carbonized and graphitized, surface treated, washed, dried, sized, and then wound. Based on the manufacturing control, PAN based carbon fiber is categorized into large tow, general purpose, and aerospace grades. Based on the degree of oxidization, carbonization, and graphitization, the material is categorized further due to their properties. These production types are general purpose, high strength, intermediate modulus, and high modulus. (Park, 2015, p. 31-44)

Biaxial sleeve is typically manufactured in the same fashion as typical rope sheath, but with carbon fiber. The fiber tow (groups of individual fiber strands) are interwoven upon a die to create the desired sleeve. The size of this die dictates the diameter of the sleeve, and the density of the tow dictates strength in the direction of the fiber. Braid angle was a significant factor in the properties of the laminate, and was determined based on the structural requirements of the finished component. If desired, the braid can be tailored to the specific application, but typically braid angle

was specified at 45 degrees for part conformability and manufacturing process simplicity. In some specialized cases, the fiber can be wound around specific part geometries (named preforms or mandrels) to conform to unique shapes or specific structural requirements. (Strong, 2008, p. 256)

## **1.1 History**

Modern composites were first used in 1937, when the first fiberglass (or glass wool) was produced and sold to the aircraft industry for use in structural aircraft components. Fiberglass, and its accompanying phenolic resin, was used for tooling of highly geometrically complex features such as compound curves that were required for the metal stamping process. The demand for fiberglass and improved resins dramatically increased during World War II, and when the war effort stopped, businesses pivoted to other industry sectors to remain in business. The automotive, private aerospace, and marine applications were considered good candidates for the technological advancement. (Strong, 2008, p. 5-6)

## **1.2 Applications**

Carbon fiber reinforced plastic members are primarily used for applications including aerospace, automotive, medical equipment civil engineering, audio equipment, sports equipment, and outdoor equipment. These applications are vastly diverse, but share the requirement of high performance components that must be tailored to the specific requirements of the end users and the system. (Park, 2015, p. 254-268) Emerging sectors such as the hobbyist, marine, and construction industries also may require the use of carbon fiber reinforced plastics as a structural material, and therefore may benefit from the approach and results outlined in the preceding research.

### **1.3 Properties**

Fiber reinforced composites are used within these applications mainly due to their high specific strength and effective modulus. Other instances in which carbon fiber reinforced plastics are implemented include those that require corrosion resistance and low coefficient of thermal expansion; both of which are mainly taken advantage of in the aerospace and automotive industries. High coefficient of restitution and radiolucency are taken advantage of mainly in the medical and biomedical industries. Other important factors are heat resistance, low general reactivity, and aesthetics, and can be taken advantage of in various industries from personal electronics to musical instruments. (Park, 2015, p. 254-268)

## **2 Problem**

Although composite materials have considerable benefits that make them useful for many existing and emerging applications, there are some issues that limit their feasibility in areas of the aerospace and dynamic mechanical applications. A notable problem is that the effective modulus after low velocity impact can be significantly lower than that of metallic materials of a given weight. Composite materials typically undergo reinforcement and sometimes matrix deformation or failure under impact conditions. This is typically due to the relatively low elongation at break of carbon fiber reinforced plastics compared to other load bearing materials such as metals, and manifests itself in the deformation of part geometry on the surface, between laminates, or on the opposite surface of the impact. Deformation and resulting effective modulus decrease is dependent on laminate thickness, impactor geometry, and impact velocity. Under impact conditions, metals typically deform but retain most structural properties of the material, and primarily lose properties due to geometry change while below the static yield strength of the material. They also tend to

distribute load in a consistent manner due to their isotropy. Carbon fiber composites usually do not incur plastic deformation in the same fashion as metals, which results in yield strengths and ultimate strengths at the same point on a stress strain curve. (Zukas, 1992, p. 79-91)

Composite applications are also limited due to the required fastening system necessary for implementation in high stress machine components. Dynamic components typically require a metallic fastening system due to the durability and formability of metal fasteners, and sometimes require the use of mechanisms that endure sliding motion. Fiber reinforced plastic composites do not typically have good wear characteristics due to the soft polymer matrix and relatively abrasive reinforcement material. Furthermore, due to the macroscopic reinforcement pattern, comparatively smaller geometries may not be reinforced, requiring the more malleable matrix to take most the load, making small fixtures less feasible. (U.S. Department of Transportation: Federal Aviation Administration, 2012, p. 7-46)

Secondary bonding dissimilar materials such as fiber reinforced composites and metals can result in laminate failure due to mechanisms such as galvanic corrosion, thermal fatigue, and pure adhesive failure due to the loading scenario and surface preparation conditions. Galvanic corrosion occurs when two dissimilar materials with dramatic differences in galvanic series rankings come in physical contact with a dielectric. When this occurs, the more noble material would reduce corrosion, and the less noble material would degrade at a higher rate. (Mandel, M. & Krüger, L., 2014, p. 1123) Thermal fatigue is the means of failure in which materials with differing levels of coefficient of thermal expansion are affixed to each other. As one material heats and expands, the other expands to a lesser degree. Heat cycling would ultimately cause the deformation and failure of the adhesive material. Pure adhesive failure occurs when two components are bonded together

in a rigid fashion without the use of concentrated load fasteners. If the two components have sufficient strength, and the strength of the adhesive is reached, the two components may remain intact and remain in contact with the adhesive, with the adhesive failing solely upon the bond line. (Shin, K. C. & Lee, J. J., 2006, p. 476).

## **2.1 Theoretical Perspective**

The theoretical perspective that highlighted this research, and the problem statement that was to be resolved, was the theory of impact mechanics of composite laminates. This theory has been extensively researched for composites using a sandwich core, but little work has been done on metal laminate impact strength. Composite and sandwich structures have been frequently used in aerospace engineering related applications due to their lightweight properties. However, these materials are very sensitive to impact damage. Most impact studies on composite and sandwich structures focus on the following aspects: dynamic response, contact mechanics of composite and sandwich structures with foreign objects, damage and failure modes of composite and sandwich structures under impact and effects of anisotropy and special core structures on impact responses. This depicts that traditional carbon fiber composites with traditional core materials have good static and dynamic strength, but have poor strength after an impact scenario. This research was intended to be implemented with a novel metallic laminate substrate, which may increase yield strength after an impact condition. This was due to the previous use and validation of metals as impact absorbing materials against projectiles and blast shrapnel. (Qiao, P., Yang, M., & Bobaru, F., 2008, p. 240)

### 3 Purpose

The purpose of this experiment was to determine the structural effects of a tubular aluminum substrate on a carbon fiber reinforced composite tube following an impact condition, and to what degree the metallic substrate enhances these properties.

### 4 Hypotheses

For this experiment, there were two supporting hypotheses, with one main hypothesis. The two supporting hypotheses ( $H_1$  and  $H_2$ ) were used to determine the validity of the experiment methodology. The one main hypothesis ( $H_3$ ) was used to ultimately determine the outcome of the experiment, and whether the sleeve condition has ultimately affected the dependent variable.

**$H_1$ :** There is equal variance of the effective modulus between each batch factor level of the analysis scenario.

The first supporting hypothesis was between the variances of the effective modulus in each batch factor level. The variance of the batch factor level within each analysis scenario (such as pre impact torsion, composite layer shear modulus, and post impact tension) was compared against the variances of the other batch factor levels within that analysis scenario. Each analysis scenario effective modulus variance was compared against the effective modulus variations of different batches, to determine the statistical significance of the difference in variance between the values. First, a normality test was performed to determine the statistical significance of the difference between the data and a perfect normal distribution. After this, a Bartlett's and Levene's equal variance test was used. The null hypothesis was that all variances were equal between the analysis scenario tests. This would indicate that the manufacturing and testing methods of the samples were

repeatable. Since there was no historical variance data to determine upper and lower standard limits, as well as no specific industry or product to determine quality limits, minimum and maximum values couldn't be determined based on the information given. Demonstrating process and manufacturing capability from equal variance would support the validity of the experiment and allow it to continue. A rejection of this hypothesis would indicate that the process was not capable, and the experiment manufacturing or testing methods would need to be revisited and improved for the experiment to move forward in a productive and repeatable fashion. Ancillary hypotheses include an insignificant batch factor contribution to the model, which signifies that batch factor level variation does not contribute to effective modulus variation in the analysis scenario.

**H<sub>2</sub>:** There is a lower effective modulus after the impact than before the impact for the non sleeve condition (0.000 sleeve thickness) factor level of both the loading scenarios.

The second supporting hypothesis was between the effective modulus of post impact change for the 0.000 sleeve thickness factor level. The 0.000 sleeve thickness factor level effective modulus was calculated, and the pre impact condition was compared against the post impact condition by finding the difference. The samples' effective modulus was compared by taking the post impact percent change to determine the difference between the two values using a boxplot. The null hypothesis was that there was a difference between the pre impact and post impact factor values. This would therefore aid in determining whether the impact procedure affected the effective modulus of the samples, and therefore determine whether the impact procedure was valid. A rejection of this hypothesis would indicate that the process was not capable, and the experiment drop impact methods would need to be revisited and improved in this area for the experiment to

move forward to further data analysis. Preliminary test samples were manufactured in addition to the main test samples to verify the provided drop height and weight, so this test was mainly a manufacturing and test repeatability verification.

**H<sub>3</sub>:** There is a lower post impact percent effective modulus change of the aluminum sleeve conditions than the non sleeve condition factor level of the experiment.

The main hypothesis of the research was between the effective modulus of the non sleeve and the aluminum sleeve factor levels. The post impact percent change of each of the sleeve thickness factor levels were compared if the two supplementary hypotheses were fulfilled. The samples' effective modulus was compared to determine the statistical significance of the change using an ANOVA, main effects and boxplots, and a Tukey pairwise comparison. The hypothesis was that there was statistically significant change between the means of each sleeve thickness factor level, and more importantly that there was a lower effective modulus decrease for the samples that have had the aluminum sleeve factor level. This would indicate that there was a difference between the post impact percent change that had the aluminum sleeve factor levels, and the post impact percent change that have a non sleeve factor level. Using main effects plots and boxplots would then show that the aluminum sleeve reduces the effective modulus post impact change, therefore increasing post impact effective modulus. A rejection of this hypothesis would indicate that the aluminum sleeve does not contribute to the overall strength of the laminate after an impact condition. It was important to note that the effective modulus of the different sample sleeve conditions were normalized based on individual sample geometry before data analysis.

## 5 Significance

Composites that have increased impact resistance and an improved means of fastening may dramatically increase the number of applications they can successfully be used in, therefore decreasing the cost of composite material implementation due to its ubiquity. This increase in composite material use has the benefit of being able to decrease weight of critical transportation and infrastructure systems, which would in turn decrease ultimate power requirements. Although relatively small amounts of carbon fiber reinforced plastics are necessary for a majority of component applications, the safety factor and therefore the added unnecessary material was quite high in composite components due to the impact requirements. (Broutman, L. J. et al, 1972, p. 13)

Utilizing aluminum substrates may decrease overall component weight by shouldering a portion of the impact energy. This can eventually decrease fossil fuel use, as well as pollution emissions. Decreasing weight of components can increase not only fuel mileage in aerospace and automotive applications, but also handling characteristics, safety, and ride quality of transportation vehicles.

The use of composites to lighten certain areas of transportation systems allows designers to add weight in areas that fulfill the customer requirements to a greater extent. Areas such as sound damping, suspension improvements, and drivetrain improvements can be made, and the associated weight penalty can be minimized due to the inclusion of carbon fiber reinforced plastic components. Furthermore, existing composite components can be manufactured more quickly and using a less skilled workforce due to the separate aluminum and carbon fiber reinforced plastic sleeves which simply need to be bonded together. In the case of more intricate components, metal pieces can be manufactured using a hydroforming process, and the composite piece may use the hydro formed component as a mold.

## **6 Literature Review**

The literature review stage was completed to determine whether the same work has been already completed. If the research to be experimented was novel, then the research can continue forward. The literature review was then used to look at similar work that has been completed in the field of research. It also allows for further insight into the underlying applications or problems that previous research was attempting to address. This can be used for further inspiration, or to determine areas of research that have been completely overlooked. The following articles are a sample of the main points that were to be emphasized among a larger list of references used to guide the methodology and process within this research experiment.

### **6.1 Applications**

Research has been completed regarding one of the specific main applications of fiber reinforced composite shafts: automotive drive shafts. These drive shafts transmit rotational energy from the transmission in the case of a rear wheel drive automobile, or from the transfer case in an all-wheel drive automobile. Energy is transferred to the front or rear differentials. This energy transfer is mainly torsional, with little axial loading and bending due to suspension travel and shaft whirl respectively. This highlights the use of composites within the application, as well as represents optimization methods for composite use in these applications. It also shows the need for impact absorption properties in the component. Findings concluded that the 45 degree fiber angle to the axis provided optimal torsional strength, while lesser fiber angles relative to the shaft axis provided increased natural frequency of the component. (Badie, M. A., Mahdi, E., & Hamouda, A. M. S., 2010, p. 1485) Considering this, a 45 degree fiber angle appeared valid for the intended loading scenarios.

## **6.2 Composite Metal Interface**

Previous research has been completed with regard to the use of thin strips of carbon fiber reinforced plastic with thin walled steel columns. In the columns, load was transferred axially, as opposed to torsionally in the drive shafts. Thin strips of carbon fiber reinforced plastic were placed along the perimeter of the members in an effort to maximize the strength of the existing structure. It also applies this technology to an original structure that was not meant to be reinforced, which incorporates a retrofitting concept. Differences between this previous work and the current work was that the current work was using a full coverage carbon fiber reinforced plastic sleeve instead of strategically placed strips. The independent variable in the previous work was the fiber placement instead of the sleeve involvement. The load of this previous research was only in the compressive axial direction, while the proposed experiment was in the axial tensile and torsional directions. Findings concluded that the strongest designs contained multiple thin carbon fiber reinforced plastic strips placed in the axial direction, and multiple strips 45 degrees to the axis. More importantly, the research concluded that a full carbon unidirectional cover axial to load was not as strong as strategically placed fiber tape. (Muteb, H. M., Kemal, A. T., & Jaber, M. H., n.d. p.623-633) Although the proposed research does not contain compressive forces, the previous research validates the fiber angle. It also invalidates the use of a unidirectional fabric in favor of a woven material.

## **6.3 Composite Impact**

Significant research has been completed regarding the impact and structural characteristics of composite materials in their neat state. The impact research depicts methods that were used only for metallic and isotropic materials, those that can be used within the metallic sectors and modified

for the composite sectors, as well as new processes that were developed solely for the anisotropic nature of composites. The previous research was concentrated around the methodology of testing for impact response of stiff anisotropic materials, and measures energy absorption instead of effective modulus after impact. This research was concentrated around the measurement of the low strain rate effective modulus after an impact, instead of the high strain rate energy absorption. This was in an effort to not only provide data more conducive to a real-world scenario, but also to encompass material that was valid for both the metallic and composite based materials used in this experiment. Findings concluded that some test methods for metals were significantly inapplicable for composite materials. Furthermore, it showed the crack formation and propagation occurring with the valid impact testing methods. (Broutman, L. J. et al, 1972, p. 1-9) Due to the crack formation on the opposite side of the impact site, the use of a metal substrate for composite support appeared valid. Current ASTM standards were used to determine loading rates that can be used as introductory drop impact values for the proposed experiment. (ASTM, 2014, para. 14)

## **7 Methodology**

The methodology that has been chosen was a quantitative research approach. The philosophical worldview that was associated with this research approach was post positivist. The research design that was chosen was experimental.

The quantitative research approach was chosen due to the nature of the experiment and the scientific method in general, as well as the audience that the research was designed to present to. Within the Manufacturing and Mechanical Systems Integration Master's program, as well as the CAST department, nearly all papers are quantitative. This allows for ease of research, as well as

credibility, as the research can be parameterized and tailored to specific problems that the audience may face.

## **7.1 Independent Variables**

The independent variables were the variables that would ultimately affect the dependent variable value. In this case, the independent variables were the sleeve condition, impact condition, and loading condition.

In this experiment, the sleeve condition was whether a 0.5” outer diameter thin aluminum tube was affixed to the sleeve ends of the sample under the carbon fiber sleeve, and the thickness of aluminum sleeve. There were three specific conditions, including a non sleeve condition (0.000 sleeve thickness factor level), a 0.020” thick aluminum sleeve (0.020 sleeve thickness factor level), and a 0.028” thick aluminum sleeve (0.028 sleeve thickness factor level). In the non sleeve condition, the carbon fiber reinforced plastic biaxial sleeve was directly adhered to the two aluminum rods using the structural adhesive, with no aluminum tube involved. In the aluminum sleeve conditions, the aluminum tube has two solid aluminum rods adhered to the inner diameter of the tube. The carbon fiber biaxial sleeve was adhered to the outer diameter of the aluminum tube using specialized metal to composite structural adhesive (Hysol E-120HP). The aluminum sleeve was hypothesized to affect the overall effective modulus change of the sample after an impact has occurred.

The impact condition of the experiment was whether the sample has undergone the specific high strain rate impact loading scenario before the other two low strain rate loading scenarios take place. There were two specific conditions, including a pre impact condition and a post impact condition.

The impact in this experiment was a hemispherical “tup” style impactor falling at a specific height from the axis of the sample. The impactor was dropped from this height using a drop tower impact system. The impactor was fully free falling, and standardized drop heights based on laminate thickness was used in preliminary testing to ensure that the impact scenario negatively affects the structural characteristics of the non sleeve samples. The impact occurred half way down the length of the shaft, at the axis of the tube geometry. In the second hypothesis, the impact force of the ball was thought to impart enough stress to damage the carbon fiber reinforced composite shell. The third hypothesis states that this impact would damage the sample with the sleeve to a lesser extent, or not to damage the sample at all, therefore decreasing the effective modulus change of the sample with the aluminum sleeve.

The loading conditions were what type of load, and therefore stress, was placed on the part. Due to the anisotropy of the carbon fiber composite and the possible effects of the composite to metal bonding, the shaft was hypothesized to react in a different manner and have different effective modulus due to different loading scenarios, which was the rationale behind using multiple different loading scenarios for the testing of impact effect. There were two specific loading conditions that the samples underwent during this experiment. These conditions were torsion and tension. It was hypothesized that the sample effective modulus was higher in the torsional loading condition than the tension loading condition due to the 45-degree orientation of the fibers relative to the axis of the sample.

The torsion test used a different testing machine than the tension testing. A Tinius Olsen torsion tester was used from the RIT Mechanical Engineering department, and measured the effective shear modulus of the samples. The sample was fastened to the machine using the bare aluminum

ends of the sample, as with the tension test. Standardized torsional strain rates were used, as with the tension testing condition. The sleeve ends were of the same diameter and length as those with the other tests, and have been made to fit the torsional tester as well. Testing occurred below the yield limit of the sample, based on preliminary testing. As with the tension test condition, supplementary samples were created and tested to the ultimate strength limit to ensure that the yield strength of the sample was not being surpassed for each test. Inclinator relative position was also monitored after torsion testing to ensure that no samples were plastically deformed.

In the tensile loading condition, an electromechanical tensile tester was used, which was supplied by the RIT MMET department. The sleeve ends have specific diameters to accommodate the jaw requirements of the tensile tester. The machine clamped on to the sleeve ends in the case of the non sleeve condition, and pulled on the tube containing the sleeve ends in the case of the aluminum sleeve scenario. Although counter intuitive, this was done to provide a more accurate comparison, as the material being displaced was directly adhered to the sleeve in both scenarios. The machine pulled axially at a specified strain rate of  $0.050''/\text{min}$  until 75% of the yield strength of the sample was reached. It then stopped and returned to its original position. This was done to ensure that the samples can be used for multiple impact conditions and testing conditions, as the samples did not deform plastically. The sleeve ends were the same for both testing methods, including torsional testing. This was done to ease manufacturing, as well as to ensure repeatability and accuracy in the data collected.

## **7.2 Dependent Variable**

The dependent variable in this experiment was the effective modulus, which was the amount of stress that occurs based on the strain imparted on the sample. The rationale behind this

measurement was that effective modulus can be measured in a reproducible manner with a single sample, and does not require the sample to be damaged in any way. This allows a single sample to be used for both testing conditions and in pre and post impact conditions, decreasing the likelihood of variation due to manufacturing processes. This was a requirement specific to the use of biaxial sleeve, as the modulus of the sample was exceptionally sensitive to the fiber orientation relative to the sample axis. Metals tend to have a deviation between their yield and ultimate strengths, while composites tend to have the yield and ultimate strengths of the same value. Carbon fiber reinforced composites also tend to have a much greater modulus and a decreased elongation at break compared to metals. (Park, 2015, p. 184) Therefore, testing effective modulus helped determine to what degree each material was contributing to the overall strength of the sample. As stated previously, preliminary samples were required as well as analytical models to ensure that the yield strength was not surpassed during general testing, as this would make the samples unusable for proceeding test conditions and impact conditions.

### **7.3 Control Variables**

The control variables in this experiment were the factors that would need to be monitored to ensure accuracy to the analytical models, as well as repeatability within the samples, testing conditions, and impact conditions. One of the control variables was the machining tolerances and surface finish of the areas of the metal that was adhered to the composite sleeve. In the case of the non sleeve sample, this was the surface finish of the sleeve ends. In the case of the aluminum sleeve samples, this was the surface finish of the metal tube. The machining tolerances was monitored to ensure reliability and repeatability of the sample data output compared to the analytical model as well as other samples. It would also be used to ensure fitment of the carbon fiber reinforced plastic

sleeve onto the outer diameter of the metal attachments, and ensure proper bond line thickness between the two materials.

The composite contact surface finish was monitored to ensure reliability and repeatability of proper adhesion between the composite and metal components of the sample. Adhesive failure was not expected to account for the mode of failure within the samples for either the non sleeve or the aluminum sleeve conditions. Analytical models were performed without accounting for adhesive failure, and any failure of the interlaminar bond between the carbon fiber reinforced plastic and metal was likely to cause unexpected effective modulus results. Therefore, a proper mechanical bond between the metal component and the adhesive was verified. This mechanical bond was ensured using sand paper after the machining process, but before the use of the chromate conversion coating. Surface roughness measurements were taken to ensure the surface was abraded to the proper depth, and the proper orientation. Analytical models have been calculated to determine proper adhesive surface area to reduce the likelihood of adhesive failure.

Curing parameters were also considered. Parameters such as curing temperature, curing humidity, and compaction were controlled to allow conformance of material properties to analytical data as well as between samples. Curing temperature must be considered due to the chemical composition of the matrix that was being used in the experiment. The epoxy resin that was used was sensitive to temperature while in its curing state. With that said, the curing temperature was similar to that of typical room temperature, and variation in room temperature would, under most circumstances, translate to a difference in curing time and would not affect the end sample effective modulus characteristics. (Axson Technologies: Marine 820 Epoxy Laminating System, 2016)

Curing humidity must be controlled to a great extent, as it has the potential to affect the effective modulus results. As with the curing temperature, humidity must be controlled due to the epoxy resin used. Epoxy resin is typically hydrophilic, and humidity has the potential to degrade the characteristics of the resin. As was the case with the temperature, average room humidity would not dramatically decrease properties, but the parameter must be considered to ensure complete understanding of the underlying effects. (Axson Technologies: Marine 820 Epoxy Laminating System, 2016)

Compaction rates have less to do with the resin used, but have a potentially dramatic effect on effective modulus results. This was due to potential geometry changes that can arise from improper composite compaction, the ability for the resin to retain air bubbles, and the ability for the resin to be exposed to humidity. Improper compaction can lead to increased composite layer thickness. This would lead to an increased overall tube geometry diameter, which would decrease stress on the composite, artificially increasing apparent effective modulus of the sample. (Park, 2015, p. 205)

Decreased compaction may also allow bubbles in the resin, which were introduced in the hardener mixing process, to remain in the composite laminate. This would in turn create stress concentrations, as well as voids with no fiber coverage, which may artificially lower the apparent effective modulus and may allow the yield stress to be attained more easily. This would allow the sample to plastically deform and would result in a sample that could no longer be used in subsequent tests. (Park, 2015, p. 205)

If air was introduced due to decreased compaction, the humidity within that air may be introduced into the resin, which would decrease the structural properties of the composite laminate. This was mitigated using a vacuum bag, which was used to isolate the resin from the atmosphere.

## **7.4 Manufacturing Procedure**

Once the materials were procured, the parts were machined and assembled into the proper component to test. The required steps were broken into the following phases; machining, aluminum sleeve assembly, carbon fiber sleeve layup, carbon fiber reinforced plastic sleeve assembly, and torsion fixture alignment tool manufacture.

### **7.4.1 Machining**

The aluminum tube was the first component to be machined. The aluminum tube was of 0.5” outer diameter, and consisted of two thicknesses; 0.020” and 0.028”. Both thicknesses were machined in the same manner, though decreased feed rates were used to ensure the thinner 0.020” samples were not deformed in the manufacturing process. Tubes were cut to length using a band saw. Although a cutoff saw would be typically used, it required a clamping mechanism to provide grip on the part circumference, which would have led to deformation of the thin walled aluminum tubing. Tube lengths were cut oversize (14.125”) to allow for a more precise cut in subsequent steps. A lathe was considered for the initial cutting operation, and would have saved subsequent steps, but would have required a tailstock holder for the full length of the tube which was not available. Instead an initial band saw operation was implemented, and a lathe was used to precisely cut the size to the required 14” length.

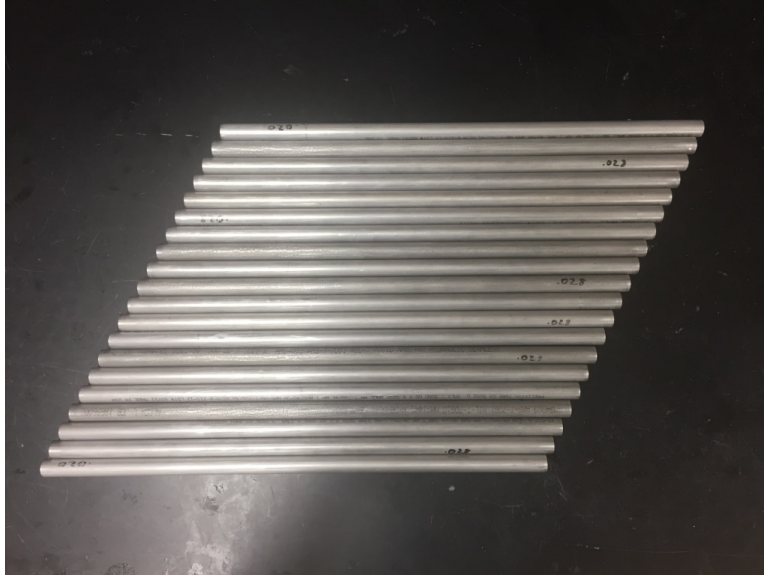


*Figure 7.1: The aluminum tubes, cut to the final length of 14".*

After the tubes were machined to size, the geometry was sanded on the adhering surfaces using a lathe and 220 grit sandpaper. They were sanded in a cross hatch pattern to maximize mechanical grip. (Rock West Composites: Composite Bond Prep 101, 2016) This surface roughness was verified using a profilometer in a subsequent step. This concluded that there was very little part to part variance, representing the validity of the sanding process. The inner circumference of the tube was then sanded using 220 grit sandpaper for the 4" of length in which it would contact the sleeve ends in the future adhering process. This surface roughness could not be verified due to the limitations of the profilometer, but similar methods and materials were used for the inner circumference as the outer circumference.

The ends were the next components to be machined. Though they were all machined to the same length of 4", they had multiple diameters. The non sleeve ends were machined to 0.465" to accommodate the thicker laminate and subsequent smaller inner diameter. The 0.020" thick sleeve ends were machined to 0.450" to accommodate the sleeve thickness and adhesive bondline

thickness. The 0.028" thick sleeve ends were machined to 0.434" to accommodate the sleeve thickness and adhesive bondline thickness in the same manner as the 0.020" thickness samples.

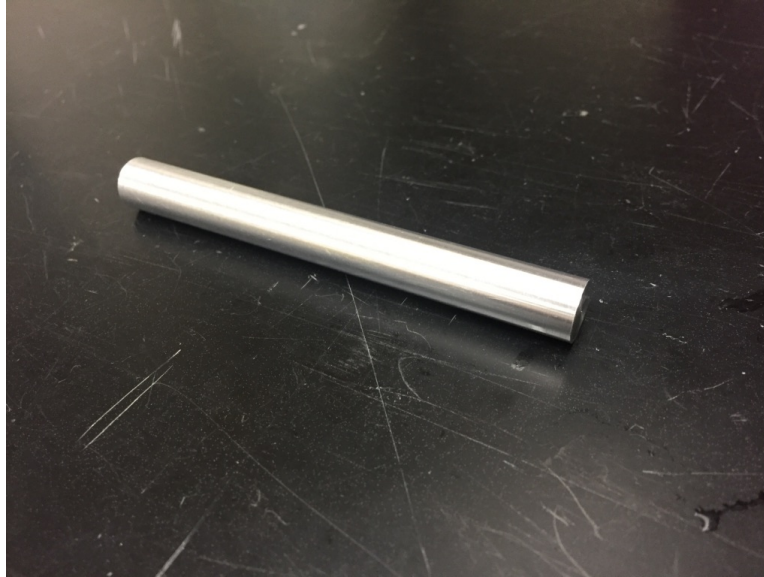


*Figure 7.2: The aluminum ends, machined to their final diameter and length.*

After the ends were machined, they were sanded using 220 grit sandpaper. They were sanded in a cross hatch pattern to maximize mechanical grip. This surface roughness was verified using a profilometer in a subsequent step.

The mandrels were the next components to be machined. Though they were all machined to the same length of 14", they had two different diameters. The mandrels for the non sleeve components were machined to 0.465" to accommodate the thicker laminate, and the sleeve mandrels were kept at the 0.5" thickness to accommodate the sleeve diameter. This step was to ensure that all sample geometries retained the same mean diameter, given the different composite layer thickness. Though the mandrels were 14" in length, the machined length was 12" this allowed for length on the side of the mandrel to handle the piece while the carbon fiber was being laid up. After turning,

all machined lengths were sanded with 400, 600, 800, and 1000 grit sandpaper. Though all sanding was done transverse to the axis of the mandrel (in the direction of rotation), 1000 grit sandpaper was also sanded along the axis to ensure ease of part removal due to the lack of loft angle.

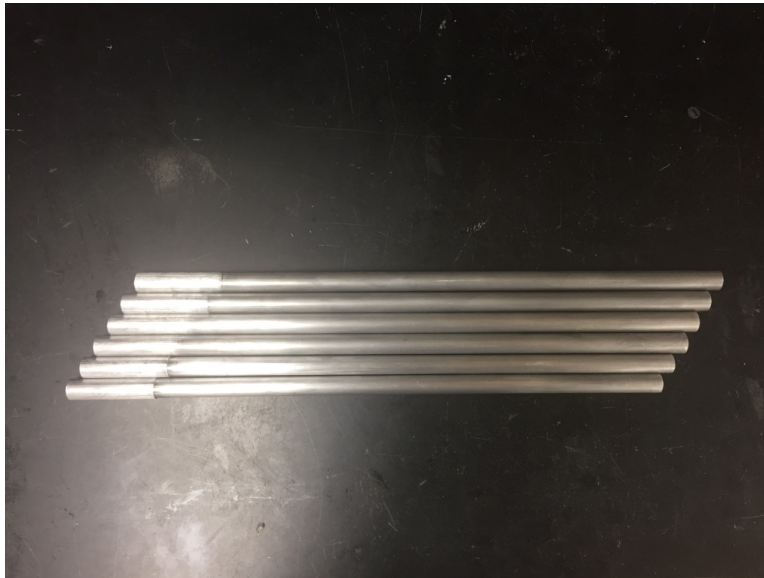


*Figure 7.3: Aluminum mandrels, machined to their final diameter and length.*

The sleeves, ends, and mandrels were then tested for surface roughness. A Mahr Federal Pocket Surf was initially used to measure surface roughness along the axis of the samples, and a Tamar HRT 3000 was used for surface roughness verification of sanding angle. All tests were run along the axis of the sample, at random locations along the length and circumference of the samples. The objective for the sleeves and ends was to achieve a desired roughness value to ensure mechanical adhesion between the adhesive and substrates. The objective for the mandrels was to achieve the lowest roughness value to ensure ease of removal of the carbon fiber reinforced plastic sleeves from the mandrels after layup.



*Figure 7.4: Surface roughness testing of aluminum end using Mahr Federal Pocket Surf.*

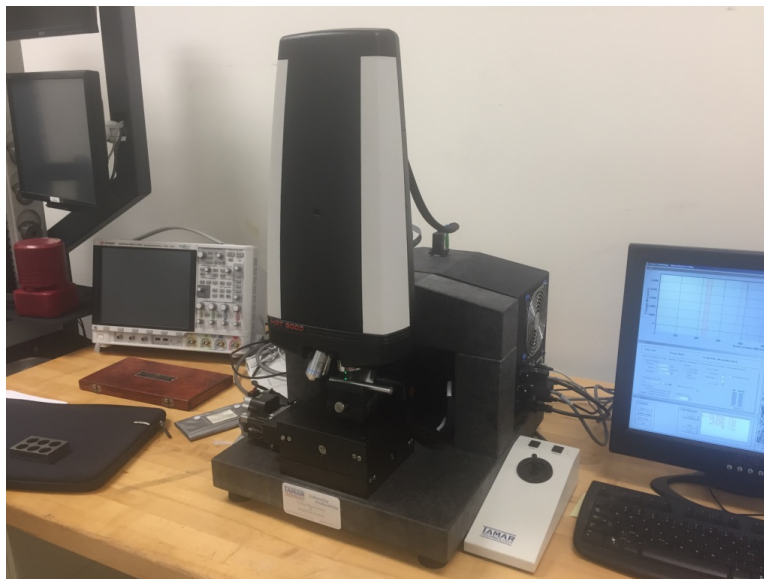


*Figure 7.5: Surface roughness testing using Tamar HRT 3000.*

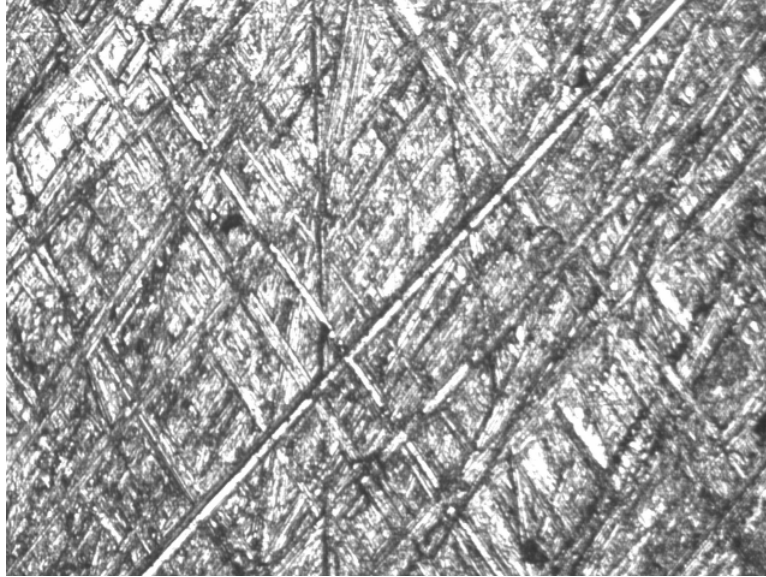


*Figure 7.6: Surface roughness image of aluminum sleeve using Tamar HRT 3000 (note 45 degree crosshatch pattern).*

After the parts were machined and tested, they were coated to prevent corrosion between the adhesive and the substrate after the adhering process. To prepare for the coating process, the sleeves and ends were cleaned using dish detergent and water. After rinsing, they were cleaned with acetone and a lint free cloth. The parts were then cleaned with Alumiprep 33, a phosphoric acid based cleaner, diluted as per the product data sheet. After rinsing with water, the parts were dried. Diluted Alodine 1001, a chromic acid based chrome conversion coating, was then applied. Parts were thoroughly rinsed with water and dried as with the Alumiprep. This concludes the coating process.

#### **7.4.2 Aluminum Sleeve Assembly**

After all parts were coated, the sleeves were adhered to the sleeve ends. Parts were adhered using Loctite Hysol EA E-120HP. Adhesive was applied to the inner circumference of the sleeves, and the outer circumference of the ends. Ends were inserted into the sleeves using a helical motion to

allow trapped air within the sleeve to escape without forming air bubbles between the sleeve and ends. 24 hours were given to ensure parts were fully cured. (Loctite: EA E-120HP, 2014)

### **7.4.3 Composite Sleeve Layup**

After the sleeve ends were inserted into the sleeve ends, the carbon fiber sleeves were laid up. This process consisted of mandrel preparation, lay up, and vacuum bagging. Mandrel preparation started with mandrel cleaning. Mandrels were cleaned first with dish detergent and water, and then rinsed with acetone and a lint free cloth. Wax was then applied. Partall Paste #2 was used due to its performance in composite part removal. Wax was applied, buffed and left to sit for an hour before the next wax layer to allow for appropriate solvent release. This process was repeated to produce four layers of wax. (Fibre Glast Developments Corporation: Parting Wax, 2010) Once the last layer was dry, Polyvinyl Alcohol (PVA) was applied to the mandrels. This material was used as a mold release agent, and as a bondline thickness producer. The ideal PVA thickness of 0.004 in (Fibre Glast Developments Corporation: PVA Release Film, 2010) was identical to that of the ideal bondline thickness of the adhesive. (Loctite: EA E-120HP, 2014) Therefore, it was implemented to increase the diameter of the mandrels to accommodate secondary bonding. An aerosol spray system was utilized to provide even coating of the PVA, and provide the necessary bondline thickness as well as runout tolerance along the mating surface between the carbon fiber reinforced plastic sleeve and the aluminum sleeve.

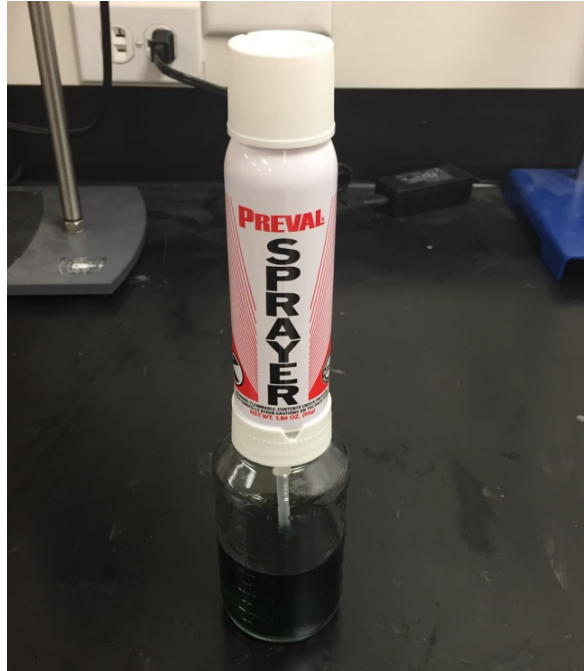


*Figure 7.7: Aerosol system used to spray PVA on to mandrels.*



*Figure 7.8: Fixture used to spray mandrels in an even manner.*

After sufficient time was given for the PVA to dry, the layup process began. A layer of dry carbon fiber biaxial sleeve of 0.5” nominal diameter was placed over the mandrel, and epoxy was placed on the sleeve. The epoxy used was AdTech 820, with the accompanying 824 hardener. This process was repeated to produce two layers for the sleeve mandrels, and four layers for the non sleeve mandrels.

When all layers of carbon fiber were applied to the mandrels, the vacuum bagging process was implemented. The samples were wrapped in ACP Composites Econolease Super Release Peel Ply. This was used to provide a breather material for even vacuum pressure distribution. A typical breather ply was considered, but would have affected the resin volume percentage of the composite due to the transfer of resin to the breather ply. A bridge of peel ply was placed across all samples to distribute vacuum pressure. ACP Composites Stretchlon 200 High Stretch Bag Film was used as a bagging film. The decreased thickness and high conformability of the film helped prevent wrinkles in the outer fiber layers. Vacuum bag sealant tape was used to seal the perimeter of the vacuum bag. Polyethylene vacuum hose was inserted into the ends of the sealing tape to produce the required vacuum.



*Figure 7.9: Vacuum bagging system used for composite sleeve manufacture.*

After 24 hours, the samples were demolded. The vacuum bag was peeled off, and the carbon fiber reinforced plastic sleeves were removed from the mandrels. A helical removal method was employed to remove the sleeves due to the lack of loft in the mandrel. This was achieved by using pliers to twist a sacrificial length of the composite tube. Once the sleeves were removed, the peel ply material was removed. The sleeves were then cut to the required 10" length. This was done using a band saw to minimize fiber tear and then sanded using a belt sander to provide a flat face. After machining of the carbon fiber reinforced plastic sleeves was completed, the residual wax and PVA was removed. This was done using a hot water bath to dissolve the PVA and release the wax. After the hot water bath, the inner surface of the sleeves were honed with 220 grit sandpaper. This was done to remove remaining residue, as well as to create a mechanical bond for the adhesive. After honing, the inner surfaces of the sleeves were rinsed with acetone to remove honing residue. Samples were placed in a convection oven at 30 degrees Celsius to remove the acetone quickly.

#### **7.4.4 Composite Sleeve Assembly**

The carbon fiber composite sleeves were assembled on the aluminum sleeves after the carbon fiber surface preparation was complete. Bonding adhesive was placed on the outer surface of the aluminum sleeves, in the area upon which the carbon fiber reinforced plastic sleeves were to be placed. The carbon fiber composite sleeves were slid onto the aluminum sleeves, and aligned so that each composite sleeve end was 2" from the end of the aluminum sleeve. Excess adhesive was removed from the sleeves. For the non sleeve samples, the aluminum ends were bonded directly to the carbon fiber reinforced plastic sleeves using the same method. This was done to ensure continuity between the aluminum sleeve and non sleeve samples. The components were left to cure at room temperature for 24 hours.

#### **7.4.5 Test Preparation**

Preliminary testing was completed first using a torsion tester. To ensure the torsion tester was adequately aligned for the individual samples, alignment tools were machined for the diameters of the specimen ends. These diameters were 0.500" for the sleeve ends, and 0.465" for the non sleeve ends.

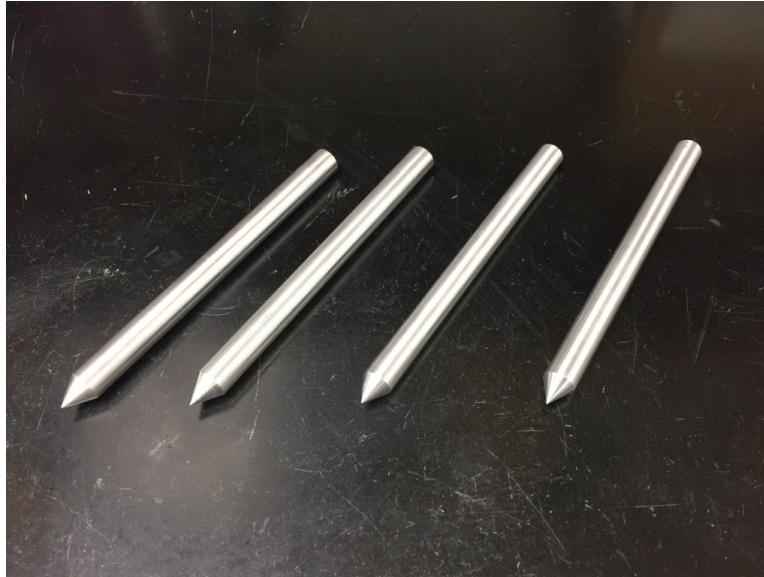


*Figure 7.10: Alignment tools used to verify concentricity in the torsion tester jaws.*

After proper alignment tools were machined, they were used to ensure the torsion tester chucks were concentric to each other. Each of the three jaws of the two chucks were adjusted individually to ensure proper compression on the samples and concentricity to each other. This was completed by using a runout gage to ensure drive chuck runout, and then the driven chuck was centered on the drive chuck.

## **7.5 Test Procedure**

Sample cross sectional drawings were used to depict the intended material layer thicknesses.

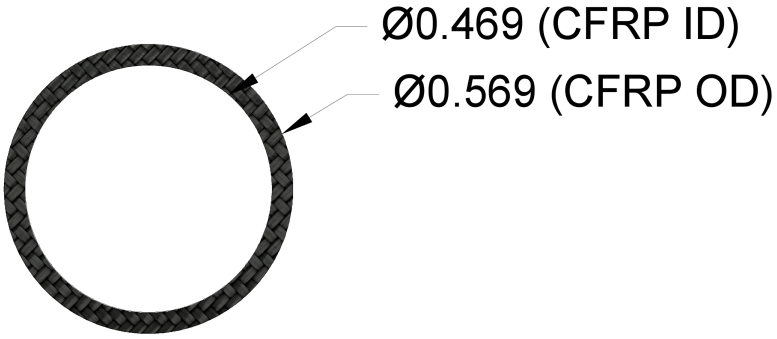


*Figure 7.11: Non sleeve/0.000 sleeve thickness factor level sample intended cross section.*

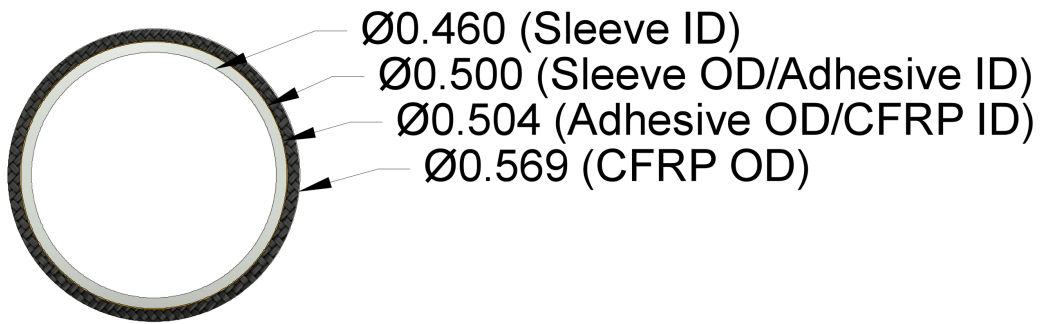


*Figure 7.12: 0.020 sleeve thickness factor level sample intended cross section.*

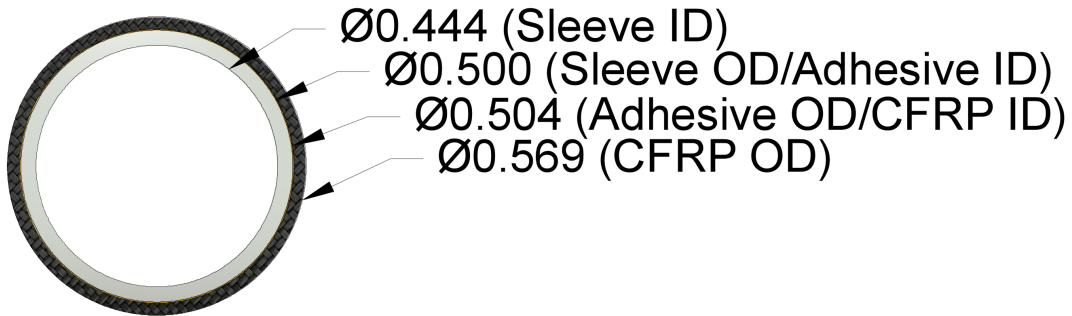


*Figure 7.13: 0.028 sleeve thickness factor level sample intended cross section.*

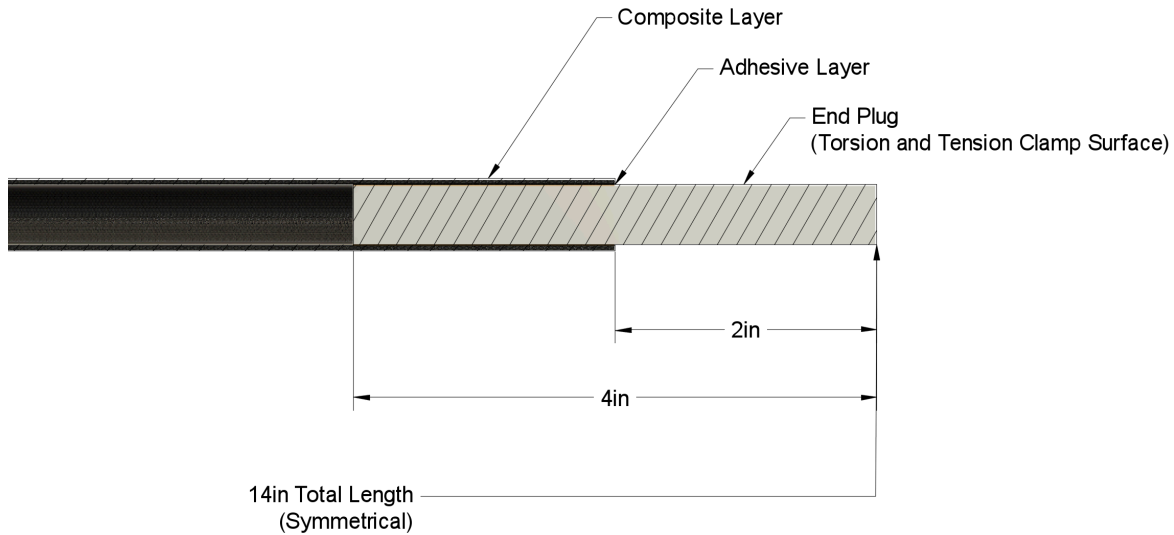


Figure 7.14: No sleeve (0.000) sample section view.

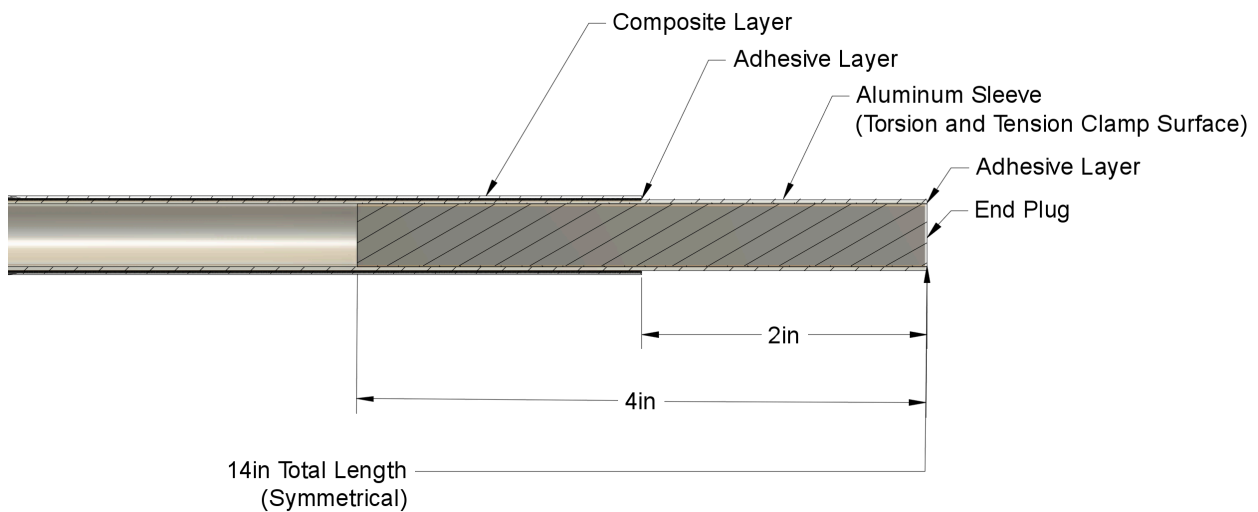


Figure 7.15: 0.020 and 0.028 sleeve thickness sample section view.

### 7.5.1 Pre and Post Impact Torsion Procedure

For the pre and post impact torsion, a Tinius Olsen 10,000 in-lb Torsion Tester was used from the Mechanical Engineering Materials Testing Lab of RIT. Torsion tester jaws were measured before each testing session to ensure concentricity of  $\pm 0.010''$ . Inclinometers were placed at both ends of the critical cross section of the sample to ensure that data collection occurred on the carbon fiber

composite and aluminum sleeve area, and did not include the torsional deflection of the end plugs. Inclinometer accuracy was 0.1 degrees. Inclinometers were placed with 6” between stations, which was the extent of the critical cross section length. A strain rate of 5 degrees per minute was implemented. This speed was primarily chosen due to the speed of data collection when manually entering the inclinometer data. Data was collected in the form of; retrieving driven inclinometer, torque, and head angle when the predetermined drive inclinometer angle was reached. When drive side inclinometer surpassed 0.5 degrees past previous data collection, data was collected for drive inclinometer, driven inclinometer, head torque, and head angle simultaneously.



*Figure 7.16: Assembled sleeve, with inclinometer fixture in place.*

A preliminary sample was tested beyond the yield strength torque values for each of the three sample sleeve types. Subsequent samples were tested to 75% of the yield strength torque value of the sample type to ensure that all samples would remain within their elastic ranges. Data was collected and analyzed by inputting data into the spreadsheet, calculating stress based on predetermined sample properties, calculating strain based on inclinometer data, creating a stress

strain graph, and determining effective modulus based on the slope of the curve. All graphs were verified to ensure that the elastic limit of the samples was not reached by determining stress strain curve linearity before calculating effective modulus.

### **7.5.2 Pre and Post Impact Tension Procedure**

For the pre and post impact tension testing, an MTS Insight 100 kN Standard Length Electromechanical tensile tester was used in conjunction with MTS TestSuite TW Elite Software in the Manufacturing and Mechanical Engineering Technology materials testing lab of RIT. A 100 kN MTS load cell was used to measure tensile force on the sample, and was reset before each sample testing session. 0.42-0.66" v-wedge tensile tester jaws were used, and set at 10" between jaw ends before the testing procedure began. This was performed to ensure that the jaws securely contacted the aluminum cylindrical ends, and were not in contact with the carbon fiber sleeve. No external sensors were implemented outside of the tension testing unit. A strain rate of 0.050"/min was implemented in accordance to ASTM D3039. (ASTM, 2014, para. 14) Head travel and head load were the two factors being measured and consequently analyzed.

A preliminary sample was tested beyond the yield strength force values for each of the three sample sleeve types. Subsequent samples were tested to 75% of the yield strength force value of the sample type to ensure that all samples would remain within their elastic ranges. Data was collected and analyzed by retrieving data from the spreadsheet created by the testing software, calculating stress based on predetermined sample properties, calculating strain based on head travel, creating a stress strain graph, and determining effective modulus based on the slope of the curve. All graphs were

verified to ensure that the elastic limit of the samples was not reached before calculating effective modulus.

### 7.5.3 Impact Procedure

For the impact procedure, a TMI Group 43-26 Falling Dart Impact Tester was used, and modified in accordance to ASTM D7136 composite drop weight impact requirements. A 0.625” steel hemispherical “tup” style impactor was machined and used in lieu of the testers original 1.5” aluminum hemispherical impactor. A steel impactor shaft was machined and implemented in lieu of the testers original aluminum shaft. Weights were added to the impactor shaft increase impactor weight to 4 lb ±0.005 lb, and were fastened to the impactor shaft to eliminate weight dislocation upon the impact event. (ASTM: D7136, 2015, para. 15)

Drop impact energy was calculated based on required impact energy using ASTM D7136 impact energy calculations (ASTM: D7136, 2015, para. 15):

$$E = C_E h \quad (8.1)$$

where:

$E$  = potential energy of impactor prior to drop, [in-lbf],

$C_E$  = specified ratio of impact energy to specimen thickness, [1500 in-lbf/in], and

$h$  = nominal thickness of specimen, [in].

Drop height was calculated based on the impact energy requirement (ASTM: D7136, 2015, para. 15):

$$d = \frac{E}{m_{dlb}} \quad (8.2)$$

where:

$d$  = drop height of impactor, [in],

$m_{dlb}$  = weight of impactor in standard gravity, [lb]

The default impactor weight was to be 12 lb, but the selected impactor weight must permit a minimum drop distance of 12". Since this weight would not permit the given minimum drop distance with the manufactured sample thickness, a lower weight of 4 lb was implemented in accordance with the ASTM standard. (ASTM: D7136, 2015, para. 15)

The ASTM D7136 test standard was used since it was intended for testing the impact capabilities of fiber reinforced composite samples. With this said, the test was tailored for the use of flat composite laminates, instead of the cylindrical shafts used in the research. For this reason, the testing parameters were modified.

The sample was placed on a flat steel plate, as opposed to the perimeter supported cavity used in the standard test method. This was carried out to ensure that a more complex three point bending event did not occur, which would have been highly dependent on sample length as well as diameter and material of the sample.

A similar laminate thickness vs. drop height calculation was implemented. This was used to allow for a standardized approach. It was also used due to the samples diameter conformity to the ASTM standard cut out depth. Minimum depth of the cavity below the sample being tested was 0.25" based on the standard. As the sample average diameter was 0.5", a complete cylinder crush would compress the impacted side of the cylinder by 0.25". This would mean that the impacted side of

the cylinder would have the same amount of post impact travel as the ASTM standard, and therefore similar calculation methods could be used. (ASTM: D7136, 2015, para. 15)

Lateral supports were used to prevent sliding due to impact, but no direct base fixture systems were implemented. This was done to prevent slipping under impact, but ensured that the majority of the impactor energy was concentrated on the local impact site of the sample.

With the 4 lb standard impactor and specified ratio of impact energy to specimen thickness, a height of 19.52” was calculated for the non sleeve samples, 19.13” for the 0.020 thickness sleeve samples, and 22. 17” for the 0.028 thickness samples. To provide a standardized impact energy among all sample sleeve factors, a drop height of 22” was implemented, and was measured from the bottom (tip) of the impactor to the expected impact site of the sample. (ASTM: D7136, 2015, para. 15)

The sample was placed on a flat plate, which served as a fixed support transverse to the impact site. Longitudinal location was determined using a test sample, ensuring the impactor contacted the samples along the axis of the cylindrical surface in a repeatable nature, and did not slide along the surface once impact occurred. Lateral supports along each side of the sample were used to minimize the likelihood of the sample sliding against the base once the impact had occurred. No supports were placed on top of the sample. This was done to ensure that any bending force created by the impact event was not artificially transferred to the impact apparatus.



*Figure 7.17: Original drop impact tester before modifications.*



*Figure 7.18: Drop impact tester after modifications.*



*Figure 7.19: Impactor as machined, not including necessary weights.*



*Figure 7.20: Impactor including necessary weights.*

The release mechanism was triggered and the impactor was dropped upon the sample. Impact depth was found using the impactor geometry. The impactor was placed in the depression caused by the impact event, and the offset from the original sample diameter (calculated from pre impact torsion and tension data) was determined to be the impact depth.

## 7.6 Data Collection

The data was collected mainly regarding the effective modulus of the samples. This was done using the tensile testing machine within the College of Applied Science and Technology and torsion tester within Kate Gleason College of Engineering of Rochester Institute of Technology. The output of these machines was what was known as a stress strain curve. This was the measurement of stress which was the applied force on the machine over the area of the sample that the force was acting upon. Strain was the amount that the sample was deforming due to the load imparted on the sample.

The data for the tension stress/strain charts was directly retrieved from the tensile testing machine. The tester outputs a stress strain diagram, alongside values for the yield and ultimate strength. Data outputs from the machine were used to input the data into a spreadsheet for further analysis. The principal point of comparison between samples was the effective modulus, which was the derivative of the stress/strain curve below the yield limit of the sample.

Data for the torsion testing was slightly different from that of the tension testing. Since there was no linear strain data that was output on the stress strain diagram, angular stress strain diagrams were employed. The torsion tester outputs strain in the form of degrees of deflection. Knowing the geometry of the sample, the equivalent strain of the material was determined. As with the tension and compression, this data was retrieved for further investigation and analysis. For ease of analysis, this data was compared solely to other torsion data to determine sample effective modulus results.

Other ancillary data that was recorded includes the surface roughness of the sleeve and sleeve ends. This data was used to support the validity of the output data supplied by the main

measurement systems, but was not analyzed as adhesive failure was limited to yielded samples. Surface roughness was thought to be a potential cause for variation in tension or torsion effective modulus, and was considered to be the cause for possible delamination between the composite and metal components. This event did not occur in the main testing below yield, so roughness measurements were not referenced.

## **7.7 Data Analysis**

Once all the samples were tested and the data was output from the machine, the data was put in a format in which it could be easily read and reviewed. This came in the form of inputting the retrieved values into a spreadsheet to save the necessary values. The effective modulus was determined by taking the derivative of the stress strain curve below the yield point. This was the main point of sample comparison and experiment validity.

The first method of analyzing the data was between the variance of the effective modulus of each sample of each loading condition of each impact and sleeve condition. To test the difference in variance, a preliminary normality test must be performed. This determines the statistical significance that the test data comes from a normally distributed population. After the normality test, a Bartlett's test was performed. This test was based around normal distributions. Then a Levene's test was performed. This test was agnostic to the distribution of the data collected, and was less conservative. Both tests would compare the variance in one test condition to all other test conditions, and provide statistical significance regarding the likelihood that all variances were equivalent to each other. If the data conforms to a normal distribution, and the variances were equal, there was sufficient evidence to determine that the manufacturing process used was

sufficient to produce repeatable samples, and the testing method was sufficient enough to provide repeatable data for the experiment.

The second method of analyzing the data was between the two impact conditions of each sleeve condition. More specifically, this was the effective modulus of each loading condition within each impact condition for the non sleeve conditions. Pre impact samples were compared to post impact samples. This was used to determine the difference in the two sample means. This analysis was used to determine whether the impact condition was effective, and negatively affected the samples regarding their effective modulus. If the resulting data shows that the impact has had no effect on the sample effective modulus, the experiment may need to be run again with an increased impactor weight or an increased drop height. If it was determined that there was statistical significance to a variation between the means of the drop impact and no impact samples, then the test analysis would continue.

The third method of analyzing the data was between the two sleeve conditions of the experiment. More specifically, it was between the two sleeve conditions of each loading condition of just the drop impact condition of the experiment. The effective modulus of the non sleeve condition of each of the loading conditions for the impact condition was compared against the aluminum sleeve condition for all loading conditions for the impact condition. This was done using a t-test statistical method, and would compare the means of the aluminum sleeve and non sleeve conditions. The statistical significance of the difference between the means was calculated, and based on the output, the hypothesis was rejected or failed to be rejected. This be the foremost determination of whether the sleeve ultimately improved the effective modulus of the sample after sample was impacted, under the two different loading conditions. This analysis was performed separately for

the different loading scenarios, as the loading condition may have affected the two sleeve conditions in a different manner.

### 7.7.1 Pre Impact Torsion Data Analysis

Data was entered in 0.5 degree increments, based on the rotation of the right (drive side) inclinometer. Right inclinometer angle, left inclinometer angle, current head torque, and current head angle were recorded. Head deflection, slip angle, and corrected head deflection were calculated, and used to determine strain along the critical cross section of the sample. Stress was determined using head torque and individual sample geometry. Sample geometry was corrected based on sample shaft outer diameter, which was measured using calipers (accurate to 0.001 in). This was performed to account for slight variation in sample torsional effective modulus due to variations in fiber reinforced composite thickness. Composite layer inner diameter and aluminum sleeve geometry were determined before the manufacturing of the samples.

Torsional stiffness of a cylinder is defined (Bauchau & Craig, 2009, p. 267):

$$H = \frac{\pi}{2} GR^4 \quad (8.3)$$

where:

H = Torsional stiffness, [(lb\*in)/rad],

G = Shear modulus, [psi], and

R = Radius, [in],

Torsional stiffness of a circular tube becomes (Bauchau et al, 2009, p. 267):

$$H = \frac{\pi}{2} G(R_o^4 - R_i^4) \quad (8.4)$$

where:

$R_o$  = Outer radius, [in], and

$R_i$  = Inner radius, [in],

Considering multiple layers within a circular tube torsional stiffness becomes (Bauchau et al, 2009, p. 267):

$$H = \frac{\pi}{2} \sum_{i=1}^N G^{[i]} \left[ \left( R_o^{[i]} \right)^4 - \left( R_i^{[i]} \right)^4 \right] \quad (8.5)$$

Considering the composite and aluminum sleeve layers:

$$H = \frac{\pi}{2} [G_a (R_{oa}^4 - R_{ia}^4) + G_c (R_{oc}^4 - R_{ic}^4)] \quad (8.6)$$

Solving for the modulus of the composite layer:

$$G_c = \frac{2H + \pi(-G_a)R_{oa}^4 + \pi G_a R_{ia}^4}{\pi R_{oc}^4 - \pi R_{ic}^4} \quad (8.7)$$

where:

$G_a$  = Shear modulus of the aluminum sleeve, [psi],

$R_{oa}$  = Outer radius of the aluminum sleeve, [in],

$R_{ia}$  = Inner radius of the aluminum sleeve, [in],

$G_c$  = Shear modulus of the composite layer, [psi],

$R_{oc}$  = Outer radius of the composite layer, [in], and

$R_{ic}$  = Inner radius of the composite layer, [in].

The shear modulus of the composite was determined based on torsional stiffness and geometry of each sample, as well as shear modulus of the sleeve material. Shear modulus of the aluminum

sleeve was taken to be 3,770,000 psi based on published data. (MatWeb Material Property Data: 6061-T6 Aluminum, 2017) Based on this, the shear modulus of the composite layer was determined for each sample. This shear modulus was analyzed to determine data validity and correlation.

Given the mean radius:

$$R_m = \frac{R_o + R_i}{2} \quad (8.8)$$

where:

$R_m$  = Mean radius, [in].

Given the wall thickness:

$$t = R_o - R_i \quad (8.9)$$

where:

t = Thickness, [in].

Given the thin wall assumption applies:

$$\frac{t}{R_m} \ll 1 \quad (8.10)$$

Torsional stiffness of a thin walled tube simplifies to (Bauchau et al, 2009, p. 267):

$$H = \frac{\pi}{2} G (R_o^2 + R_i^2) (R_o + R_i) (R_o - R_i) \quad (8.11)$$

$$H \approx 2\pi G t R_m^3 \quad (8.12)$$

This is due to the formula:

$$H = 2\pi G_c t_c R_{mc}^3 + 2\pi G_a t_a R_{ma}^3 \quad (8.13)$$

where:

$t_c$  = Thickness of composite layer, [in],

$R_{mc}$  = Mean radius of composite layer, [in],

$t_a$  = Thickness of aluminum sleeve, [in], and

$R_{ma}$  = Mean radius of aluminum sleeve, [in].

Since the mean radius and thickness of the composite layer and aluminum sleeve are similar relative to the radius of the sample:

$$H = 2\pi(G_c + G_a)t_t R_m^3 \quad (8.14)$$

$$H = G_t t R_m^3 \quad (8.15)$$

where:

$t_t$  = Thickness of total sample, [in],

$R_m$  = Mean radius of sample, [in], and

$G_t$  = Shear modulus of composite and aluminum layers, [psi].

This formula allows for the calculation of sample modulus, and therefore sample stress, by means of combining all sample layers. This creates a situation in which the sample effective stress can be determined using typical single layer tube calculations, as long as all layers are accounted for in the sample geometry.

Torsional stiffness of a thin walled tube simplification, given multiple layers. Torsional stiffness is the weighted average of the shear moduli of the layers. (Bauchau et al, 2009, p. 267)

$$H = \frac{\pi}{2} \sum_{i=1}^N G^i t^i \left( \frac{R_o^{[i]} + R_i^{[i]}}{2} \right)^3 \quad (8.16)$$

where:

[i] = Each layer,

N = Number of layers,

G = Shear modulus of each layer, [psi],

t = Thickness of each layer, [in],

$R_o$  = Outer radius of each layer, [in], and

$R_i$  = Inner radius of each layer, [in].

Sample calculation comparisons between the original circular tube torsional stiffness and simplified circular tube torsional stiffness were made. Stiffness results showed a deviation of less than 5%, signaling the validity of the simplified calculations within this geometry. This was likely due to the sample's minimal thickness relative to the radius of the cross section (thin wall assumption). Therefore, in measuring stiffness, the simplified calculations were implemented, which considered the aluminum sleeve and composite sleeve as a single unit with a unified modulus and thickness.

It is important to note that “effective modulus” is referenced instead of “modulus” in subsequent analysis. This is because the modulus of the sample material does not change greatly before and after impact, in the case of the aluminum and the non ruptured composite samples. Though this is the case, the effective modulus changed due to geometry change, sleeve delamination, and fiber rupture due to the impact event. Effective modulus of the samples was calculated instead of sample stiffness to ensure that the differences in geometry between each sample due to manufacturing process variability were not introduced into the data and were adequately accounted for, but is not necessarily reflective of the actual material properties.

The shear stress in a circular tube due to torsion was defined as:

$$\tau = \frac{Tr_o}{J} \quad (8.17)$$

where:

$\tau$  = Shear stress, [psi],

T = Applied torque, [in\*lb],

$r_o$  = Outer radius of the tube, [in], and

J = Polar moment of inertia of the tube geometry, [in<sup>4</sup>].

The polar moment of inertia in a thin walled tube was defined as:

$$J = \pi \frac{D^4 - d^4}{32} \quad (8.18)$$

where:

D = Outer diameter of the tube, [in], and

d = Inner diameter of the tube, [in].

Shear strain in a circular tube due to torsion was defined as:

$$\gamma = \frac{\theta r_o}{L} \quad (8.19)$$

where:

$\gamma$  = Shear strain, [in/in],

$\theta$  = Angular deflection, [radians],

$r_o$  = Outer radius of the tube, [in], and

L = Length of tube between contact points, [in].

A stress/strain curve was created based on the values, and a trend line was fitted to the data points. Any values that surpassed the sample yield values (occurring in the initial failure test samples) were omitted to ensure that the curve only followed the elastic region of the sample. The slope of the trend line was recorded as the effective modulus of the sample.

Data was analyzed using Minitab statistical data analysis software. A traditional ANOVA was calculated using a General Linear Model. Model adequacy was determined based on a standardized residual normal probability plot, and Bartlett's and Levene's tests. Factor comparisons were calculated using a Tukey test method and general trend inferences were formed based on boxplots and main effects plots.

Design type: Multifactor, mixed effects.

Effect type:

Batch: Random, since the batches in the model were assumed to represent a greater population.

Sleeve thickness: Fixed, since it was assumed that if the experiment were run again, the same thicknesses would be used.

## General Linear Model: Mean Effe. Shear Modulus (psi) versus Batch, Sleeve Thickness

Method

Factor coding (-1, 0, +1)

Factor Information

Factor	Type	Levels	Values
Batch	Random	5	1, 2, 3, 4, 5
Sleeve Thickness	Fixed	3	0.000, 0.020, 0.028

Analysis of Variance

Source	DF	Adj SS	Adj MS	F-Value	P-Value
Batch	4	59854411174	14963602793	0.48	0.753
Sleeve Thickness	2	9.25798E+11	4.62899E+11	14.74	0.000
Error	22	6.90783E+11	31399240547		
Lack-of-Fit	8	1.25516E+11	15689556706	0.39	0.909
Pure Error	14	5.65267E+11	40376202742		
Total	28	1.64509E+12			

Model Summary

S	R-sq	R-sq(adj)	R-sq(pred)
177198	58.01%	46.56%	27.58%

*Figure 7.21: General linear model output of effective shear modulus for pre impact torsion samples.*

Based on the analysis, the sleeve thickness factor appeared significant. The batch factor did not appear significant.

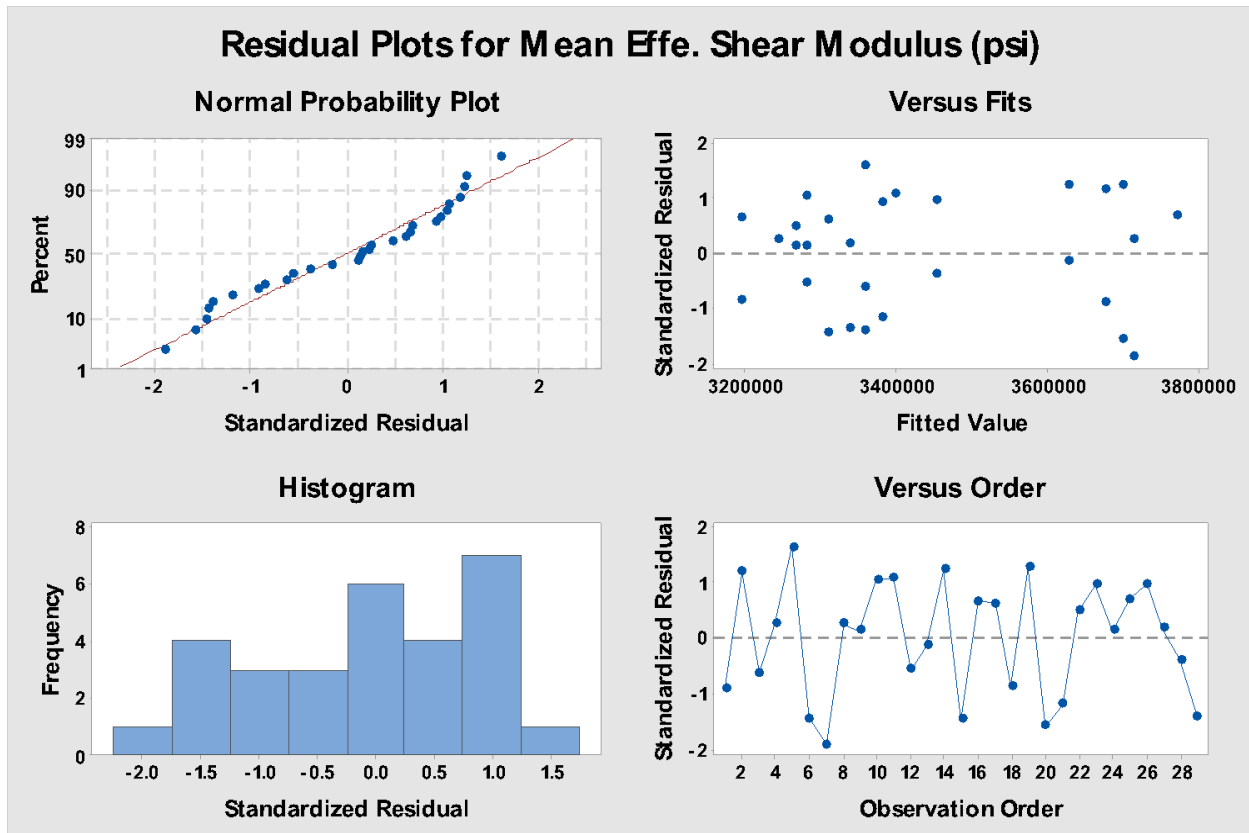
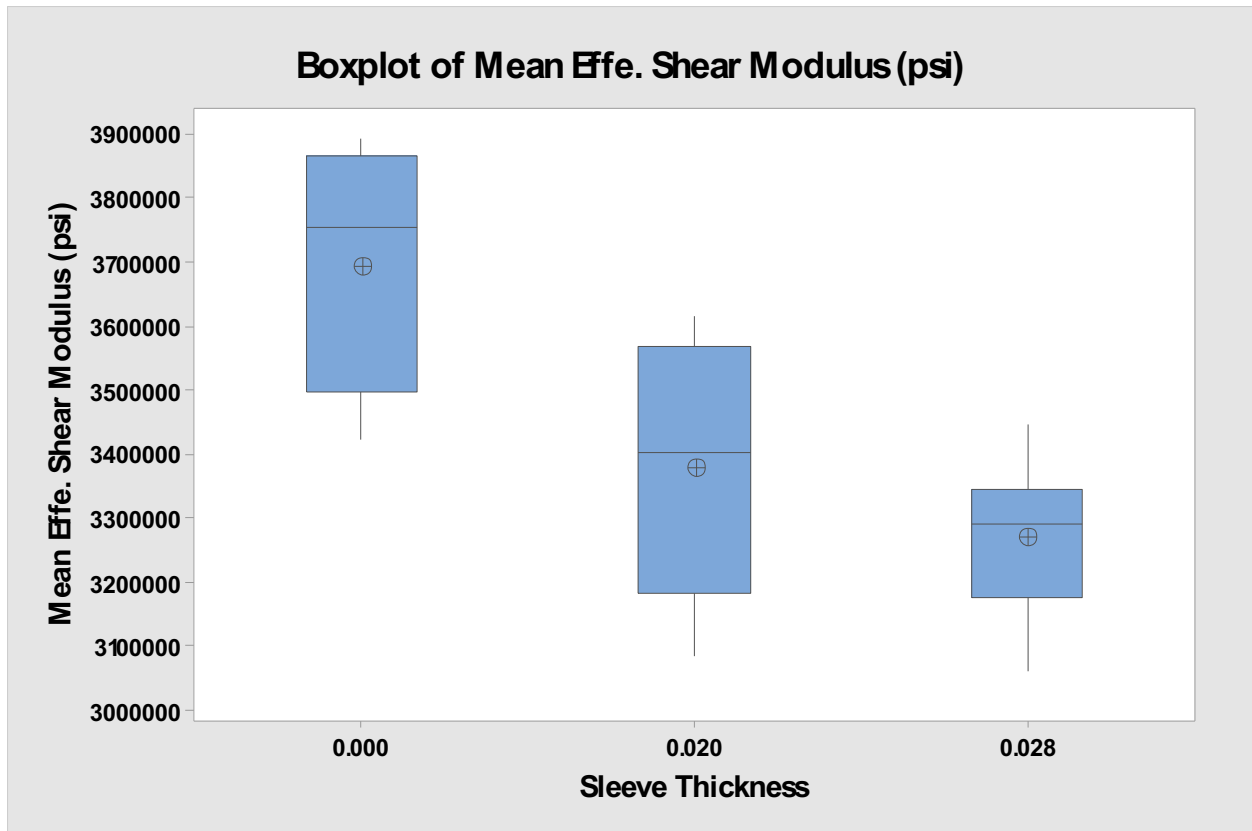


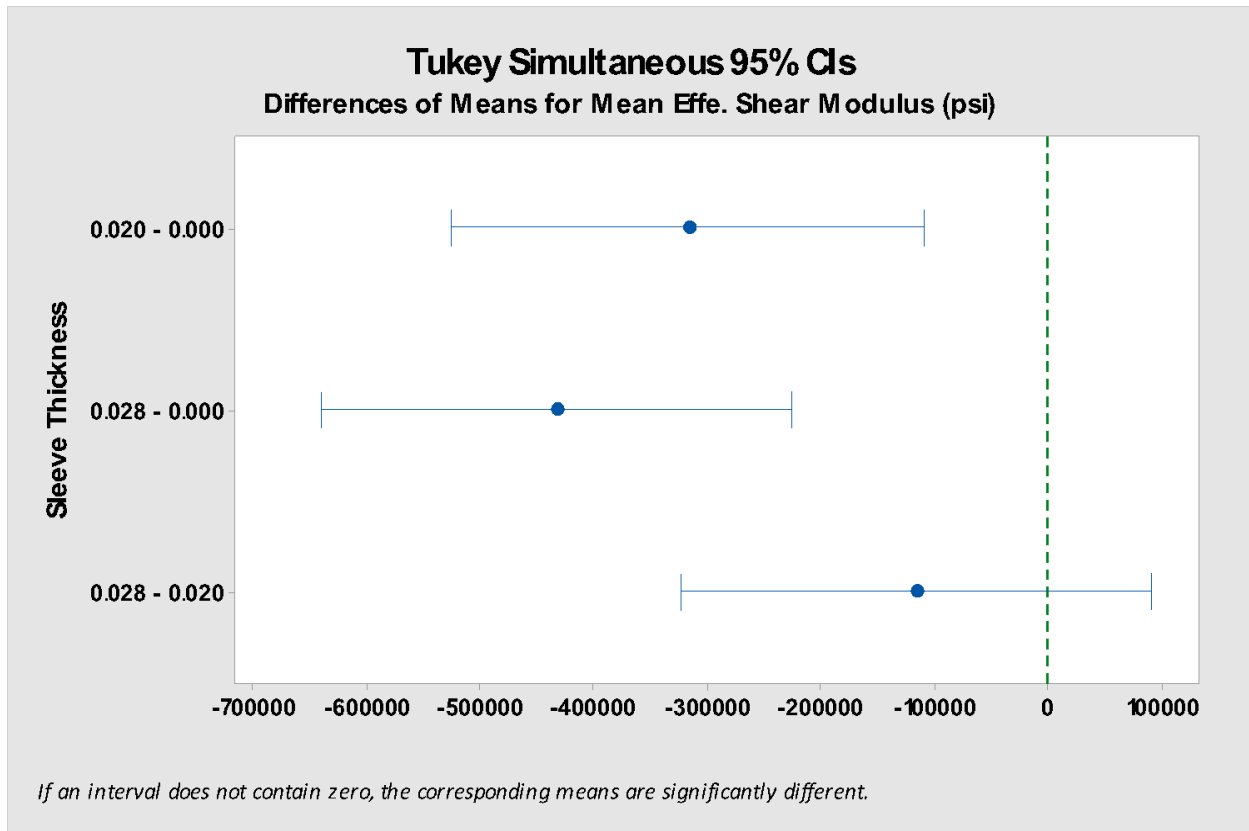
Figure 7.22 Residual plots for shear modulus of pre impact torsion samples.

Based on the normal probability plot of standardized residuals, the data appeared to come from a normal population. There appeared to be a cubic line formation through the normal line. This did not appear to be a cause for concern. This normality was verified quantitatively in a subsequent step. Based on the standardized residuals vs. fits graph, the data appeared to have equal variance. The frequency vs. standardized residual histogram showed values between -2 and 1.5. Therefore, there did not appear to be a cause for concern in this plot.



*Figure 7.23: Boxplot of shear modulus for each sleeve thickness factor level.*

Based on the plot of effective modulus vs. sleeve thickness, a correlation could be determined. As the sleeve thickness increased (with the 0.000 thickness being the sample with non sleeve condition), the effective modulus decreased. Variance appeared to decrease from the 0.000 and 0.020 sleeve thickness factor levels to the 0.028 sleeve thickness factor level.



**Tukey Pairwise Comparisons: Response = Mean Effe. Shear Modulus (psi), Term = Sleeve Thicknes**

Grouping Information Using the Tukey Method and 95% Confidence

Sleeve Thickness	N	Mean	Grouping
0.000	9	3697966	A
0.020	10	3380849	B
0.028	10	3264860	B

Means that do not share a letter are significantly different.

*Figure 7.24: Tukey pairwise comparisons of shear modulus for the sleeve thickness factor levels.*

The Tukey pairwise comparison of effective modulus vs. sleeve thickness shows the 0.000 factor level as coming from a different group than the 0.020 and 0.028 sleeve thickness factor levels, which were statistically similar.

### 7.7.2 Composite Layer Data Analysis

The composite layer modulus was calculated in an effort to isolate the effective modulus contribution of the composite material to the sample geometry. Assumptions were made regarding sleeve material shear modulus based on published data. The geometry of each sample was calculated individually to determine an accurate composite material property. The shear modulus and cross sectional area of the adhesive were not considered, as the area of the adhesive was insignificant compared to the sleeve and composite layer.

Design type: Multifactor, mixed effects.

Effect type:

Batch: Random, since the batches in the model were assumed to represent a greater population.

Sleeve thickness: Fixed, since it was assumed that if the experiment were run again, the same thicknesses would be used.

## General Linear Model: Composite Shear Modulus (psi) versus Batch, Sleeve Thickness (in)

Method

Factor coding (-1, 0, +1)

Factor Information

Factor	Type	Levels	Values
Batch	Random	5	1, 2, 3, 4, 5
Sleeve Thickness (in)	Fixed	3	0.000, 0.020, 0.028

Analysis of Variance

Source	DF	Adj SS	Adj MS	F-Value	P-Value
Batch	4	2.65739E+16	6.64348E+15	1.09	0.386
Sleeve Thickness (in)	2	1.15372E+18	5.76858E+17	94.64	0.000
Error	22	1.34092E+17	6.09508E+15		
Lack-of-Fit	8	3.59210E+16	4.49012E+15	0.64	0.733
Pure Error	14	9.81709E+16	7.01221E+15		
Total	28	1.34956E+18			

Model Summary

S	R-sq	R-sq(adj)	R-sq(pred)
78071020	90.06%	87.35%	83.06%

*Figure 7.25: General linear model output of composite layer shear modulus for all samples.*

Based on the analysis, the sleeve thickness factor appeared significant.

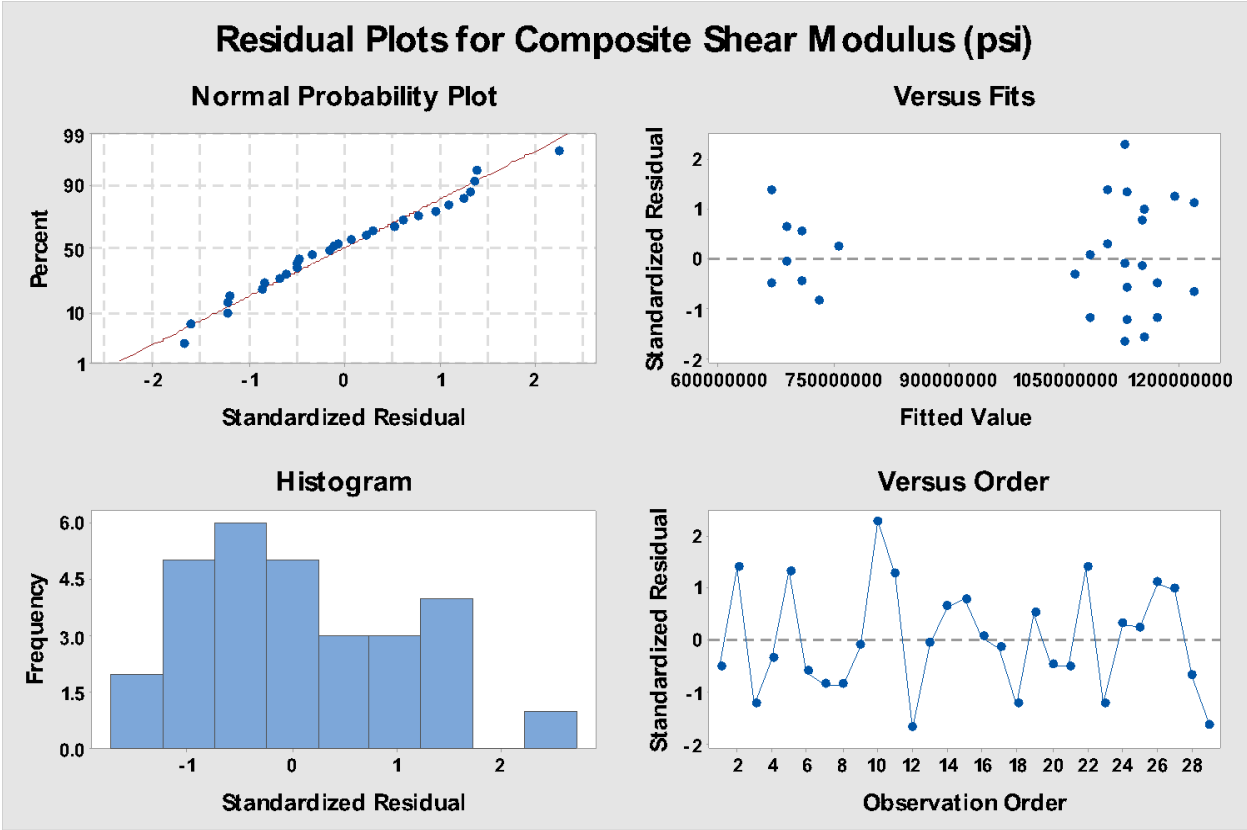


Figure 7.26: Residual plots for composite shear modulus of all samples.

Based on the normal probability plot of standardized residuals, the data appeared to come from a normal population. There appeared to be a cubic line formation through the normal line. This did not appear to be a cause for concern. This normality was verified quantitatively in a subsequent step. Based on the standardized residuals vs. fits graph, the data appeared to have equal variance. The frequency vs. standardized residual histogram showed values between -1 and 2. Therefore, there did not appear to be a cause for concern in this plot.

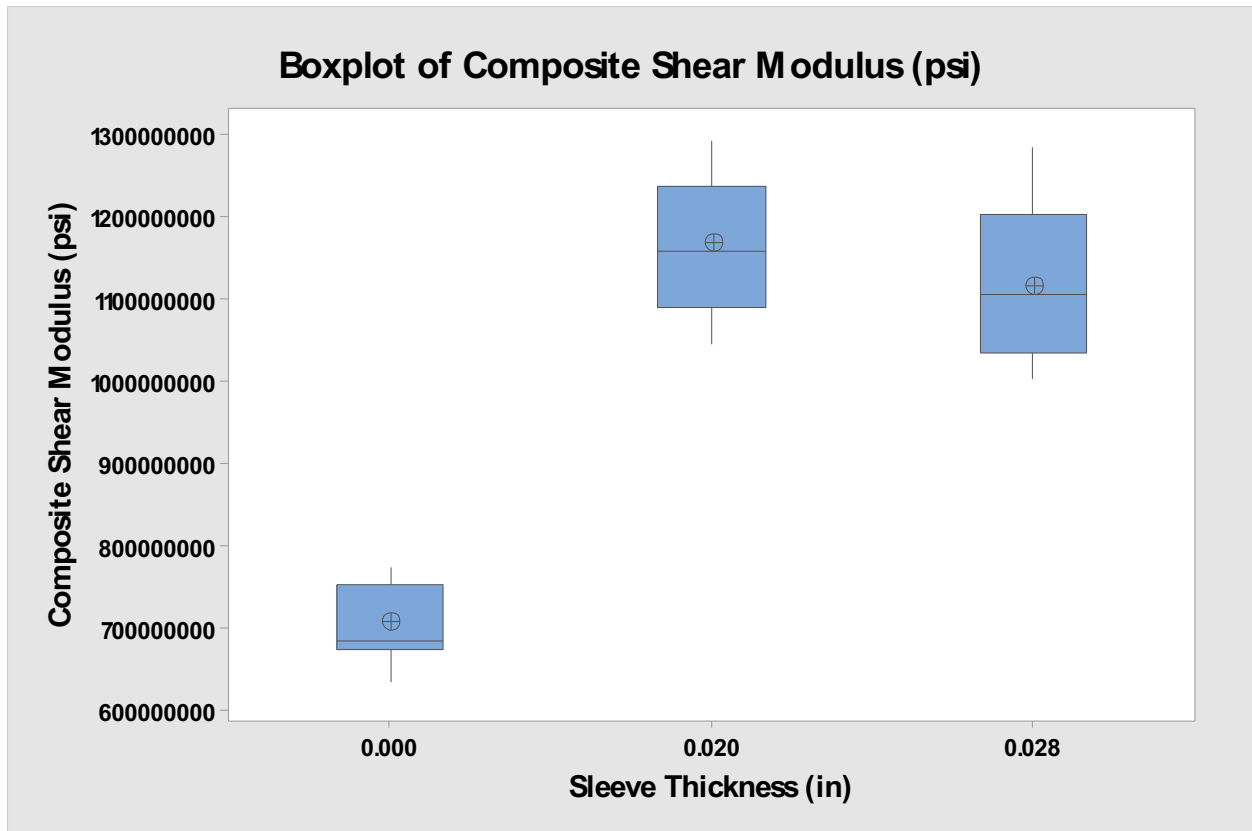
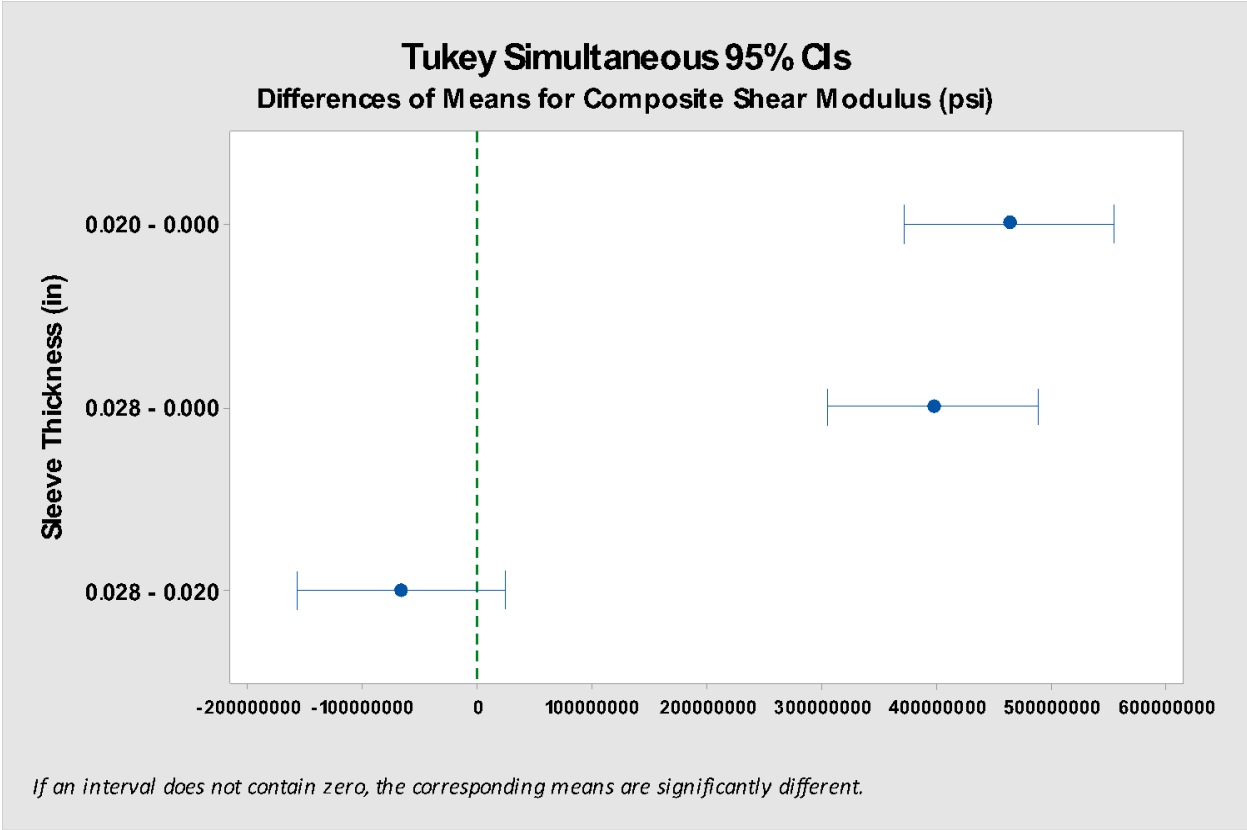


Figure 7.27: Boxplot of composite shear modulus for each sleeve thickness factor level.

Based on the plot of effective modulus vs. sleeve thickness, a correlation could be determined. As the sleeve thickness increased (with the 0.000 thickness being the sample with non sleeve condition), the composite layer shear modulus increased. Variance appeared to increase from the 0.000 sleeve thickness factor level to the 0.020 and 0.028 sleeve thickness factor levels.



**Tukey Pairwise Comparisons: Response = Composite Shear Modulus (psi), Term = Sleeve Thickness**

Grouping Information Using the Tukey Method and 95% Confidence

Sleeve Thickness (in)	N	Mean	Grouping
0.020	10	1172967984	A
0.028	10	1106784322	A
0.000	9	710023716	B

Means that do not share a letter are significantly different.

Figure 7.28: Tukey pairwise comparisons of shear modulus for the sleeve thickness factor levels.

The Tukey pairwise comparison of effective modulus vs. sleeve thickness shows the 0.000 factor level as coming from a different group than the 0.020 and 0.028 sleeve thickness factor levels, which were statistically similar.

### 7.7.3 Pre Impact Tension Data Analysis

Data was entered automatically from the MTS tensile tester at a rate of 10Hz. Crosshead travel and crosshead load were recorded into a comma delimited excel spreadsheet by default after each test. Original test length and crosshead travel were used to determine nominal strain. Stress was determined using head load and sample geometry. Sample geometry was corrected based on sample shaft outer diameter to account for slight variation in fiber reinforced composite thickness due to manufacturing processes.

Axial stress in a tube was defined:

$$\pi = \frac{F}{A} \quad (8.20)$$

where:

$\pi$  = Axial stress in the tube, [psi],

F = Axial force on the tube, [lbf], and

A = Cross sectional area of the tube [ $\text{in}^2$ ].

Cross sectional area of the tube was defined:

$$A = \pi \frac{D^2 - d^2}{4} \quad (8.21)$$

where:

D = Outer diameter of the tube, [in], and

d = Inner diameter of the tube, [in].

A stress/strain curve was created based on the values. A bilinear trend was noted on 27 of the 29 stress/strain curves. This bilinear trend was determined to be typical for some composite tensile

sample curves. (ASTM, 2014, para. 14) Stiffness was typically calculated based on the slope on the left side of the transition point of the bilinear curve. Due to the small degree of linearity on the left side of the transition point, the right side of the transition point was used to calculate slope and therefore effective modulus.

To form the line upon which effective modulus was calculated, a linear trend line with a non zero intercept was created. Any values that surpassed the sample yield values (occurring in the initial failure tests) were omitted to ensure that the curve only followed the elastic region of the sample. Values in the low stress region of the stress/strain curve were cropped from the dataset to highlight the upper portion of the curve. These values were cropped until the  $R^2$  value of the line depicting the data reached 0.99. This signified that the trend line described the linear region of the data to the right of the stress/strain curve transition point. The slope of the trend line was recorded as the effective modulus of the sample, and did not consider the intercept point of the line. This was due to the complex nature of the composite sleeve strain interaction, contributing to the bilinear trend.

Samples that were tested beyond their yield limits in the previous torsion tests were removed from this tension analysis. Data was analyzed using Minitab statistical data analysis software. A traditional ANOVA was calculated using a General Linear Model. Model adequacy was determined based on a standardized residual normal probability plot, and Bartlett's and Levene's tests. Factor comparisons were calculated using a Tukey test method and general trend inferences were formed based on boxplots and main effects plots.

The dataset was analyzed, and was not found to not follow a normal distribution, and had minor equal variance issues. The normal distribution p-value was found to be 0.007, and would cause for a rejection of the hypothesis that the data came from a normal distribution. Consideration was

made regarding potential outliers. A boxplot was created for effective modulus, categorized among sleeve thickness. Outliers were found among sleeve thickness factor levels 0.000 and 0.020. B5S1 and B5S4 were found to be outliers, and were removed. The following data analysis was completed after outlier removal.

Design type: Multifactor, mixed effects.

Effect type:

Batch: Random, since the batches in the model were assumed to represent a greater population.

Sleeve thickness: Fixed, since it was assumed that if the experiment were run again, the same thicknesses would be used.

## General Linear Model: Mean Effe. Tens. Modulus (psi) versus Batch, Sleeve Thickness (in)

### Method

Factor coding (-1, 0, +1)

### Factor Information

Factor	Type	Levels	Values
Batch	Random	5	1, 2, 3, 4, 5
Sleeve Thickness (in)	Fixed	3	0.000, 0.020, 0.028

### Analysis of Variance

Source	DF	Adj SS	Adj MS	F-Value	P-Value
Batch	4	73581427872	18395356968	0.56	0.696
Sleeve Thickness (in)	2	1.60408E+12	8.02039E+11	24.32	0.000
Error	17	5.60543E+11	32973122997		
Lack-of-Fit	7	1.86431E+11	26632941672	0.71	0.665
Pure Error	10	3.74112E+11	37411249925		
Total	23	2.40235E+12			

### Model Summary

S	R-sq	R-sq(adj)	R-sq(pred)
181585	76.67%	68.43%	57.23%

*Figure 7.29: General linear model output of effective tensile modulus for pre impact tension samples.*

Based on the analysis, the sleeve thickness factor appeared significant. The batch factor did not appear to be significant.

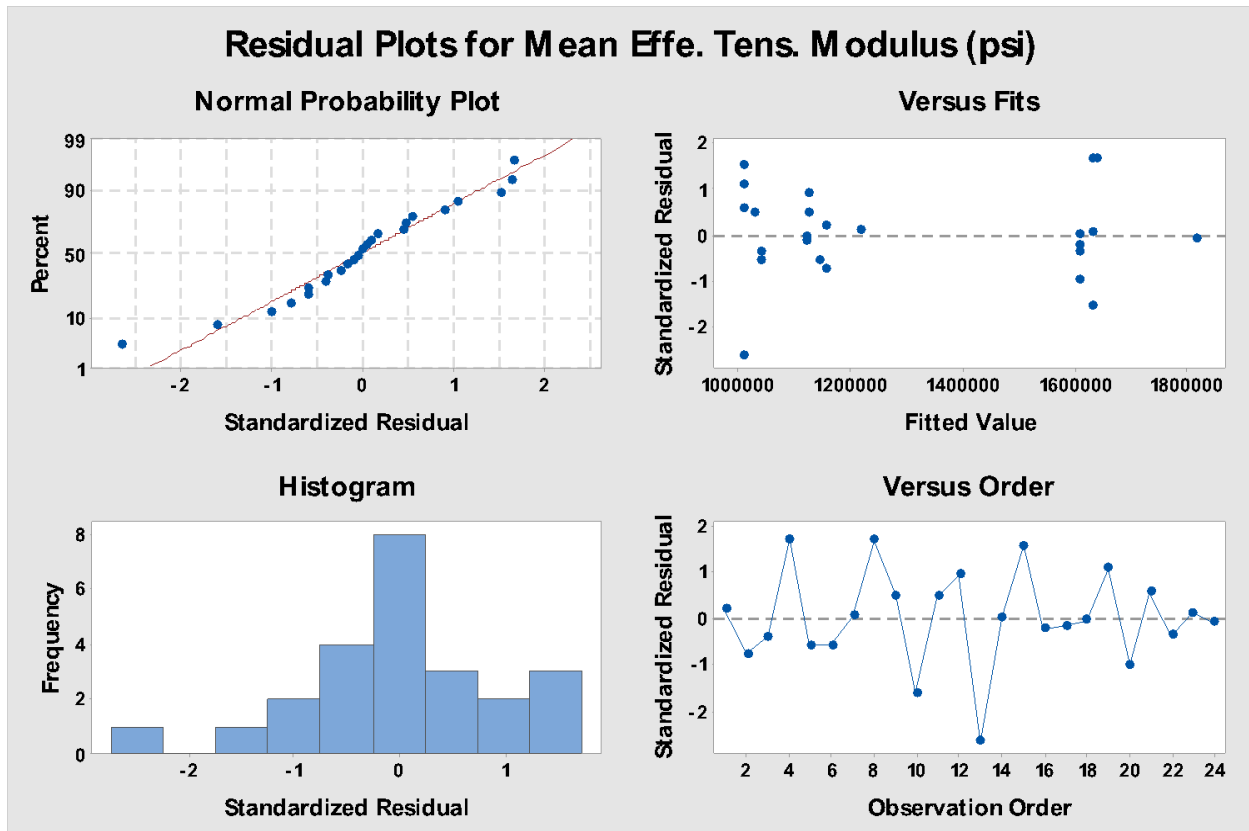
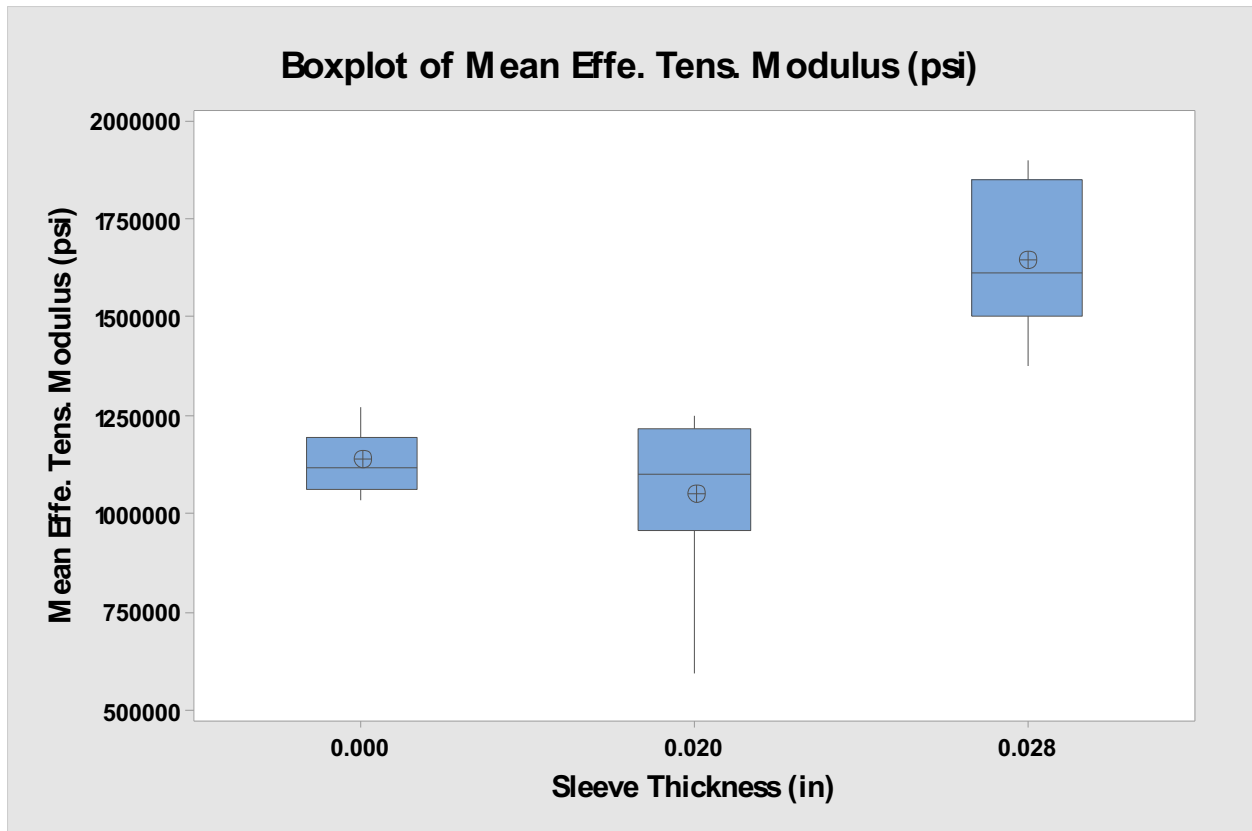


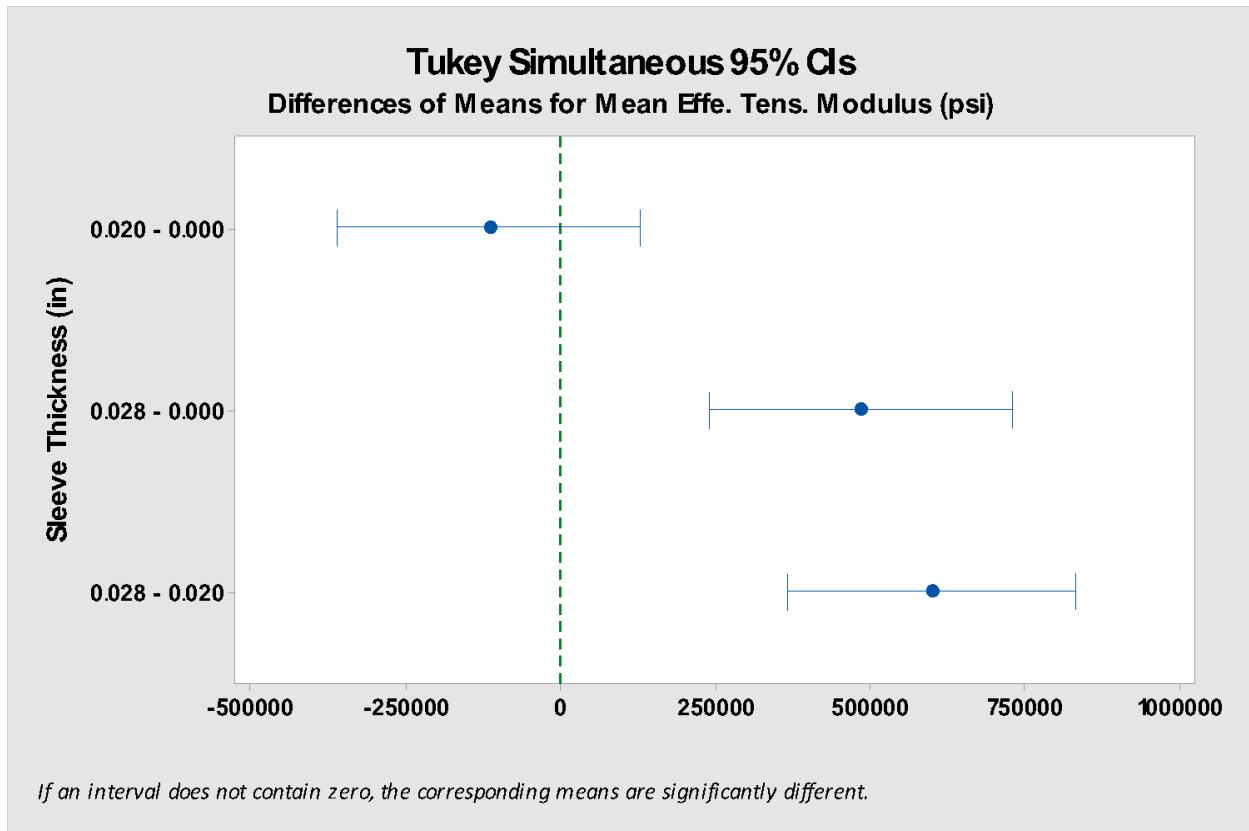
Figure 7.30: Residual plots for tensile modulus of pre impact tension samples.

Based on the normal probability plot of standardized residuals, the data appeared to come from a normal population. This normality was verified quantitatively in a subsequent step. Based on the standardized residuals vs. fits graph, the data appeared to have equal variance. The frequency vs. standardized residual histogram showed values between -2 and 1. Therefore, there did not appear to be a cause for concern in this plot.



*Figure 7.31: Boxplot of tensile modulus for each sleeve thickness factor level.*

Based on the plot of effective modulus vs. sleeve thickness, a correlation could be determined. As the sleeve thickness increased (with the 0.000 thickness being the sample with non sleeve condition), the effective modulus increased. Variance appeared to increase as sleeve thickness increases as well.



**Tukey Pairwise Comparisons: Response = Mean Effe. Tens. Modulus (psi), Term = Sleeve Thicknes**

Grouping Information Using the Tukey Method and 95% Confidence

Sleeve Thickness (in)	N	Mean	Grouping
0.028	9	1661468	A
0.000	7	1176014	B
0.020	8	1060560	B

Means that do not share a letter are significantly different.

*Figure 7.32: Tukey pairwise comparisons of tensile modulus for the sleeve thickness factor levels.*

The Tukey pairwise comparison of effective modulus vs. sleeve thickness shows the 0.00 and 0.020 thickness factor levels as coming from a different group as the 0.028 sleeve thickness factor level samples.

#### 7.7.4 Impact Data Analysis

Data was collected based on the difference between original sample diameter and post impact sample diameter. Original sample diameter was collected based on average sample diameter found for pre impact tension and torsion stress calculations. Post impact sample diameter was determined using the impactor geometry used.

Impactor length was first determined, and used as an offset for further diameter calculations. The impactor was placed at the impact site, and calipers were used to measure the distance from the opposite side of the sample to the impact (facing the impact apparatus base), to the impactor base. The impactor length was subtracted to determine post impact sample diameter. Post impact sample diameter was subtracted from pre impact sample diameter to determine depression depth. This depth was used as a comparison for data analysis.

Samples that were tested beyond their yield limits in the previous torsion and tension tests were removed from this impact analysis. Data was analyzed using Minitab statistical data analysis software. A traditional ANOVA was calculated using a General Linear Model. Model adequacy was determined based on a standardized residual normal probability plot, and Bartlett's and Levene's tests. Factor comparisons were calculated using a Tukey test method and general trend inferences were formed based on boxplots and main effects plots.

Design type: Multifactor, mixed effects.

Effect type:

Batch: Random, since the batches in the model were assumed to represent a greater population.

Sleeve thickness: Fixed, since it was assumed that if the experiment were run again, the same thicknesses would be used.

**General Linear Model: Depression Depth (in) versus Batch, Sleeve Thickness (in)**

Method

Factor coding (-1, 0, +1)

Factor Information

Factor	Type	Levels	Values
Batch	Random	5	1, 2, 3, 4, 5
Sleeve Thickness (in)	Fixed	3	0.000, 0.020, 0.028

Analysis of Variance

Source	DF	Adj SS	Adj MS	F-Value	P-Value
Batch	4	0.002969	0.000742	0.92	0.477
Sleeve Thickness (in)	2	0.017774	0.008887	11.01	0.001
Error	16	0.012915	0.000807		
Lack-of-Fit	7	0.002158	0.000308	0.26	0.956
Pure Error	9	0.010757	0.001195		
Total	22	0.038918			

Model Summary

S	R-sq	R-sq(adj)	R-sq(pred)
0.0284110	66.81%	54.37%	32.42%

*Figure 7.33: General linear model output of depression depth for all samples.*

Based on the analysis, the sleeve thickness factor appeared significant.

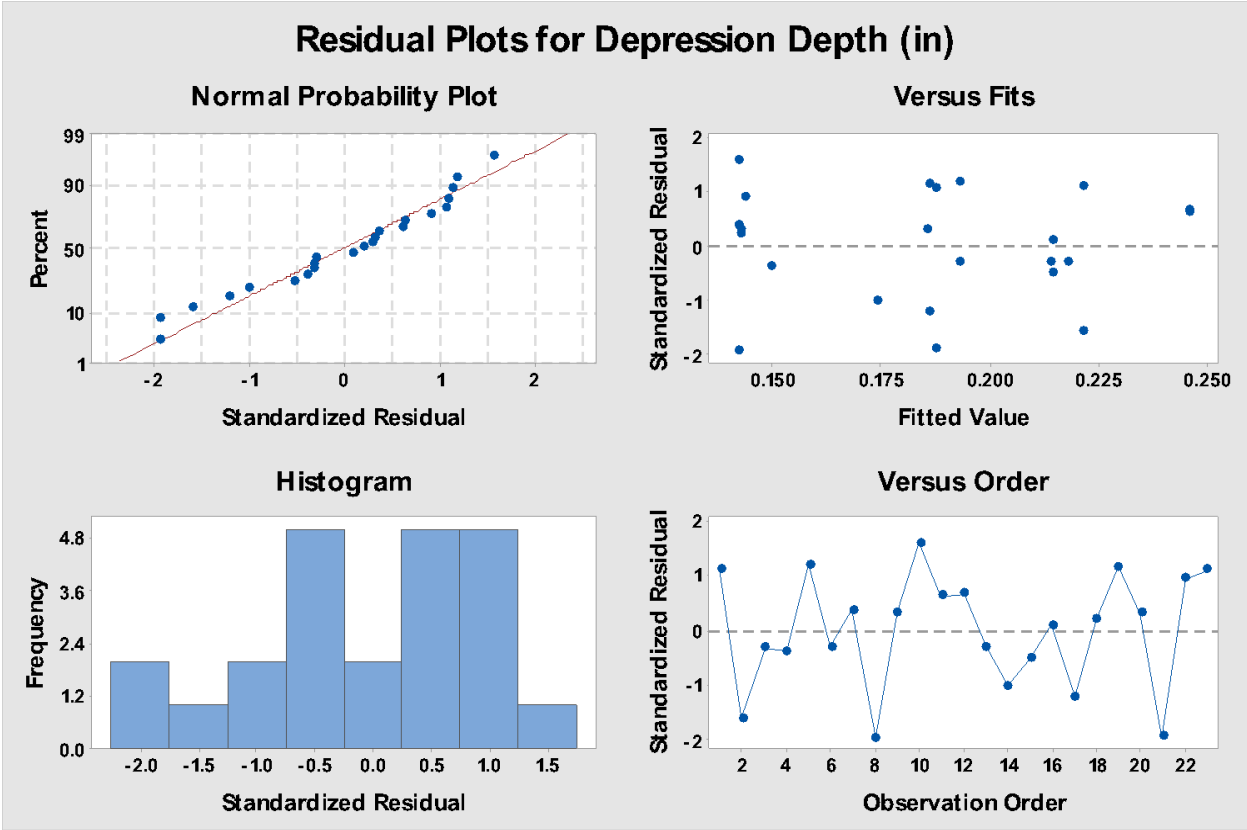
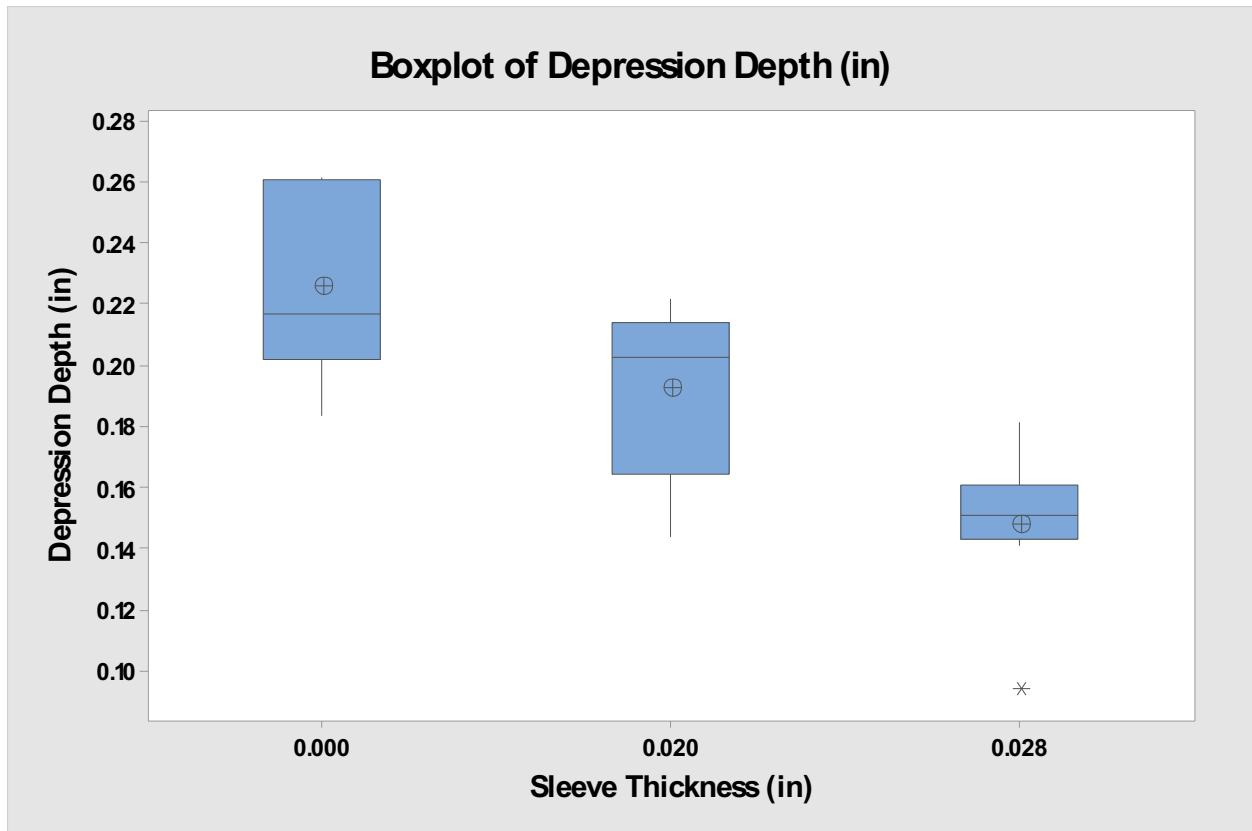


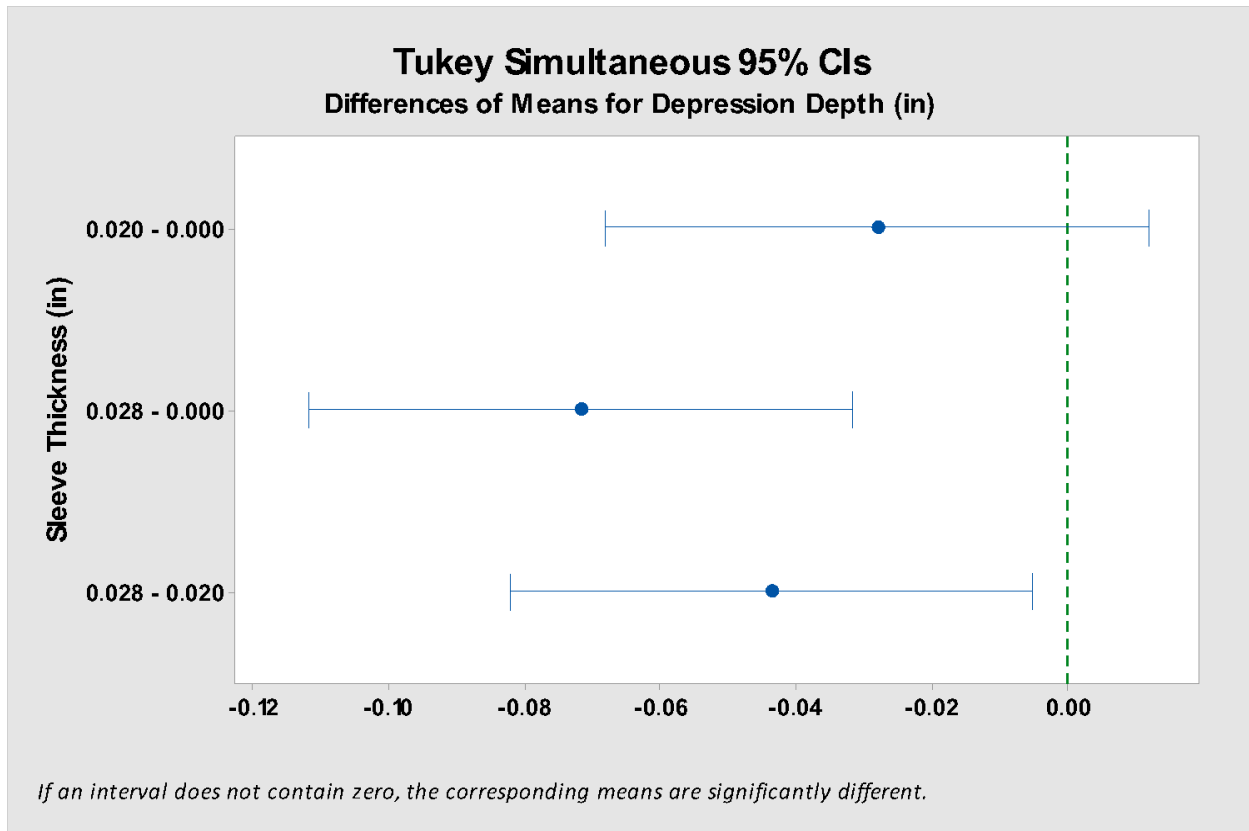
Figure 7.34: Residual plots for depression depth of all samples.

Based on the normal probability plot of standardized residuals, the data appeared to come from a normal population. There appeared to be a cubic line formation through the normal line. This did not appear to be a cause for concern. This normality was verified quantitatively in a subsequent step. Based on the standardized residuals vs. fits graph, the data appeared to have equal variance. The frequency vs. standardized residual histogram showed values between -2 and 1.5. Therefore, there did not appear to be a cause for concern in this plot.



*Figure 7.35: Boxplot of depression depth for each sleeve thickness factor level.*

Based on the plot of Depression depth vs. sleeve thickness, a correlation could be determined. As the sleeve thickness increased (with the 0.000 thickness being the sample with non sleeve condition), the depression depth decreased. Variance appeared to decrease as the sleeve thickness factor level increased.



**Tukey Pairwise Comparisons: Response = Depression Depth (in), Term = Sleeve Thickness (in)**

Grouping Information Using the Tukey Method and 95% Confidence

Sleeve Thickness (in)	N	Mean	Grouping
0.000	7	0.222134	A
0.020	8	0.194099	A
0.028	8	0.150420	B

Means that do not share a letter are significantly different.

*Figure 7.36: Tukey pairwise comparisons of depression depth for the sleeve thickness factor levels.*

The Tukey pairwise comparison of Depression depth vs. sleeve thickness shows the non sleeve and 0.020 sleeve thickness factor levels as coming from a different group as the 0.028 sleeve thickness factor levels.

### **7.7.5 Post Impact Torsion Data Analysis**

Post-impact torsion data analysis occurred in a similar fashion as the pre impact torsion test data analysis. No changes were made to the data collection methods to produce accurate difference measurements.

Samples that were tested beyond their yield limits in the previous torsion and tension tests were removed from this torsion analysis. Data was analyzed using Minitab statistical data analysis software. A traditional ANOVA was calculated using a General Linear Model. Model adequacy was determined based on a standardized residual normal probability plot, and Bartlett's and Levene's tests. Factor comparisons were calculated using a Tukey test method and general trend inferences were formed based on boxplots and main effects plots.

Design type: Multifactor, mixed effects.

Effect type:

Batch: Random, since the batches in the model were assumed to represent a greater population.

Sleeve thickness: Fixed, since it was assumed that if the experiment were run again, the same thicknesses would be used.

## General Linear Model: Mean Effe. Shear Modulus (psi) versus Batch, Sleeve Thickness (in)

Method

Factor coding (-1, 0, +1)

### Factor Information

Factor	Type	Levels	Values
Batch	Random	5	1, 2, 3, 4, 5
Sleeve Thickness (in)	Fixed	3	0.000, 0.020, 0.028

### Analysis of Variance

Source	DF	Adj SS	Adj MS	F-Value	P-Value
Batch	4	96401247129	24100311782	0.23	0.920
Sleeve Thickness (in)	2	1.28394E+13	6.41969E+12	60.27	0.000
Error	16	1.70425E+12	1.06516E+11		
Lack-of-Fit	7	2.53237E+11	36176653084	0.22	0.969
Pure Error	9	1.45101E+12	1.61224E+11		
Total	22	1.68642E+13			

### Model Summary

S	R-sq	R-sq(adj)	R-sq(pred)
326367	89.89%	86.10%	80.51%

*Figure 7.37: General linear model output of effective shear modulus for post impact torsion samples.*

Based on the analysis, the sleeve thickness factor appeared significant.

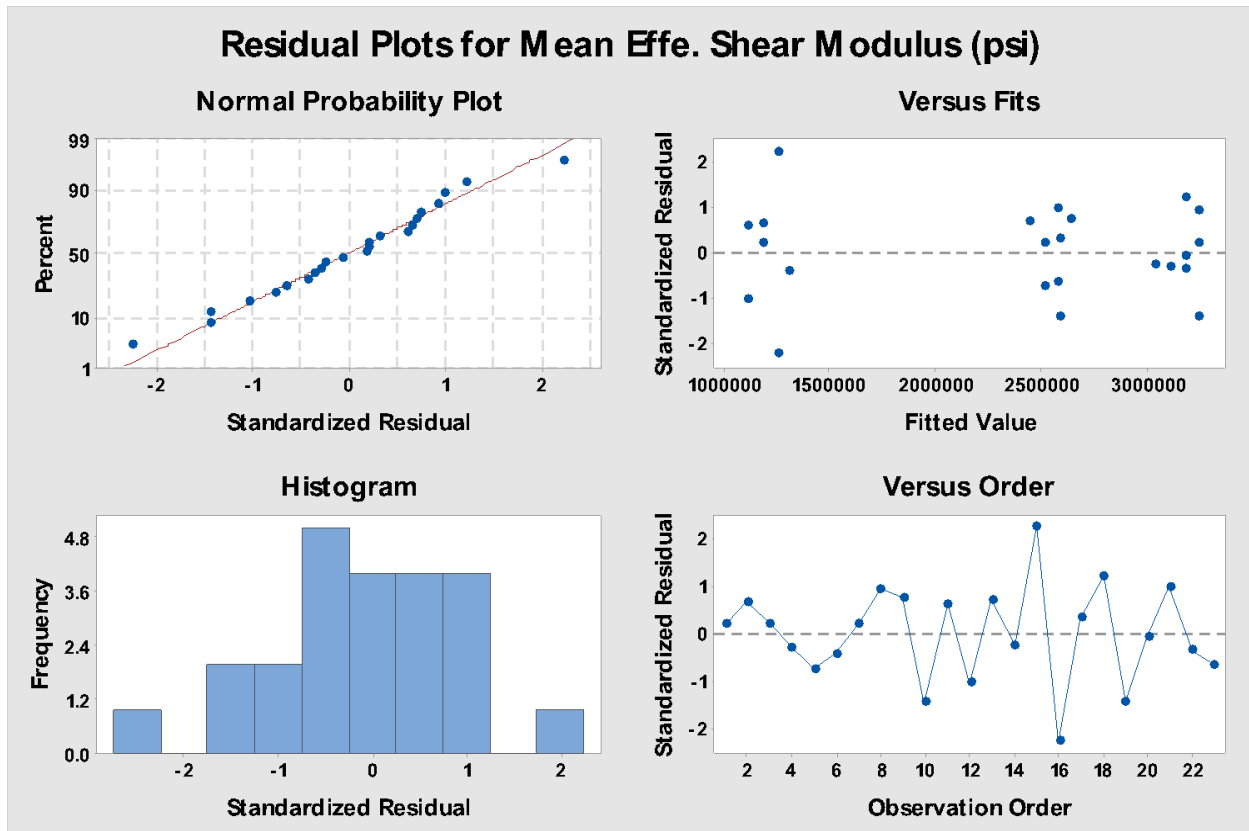


Figure 7.38: Residual plots for shear modulus of post impact torsion samples.

Based on the normal probability plot of standardized residuals, the data appeared to come from a normal population. There appeared to be a cubic line formation through the normal line. This did not appear to be a cause for concern. This normality was verified quantitatively in a subsequent step. Based on the standardized residuals vs. fits graph, the data appeared to have equal variance. The frequency vs. standardized residual histogram showed values between -2 and 2. Therefore, there did not appear to be a cause for concern in this plot.

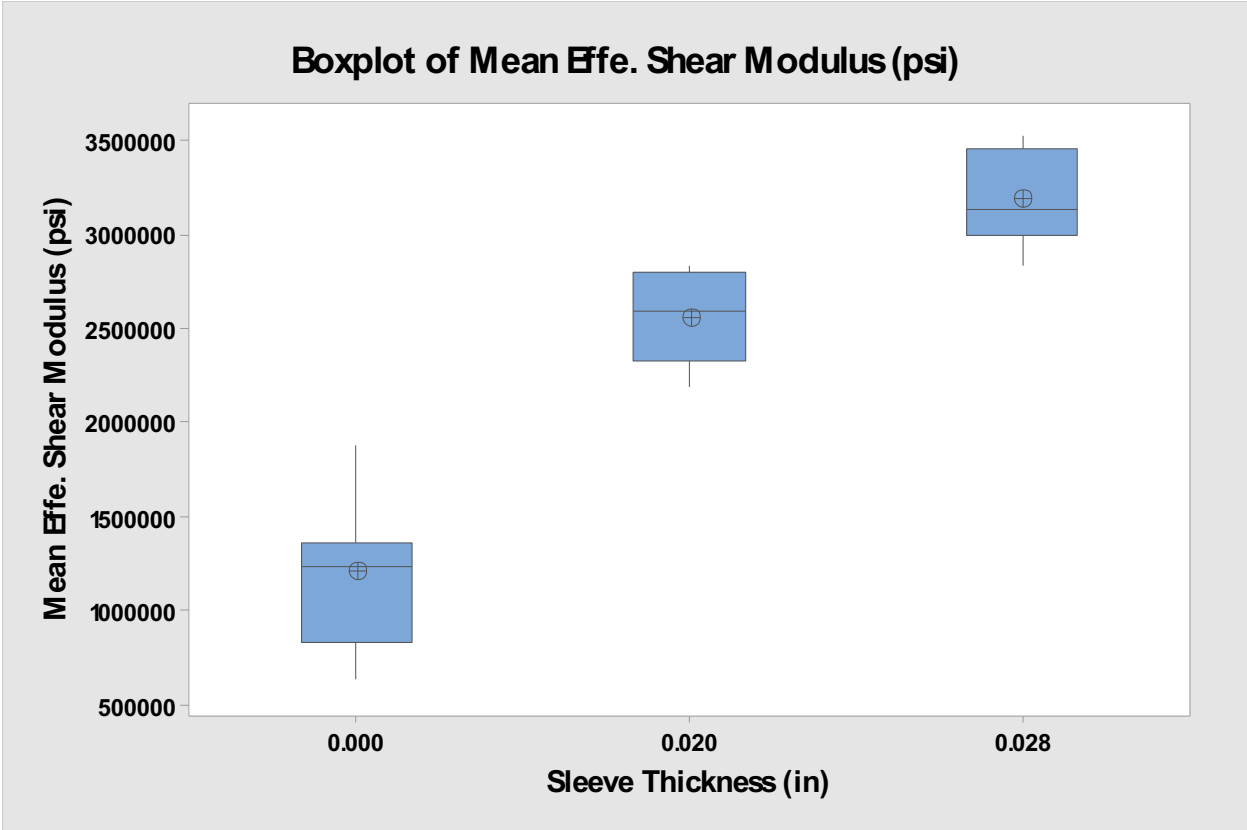
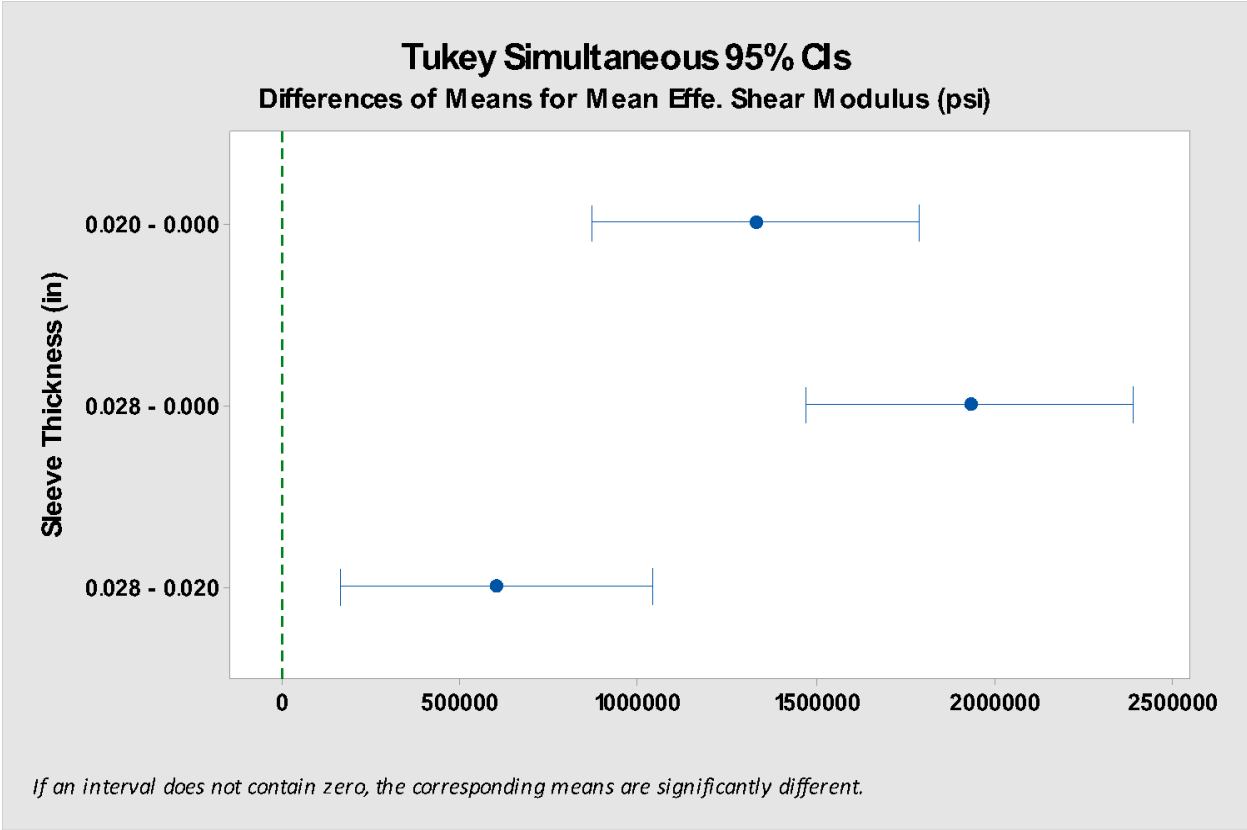


Figure 7.39: Boxplot of shear modulus for each sleeve thickness factor level.

Based on the plot of effective modulus vs. sleeve thickness, a correlation could be determined. As the sleeve thickness increased (with the 0.000 thickness being the sample with non sleeve condition), the effective modulus increased. Variance appeared to remain the same as sleeve thickness factor level increased.



**Tukey Pairwise Comparisons: Response = Mean Effe. Shear Modulus (psi), Term = Sleeve Thicknes**

Grouping Information Using the Tukey Method and 95% Confidence

Sleeve Thickness (in)	N	Mean	Grouping
0.028	8	3152127	A
0.020	8	2550974	B
0.000	7	1221475	C

Means that do not share a letter are significantly different.

*Figure 7.40: Tukey pairwise comparisons of shear modulus for the sleeve thickness factor levels.*

The Tukey pairwise comparison of effective modulus vs. sleeve thickness shows the 0.000, 0.020, and 0.028 sleeve thickness factor levels as coming from three separate groups, and were significantly different.

### 7.7.6 Post Impact Tension Data Analysis

Post impact tension data analysis occurred in a similar fashion as the pre impact tension test data analysis. No changes were made to the data collection methods to produce accurate contrast measurements.

Data was analyzed using Minitab statistical data analysis software. A traditional ANOVA was calculated using a General Linear Model. Model adequacy was determined based on a standardized residual normal probability plot, and Bartlett's and Levene's tests. Factor comparisons were calculated using a Tukey test method and general trend inferences were formed based on boxplots and main effects plots.

The dataset was analyzed, and the sleeve thickness factor was found to not be significant. The sleeve thickness factor was found to not be significant. The sleeve thickness factor p-level was found to be 0.230, and the batch factor was found to be 0.111, showing the batch factor as more significant than the sleeve thickness factor. Consideration was made regarding potential outliers. A boxplot was created for effective modulus, categorized among sleeve thickness. An outlier was found among 0.020 sleeve thickness factor level. B5S4 was found to be outliers, and were removed. This was found to be an outlier for the pre impact tension test as well. The following data analysis was completed after outlier removal.

Design type: Multifactor, mixed effects.

Effect type:

Batch: Random, since the batches in the model were assumed to represent a greater population.

Sleeve thickness: Fixed, since it was assumed that if the experiment were run again, the same thicknesses would be used.

**General Linear Model: Mean Effe. Tens. Modulus (psi) versus Batch, Sleeve Thickness (in)**

Method

Factor coding (-1, 0, +1)

Factor Information

Factor	Type	Levels	Values
Batch	Random	5	1, 2, 3, 4, 5
Sleeve Thickness (in)	Fixed	3	0.000, 0.020, 0.028

Analysis of Variance

Source	DF	Adj SS	Adj MS	F-Value	P-Value
Batch	4	7.36899E+11	1.84225E+11	1.50	0.262
Sleeve Thickness (in)	2	4.19486E+12	2.09743E+12	17.13	0.000
Error	12	1.46963E+12	1.22469E+11		
Lack-of-Fit	6	8.33134E+11	1.38856E+11	1.31	0.376
Pure Error	6	6.36492E+11	1.06082E+11		
Total	18	7.80320E+12			

Model Summary

S	R-sq	R-sq(adj)	R-sq(pred)
349956	81.17%	71.75%	44.61%

*Figure 7.41: General linear model output of effective tensile modulus for post impact tension samples.*

Based on the analysis, the sleeve thickness factor appeared significant.

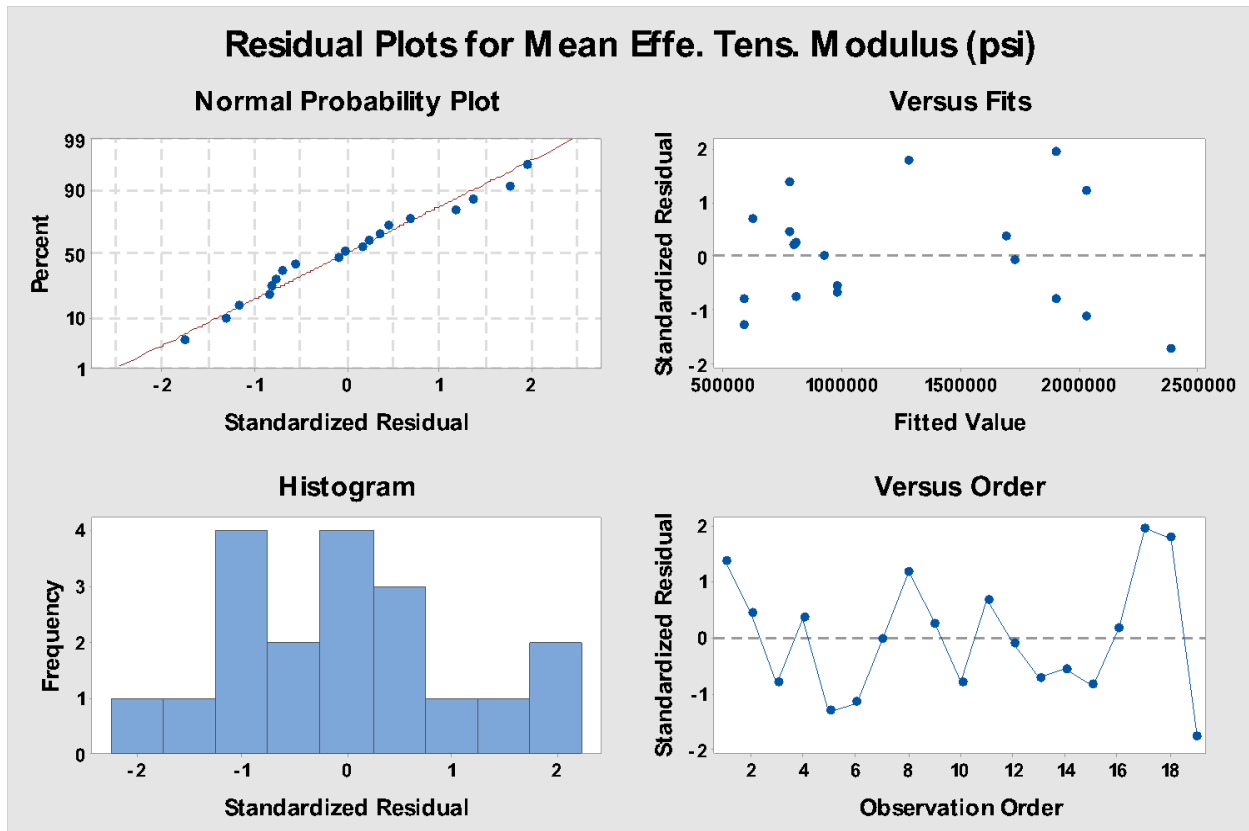


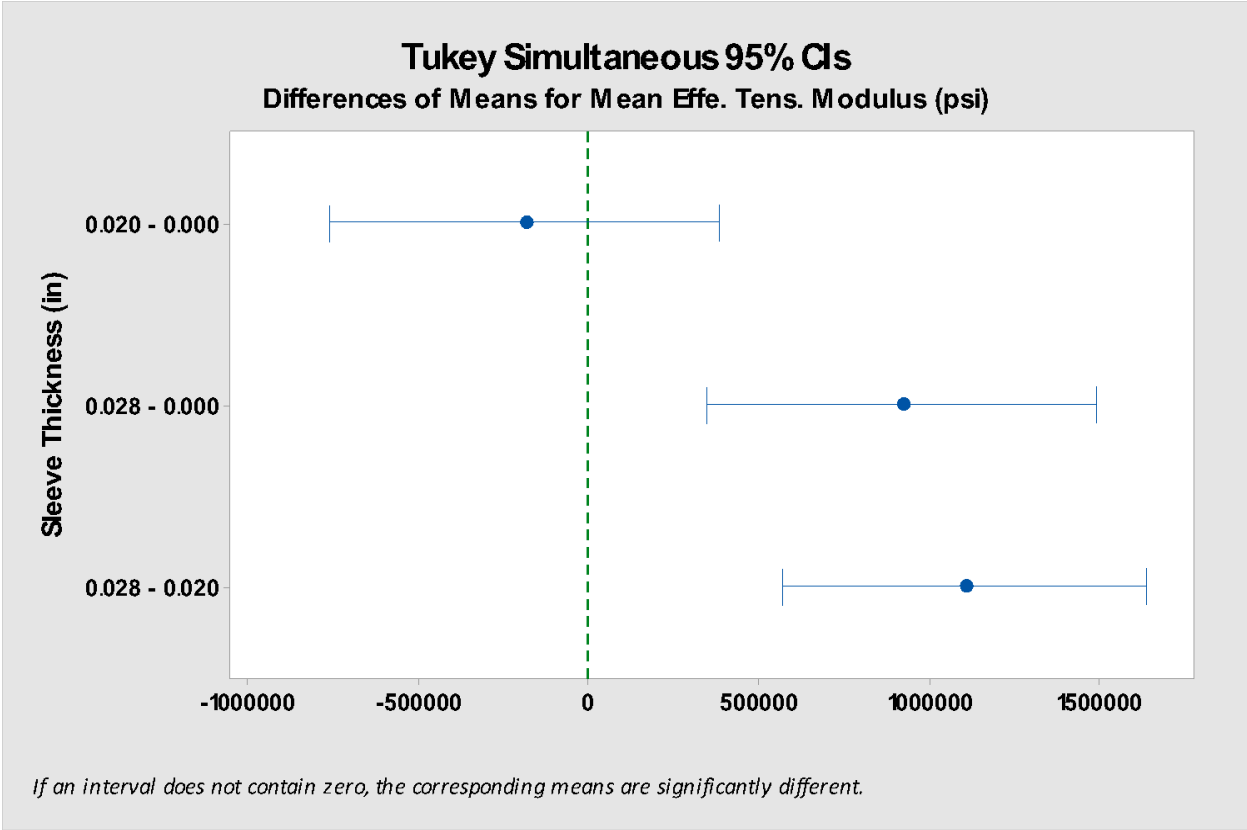
Figure 7.42: Residual plots for tensile modulus of post impact tension samples.

Based on the normal probability plot of standardized residuals, the data appeared to come from a normal population. There appeared to be a cubic line formation through the normal line. This did not appear to be a cause for concern. This normality was verified quantitatively in a subsequent step. Based on the standardized residuals vs. fits graph, the data appeared to have equal variance. The frequency vs. standardized residual histogram showed values between -2 and 2. Therefore, there did not appear to be a cause for concern in this plot.



*Figure 7.43: Boxplot of tensile modulus for each sleeve thickness factor level.*

Based on the plot of effective modulus vs. sleeve thickness, a correlation could be determined. As the sleeve thickness increased (with the 0.000 thickness being the sample with non sleeve condition), the effective modulus remained the same for the 0.000 and 0.020 sleeve thickness factor levels, and increased for the 0.028 sleeve thickness factor level. Variance appeared to increase from the 0.000 sleeve thickness factor level to the 0.020 and 0.028 sleeve thickness factor levels.



**Tukey Pairwise Comparisons: Response = Mean Effe. Tens. Modulus (psi), Term = Sleeve Thicknes**

Grouping Information Using the Tukey Method and 95% Confidence

Sleeve Thickness (in)	N	Mean	Grouping
0.028	7	1943495	A
0.000	6	1024439	B
0.020	6	839663	B

Means that do not share a letter are significantly different.

*Figure 7.44: Tukey pairwise comparisons of tensile modulus for the sleeve thickness factor levels.*

The Tukey pairwise comparison of effective modulus vs. sleeve thickness shows the 0.000 and 0.020 sleeve thickness factor levels as being similar, coming from a different group as the 0.028 sleeve thickness factor level.

### 7.7.7 Post Impact Torsion Change Data Analysis

For each sample, the post impact effective modulus was subtracted from the pre impact effective modulus and divided by the pre impact effective modulus, calculating the percent change in effective modulus due to the impact event. Two samples were found to have slightly increased in effective modulus after impact within the 0.028 sleeve thickness factor level. Though this was considered unlikely, the data was still considered as it was not found to be an outlier.

Data was analyzed using Minitab statistical data analysis software. A traditional ANOVA was calculated using a General Linear Model. Model adequacy was determined based on a standardized residual normal probability plot, and Bartlett's and Levene's tests. Factor comparisons were calculated using a Tukey test method and general trend inferences were formed based on boxplots and main effects plots.

Design type: Multifactor, mixed effects.

Effect type:

Batch: Random, since the batches in the model were assumed to represent a greater population.

Sleeve thickness: Fixed, since it was assumed that if the experiment were run again, the same thicknesses would be used.

## General Linear Model: Mean Eff. Shear Mod. % Change versus Batch, Sleeve Thickness (in)

Method

Factor coding (-1, 0, +1)

Factor Information

Factor	Type	Levels	Values
Batch	Random	5	1, 2, 3, 4, 5
Sleeve Thickness (in)	Fixed	3	0.000, 0.020, 0.028

Analysis of Variance

Source	DF	Adj SS	Adj MS	F-Value	P-Value
Batch	4	32.0	8.00	0.10	0.982
Sleeve Thickness (in)	2	13920.6	6960.32	84.04	0.000
Error	16	1325.2	82.82		
Lack-of-Fit	7	176.2	25.17	0.20	0.978
Pure Error	9	1149.0	127.67		
Total	22	17049.9			

Model Summary

S	R-sq	R-sq(adj)	R-sq(pred)
9.10066	92.23%	89.31%	85.05%

*Figure 7.45: General linear model output of effective shear modulus percent change for the torsion samples.*

Based on the analysis, the sleeve thickness factor appeared significant.

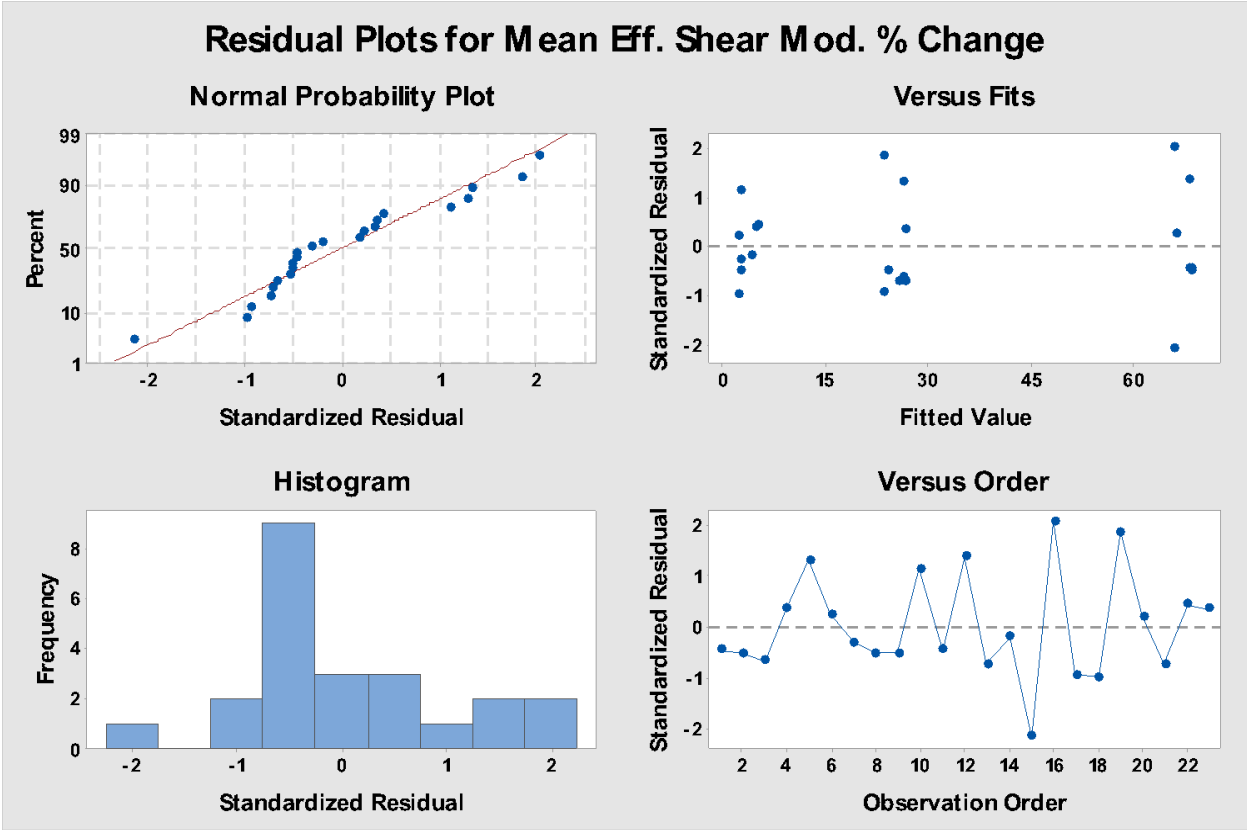
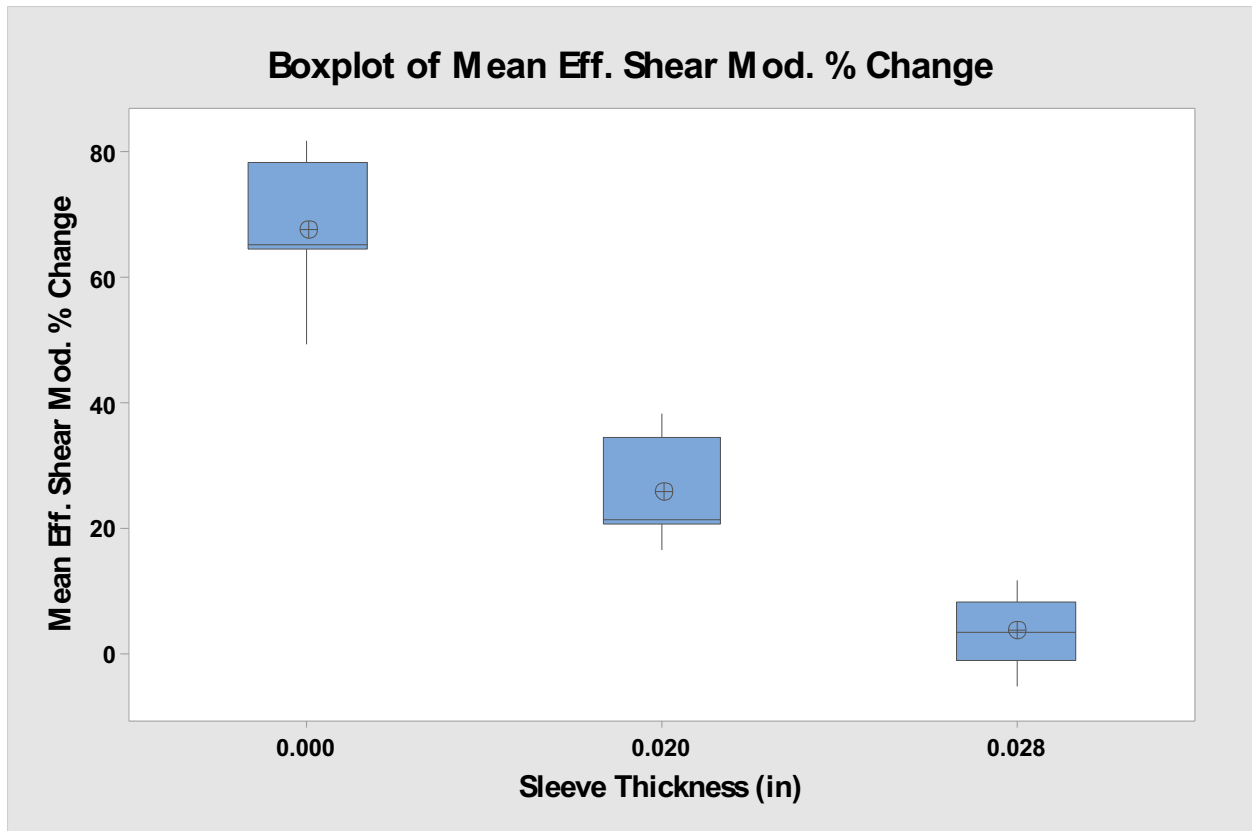


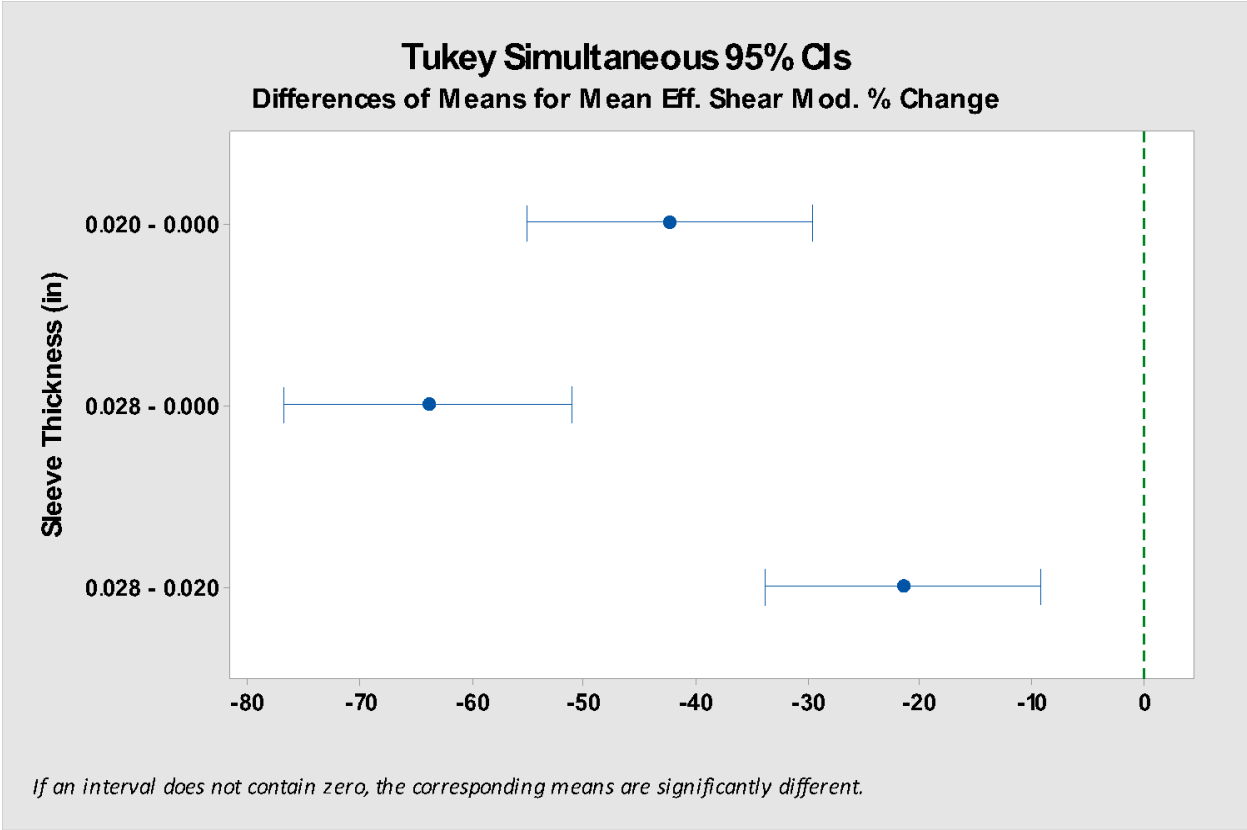
Figure 7.46: Residual plots for shear modulus percent change of torsion samples.

Based on the normal probability plot of standardized residuals, the data appeared to come from a normal population. There appeared to be a cubic line formation through the normal line. This did not appear to be a cause for concern. This normality was verified quantitatively in a subsequent step. Based on the standardized residuals vs. fits graph, the data appeared to have equal variance. The frequency vs. standardized residual histogram showed values between -2 and 2. Therefore, there did not appear to be a cause for concern in this plot.



*Figure 7.47: Boxplot of shear modulus percent change for each sleeve thickness factor level.*

Based on the plot of effective modulus vs. sleeve thickness, a correlation could be determined. As the sleeve thickness increased (with the 0.000 thickness being the sample with non sleeve condition), the effective modulus change decreased. Variance appeared to decrease slightly as the sleeve thickness factor level increased.



**Tukey Pairwise Comparisons: Response = Mean Eff. Shear Mod. % Change, Term = Sleeve Thickness**

Grouping Information Using the Tukey Method and 95% Confidence

Sleeve Thickness (in)	N	Mean	Grouping
0.000	7	67.6331	A
0.020	8	25.2753	B
0.028	8	3.7654	C

Means that do not share a letter are significantly different.

*Figure 7.48: Tukey pairwise comparisons of shear modulus percent change for the sleeve thickness factor levels.*

The Tukey pairwise comparison of effective modulus vs. sleeve thickness shows the non sleeve, 0.020 sleeve thickness, and 0.028 sleeve thickness factor levels as coming from three separate groups, and were significantly different.

### 7.7.8 Post Impact Tension Change Data Analysis

For each sample, the post impact effective modulus was subtracted from the pre-impact effective modulus and divided by the pre impact effective modulus, calculating the percent change in effective modulus due to the impact event.

The dataset was analyzed, and the sleeve thickness factor level was found to not be significant. The batch factor level was found to be more significant, which alluded to possible issues in the analysis. A boxplot was created of effective modulus vs. sleeve thickness factor, and no outliers were found. The 0.020 sleeve thickness factor level variance was found to be large relative to the other two factor levels. This appeared to be driven by the large variance of the post impact torsion 0.020 sleeve thickness factor level which was also higher than the other two sleeve thickness factor levels.

The 0.020 sleeve thickness factor level was removed, as it was shown to contribute enough variance to the model to make the sleeve thickness factor insignificant. The primary rationale behind the 0.020 sleeve thickness factor level variance is the effective modulus change between the aluminum sleeve and carbon fiber composite sleeve components, as well as the adhesive strength between the two components. The high modulus of the carbon fiber sleeve, alongside the lower modulus of the thinner aluminum sleeve, may have caused a shear event. This may have surpassed the adhesive shear strength, resulting in adhesive failure along the aluminum interface. This has been noted in the pre and post impact yield samples in the 0.020 sleeve thickness factor level.

Data was analyzed using Minitab statistical data analysis software. A traditional ANOVA was calculated using a General Linear Model. Model adequacy was determined based on a standardized residual normal probability plot, and Bartlett's and Levene's tests. Factor comparisons were calculated using a Tukey test method and general trend inferences were formed based on boxplots and main effects plots.

Design type: Multifactor, mixed effects.

Effect type:

Batch: Random, since the batches in the model were assumed to represent a greater population.

Sleeve thickness: Fixed, since it was assumed that if the experiment were run again, the same thicknesses would be used.

## General Linear Model: Mean Effe. Tens. Mod. % Change versus Batch, Sleeve Thickness (in)

Method

Factor coding (-1, 0, +1)

Factor Information

Factor	Type	Levels	Values
Batch	Random	5	1, 2, 3, 4, 5
Sleeve Thickness (in)	Fixed	2	0.000, 0.028

Analysis of Variance

Source	DF	Adj SS	Adj MS	F-Value	P-Value
Batch	4	1526	381.6	0.50	0.739
Sleeve Thickness (in)	1	4141	4140.8	5.40	0.053
Error	7	5364	766.3		
Lack-of-Fit	2	1631	815.3	1.09	0.404
Pure Error	5	3734	746.7		
Total	12	14402			

Model Summary

S	R-sq	R-sq(adj)	R-sq(pred)
27.6820	62.75%	36.15%	*

*Figure 7.49: General linear model output of effective tensile modulus percent change for tensile samples.*

Based on the analysis, no factors appear significant.

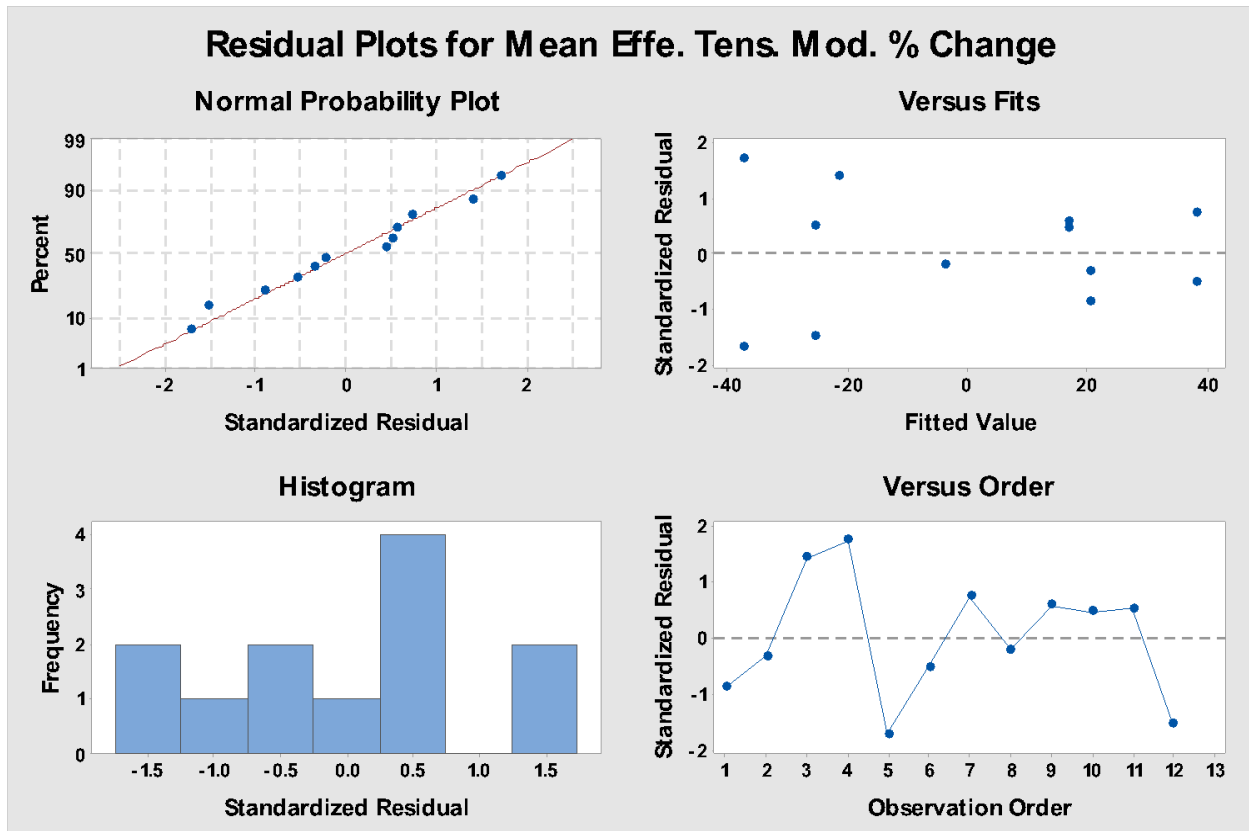
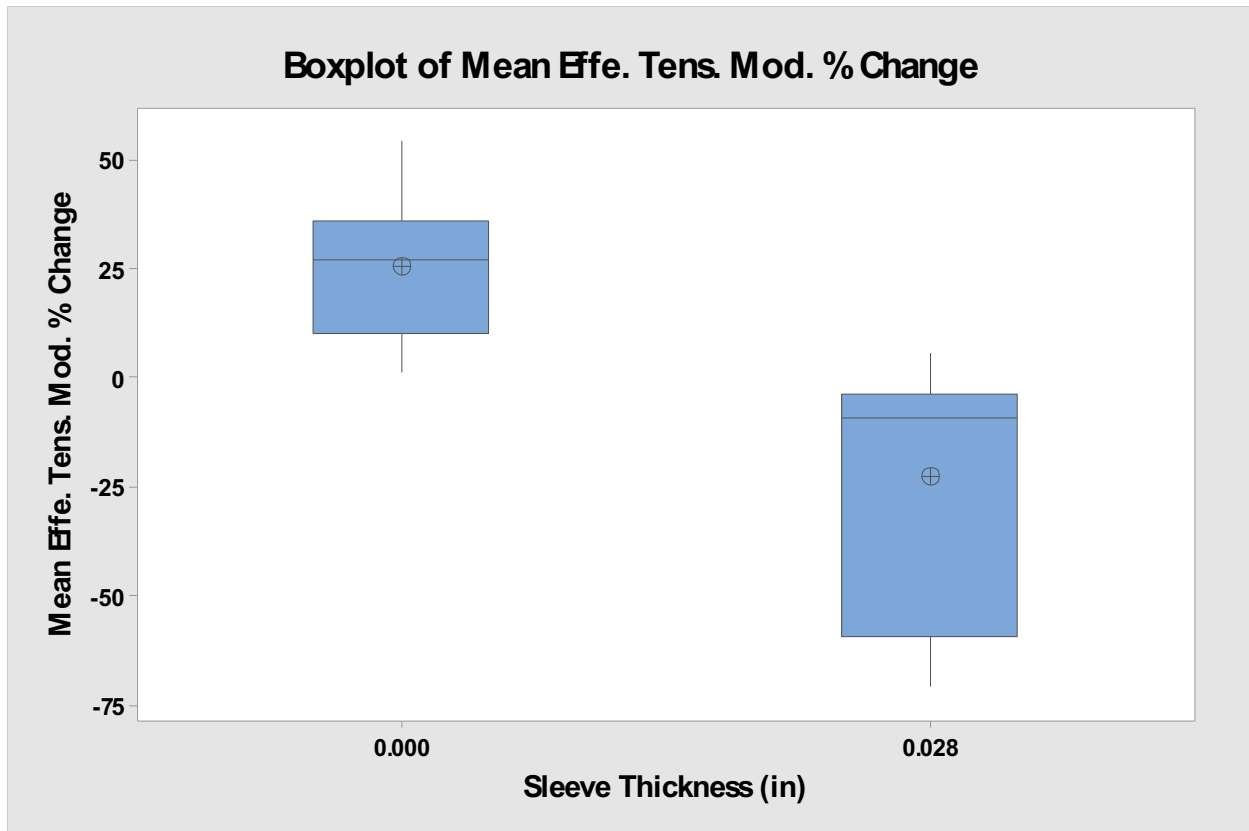


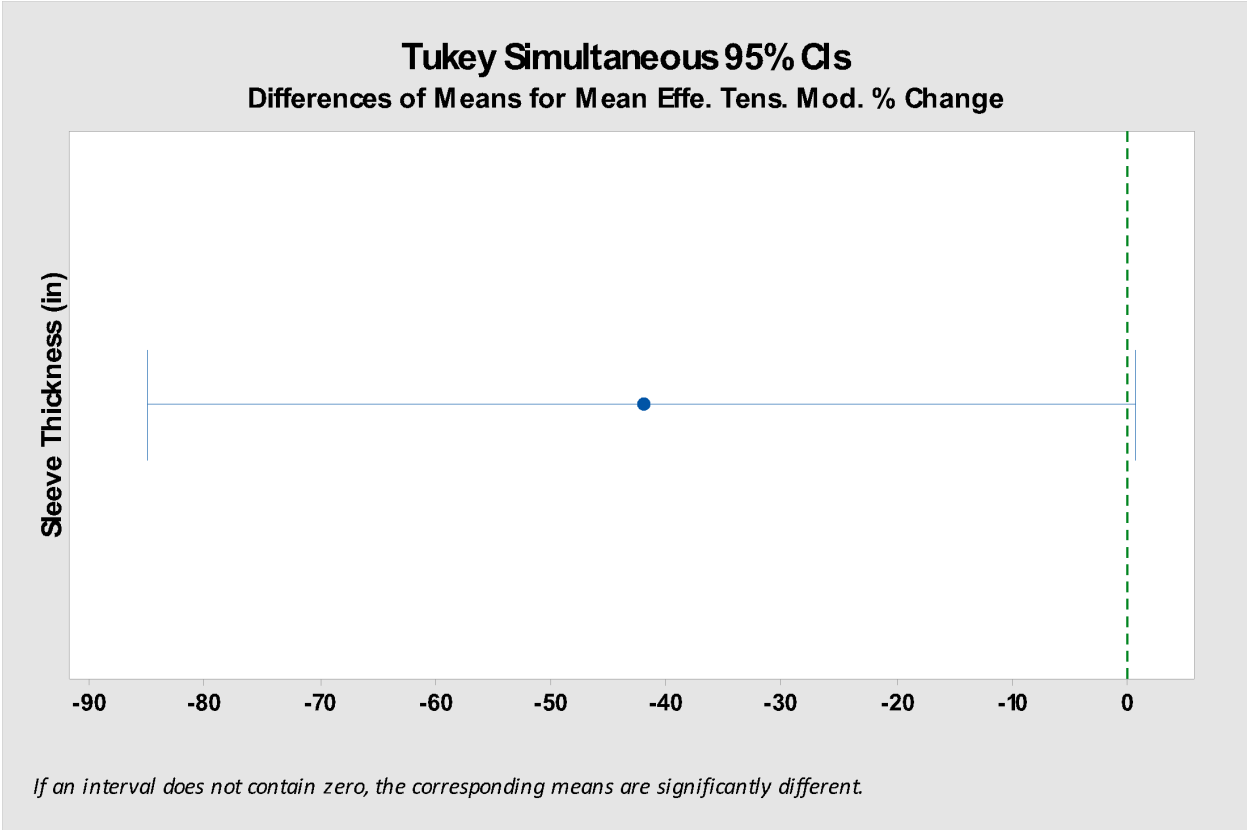
Figure 7.50: Residual plots of tensile modulus percent change of tension samples.

Based on the normal probability plot of standardized residuals, the data appeared to come from a normal population. There appeared to be a cubic line formation through the normal line. This did not appear to be a cause for concern. This normality was verified quantitatively in a subsequent step. Based on the standardized residuals vs. fits graph, the data appeared to have equal variance. The frequency vs. standardized residual histogram showed values between -1.5 and 1.5. Therefore, there did not appear to be a cause for concern in this plot.



*Figure 7.51: Boxplot of shear modulus for the sleeve thickness factor levels.*

Based on the plot of effective modulus vs. sleeve thickness, a correlation could be determined. As the sleeve thickness increased (with the 0.000 thickness being the sample with non sleeve condition), the effective modulus change decreased. Variance appeared to increase as the sleeve thickness factor level increased.



**Tukey Pairwise Comparisons: Response = Mean Effe. Tens. Mod. % Change, Term = Sleeve Thicknes**

```

Grouping Information Using the Tukey Method and 95% Confidence
|
Sleeve
Thickness
(in)      N      Mean  Grouping
0.000     6    22.5998  A
0.028     7   -19.5268  A

Means that do not share a letter are significantly different.

```

*Figure 7.52: Tukey pairwise comparisons of tensile modulus percent change for the sleeve thickness factor levels.*

The Tukey pairwise comparison of effective modulus vs. sleeve thickness shows the non sleeve and 0.028 sleeve thickness factor levels as coming from the same group.

## **7.8 Observations**

### **7.8.1 Pre Impact Torsion Observations**

The initial test samples for each of the three sleeve thickness factor levels were tested to their maximum yield torque. These maximum yield torque values were used for subsequent samples, which were subjected to 75% of the sleeve factor levels yield torque. They also were used to monitor the mode of failure for each of the test events.

For the 0.000 sleeve thickness factor level, the yielded sample made audible cracking noises before the yield point. At the yield point, no visible changes occurred, though successive cracking noises and a decrease in torsion tester head torque signaled yield point. For the 0.020 sleeve thickness factor level, the sample made subtle audible cracking noises before the yield point. At the yield point, no visible changes occurred, though a decrease in torsion tester head torque signaled yield point. For the 0.028 sleeve thickness factor level, the sample made some audible cracking noises before the yield point. At the yield point, no visible changes occurred, though a decrease in torsion tester head torque signaled yield point.

Based on the GLM ANOVA output (Figure 7.21), the batch\*sleeve thickness interaction was not significant, and was therefore removed. The sleeve thickness factor appeared to be significant. Therefore, the mean response for the sleeve thickness factor levels were not all the same. This corresponds with the initial requirements for experiment validity, and was further analyzed in a subsequent step. The batch factor did not appear to be significant. Therefore, the mean response

for the batch factor levels were the same. This also corresponds with the initial requirements for experiment validity, and was further analyzed in a subsequent step.

The data was found to be normally distributed, and have equal variances among the batch factors (Figure 7.22). Therefore, the model was assumed to be adequate. Since the batch factor was determined to not have any statistically different levels, batch to batch variation was assumed to be negligible, reinforcing experiment validity. Since batch factors have equal variance and come from a normal population, sample manufacturing and data collection process was assumed to offer repeatable results that can be used for further analysis.

The boxplot for effective modulus vs. sleeve thickness (Figure 7.53) showed that as the sleeve thickness increased from the 0.000 level to the 0.020 and then to the 0.028 level, the effective modulus decreased. The degree to which the effective modulus decreased was analyzed in a subsequent step.

The Tukey pairwise comparison test analysis (Figure 7.24) concluded that the 0.000 sleeve thickness factor level was statistically different from the 0.020 and 0.028 sleeve thickness factor levels. Based on this data, as well as the boxplot and main effects plots, it can be concluded that the 0.000 sleeve thickness factor level was statistically higher than the 0.020 and 0.028 sleeve thickness factor levels, which were statistically similar.

Rationale behind the difference in means between the three sleeve thickness factor levels was the degree of carbon fiber reinforced plastic in each of the factor levels. The 0.00 sleeve thickness samples had non sleeve, and were therefore entirely carbon fiber reinforced plastic. Since the carbon fiber biaxial sleeve contains nearly all fibers in the 45-degree direction to the axis, most

fibers were in pure tension or compression when subjected to a torsional loading scenario. This translates to a higher sample effective modulus. As with the 0.000 sleeve thickness factor level samples, the 0.020 sleeve thickness samples provide higher effective modulus due to their higher percentage of fiber to aluminum.

### **7.8.2 Composite Layer Observations**

Based on the GLM ANOVA output, (Figure 7.25) the batch\*sleeve thickness interaction was not significant, and was therefore removed. The sleeve thickness factor appeared to be significant. Therefore, the mean response for the sleeve thickness factor levels were not all the same. This corresponds with the initial requirements for experiment validity, and was further analyzed in a subsequent step. The batch factor did not appear to be significant. Therefore, the mean response for the batch factor levels were the same. This also corresponds with the initial requirements for experiment validity, and was further analyzed in a subsequent step.

The data was found to be normally distributed, and have equal variances among the batch factors (Figure 7.26). Therefore, the model was assumed to be adequate. Since the batch factor was determined to not have any statistically different levels, batch to batch variation was assumed to be negligible, reinforcing experiment validity. Since batch factors have equal variance and come from a normal population, sample manufacturing and data collection process was assumed to offer repeatable results that can be used for further analysis.

The boxplot for composite layer modulus vs. sleeve thickness (Figure 7.27) showed that as the sleeve thickness increased from the 0.000 level to the 0.020 level, the modulus increased, and as

the sleeve thickness increased from the 0.020 level to the 0.028 level, the modulus slightly decreased. The degree to which the modulus changed was analyzed in a subsequent step.

The Tukey pairwise comparison test analysis (Figure 7.28) concluded that the 0.000 sleeve thickness factor level was statistically different from the 0.020 and 0.028 sleeve thickness factor levels. Based on this data, as well as the boxplot and main effects plots, it can be concluded that the 0.000 sleeve thickness factor level was statistically lower than the 0.020 and 0.028 sleeve thickness factor levels, which were statistically similar.

Rationale behind the difference in means between the three sleeve thickness factor levels was the shear strength of the adhesive, a sleeve shear modulus that was different from the published values, and fiber angle relative to the sample axis. Ideally, the composite layer shear modulus should be the same for each sleeve thickness factor level. An increase in composite layer modulus may be due to the cross sectional area of the adhesive, which was not accounted for in the shear modulus calculations. Torsional effective modulus that was not accounted for in the sleeve was determined to be caused by the composite layer, regardless of other intermediate layers. This is the least likely reason for modulus deviation due to the minimal cross sectional area of the adhesive.

Another reason for modulus deviation between sleeve thickness factor levels may be that the published values for the aluminum sleeve were not indicative of actual material properties. If the aluminum sleeve material had a higher shear modulus than the published values, the calculations would assume that the sleeve was contributing less effective modulus to the sample than what was occurring. This is a potential area of concern, but the shear modulus would have to be inaccurate by more than an order of magnitude to make an appreciable effect. Therefore, it may contribute, but is not the main contributor to deviation.

The last reason for modulus deviation between sleeve thickness factor levels is the change in fiber angle relative to the axis. The same size of biaxial sleeve was used for all layers of the samples. For this reason, as the biaxial sleeves are layered and build thickness, the fiber angle relative to the sample axis changes from a more axial fiber direction to a more transverse direction. The 0.020 and 0.028 sleeve thickness factor level samples would therefore have a greater percent of fiber cross sectional area with a more transverse fiber orientation. This is because they were laid up on a 0.5” mandrel instead of the 0.465” mandrel for the 0.000 sleeve thickness factor level samples. This is likely to be the reason for the modulus deviation, and would require the use of advanced manufacturing procedures and composite materials to alleviate.

### **7.8.3 Pre Impact Tension Observations**

The initial test samples were used to determine the yield tensile force for each of the three sleeve factor levels. These values were used for subsequent samples, which were subjected to 75% of the sleeve factor levels yield force. They also were used to monitor the mode of failure for each of the test events.

For the 0.000 sleeve thickness factor level, the yielded sample made no audible cracking noises before the yield point. At the yield point, there was visible and significant necking in the center of the sample critical cross section. A decrease in tensile tester head force also signaled yield point. Upon head travel return after the test session, the sample retained its visible deformation in the form of cross sectional necking.

For the 0.020 sleeve thickness factor level, the sample made no audible cracking noises before the yield point. At the yield point there appeared to be no composite damage, but there appeared to be

composite to aluminum delamination (adhesive failure). The aluminum tube appeared to pull through the composite tube. A decrease in torsion tester head torque also signaled the yield point. Upon head travel return after the test session, the sample retained its visible deformation in the form of sleeve pullout, though around 75% of the sleeve length that was removed, retracted back into the composite sleeve.

For the 0.028 sleeve thickness factor level, the sample made no audible cracking noises before the yield point. At the yield point, no visible changes occurred, though a decrease in torsion tester head torque signaled yield point. Upon head travel return after the test session, the sample showed no signs of visible deformation, as the aluminum sleeve and composite sleeve deflected equally.

Based on the GLM ANOVA output (Figure 7.29), the batch\*sleeve thickness interaction was not able to be calculated, and was therefore removed. The sleeve thickness factor appeared to be significant. Therefore, the mean response for the sleeve thickness factor levels were not all the same. This corresponds with the initial requirements for experiment validity, and was further analyzed in a subsequent step. The batch factor did not appear to be significant. Therefore, the mean response for the batch factor levels were similar. This also corresponds with the initial requirements for experiment validity, and was further analyzed in a subsequent step.

The data was found to be normally distributed, and have equal variances among the batch factors (Figure 7.30), after outliers were removed. Therefore, the model was assumed to be adequate. Since the batch factor was determined to not have any statistically different levels, batch to batch variation was assumed to be negligible, reinforcing experiment validity. Since the batch factor has equal variance and come from a normal population, sample manufacturing and data collection was assumed to offer repeatable results that can be used for further analysis.

The boxplot for effective modulus vs. sleeve thickness (Figure 7.31) showed that as the sleeve thickness increased from the 0.000 factor level to the 0.020 factor level, the effective modulus remained the same. As the sleeve thickness increased from the 0.020 factor level to the 0.028 factor level, the effective modulus increased. The degree to which the effective modulus decreased was analyzed in a subsequent step.

The Tukey pairwise comparison test analysis (Figure 7.32) concluded that the 0.000 and 0.020 sleeve thickness factor levels were statistically different from the 0.028 sleeve thickness factor level. Based on this data, as well as the boxplot and main effects plots, it can be concluded that the 0.00 and 0.020 sleeve thickness factor levels were similar, and were significantly lower than the 0.028 sleeve thickness factor level.

Rationale behind the difference in means between the 0.00 and 0.020 sleeve thickness factor and the 0.028 sleeve thickness factor level was the degree of carbon fiber reinforced plastic in each of the factor levels. The 0.00 sleeve thickness factor level had four layers of carbon fiber reinforced plastic, with no aluminum sleeve. All layers were 45 degrees to the axis of the sample, and therefore 45 degrees to the stress imparted on the fibers. This was considered to be the worst case scenario with regards to material effective modulus and ultimate strength, as there were both shear stresses and stresses perpendicular to the fiber orientation. With the 0.020 sleeve thickness factor level, there was material other than the fiber reinforced plastic to distribute the tension force. The degree to which the load was distributed increased as the sleeve thickness increased. Note that stress, and therefore effective modulus, was corrected for material thickness between all three factor levels.

#### 7.8.4 Impact Observations

Based on the GLM ANOVA output (Figure 7.33), the batch\*sleeve thickness interaction was not found to be significant. The sleeve thickness factor appeared to be significant. Therefore, the mean response for the sleeve thickness factor levels were not all the same. This corresponds with the initial requirements for experiment validity, and was further analyzed in a subsequent step. The batch factor did not appear to be significant. Therefore, the mean response for the batch factor levels were the same. This also corresponds with the initial requirements for experiment validity, and was further analyzed in a subsequent step.

The data was found to be normally distributed, and have equal variances among the batch factors (Figure 7.34). Therefore, the model was assumed to be adequate. Since the batch factor was determined to not have any statistically different levels, batch to batch variation was assumed to be negligible, reinforcing experiment validity. Since sleeve thickness and batch factors have equal variance and come from a normal population, sample manufacturing and data collection was assumed to offer repeatable results that can be used for further analysis.

The boxplot for Depression depth vs. sleeve thickness (Figure 7.35) showed that as the sleeve thickness increased from the 0.000 level to the 0.020 and then to the 0.028 level, the depression depth decreased. The degree to which the depression depth decreased was analyzed in a subsequent step.

The Tukey pairwise comparison test analysis (Figure 7.36) concluded that the .000 and 0.020 sleeve thickness factor levels were statistically different from the 0.028 sleeve thickness factor level. Based on this data, as well as the boxplot and main effects plots, it can be concluded that the

0.000 and 0.020 sleeve thickness factor levels were similar, and statistically higher than the 0.028 sleeve thickness factor level.

Rationale behind the difference in means between the three sleeve thickness factor levels was the basis for the subject of the research. All samples in the 0.000 sleeve thickness factor level had a complete rupture at the site of impact. Fiber breakage and separation were noted on all samples, with minimal fiber damage or sample deformation beyond the diameter of the hemispherical impactor.

Conversely, both the 0.020 and 0.028 sleeve thickness factor levels (Figures 7.54 and 7.55) had no visible fiber breakage or fiber to matrix delamination on any samples. On the 0.020 sleeve thickness factor levels, sample deformation was noted on three times the diameter of the impactor near the impact site. This deformation was in the form of surface denting. Sample bending was noted on all samples, but did not exceed 1" along the 14" length of the samples, and therefore did not interfere with torsion or tension test processes.

On the 0.028 sleeve thickness factor levels, sample deformation was noted on two times the diameter of the impactor near the impact site. This deformation was in the form of surface denting. Sample bending was noted on some samples, and did not exceed 0.5" along the 14" length of the samples. A rudimentary "tap test" was performed on 0.020 and 0.028 sleeve thickness factor level samples, and audible fiber to sleeve delamination was noted on all samples. Delamination appeared along no more than the diameter of the impactor, but the accuracy of the test limited the precision to which the delamination was present.



*Figure 7.54: Non sleeve (0.000 sleeve thickness factor level) post impact cross section.*

Complete fiber and matrix rupture was noted along the sample cross section, with delamination along the area of the impact site. No sample deformation was noted beyond the area of the impact site.



*Figure 7.55: 0.020 sleeve thickness factor level post impact cross section.*

No fiber rupture noted along the sample cross section, with some fiber to matrix delamination along half the diameter of the sample. There was significant sleeve to composite delamination. A 0.087" aluminum sleeve to composite void was noted.



*Figure 7.56: 0.028 sleeve thickness factor level post impact cross section.*

No fiber rupture noted along the sample cross section, with no fiber to matrix delamination. There was some sleeve to composite delamination. A 0.049" aluminum sleeve to composite void was noted.

### **7.8.5 Post Impact Torsion Observations**

The initial test samples were used to determine the yield torque for each of the three sleeve factor levels after the impact, as the yield point was assumed to have decreased and therefore required additional yield samples to identify post impact yield torque. These values were used for subsequent samples, which were subjected to 75% of the sleeve factor levels yield torque. They also were used to monitor the mode of failure for each of the test events.

For the 0.000 sleeve thickness factor level, the yielded sample made some audible cracking noises before the yield point. At the yield point, the sample appeared to twist about the portion of the cross section that was unaffected by the impact. This appeared to elongate the once circular impact site at 45 degrees from the axis of the sample. A decrease in torsion tester head torque also signaled yield point. For the 0.020 sleeve thickness factor level, the sample made subtle audible cracking noises before the yield point. At the yield point, no visible changes occurred, though a decrease in torsion tester head torque signaled yield point. For the 0.028 sleeve thickness factor level, the sample made minimal audible cracking noises before the yield point. At the yield point, no visible changes occurred, though a decrease in torsion tester head torque signaled yield point.

Based on the GLM ANOVA output (Figure 7.37), the batch\*sleeve thickness interaction was not able to be calculated, and was therefore removed. The sleeve thickness factor appeared to be significant. Therefore, the mean response for the sleeve thickness factor levels were not all the same. This corresponds with the initial requirements for experiment validity, and was further analyzed in a subsequent step. The batch factor did not appear to be significant. Therefore, the mean response for the batch factor levels were the same. This also corresponds with the initial requirements for experiment validity, and was further analyzed in a subsequent step.

The data was found to be normally distributed, and have equal variances among the batch factors (Figure 7.38). Therefore, the model was assumed to be adequate. Since the batch factor was determined to not have any statistically different levels, batch to batch variation was assumed to be negligible, reinforcing experiment validity. Since batch factors have equal variance and come from a normal population, sample manufacturing and data collection was assumed to offer repeatable results that can be used for further analysis.

The boxplot for effective modulus vs. sleeve thickness (Figure 7.39) showed that as the sleeve thickness increased from the 0.000 level to the 0.020 and then to the 0.028 level, the effective modulus increased. This was the opposite effect as the pre impact torsion test results. The degree to which the effective modulus increased was analyzed in a subsequent step.

The Tukey pairwise comparison test analysis (Figure 7.40) concluded that the 0.000, 0.020, and 0.028 sleeve thickness factor levels formed three separate groups. Based on this data, as well as the boxplot and main effects plots, it can be concluded that the effective modulus of the 0.000 sleeve thickness factor level was statistically lower than the 0.020 sleeve thickness factor level, and the effective modulus of the 0.020 sleeve thickness factor level was statistically lower than the 0.028 sleeve thickness factor level.

#### **7.8.6 Post Impact Tension Observations**

The initial test samples were used to determine the yield force for each of the three sleeve factor levels after the impact, as the yield point was assumed to have decreased and therefore required additional yield samples to identify post impact yield force. These values were used for subsequent samples, which were subjected to 75% of the sleeve factor levels yield force. They also were used to monitor the mode of failure for each of the test events.

For the 0.000 sleeve thickness factor level, the yielded sample made no audible cracking noises before the yield point. At the yield point, there was some necking in the center of the sample critical cross section. A decrease in tensile tester head force also signaled yield point. Upon head travel return after the test session, the sample retained its visible deformation in the form of cross sectional necking.

For the 0.020 sleeve thickness factor level, the sample made no audible cracking noises before the yield point. At the yield point there appeared to be no composite damage, but there appeared to be composite to aluminum delamination (adhesive failure). The aluminum tube appeared to pull through the composite tube. A decrease in torsion tester head torque also signaled the yield point. Upon head travel return after the test session, the sample retained its visible deformation in the form of sleeve pullout, though around 50% of the sleeve length that was removed, retracted back into the composite sleeve.

For the 0.028 sleeve thickness factor level, the sample made subtle audible cracking noises before the yield point. At the yield point, no visible changes occurred, though a decrease in torsion tester head torque signaled yield point. Upon head travel return after the test session, the sample showed no signs of visible deformation, as the aluminum sleeve and composite sleeve deflected equally.

Based on the GLM ANOVA output (Figure 7.41), the batch\*sleeve thickness interaction was not able to be calculated, and was therefore removed. The sleeve thickness factor appeared to be significant. Therefore, the mean response for the sleeve thickness factor levels were not all the same. This corresponds with the initial requirements for experiment validity, and was further analyzed in a subsequent step. The batch factor did not appear to be significant. Therefore, the mean response for the batch factor levels were the same. This also corresponds with the initial requirements for experiment validity, and was further analyzed in a subsequent step.

The data was found to be normally distributed, and have equal variances among the batch factors (Figure 7.42). Therefore, the model was assumed to be adequate. Since the batch factor was determined to not have any statistically different levels, batch to batch variation was assumed to be negligible, reinforcing experiment validity. Since batch factors have equal variance and come

from a normal population, sample manufacturing and data collection was assumed to offer repeatable results that can be used for further analysis.

The boxplot for effective modulus vs. sleeve thickness (Figure 7.43) showed that as the sleeve thickness increased from the 0.000 factor level to the 0.020 factor level, the effective modulus remained the same. As the sleeve thickness increased from the 0.020 factor level to the 0.028 factor level, the effective modulus increased. The degree to which the effective modulus decreased was analyzed in a subsequent step.

The Tukey pairwise comparison test analysis (Figure 7.44) concluded that the 0.000 and 0.020 sleeve thickness factor levels were statistically different from the 0.028 sleeve thickness factor level. Based on this data, as well as the boxplot and main effects plots, it can be concluded that the 0.00 and 0.020 sleeve thickness factor levels were similar, and were significantly lower than the 0.028 sleeve thickness factor level.

### **7.8.7 Post Impact Torsion Change Observations**

Based on the GLM ANOVA output (Figure 7.45), the batch\*sleeve thickness interaction was not able to be calculated, and was therefore removed. The sleeve thickness factor appeared to be significant. Therefore, the mean response for the sleeve thickness factor levels were not all the same. This corresponds with the initial requirements for experiment validity, and was further analyzed in a subsequent step. The batch factor did not appear to be significant. Therefore, the mean response for the batch factor levels were the same. This also corresponds with the initial requirements for experiment validity, and was further analyzed in a subsequent step.

The data was found to be normally distributed, and have equal variances among the batch factors (Figure 7.46). Therefore, the model was assumed to be adequate. Since the batch factor was determined to not have any statistically different levels, batch to batch variation was assumed to be negligible, reinforcing experiment validity. Since batch factors have equal variance and come from a normal population, sample manufacturing and data collection was assumed to offer repeatable results that can be used for further analysis.

The boxplot for effective modulus vs. sleeve thickness (Figure 7.47) showed that as the sleeve thickness increased, the effective modulus change decreased. The degree to which the effective modulus change decreased was analyzed in a subsequent step.

The Tukey pairwise comparison test analysis (Figure 7.48) concluded that the 0.000, 0.020, and 0.028 sleeve thickness factor levels formed three separate groups. Based on this data, as well as the boxplot and main effects plots, it can be concluded that the effective modulus change of the 0.000 sleeve thickness factor level was statistically higher than the 0.020 sleeve thickness factor level, and the effective modulus change of the 0.020 sleeve thickness factor level was statistically higher than the 0.028 sleeve thickness factor level. Therefore, the torsional effective modulus has changed most for the 0.000 sleeve thickness factor level, and least for the 0.028 sleeve thickness factor level. This serves to fail to reject the null hypothesis that this research highlights, in the torsion loading scenario.

Rationale behind the difference in means between the three sleeve thickness factor levels was the basis for the research. For the 0.000 sleeve thickness factor level, after the impact event, there was a substantial degree of matrix and reinforcement rupture. Fiber breakage removed a considerable amount of material from the cross section, and created a complex loading scenario in which the

torsional forces were transmitted to discontinuous fibers. This led to the fiber-matrix shear strength contributing greatest to torsional effective modulus within the 0.000 sleeve thickness factor level samples. For the 0.020 and 0.028 sleeve thickness factor levels, fiber and matrix breakage was not a significant contributor to the effective modulus decrease. Geometry change and composite to sleeve delamination was the main contributor to effective modulus decrease, increasing overall sample effective modulus compared to the 0.000 sleeve thickness factor level.

### **7.8.8 Post Impact Tension Change Observations**

Based on the GLM ANOVA output (Figure 7.49), the batch\*sleeve thickness interaction was not able to be calculated, and was therefore removed. The sleeve thickness factor appeared to not be significant. Therefore, the mean response for the sleeve thickness factor levels were all the same. This did not correspond with the initial requirements for experiment validity, but was further analyzed in a subsequent step. The batch factor also did not appear to be significant. Therefore, the mean response for the batch factor levels were the same. This does correspond with the initial requirements for experiment validity, and was further analyzed in a subsequent step.

The data was found to be normally distributed, and have equal variances among the batch factors (Figure 7.50). Therefore, the model was assumed to be adequate. Since the batch factor was determined to not have any statistically different levels, batch to batch variation was assumed to be negligible, reinforcing experiment validity. Since batch factors have equal variance and come from a normal population, sample manufacturing and data collection was assumed to offer repeatable results that can be used for further analysis.

The boxplot for effective modulus vs. sleeve thickness (Figure 7.51) showed that as the sleeve thickness increased, the effective modulus change decreased. Considering this, the effective modulus change decreased to a negative mean for the 0.028 sleeve thickness factor level. This theoretically means that the 0.028 sleeve thickness factor level samples increased in effective modulus after the impact event. The degree to which the effective modulus change decreased was analyzed in a subsequent step.

The Tukey pairwise comparison test analysis (Figure 7.52) concluded that the 0.000 and 0.028 sleeve thickness factor levels were from the same group. Based on this data, as well as the boxplot and main effects plots, it can be concluded that the effective modulus change of the 0.000 sleeve thickness factor level was statistically the same as the 0.028 sleeve thickness factor level. This serves to reject the null hypothesis that this research highlights, in the tension loading scenario. With this said the ANOVA and Tukey pairwise comparisons, and therefore the ultimate conclusion, appeared to be mainly driven by the high variances of the sleeve thickness factor levels. This is due to the visible difference in effective modulus change when viewing the main effects plot of the sleeve thickness factor levels. Enhanced manufacturing processes or testing techniques may serve to decrease variance, translating to an increase in significance of the sleeve thickness factor and the formation of separate groups within the Tukey pairwise comparison.

Rationale behind the difference in means between the two sleeve thickness factor levels was the basis for the research. For the 0.000 sleeve thickness factor level, after the impact event, there was a substantial degree of matrix and reinforcement rupture. Fiber breakage removed a considerable amount of material from the cross section, and created a complex loading scenario in which the tensile forces were transmitted to discontinuous fibers. This led to the fiber-matrix shear strength

contributing greatest to torsional effective modulus within the 0.000 sleeve thickness factor level samples. For the 0.028 sleeve thickness factor levels, fiber and matrix breakage was not a significant contributor to the effective modulus decrease, as there was no visible fiber damage. Geometry change and composite to sleeve delamination was the main contributor to effective modulus change, translating to a decrease in effective modulus change compared to the 0.000 sleeve thickness factor level.

### **7.8.9 Torsion Effective Modulus vs. Density Comparison**

To gain a greater understanding regarding whether certain sleeve conditions should be used for certain applications, as well as whether the additional post impact structural characteristics were worth the increase in additional weight, a specific effective modulus may provide important insight.

Density of the 0.000 sleeve thickness factor level samples was found by determining the density of the layers of composite, as there was no internal sleeve.

Total sample density was defined:

$$\rho_t = V_s \rho_s + V_c \rho_c \quad (8.22)$$

where:

$\rho_t$  = Density of the total sample, [lb/in<sup>3</sup>],

$V_s$  = Volume ratio of the sleeve,

$\rho_s$  = Density of the sleeve, [lb/in<sup>3</sup>],

$V_c$  = Volume ratio of the composite, and

$\rho_c$  = Density of the composite, [lb/in<sup>3</sup>].

Sleeve volume ratio was defined (Strong, 2008, p. 316):

$$V_s = \frac{A_s}{A_t} \quad (8.23)$$

where:

$V_s$  = Volume ratio of the sleeve,

$A_s$  = Cross sectional area of the sleeve, [in<sup>2</sup>], and

$A_t$  = Cross sectional area of the total sample, [in<sup>2</sup>].

Composite density was defined (Strong, 2008, p. 316):

$$\rho_c = V_f \rho_f + V_m \rho_m \quad (8.24)$$

where:

$\rho_c$  = Density of the composite, [lb/in<sup>3</sup>],

$V_f$  = Volume ratio of the fibers,

$\rho_f$  = Density of the fibers, [lb/in<sup>3</sup>],

$V_m$  = Volume ratio of the matrix, and

$\rho_m$  = Density of the matrix, [lb/in<sup>3</sup>].

Volume ratio of the fibers was defined (Strong, 2008, p. 317):

$$V_f = \left( 1 + \frac{1}{\left(\frac{W_f}{W_m}\right) + \left(\frac{\rho_m}{\rho_f}\right)} \right)^{-1} \quad (8.25)$$

where:

$W_f$  = Weight of the fibers, [lb],

$W_m$  = Weight of the matrix, [lb],

Volume ratio of the matrix was defined:

$$V_m = 1 - V_f \quad (8.26)$$

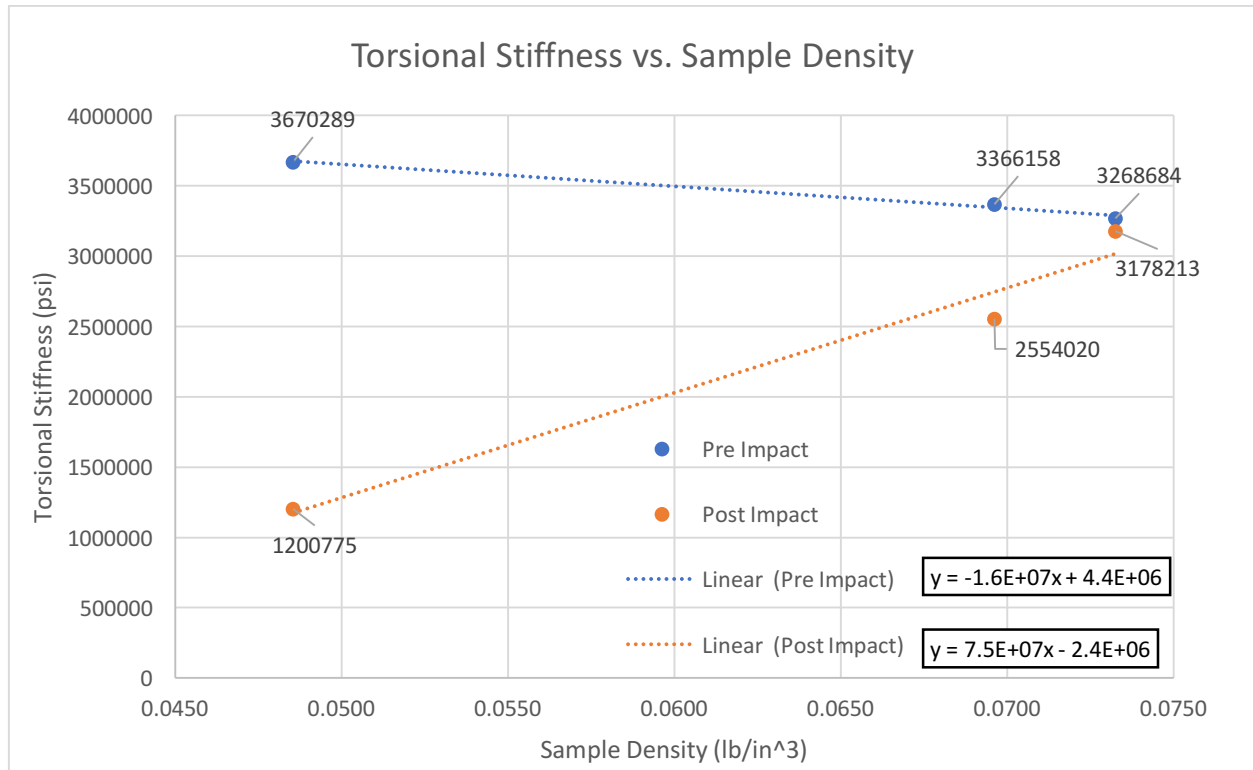


Figure 7.57: Plot of effective shear modulus vs. sample average density.

The chart of torsional effective modulus vs. sample density was useful for the determination of damage sensitivity given the weight increase due to the aluminum sleeve. It also brings to light some factors, due to the fact that the difference between pre and post impact torsional effective modulus was minimal for the 0.028 sleeve thickness factor level. There was a potential that, given a certain percentage of composite and aluminum, that there would be no effective modulus change due to impact. This post impact trend is likely to diverge from the pre impact line as impact energy

increases, which would in turn translate into a greater percent of aluminum necessary to retain post impact effective modulus characteristics. It is important to consider that component designers typically use additional layers for composite components that may encounter an impact event. Therefore, though the material density may be the same, part weight may increase due to the increased composite volume. This factor has the potential to further increase the advantages of the aluminum substrate.

## **8 Limitations**

As with any physical quantitative experiment, there were few variables that were being studied, but more variables that need to be controlled and monitored to ensure repeatability. It was not logistically feasible to control and monitor all variables due to time and monetary constraints placed on the experiment. Due to this, it was important to determine what parameters were most important, and which ones contribute the greatest to the dependent variable.

One main limitation of this experiment was the relatively low number of samples. 29 samples were tested in total, and once the grouping was divided between all the loading, impact, and sleeve scenarios, the individual sample size of around 10 samples per sleeve thickness factor level was not statistically significant. Therefore, supplementary hypotheses have been put in place to control the scenario and ensure that though the sample size was low, the data collected was reflective of the underlying condition. Even with this control, there may be manufacturing and material variability that would require further control and monitoring to ensure data validity.

Another limitation to this experiment was the relatively specialized sample geometry. Although measures were taken to ensure that this shaft geometry was as general as possible, it was

specialized compared to the flat samples that were conventionally tested. This experiment takes a more specialized approach to impact on composite components that may uncover new data, but this data would not be applicable for all composite lamination types. Therefore, primarily high curvature component geometries were able to implement the resulting data. The 0.5" shaft geometry, and more specifically the thin walled shaft undergoing an impact loading scenario, produced a complex combination of forces and stresses that would produce very different results than those of a flat plate. Depending on the impact and relative material thickness, the indenter may puncture the sample, conically deform the sample in a local manner, or cause the sample to form an ellipsoidal cross section. In the case of this research, the indenter produced a puncture in the non sleeve samples, an ellipsoidal cross section in the 0.020 sleeve thickness factor level samples, and a hemispherical deformation in the 0.028 sleeve thickness factor level samples. These varied failure modes are more complex compared to the typical flat plate impact conditions that were currently used to test composites and metals. These different modes of impact absorption would translate to different effective modulus results and different modes of failure depending on the loading scenario. This was further complicated with complex part geometry that the end user may implement, which may require further investigation to ensure comparability to the data of this experiment.

Along with the specialized sample geometry was the specialized sleeve material. A 6061 T6 aluminum was chosen due to its ubiquity within the mechanical engineering field. It has good formability, machinability, weldability, low density compared to other metals, and was relatively common due to these characteristics. Furthermore, aluminum was known for its impact absorption properties, as it was commonly used in crushable crash structures. (Qiao, P., Yang, M., & Bobaru, F., 2008, p. 241) For this reason, it was a relatively cost effective solution to many design

problems. Materials such as 4130 chrome moly steel and grade 5 titanium have a greater level of toughness, but were not commonly available in the thinner tube geometries required for this experiment. It was also important to note that aluminum has a higher specific strength than steel, which may improve performance depending in intended use. Lower degrees of machinability in the two materials also would result in greater difficulties in attaining this geometry, as well as a lower degree of repeatability. Any sleeve materials that have different impact resistance at this impact force and velocity may have different characteristics under structural loading after the impact condition.

The relatively specialized composite material was also a potential limitation. A 2k biaxial sleeve was used to provide a uniform cross section. A biaxial sleeve has a more streamlined layup process, which can potentially translate to an increased number of market sectors that could benefit from the technology. Alongside manufacturing, biaxial sleeve has an improved process repeatability compared to conventional flat fabrics. It also has a high degree of interwoven material that increases crimping. Fabric crimping decreases effective modulus, but increases impact resistance due to the straightening of the fibers under directional load. This leads to a more progressive failure mode, further enhanced by the crack stopping ability of the fiber cross over points. As with the sample sleeve material, any other fabric type or weave pattern may change results of the effective modulus both before and after the impact condition. (Strong, 2008, p. 256) With this said, it is important to note that variance in the tensile loading scenario may be attributed to a difference in fiber orientation relative to the sample axis as the biaxial sleeve layers are built upon one another. This is due to the nature of the biaxial sleeve fiber weave process, and would require different material types (such as a plain weave fabric) to overcome the variance issue.

A specialized impact scenario was also generated for the purposes of this experiment. An impactor was to be dropped vertically a specified distance onto the longitudinal axis of the sample, half way down the length of the test area. The geometry of the impactor was that of a blunt bullet nose. For sharp indenter impact or flat plate impact, different impactor and sample geometries should be considered. For other tests, a higher velocity impact may be more suitable as well. Different applications would require different parameters. This experiment was intended primarily for automotive, transportation, and subsonic impact aerospace applications with blunt impactors, which was the rationale behind the relatively low impact velocity and bullet nose of the impactor.

## **9 Future Work**

Work beyond the scope of this experiment should include improving upon the limitations of the research, as well as including independent features that may improve the usability of the output data. Limitations of the research include the decreased sample size of the experiment, specialized geometry, specialized materials, and specialized impact scenario. Independent features include computer simulation controls and advanced beam designs. The most apparent and logical step for future work would likely include an expanded degree of fiber to metal ratios as well as an expanded range of impact energies and velocities.

The sample size was determined based on previous knowledge of the processes required to acquire the data, and may be increased based on perceived process capability. It can affect the mean data output, which can affect the overall results of the experiment. If the variance in the data was determined to be too great for the intended applications, an improved manufacturing and testing process may be necessary to provide useful information. Increasing sample size may also provide insight into the underlying conditions that were causing the variance in the output data.

The geometry used within the experiment was determined based on conventional metal and composite test experiments. It also represents the capabilities of the machines used in the tensile and torsional load testing procedures. This may not fit the requirements of certain component geometries or layup schedules. It may also not conform to the degree of metal and composite used in specific applications. Therefore, it may be necessary to implement more specific geometries that were more tailored to their intended products.

The materials used represent common materials used in automotive and aerospace applications. Their properties represent those which would provide a good foundation for subsequent research. This may not properly represent other applications or specific products, and therefore other materials may need to be used to properly characterize their behavior. As stated earlier, 4130 chrome moly steel and grade 5 titanium appear to be the natural stepping stones due to their use in various industries, as well as their impact properties. With that said, the use of other materials in the given sample geometry would be dependent upon the results of the proposed experiment.

Fiber and sleeve dimensions, and therefore, the ultimate fiber to metal ratio, was dependent on readily available components and conformance to the provided testing equipment. This provided important points of comparison, but further information could be gained by including a greater degree of fiber to metal volume variation. Custom substrate thicknesses could be implemented to simplify different volume ratios, and different tube diameters could represent various applications.

## **10 Conclusion**

Carbon fiber reinforced plastic in its neat state has historically had relatively low yield strength after significant impact. The hypothesis was that the metallic substrate may exhibit a lesser

decrease in sample effective modulus after significant impact. The first supporting hypothesis was that there was equal variance of the means between the three sleeve thickness factor levels of the same analysis scenario, and an insignificant batch factor contribution. The second supporting hypothesis was that there was a higher mean yield strength before the significant impact than after the impact.

The methodology that has been chosen was a quantitative research approach, with the accompanying post positivist worldview and experimental research design. The independent variables were the sleeve condition, impact condition, and loading condition. Within the sleeve condition, there was the non sleeve variable and two aluminum sleeve variables (0.000, 0.020, and 0.028 sleeve thickness factor levels). There was a pre impact and post impact scenario, and a torsion and tension loading scenario. These conditions, and underlying variables, were altered to affect the dependent variable, which is effective modulus. This was the data that was ultimately calculated based on the experimental data collection.

The instruments that were used were based on the loading scenario necessary. For torsion, a Tinius Olsen torsion tester was used. For tension, an MTS tensile tester was used. Stress strain diagrams were created to determine effective modulus for both loading conditions. The output effective modulus calculations were used within the data analysis to test the hypothesis.

For the pre impact torsion, pre impact tension, post impact torsion, and post impact tension data analysis scenarios, the data was found to have an insignificant batch factor model contribution, come from a normal distribution, and had equal variance among the batch factor. This helped prove manufacturing process and test process validity. For the pre impact tension analysis scenario, the data was found to have an insignificant batch factor model contribution, come from a normal

distribution, and had equal variance among the batch factor. This helped further prove manufacturing process and test process validity. The model adequacy analysis performed ultimately resulted in the failure to reject the null hypothesis for  $H_1$  (the equal variance of the means, as well as batch factor contribution).

For the composite layer analysis scenario, the data was found to have an insignificant batch factor model contribution, come from a normal distribution, and had equal variance among the batch factor. This helped show the difference in composite layer modulus by removing the effects of the aluminum sleeve. It showed that the composite layer shear modulus was higher in the two aluminum sleeve factor levels, alluding to a difference in fiber orientation relative to the sample axis in the non sleeve factor level.

For the post impact torsion change analysis scenario, the data was found to have an insignificant batch factor model contribution, come from a normal distribution, and had equal variance among the batch factor. Furthermore, the boxplot showed a percent change in effective modulus between the pre and post impact non sleeve factor level. This resulted in the failure to reject the null hypothesis for  $H_2$  under the torsion loading scenario (pre and post impact decrease in the effective modulus mean for the non sleeve factor level).

The Tukey pairwise comparisons for the post impact torsion change analysis scenario showed a distinct difference in the percent change of the effective modulus among the three factor levels. The percent change was highest for the 0.000 sleeve thickness factor level, decreased significantly for the 0.020 sleeve thickness factor level, and again decreased significantly for the 0.028 sleeve thickness factor level. This resulted in the failure to reject the null hypothesis for  $H_3$  under the

torsion loading scenario (lower post impact percent change in the aluminum sleeve factor levels compared to the non sleeve factor level).

For the post impact tension change analysis scenario, the data was found to have an insignificant batch factor model contribution, come from a normal distribution, and had equal variance among the batch factor, after the 0.020 sleeve thickness factor level was removed from the dataset. The data was also found to have an insignificant sleeve thickness factor though, which alluded to issues with the variance of the factor levels. The boxplot showed a percent change in effective modulus between the pre and post impact non sleeve factor level. This resulted in the failure to reject the null hypothesis for  $H_2$  under the tension loading scenario (post impact decrease in the effective modulus mean for the non sleeve factor level).

The Tukey pairwise comparisons for the post impact torsion change analysis scenario showed no significant difference in the percent change of the effective modulus among the two factor levels. This resulted in the rejection of the null hypothesis for  $H_3$  under the tension loading scenario (lower post impact percent change in the aluminum sleeve factor levels compared to the non sleeve factor level). This was likely due to the high degree of variance among each of the sleeve thickness factor levels, since the boxplot clearly showed a difference in means among the factor levels.

## **11 Bibliography**

ASTM International. (2015, March). *Standard Test Method for Measuring the Damage Resistance of a Fiber-Reinforced Polymer Matrix Composite to a Drop-Weight Impact Event*. (Standard Designation: D7136/D7136M–15). Available from <http://www.astm.org>

Used as a reference for the calculation of drop weight impactor height, and for the modification of original drop impactor.

ASTM International. (2014, May). *Standard Test Method for Tensile Properties of Polymer Matrix Composite Materials*. (Standard Designation: D3039/D3039M-14). Available from <http://www.astm.org>

Used as a reference for the determination of testing parameters for the tensile testing research section.

Axson Technologies: AdTech Marine Systems. (2016). *Marine 820 Epoxy Laminating Systems*. Retrieved from [http://www.axson-technologies.com/sites/default/files/TDS%20-%20Marine%20820%20160524\\_1.pdf](http://www.axson-technologies.com/sites/default/files/TDS%20-%20Marine%20820%20160524_1.pdf)

Used as a reference for the material properties, and proper preparation procedures, of the matrix material used in the research.

Badie, M. A., Mahdi, E., & Hamouda, A. M. S., (2010). *Materials and Design. An investigation into carbon/glass fiber reinforced epoxy composite automotive drive shaft*. 32(2011), 1485-1500.

Used as a reference for the literature review to compare other types of metallic substrate fiber reinforced material composition, as well as their applications. Provides context for the usability of the output data.

Bauchau, O.A., & Craig, J.I. (2009). *Structural Analysis: With Applications to Aerospace Structures*. New York: Springer Science and Business Media.

Used as a reference for the calculation of tensile and torsional stiffness. Used for equations, and for the understanding of the underlying structural effects.

Broutman, L. J. et al, (1972). Air Force Office of Scientific Research. *Impact strength and toughness of fiber composite materials*. AD-753 101, 1-9.

Used as a reference for the original impact strength of composite materials, and carbon fiber reinforced components. Although matrix materials have come a long way since 1972, the principles mentioned in the research were still valid and present a means of measuring strength after an impact scenario.

U.S. Department of Transportation: Federal Aviation Administration. (2012). *Chapter 7: Advanced Composite Materials*. Retrieved from Aviation Maintenance Handbook: Airframe Volume 1: [https://www.faa.gov/regulations\\_policies/handbooks\\_manuals/aircraft/amt\\_airframe\\_handbook/](https://www.faa.gov/regulations_policies/handbooks_manuals/aircraft/amt_airframe_handbook/)

Used as a reference for determining the issues associated with composites, as well as the methods used to repair and improve composite materials.

Creswell, J. W. (2013). *Research design: Qualitative, quantitative, and mixed methods approaches (4th ed.)*. Thousand Oaks, CA: SAGE Publications.

Acts as a reference guide for the architecture of the research proposal.

Fibre Glast Developments Corporation. (2010). *Product Data Sheet: Parting Wax*. Retrieved from <http://cdn.fibreglast.com/downloads/00148-B.pdf>

Used as a reference for expected product performance, as well as to ensure that the product was being used properly.

Fibre Glast Developments Corporation. (2010). *Product Data Sheet: PVA Release Film*. Retrieved from <http://cdn.fibreglast.com/downloads/00143-B.pdf>

Used as a reference for expected product performance, as well as to ensure that the product was being used properly.

Henkel: Loctite. (2014). *Technical Data Sheet: Loctite EA E-120HP*. Retrieved from [https://tds.us.henkel.com/NA/UT/HNAUTTDS.nsf/web/8FD3ABAA09A649FE882571870000DB2F/\\$File/EA%20E-120HP-EN.pdf](https://tds.us.henkel.com/NA/UT/HNAUTTDS.nsf/web/8FD3ABAA09A649FE882571870000DB2F/$File/EA%20E-120HP-EN.pdf)

Used as a reference for expected product performance, as well as to ensure that the product was being used properly.

Mandel, M. & Krüger, L. (2014). *Long-term corrosion behaviour of EN AW-6060-T6 in an aluminium/carbon-fibre reinforced polymer self-piercing rivet joint*. *Mat.-wiss. u. Werkstofftech*, 45: 1123–1129. doi:10.1002/mawe.201400352

Used as a reference for determining the corrosion effects of carbon fiber contact with aluminum.

MatWeb Material Property Data. (2017). *Aluminum 6061-T6; 6061-T651*. Retrieved from <http://www.matweb.com/search/DataSheet.aspx?MatGUID=b8d536e0b9b54bd7b69e4124d8f1d20a&ckck=1>

Used as a reference for determining the mechanical characteristics of the 6061-T6 aluminum sleeve.

Maringer, R. E., (1966). *Volume I: Damping Capacity of Materials*. Redstone Arsenal, Alabama: Redstone Scientific Information Center.

Used as a reference for determining the damping characteristics of common materials.

Muteb, H. M., Kemal, A. T., & Jaber, M. H., (n.d.) The Iraqui Journal for Mechanical and Material Engineering, Special Issue. *Experimental investigation for improving the performance of thin walled tubular steel columns using CFRP strips*. (n.v.) Retrieved from <http://www.iasj.net/iasj?func=fulltext&aId=45098>. p. 623-634.

Used as a reference for the use of carbon fiber based composites with thin walled steel members. Determines validity of the two materials being used in conjunction with each other, as well as the application that surround the use of the materials.

Park, S. J., (2015). *Springer Series in Materials Science vol. 210: Carbon Fibers*. Dordrecht: Springer Science and Business Media.

Used as a reference for the manufacturing process of carbon fiber, and the classification of various types of carbon fiber. Used to give context for the advantages and disadvantages of carbon fiber reinforced composites.

Qiao, P., Yang, M., & Bobaru, F. (2008). *Impact mechanics and high-energy absorbing materials: review*. Faculty Publications from the Department of Engineering Mechanics, 239-241.

Used as a reference for the structural mechanics of the samples in question. Allows formation of hypotheses in a constructive manner.

Rock West Composites. (2016). *Composite Bond Prep 101*. Retrieved from [https://www.rockwestcomposites.com/media/wysiwyg/Procedure\\_for\\_Bonding\\_-\\_General\\_1.pdf](https://www.rockwestcomposites.com/media/wysiwyg/Procedure_for_Bonding_-_General_1.pdf)

Used as a reference for the proper secondary bonding preparations, mainly for the use of bonding the carbon fiber reinforced composite layers onto the aluminum sleeves.

Shin, K. C. & Lee, J. J. (2006). *Effects of thermal residual stresses on failure of co-cured lap joints with steel and carbon fiber–epoxy composite adherends under static and fatigue tensile loads*. *Composites Part A: Applied Science and Manufacturing*, Volume 37, Issue 3. p. 476-487. <http://dx.doi.org/10.1016/j.compositesa.2005.03.031>.

Used as a reference for the thermal degradation of composite materials with reference to the adhesive joint bonding properties. (<http://www.sciencedirect.com/science/article/pii/S1359835X05002307>)

Strong, B. A., (2008). *Fundamentals of Composites Manufacturing: Materials, Methods, and applications*. Dearborn, MI: Society of Manufacturing Engineers.

Used as a reference for the history, and basic structural mechanics of the samples in question. Provides basic structural calculations and references for the loading conditions that the samples would undergo.

U.S. Department of Transportation: Federal Aviation Administration. (2011). *Determining the Fatigue Life of Composite Aircraft Structures Using Life and Load-Enhancement Factors*. Springfield, Virginia: National Technical Information Services.

Used as a reference for post impact structural characteristics of fiber reinforced composite materials such as carbon fiber reinforced plastics.

Zukas, J. A. (1992). *Impact Dynamics*. New York, NY: Wiley.

Used as a reference for the impact characterization of fiber reinforced materials, to give context for the failure modes of the fiber and matrix.

## 12 Appendix

### 12.1 Machining



*Figure 12.1: Aluminum sleeves, machined to their final length.*



*Figure 12.2: Surface roughness testing of aluminum sleeve using Mahr Federal Pocket Surf.*

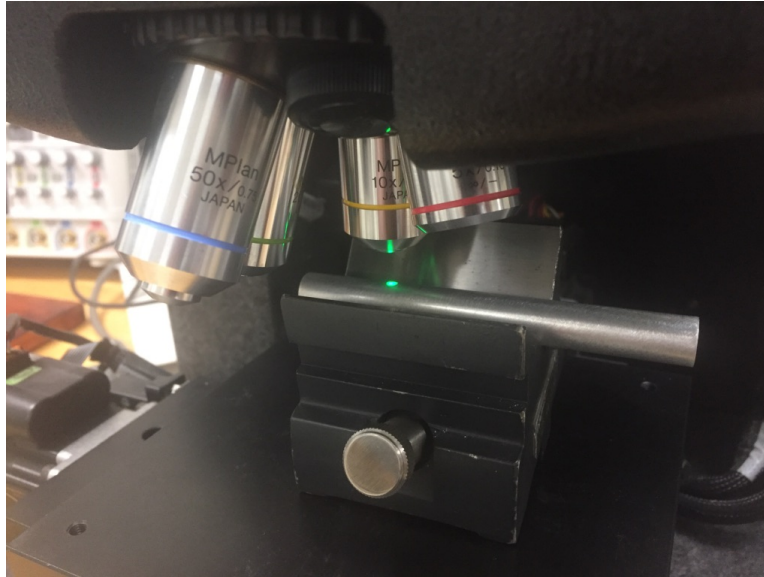


*Figure 12.3: Surface roughness testing of aluminum ends using Tamar HRT 3000.*

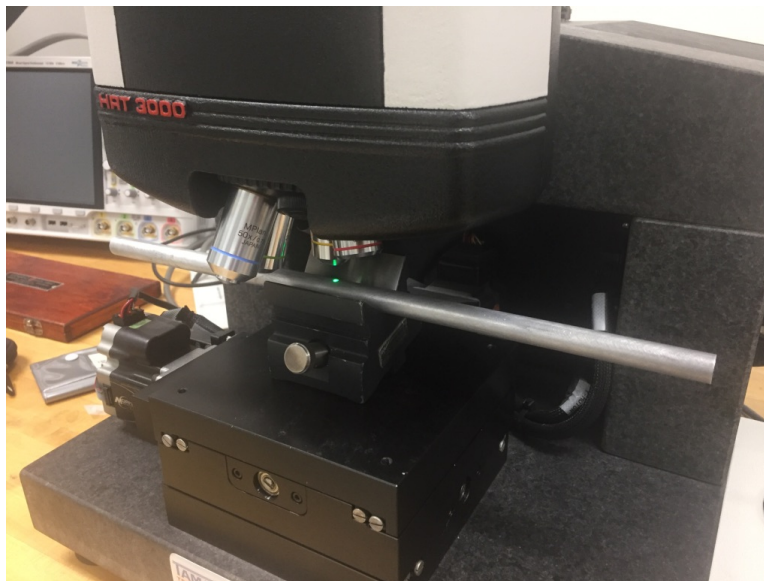


*Figure 12.4: Surface roughness testing of aluminum sleeve using Tamar HRT 3000.*

## 12.2 Pre Impact Torsion Data Analysis

### General Linear Model: Mean Effe. Shear Modulus (psi) versus Batch, Sleeve Thickness

Method

Factor coding (-1, 0, +1)

Factor Information

Factor	Type	Levels	Values
Batch	Random	5	1, 2, 3, 4, 5
Sleeve Thickness	Fixed	3	0.000, 0.020, 0.028

Analysis of Variance

Source	DF	Adj SS	Adj MS	F-Value	P-Value
Batch	4	73281536597	18320384149	1.09	0.411 x
Sleeve Thickness	2	8.79153E+11	4.39576E+11	25.89	0.000 x
Batch*Sleeve Thickness	8	1.25516E+11	15689556706	0.39	0.909
Error	14	5.65267E+11	40376202742		
Total	28	1.64509E+12			

x Not an exact F-test.

Model Summary

S	R-sq	R-sq(adj)	R-sq(pred)
200938	65.64%	31.28%	*

*Figure 12.5: General linear model output of effective shear modulus for pre impact torsion samples.*

Based on the analysis, the sleeve thickness factor appeared significant. The batch\*sleeve thickness interaction does not appear significant, and therefore was reduced.

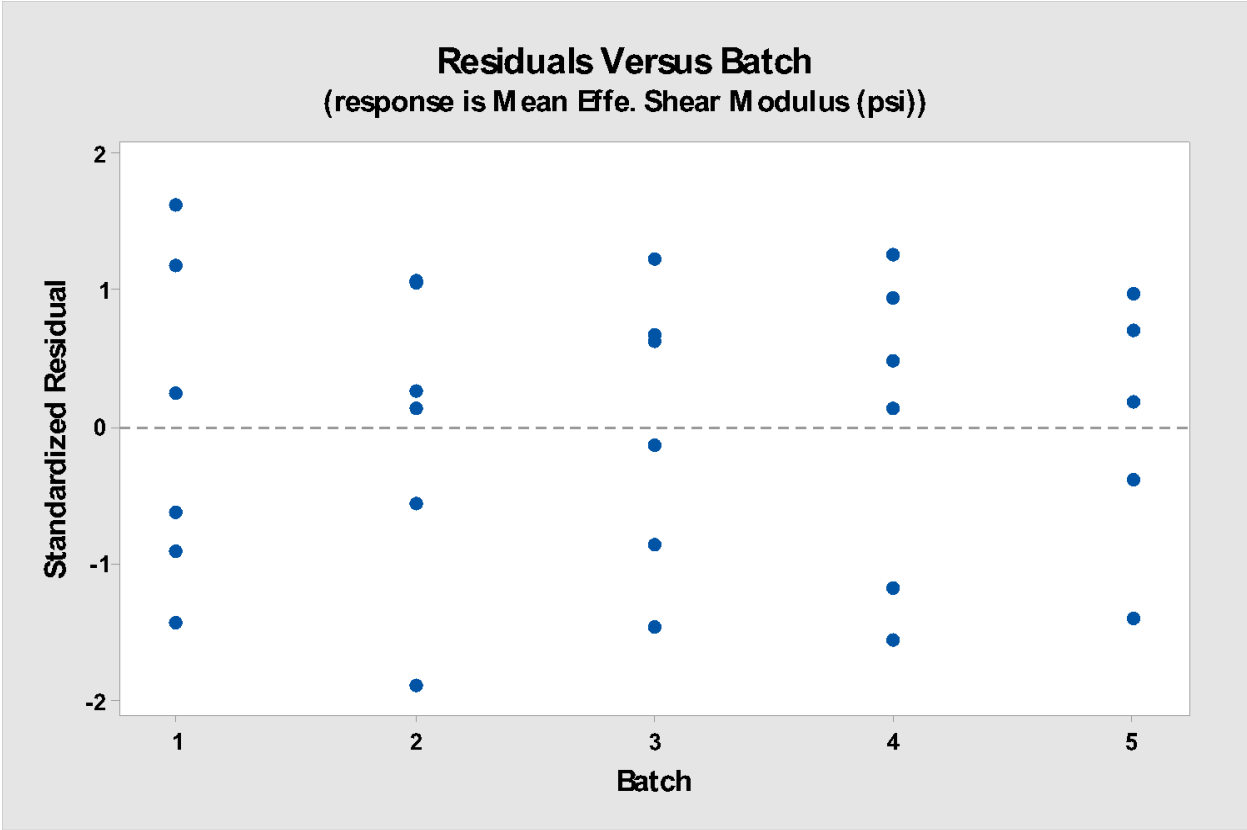


Figure 12.6: Residuals vs. batch for pre impact torsion samples.

Based on the residuals vs. batch plot, the data appeared to have equal variance.

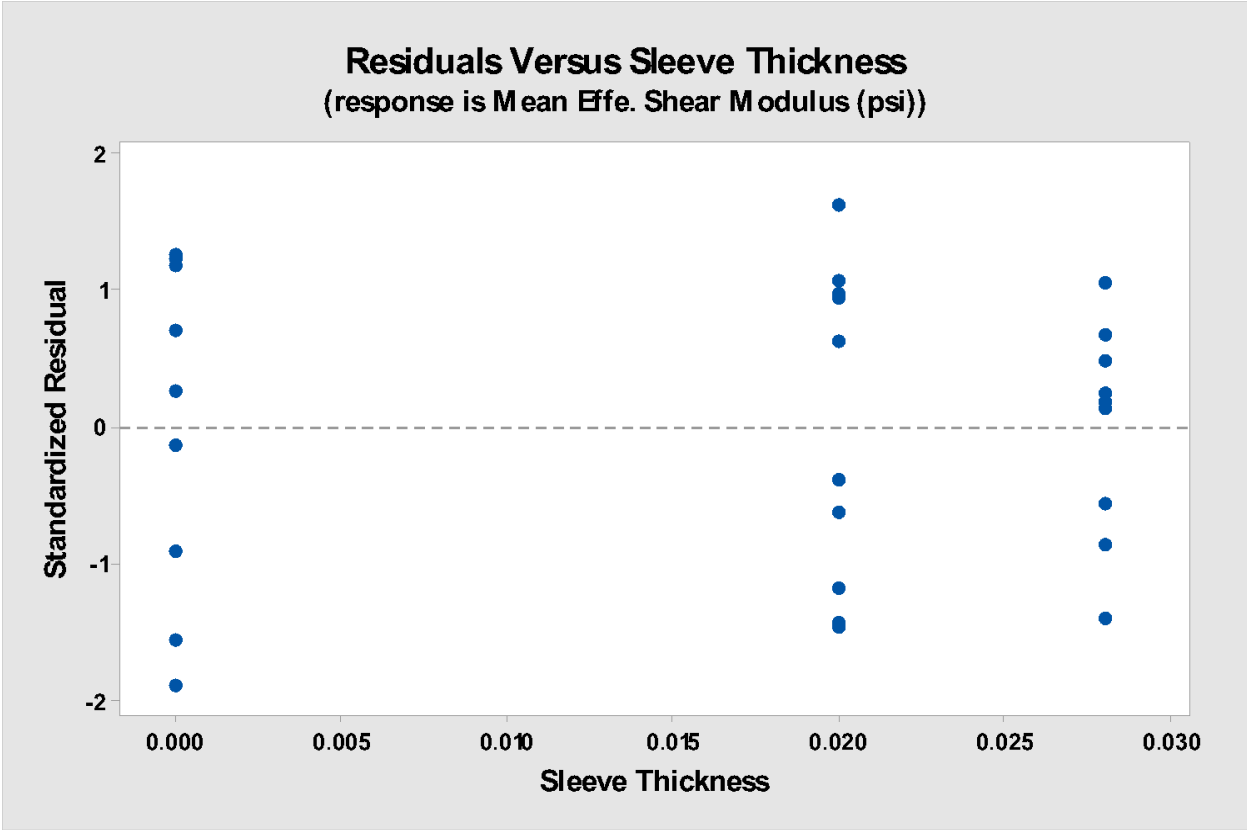


Figure 12.7: Residuals vs. sleeve thickness for pre impact torsion samples.

Based on the residuals vs. sleeve thickness plot, the data appeared to have equal variance.

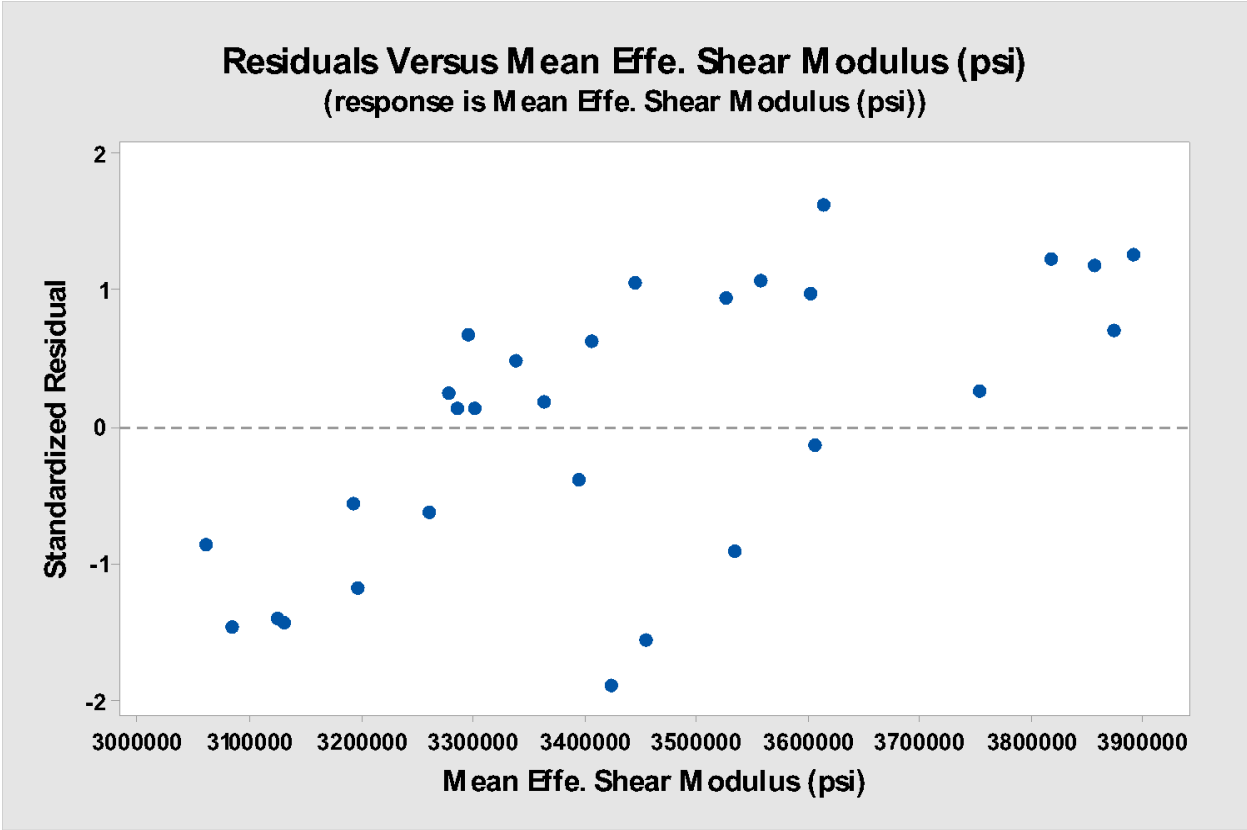
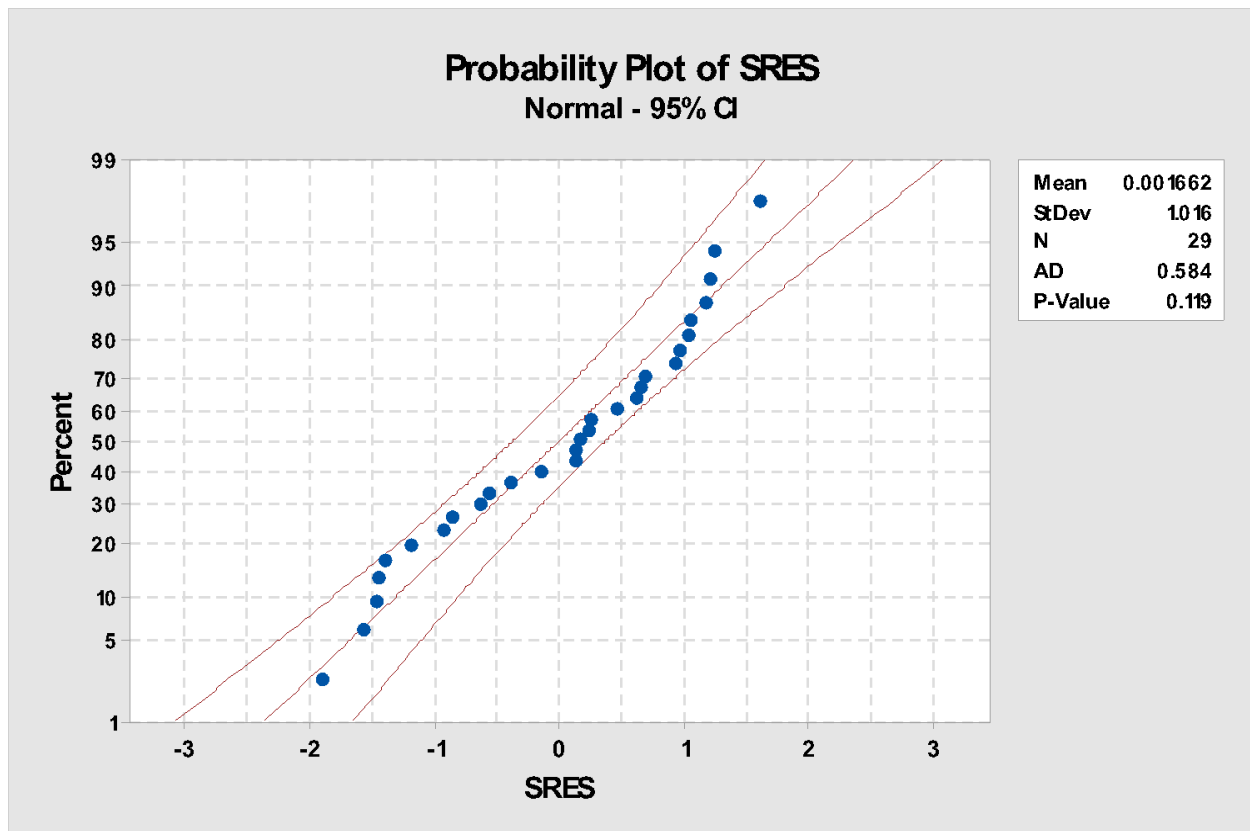


Figure 12.8: Residuals vs. effective shear modulus for pre impact torsion samples.

Based on the residuals vs. effective modulus plot, the data appeared to have equal variance.



*Figure 12.9: Normal probability plot for pre impact torsion samples.*

The normal probability plot of standardized residuals showed a p value of 0.119, greater than the  $\alpha$  of 0.05. Therefore, it was necessary to fail to reject the null hypothesis that the data comes from a normal population.

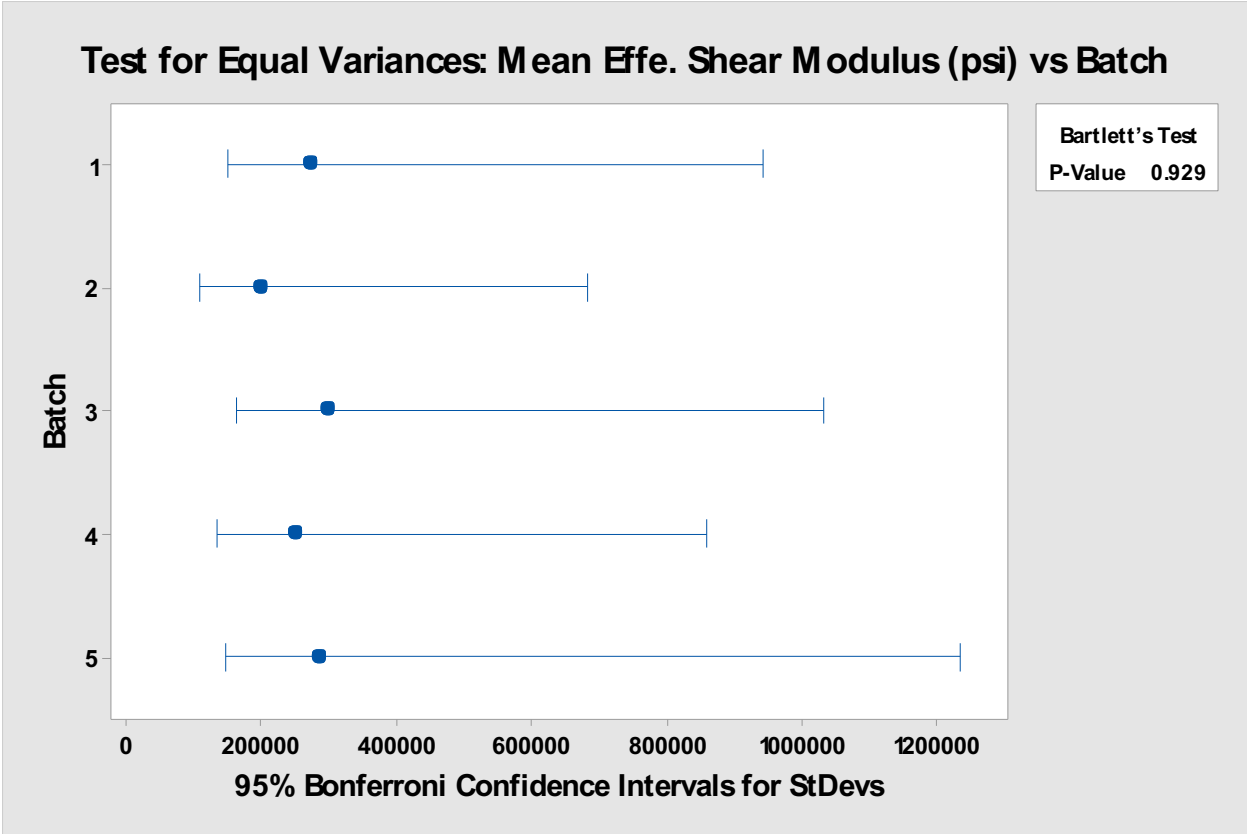
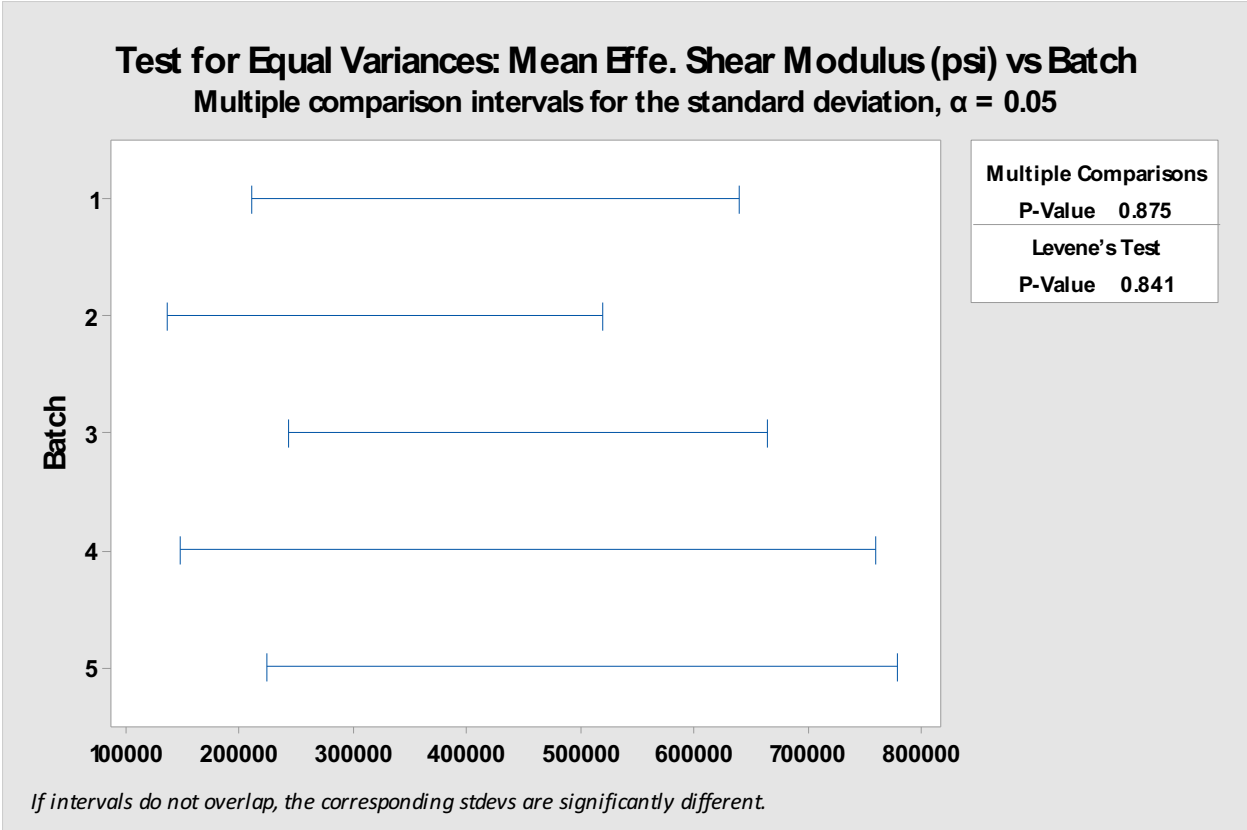


Figure 12.10: Bartlett's vs. batch test for pre impact torsion samples.

The Bartlett's test for equal variances (which was based on the assumption of a normal distribution) showed a p-value of 0.929, greater than the  $\alpha$  of 0.05. Therefore, it was necessary to fail to reject the null hypothesis that the data has equal variance for this factor.



*Figure 12.11: Levene's vs. batch test for pre impact torsion samples.*

The Levene's test for equal variances (which was not based on the assumption of a normal distribution) showed a p-value of 0.841, greater than the  $\alpha$  of 0.05. Therefore, it was necessary to fail to reject the null hypothesis that the data has equal variance for this factor.

### Test for Equal Variances: Mean Effe. Shear Modulus (psi) vs Sleeve Thickness

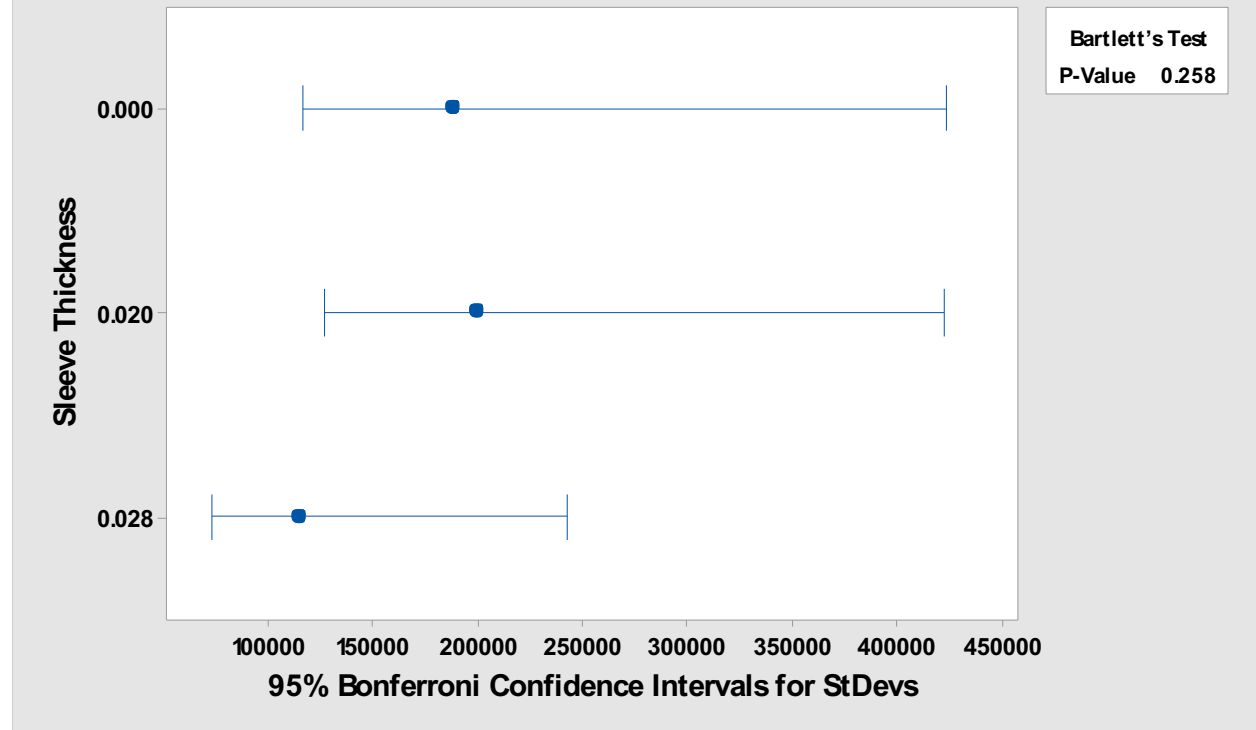
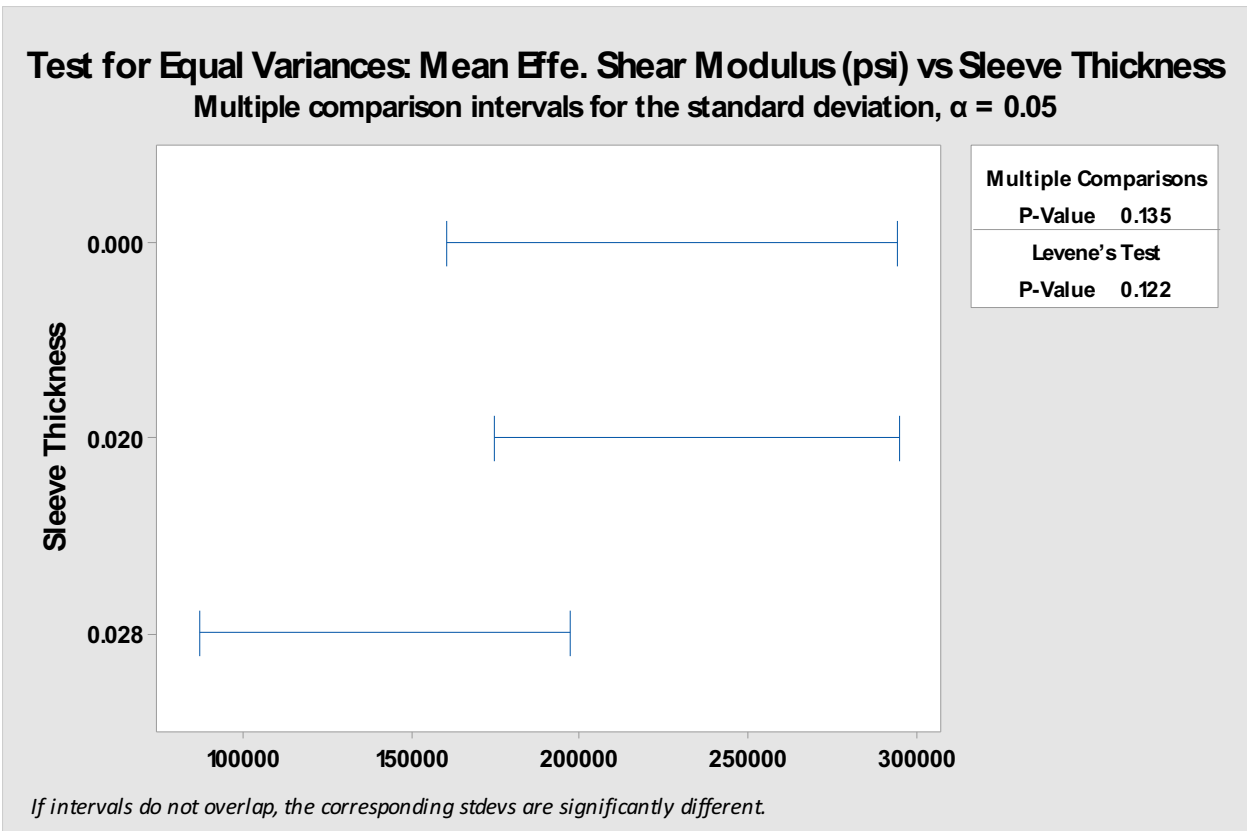


Figure 12.12: Bartlett's vs. sleeve thickness test for pre impact torsion samples.

The Bartlett's test for equal variances showed a p-value of 0.258, greater than the  $\alpha$  of 0.05. Therefore, it was necessary to fail to reject the null hypothesis that the data has equal variance for this factor.



*Figure 12.13: Levene's vs. sleeve thickness test for pre impact torsion samples.*

The Levene's test for equal variances showed a p-value of 0.122, greater than the  $\alpha$  of 0.05. Therefore, it was necessary to fail to reject the null hypothesis that the data has equal variance for this factor.

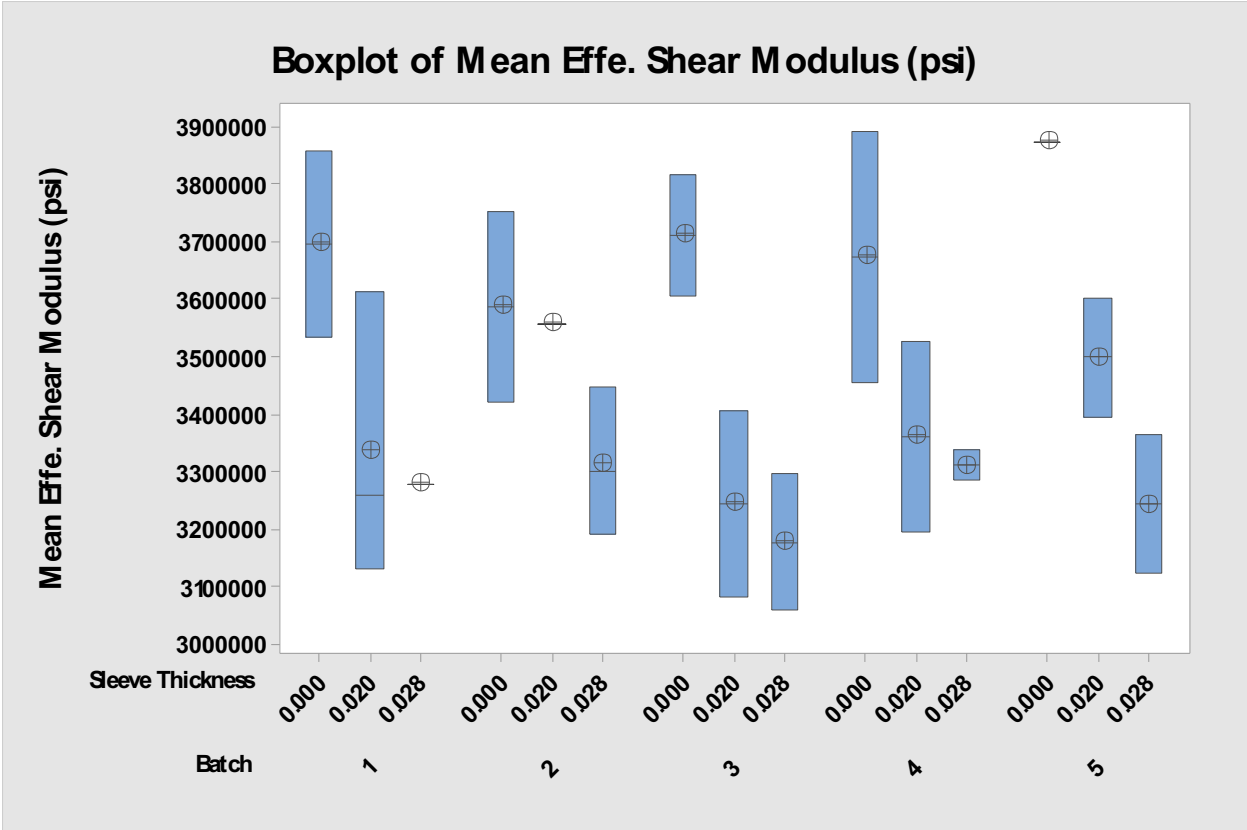


Figure 12.14: Boxplot of shear modulus vs. batch and sleeve thickness for pre impact torsion samples.

Based on the plot of effective modulus vs. batch and sleeve thickness, no higher level correlations could be determined. The batch factor was removed to help determine correlation.

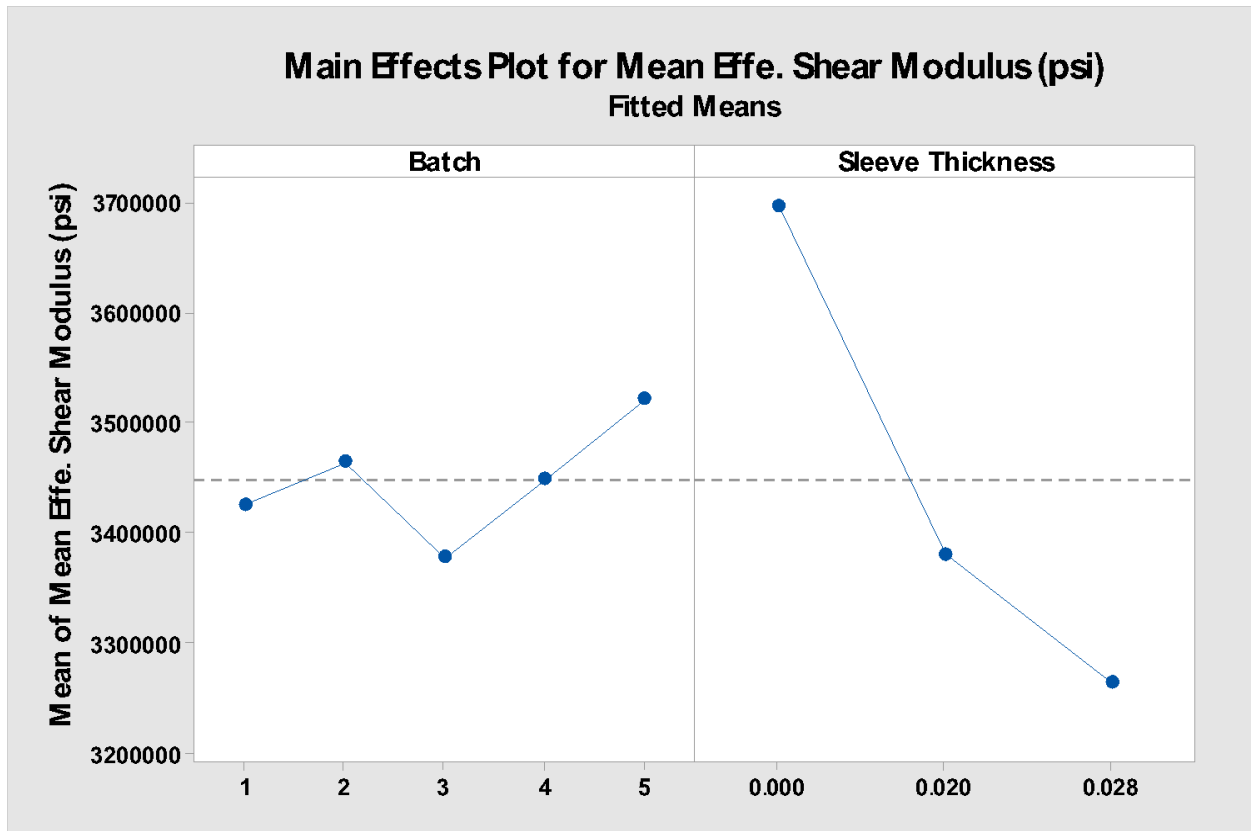


Figure 12.15: Main effects plot for pre impact torsion samples.

The main effects plot shows the batch factor levels as contributing the least to effective modulus response variance. Sleeve thickness factor levels appear to contribute the greatest to effective modulus response variance.

## 12.3 Composite Layer Data Analysis

### General Linear Model: Composite Shear Modulus (psi) versus Batch, Sleeve Thickness (in)

Method

Factor coding (-1, 0, +1)

Factor Information

Factor	Type	Levels	Values
Batch	Random	5	1, 2, 3, 4, 5
Sleeve Thickness (in)	Fixed	3	0.000, 0.020, 0.028

Analysis of Variance

Source	DF	Adj SS	Adj MS	F-Value	P-Value	
Batch	4	2.91418E+16	7.28546E+15	1.58	0.259	x
Sleeve Thickness (in)	2	1.08079E+18	5.40393E+17	116.93	0.000	x
Batch*Sleeve Thickness (in)	8	3.59210E+16	4.49012E+15	0.64	0.733	
Error	14	9.81709E+16	7.01221E+15			
Total	28	1.34956E+18				

x Not an exact F-test.

Model Summary

S	R-sq	R-sq(adj)	R-sq(pred)
83738922	92.73%	85.45%	*

*Figure 12.16: General linear model of composite shear modulus for pre impact torsion samples.*

Based on the analysis, the sleeve thickness factor appeared significant. The batch\*sleeve thickness interaction does not appear significant, and therefore was reduced.

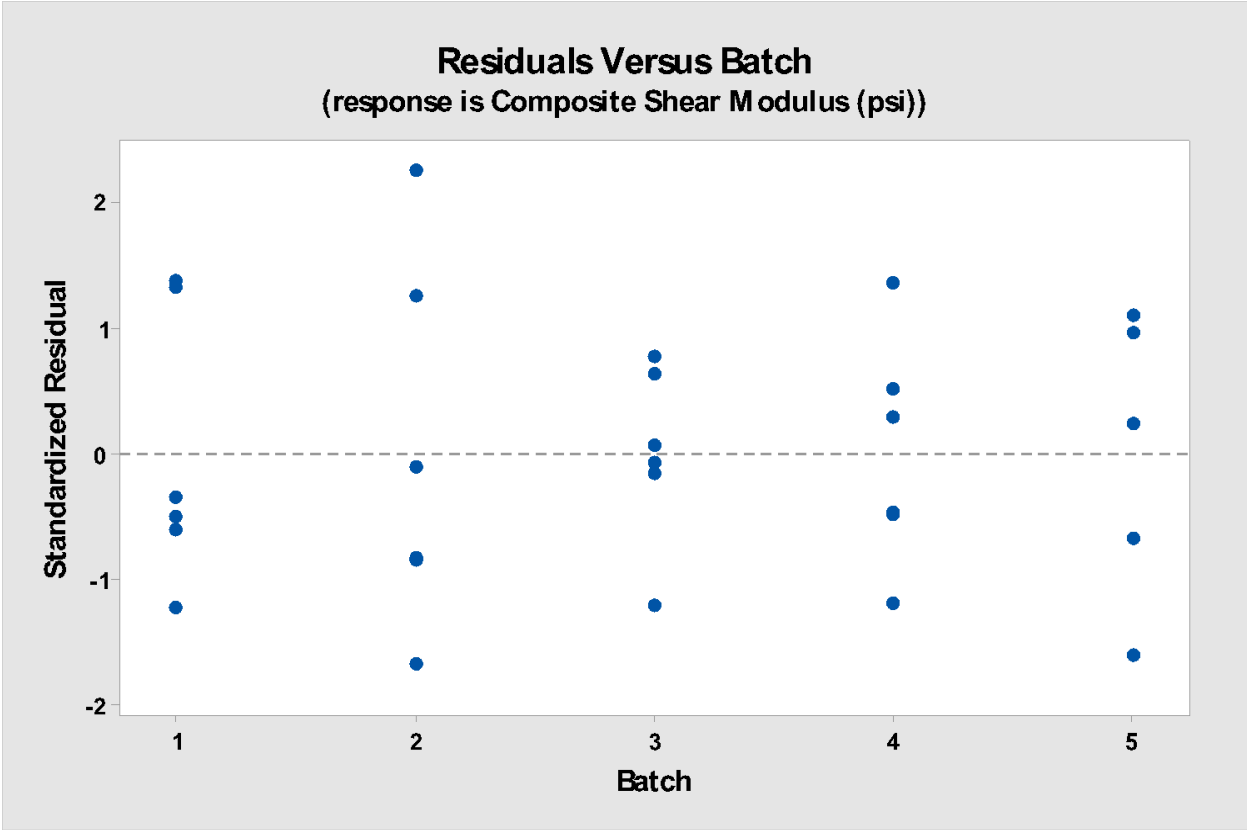


Figure 12.17: Residuals vs. batch for pre impact torsion samples.

Based on the residuals vs. batch plot, the data appeared to have equal variance.

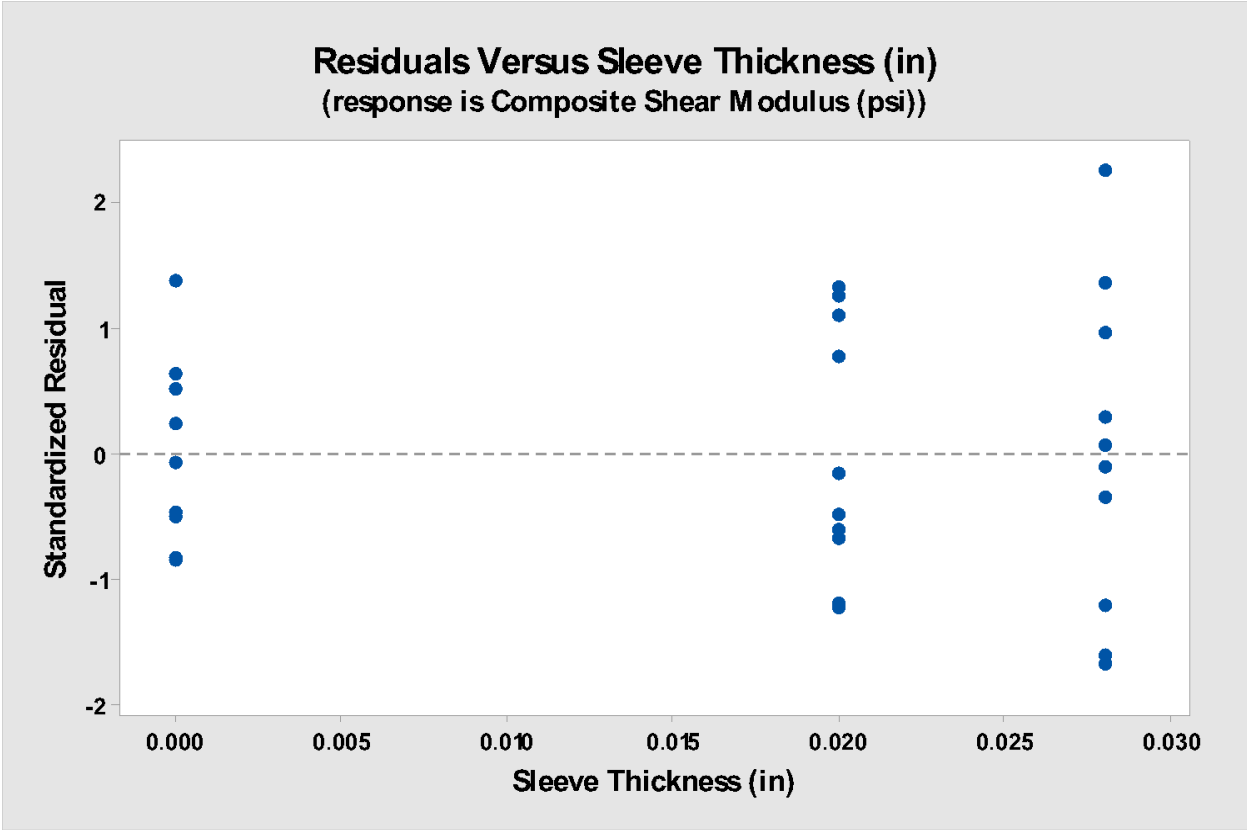


Figure 12.18: Residuals vs. sleeve thickness for pre impact torsion samples.

Based on the residuals vs. sleeve thickness plot, the data appeared to have equal variance.

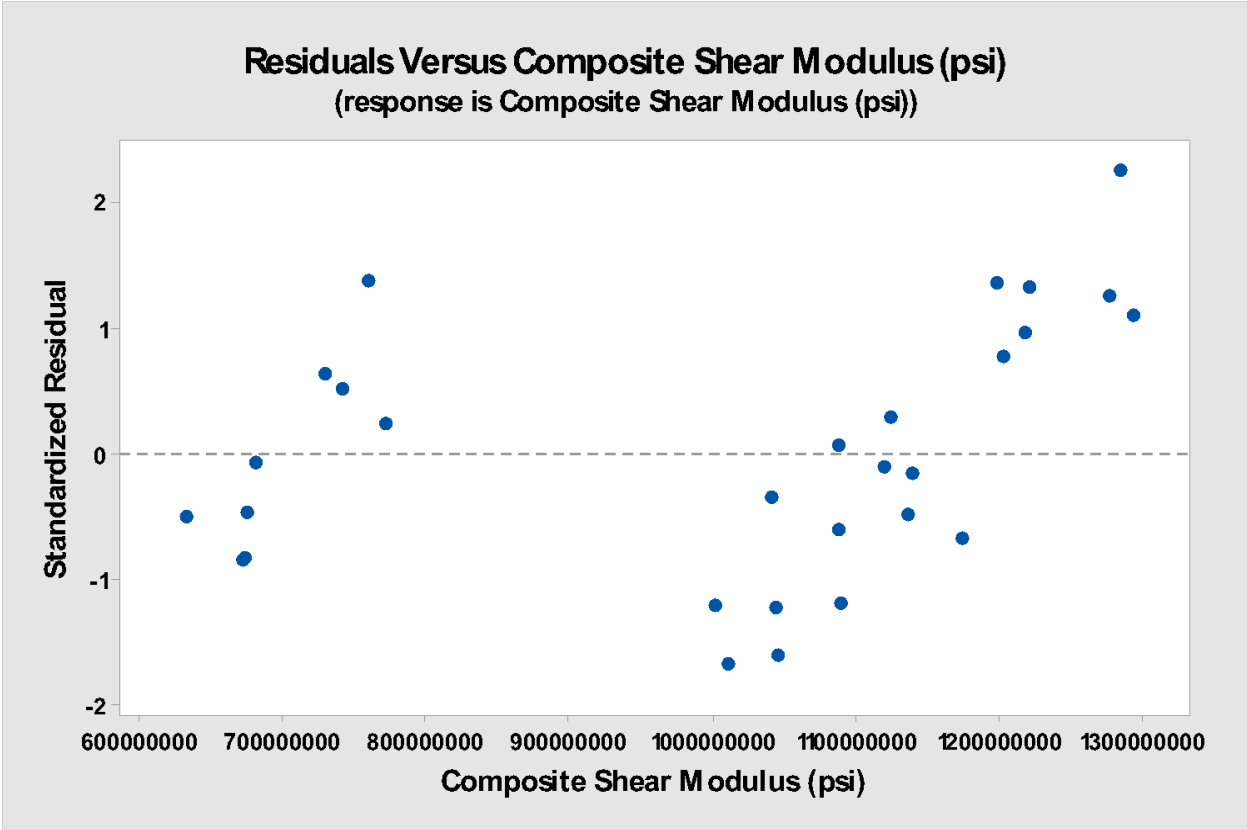
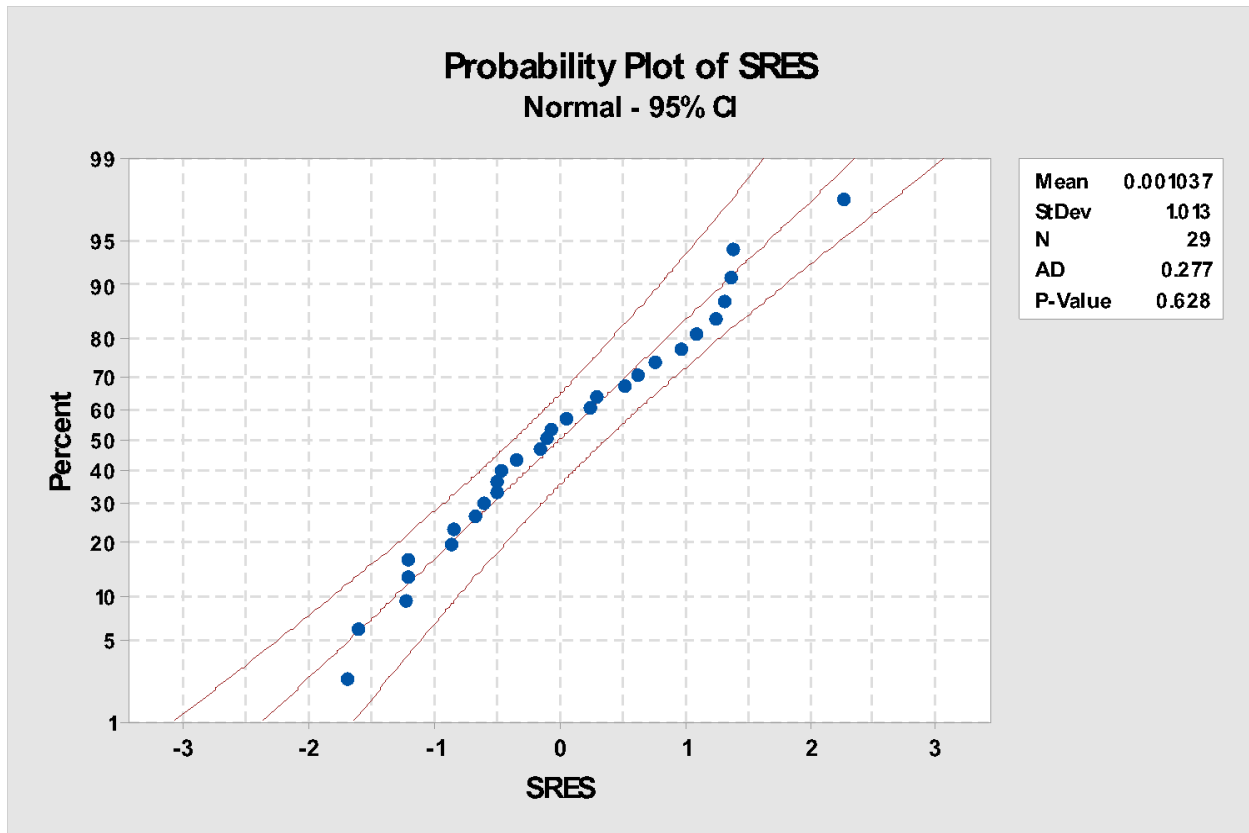


Figure 12.19: Residuals vs. composite shear modulus for pre impact torsion samples.

Based on the residuals vs. effective modulus plot, the data appeared to have equal variance.



*Figure 12.20: Normal probability plot for pre impact torsion samples.*

The normal probability plot of standardized residuals showed a p value of 0.628, greater than the  $\alpha$  of 0.05. Therefore, it was necessary to fail to reject the null hypothesis that the data comes from a normal population.

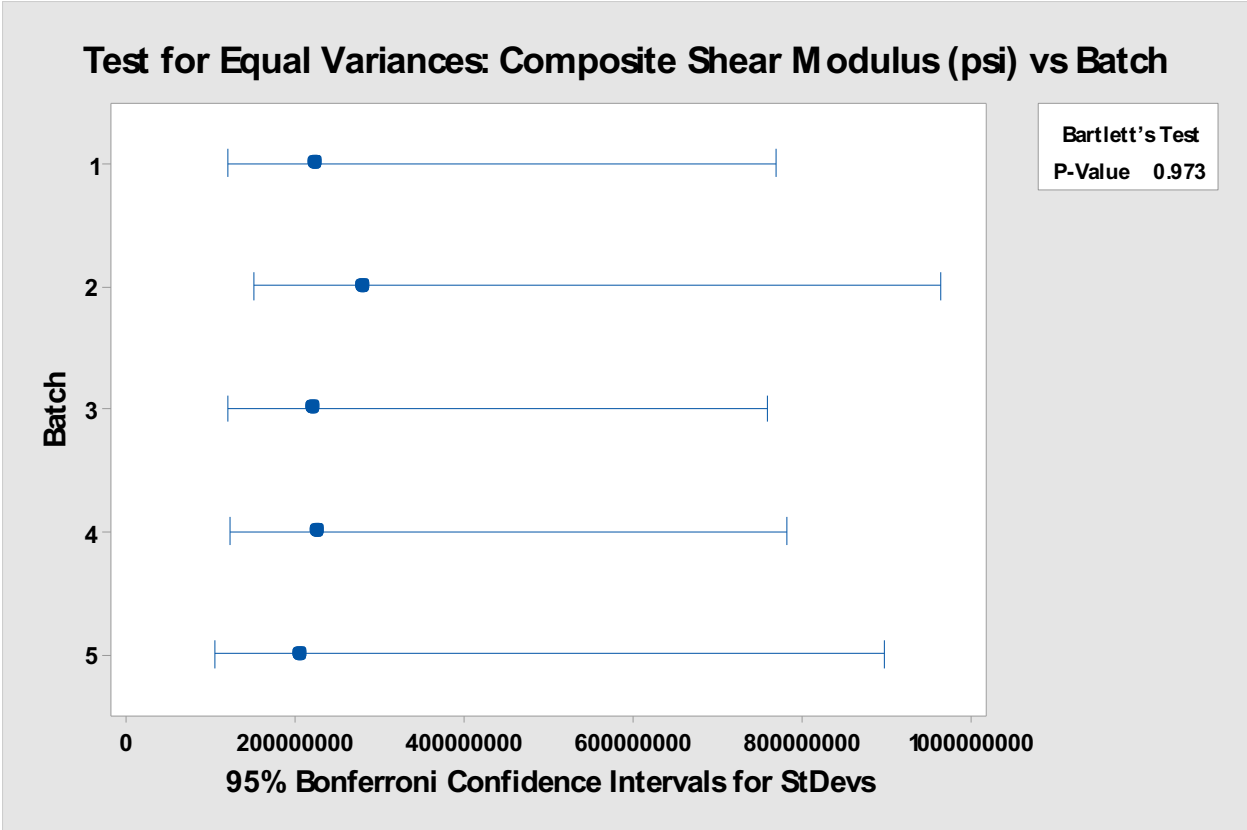
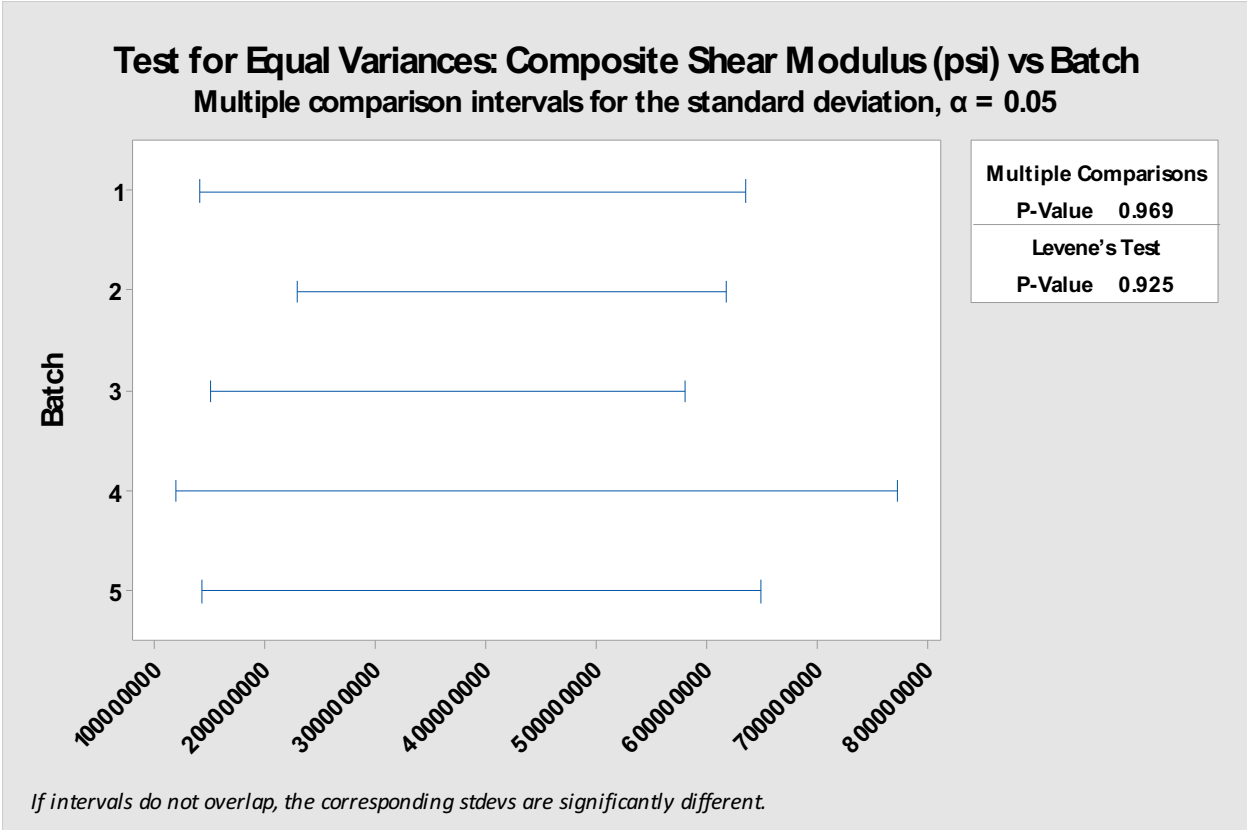


Figure 12.21: Bartlett's vs. batch for pre impact torsion samples.

The Bartlett's test for equal variances showed a p-value of 0.973, greater than the  $\alpha$  of 0.05. Therefore, it was necessary to fail to reject the null hypothesis that the data has equal variance for this factor.



*Figure 12.22: Levene's vs. batch test for pre impact torsion samples.*

The Levene's test for equal variances showed a p-value of 0.925, greater than the  $\alpha$  of 0.05. Therefore, it was necessary to fail to reject the null hypothesis that the data has equal variance for this factor.

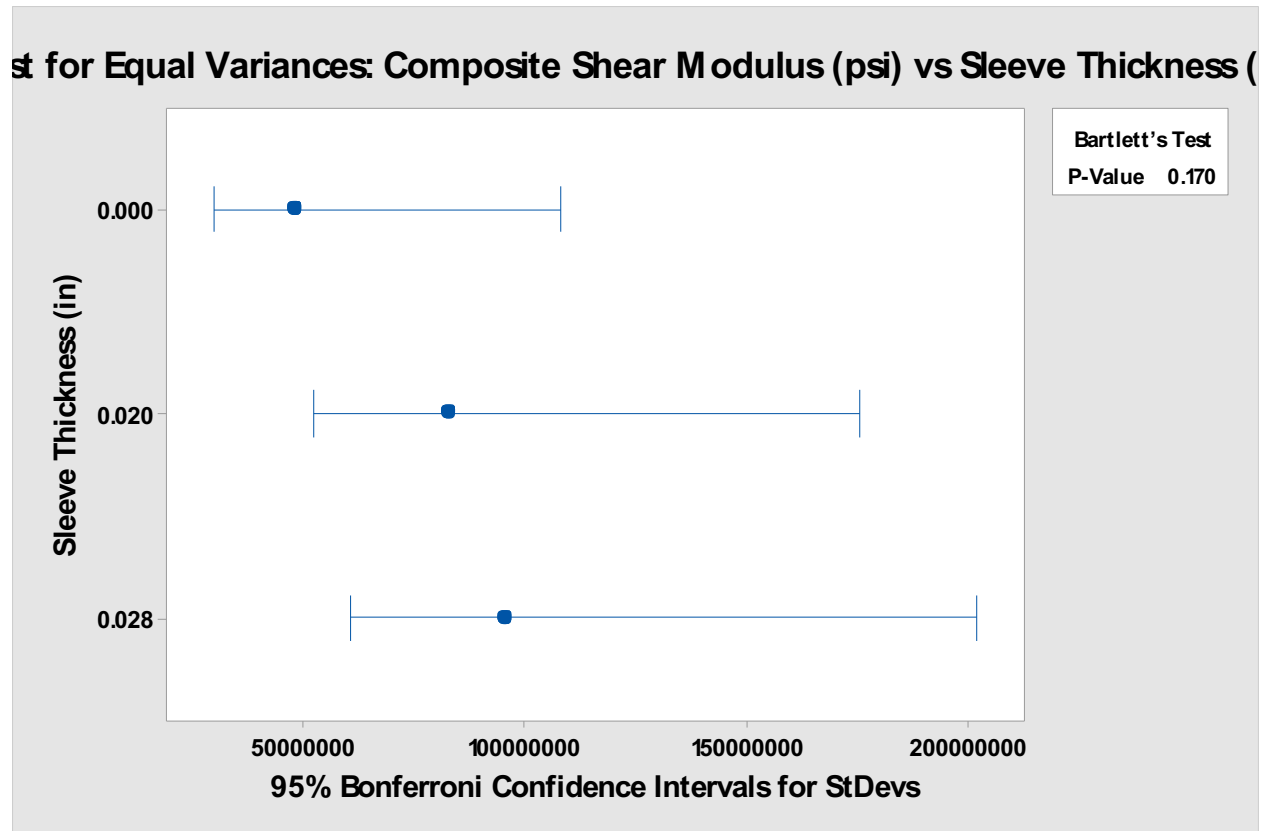
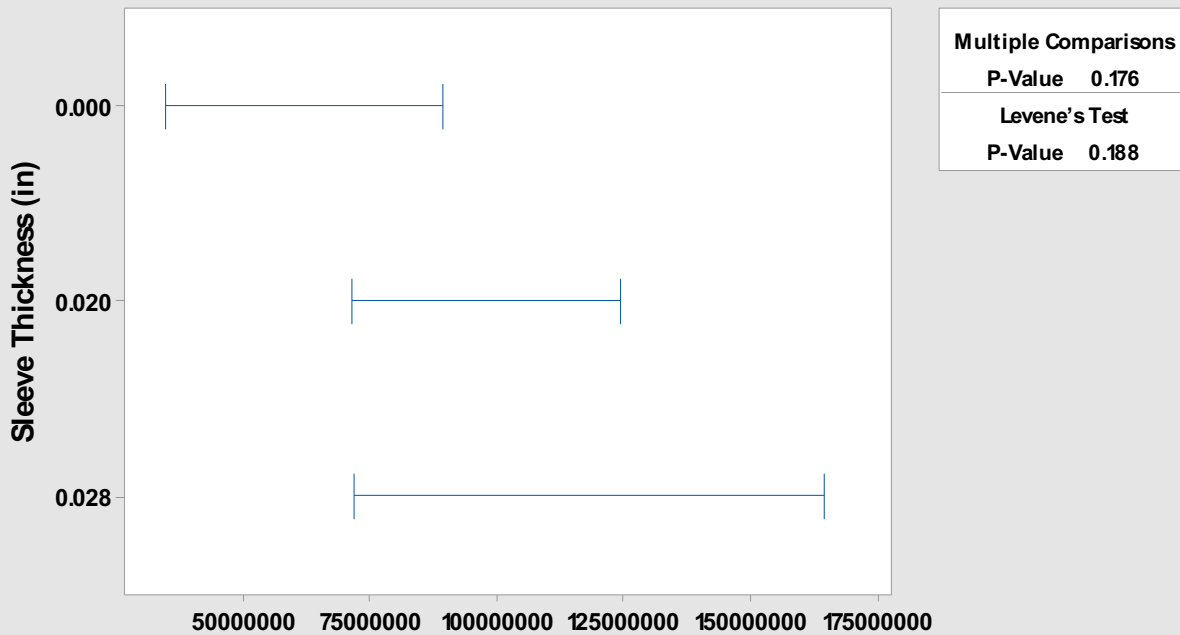


*Figure 12.23: Bartlett's vs. sleeve thickness test for pre impact torsion samples.*

The Bartlett's test for equal variances showed a p-value of 0.170, greater than the  $\alpha$  of 0.05. Therefore, it was necessary to fail to reject the null hypothesis that the data has equal variance for this factor.

**Test for Equal Variances: Composite Shear Modulus (psi) vs Sleeve Thickness (in)**  
**Multiple comparison intervals for the standard deviation,  $\alpha = 0.05$**



*If intervals do not overlap, the corresponding stdevs are significantly different.*

*Figure 12.24: Levene's vs. sleeve thickness test for pre impact torsion samples.*

The Levene's test for equal variances showed a p-value of 0.188, greater than the  $\alpha$  of 0.05. Therefore, it was necessary to fail to reject the null hypothesis that the data has equal variance for this factor.

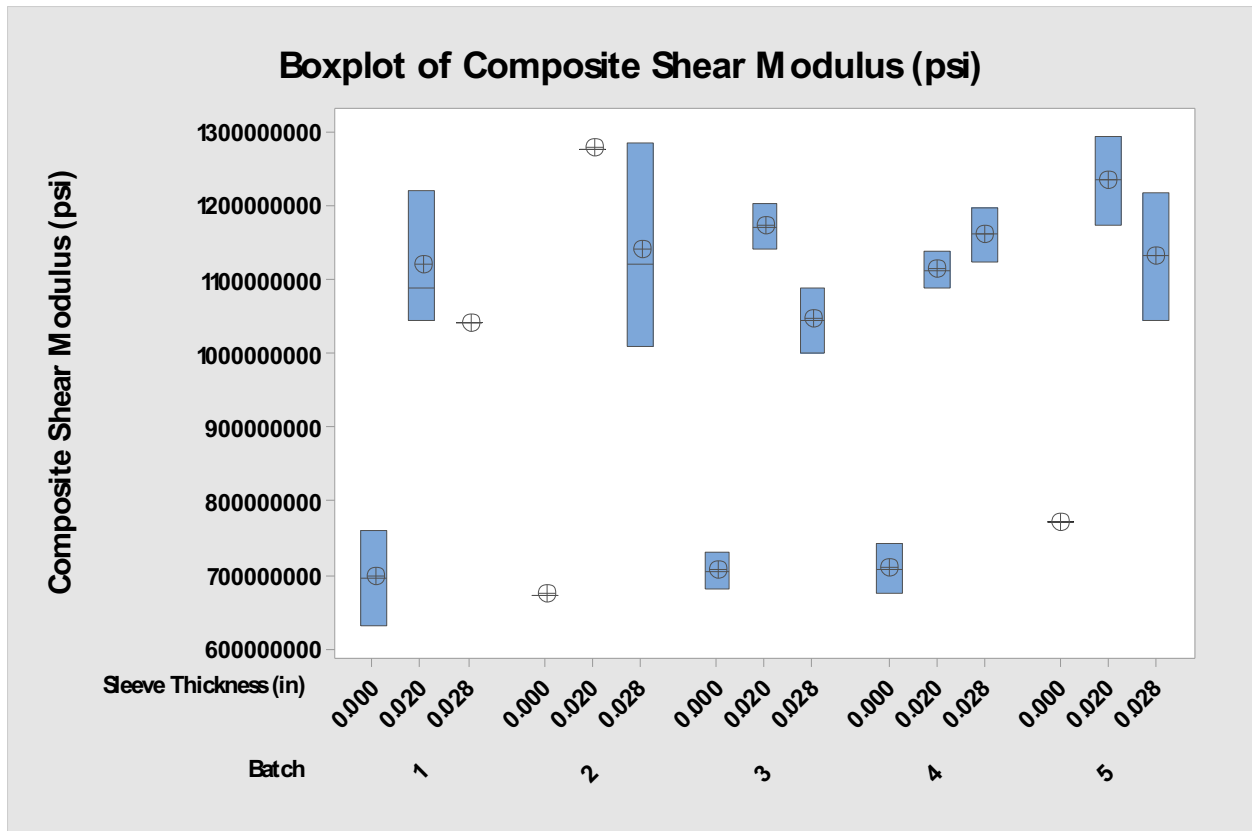


Figure 12.25: Boxplot of shear modulus vs. batch and sleeve thickness for pre impact torsion samples.

Based on the plot of effective modulus vs. batch and sleeve thickness, no higher level correlations could be determined. The batch factor was removed to help determine correlation.

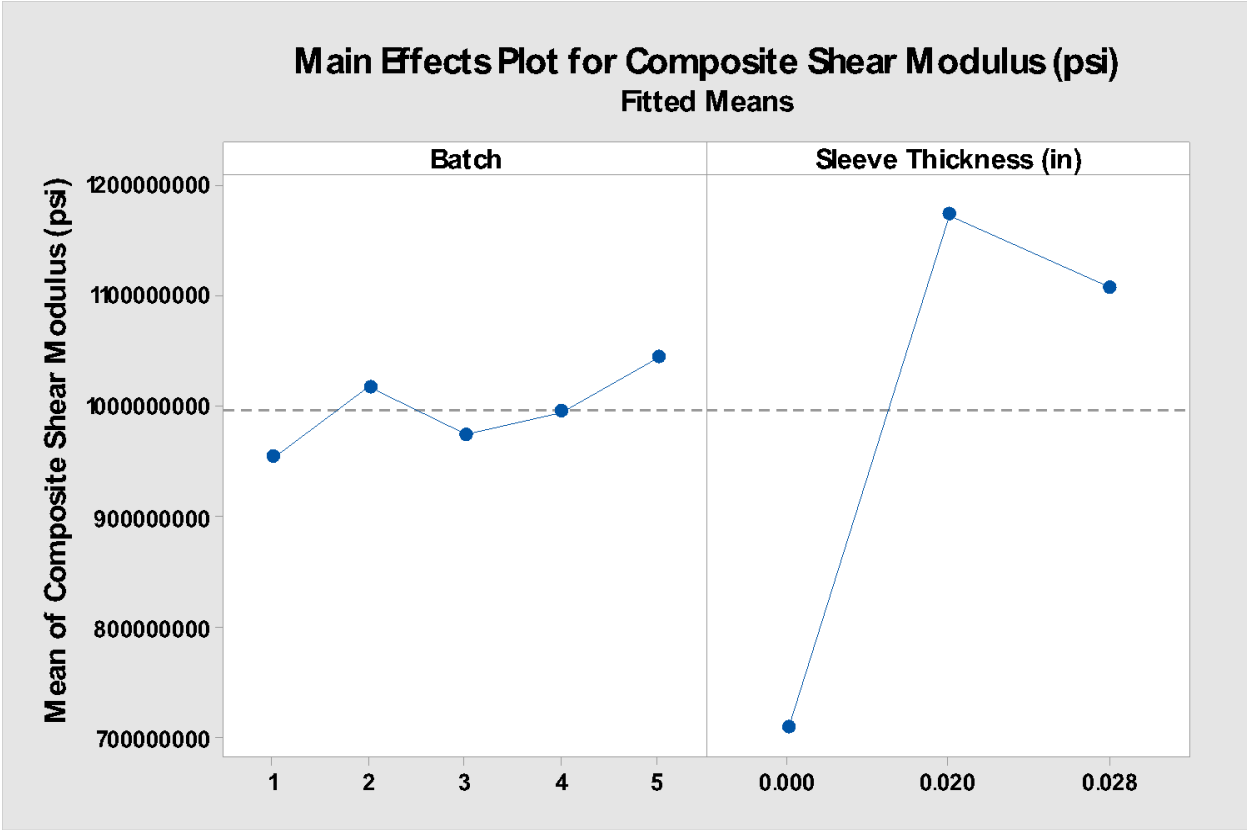


Figure 12.26: Main effects plot of shear modulus for pre impact torsion samples.

The main effects plot shows the batch factor levels as contributing the least to effective modulus response variance. Sleeve thickness factor levels appear to contribute the greatest to effective modulus response variance.

## 12.4 Pre Impact Tension Data Analysis

### General Linear Model: Mean Effe. Tens. Modulus (psi) versus Batch, Sleeve Thickness (in)

The following terms cannot be estimated and were removed:  
Batch\*Sleeve Thickness (in)

Method

Factor coding (-1, 0, +1)

Factor Information

Factor	Type	Levels	Values
Batch	Random	5	1, 2, 3, 4, 5
Sleeve Thickness (in)	Fixed	3	0.000, 0.020, 0.028

Analysis of Variance

Source	DF	Adj SS	Adj MS	F-Value	P-Value
Batch	4	73581427872	18395356968	0.56	0.696
Sleeve Thickness (in)	2	1.60408E+12	8.02039E+11	24.32	0.000
Error	17	5.60543E+11	32973122997		
Lack-of-Fit	7	1.86431E+11	26632941672	0.71	0.665
Pure Error	10	3.74112E+11	37411249925		
Total	23	2.40235E+12			

Model Summary

S	R-sq	R-sq(adj)	R-sq(pred)
181585	76.67%	68.43%	57.23%

*Figure 12.27: General linear model of tensile modulus for pre impact tension samples.*

Based on the analysis, the sleeve thickness factor appeared significant. The batch factor did not appear to be significant. The batch\*sleeve thickness factor could not be estimated, and was therefore reduced.

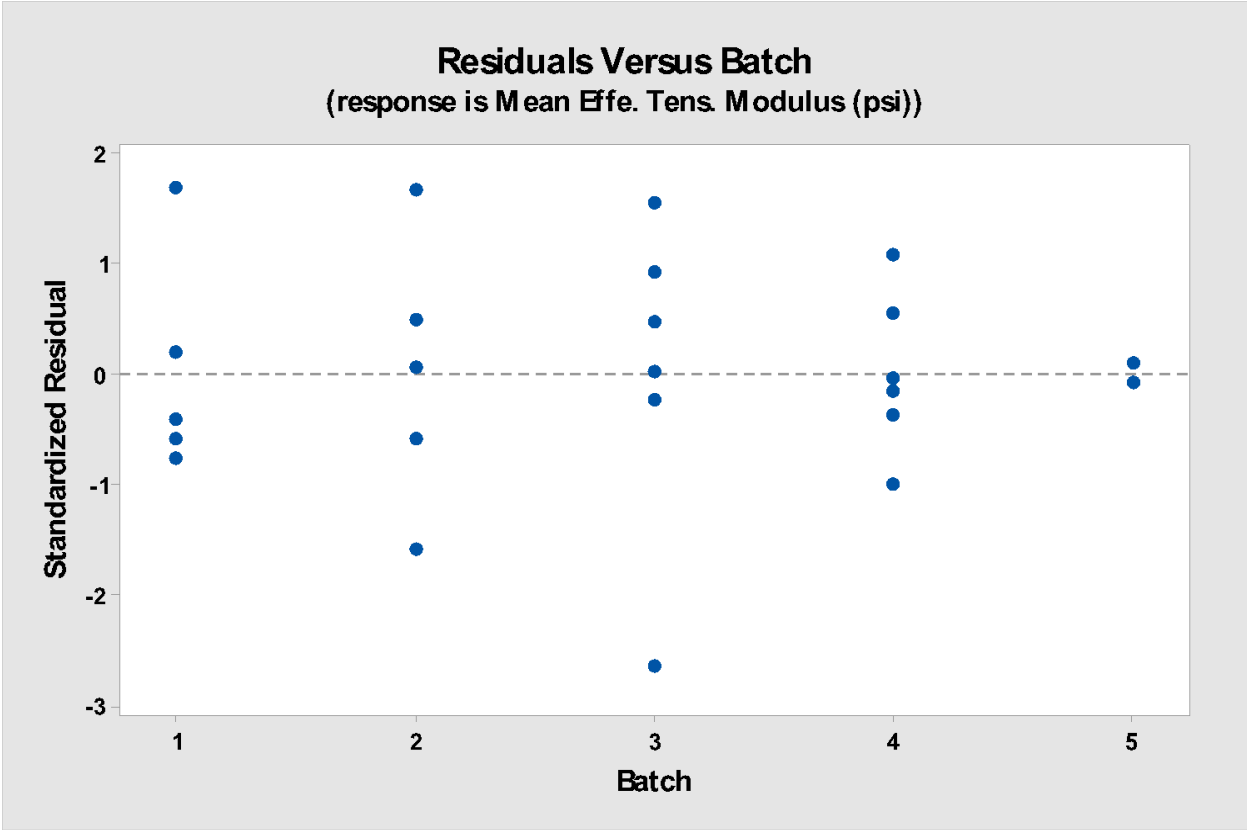


Figure 12.28: Residuals vs. batch for pre impact tension samples.

Based on the residuals vs. batch plot, the data appeared to have equal variance.

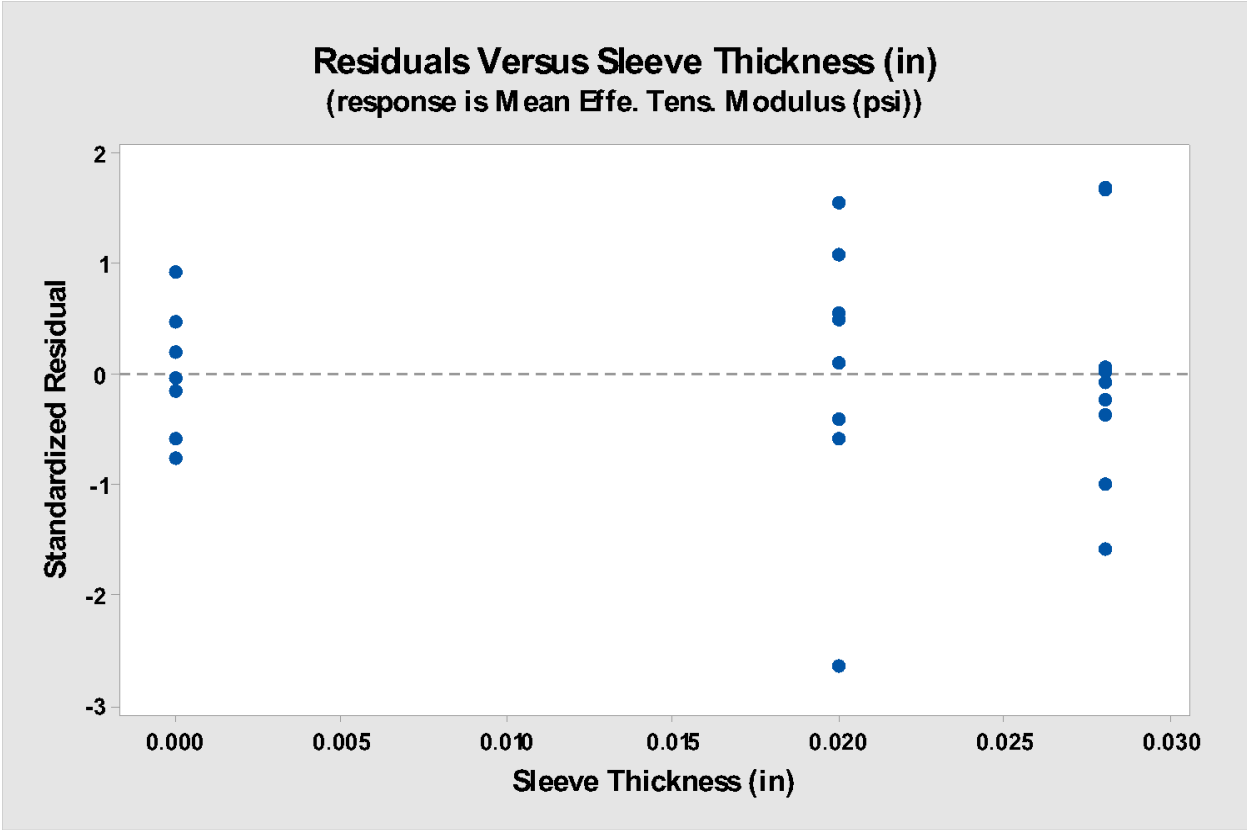


Figure 12.29: Residuals vs. sleeve thickness for pre impact tension samples.

Based on the residuals vs. sleeve thickness plot, the data appeared to have equal variance.

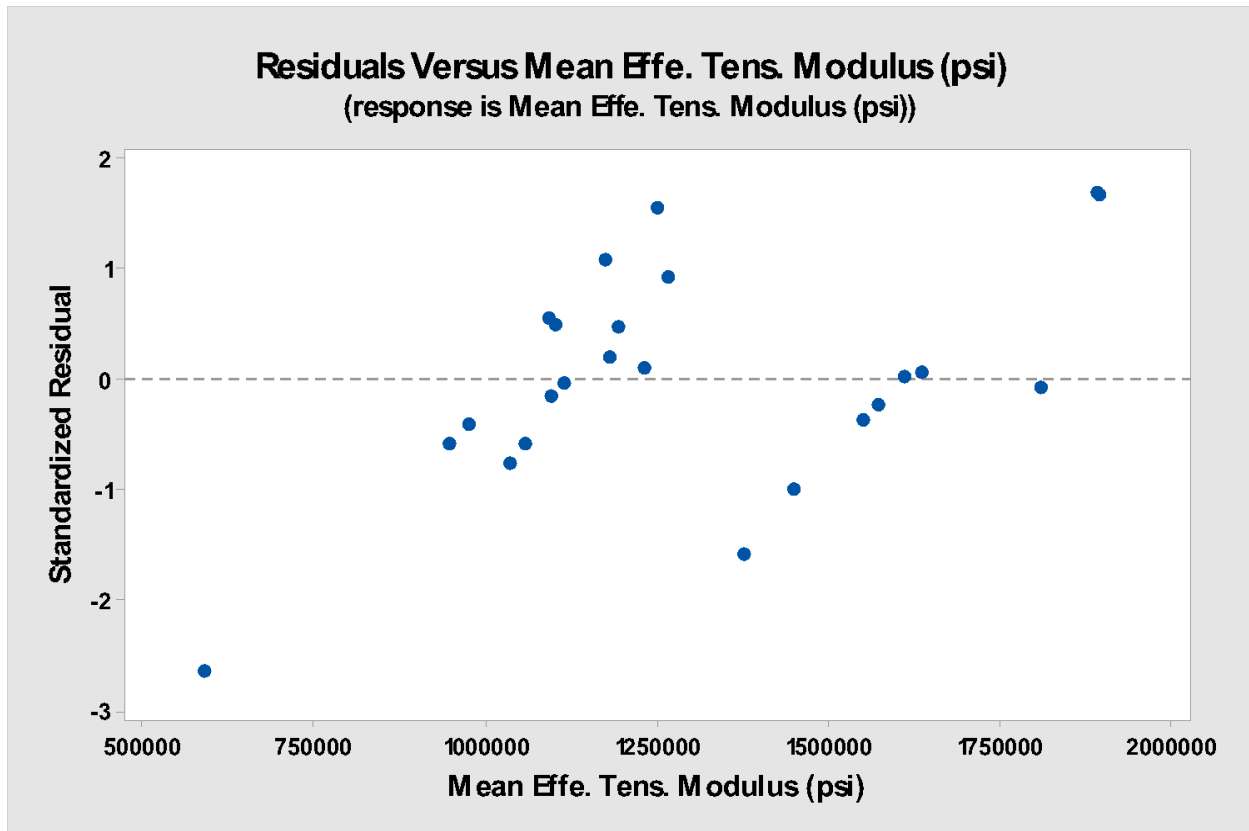
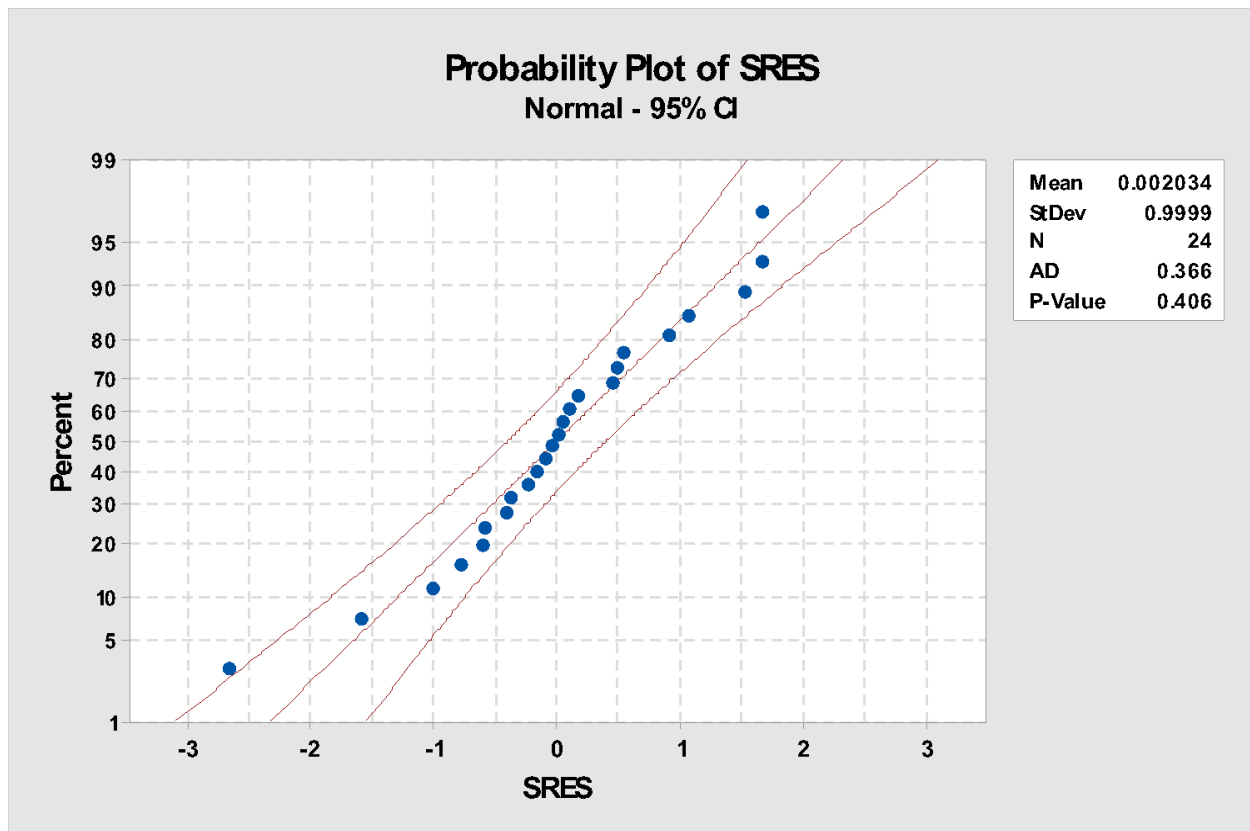


Figure 12.30: Residuals vs. effective tensile modulus for pre impact tension samples.

Based on the residuals vs. effective modulus plot, the data appeared to have equal variance.



*Figure 12.31: Normal probability plot for pre impact tension samples.*

The normal probability plot of standardized residuals showed a p value of 0.406, greater than the  $\alpha$  of 0.05. Therefore, it was necessary to fail to reject the null hypothesis that the data comes from a normal population.

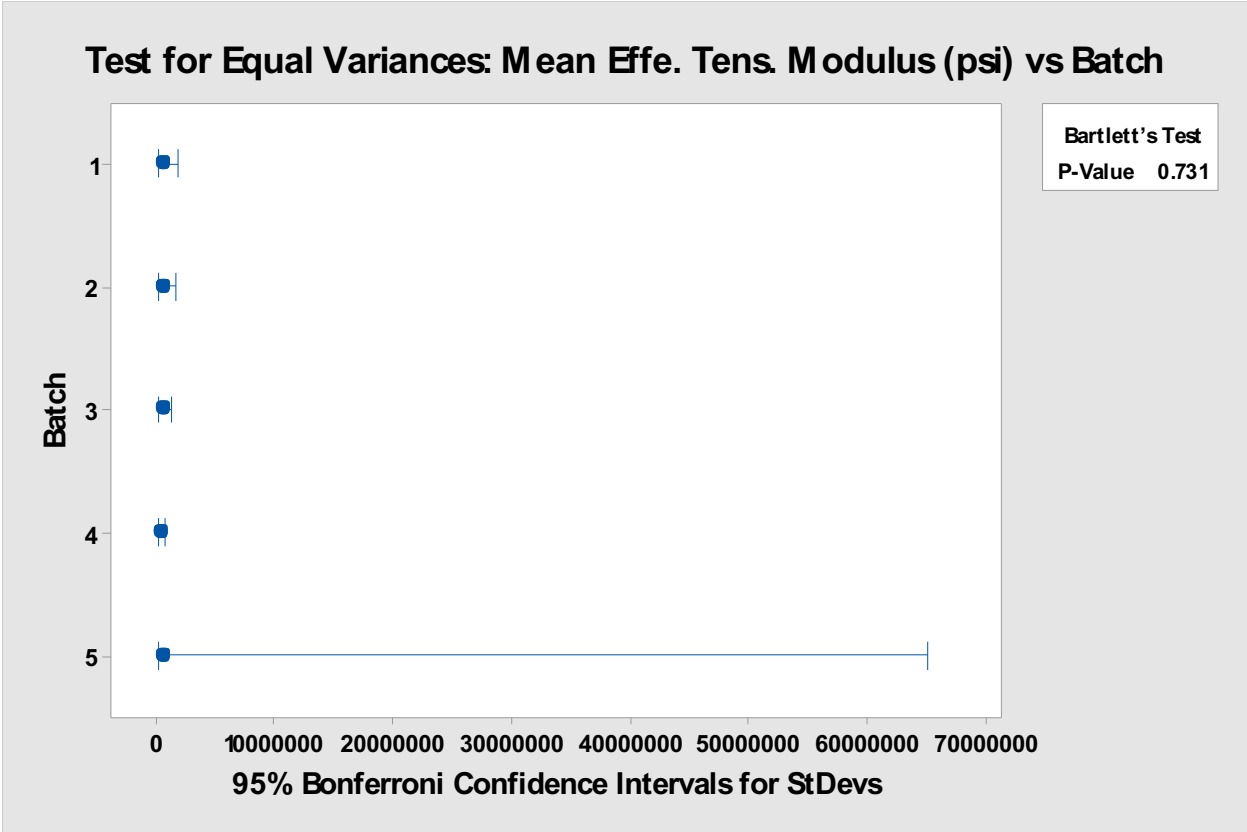


Figure 12.32: Bartlett's vs. batch test for pre impact tension samples.

The Bartlett's test for equal variances showed a p-value of 0.731, greater than the  $\alpha$  of 0.05. Therefore, it was necessary to fail to reject the null hypothesis that the data has equal variance for this factor.

### Test for Equal Variances: Mean Effe. Tens. Modulus (psi) versus Batch

Method

Null hypothesis All variances are equal  
Alternative hypothesis At least one variance is different  
Significance level  $\alpha = 0.05$

95% Bonferroni Confidence Intervals for Standard Deviations

Batch	N	StDev	CI
1	5	392881	( 66995, 4752091)
2	5	356068	(120138, 2176659)
3	6	366369	( 99240, 2369974)
4	6	201036	( 29816, 2375132)
5	2	408478	( *, *)

Individual confidence level = 99%

Tests

Method	Test	
	Statistic	P-Value
Multiple comparisons	-	0.746
Levene	0.25	0.903

\* NOTE \* The graphical summary cannot be displayed because the multiple comparison intervals cannot be calculated.

Figure 12.33: Levene's vs. batch test for pre impact tension samples.

The Levene's test for equal variances showed a p-value of 0.903, greater than the  $\alpha$  of 0.05. Therefore, it was necessary to fail to reject the null hypothesis that the data has equal variance for this factor. Due to the nature of the multiple comparisons test, and since there were just two samples within the batch 5 factor level, a graphical summary could not be presented.

st for Equal Variances: Mean Effe. Tens. Modulus (psi) vs Sleeve Thickness (

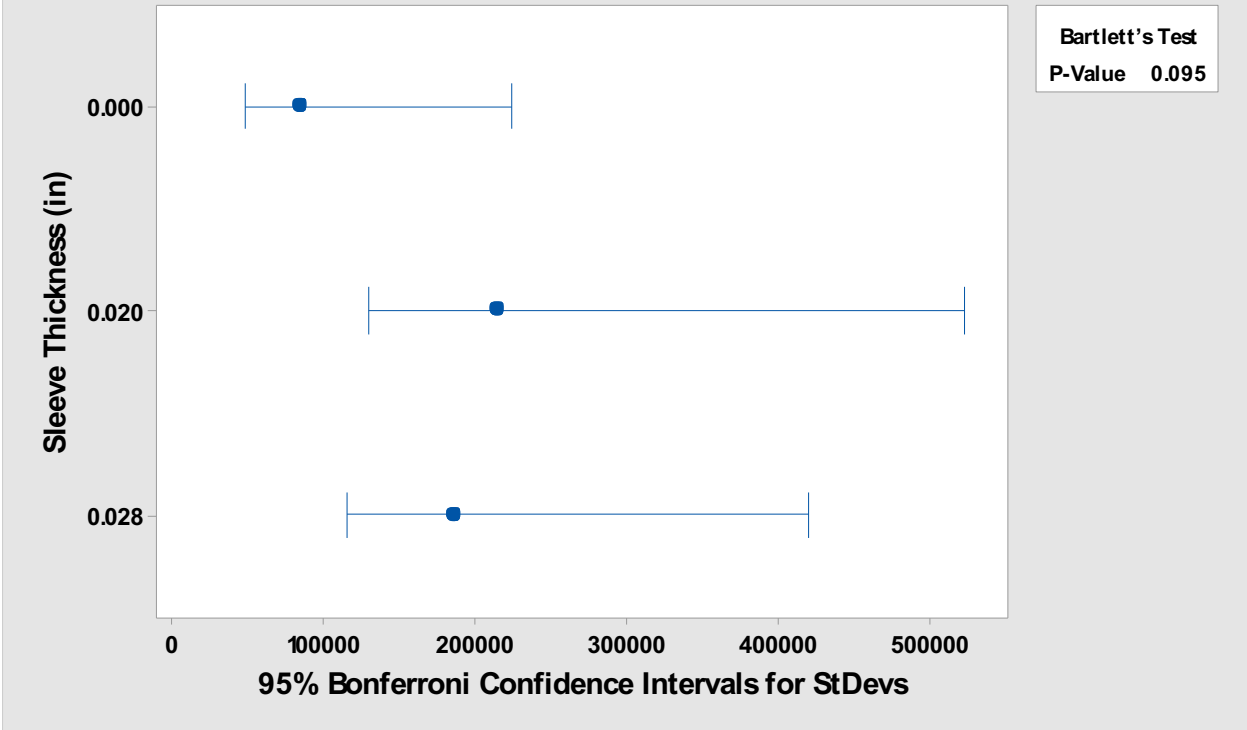
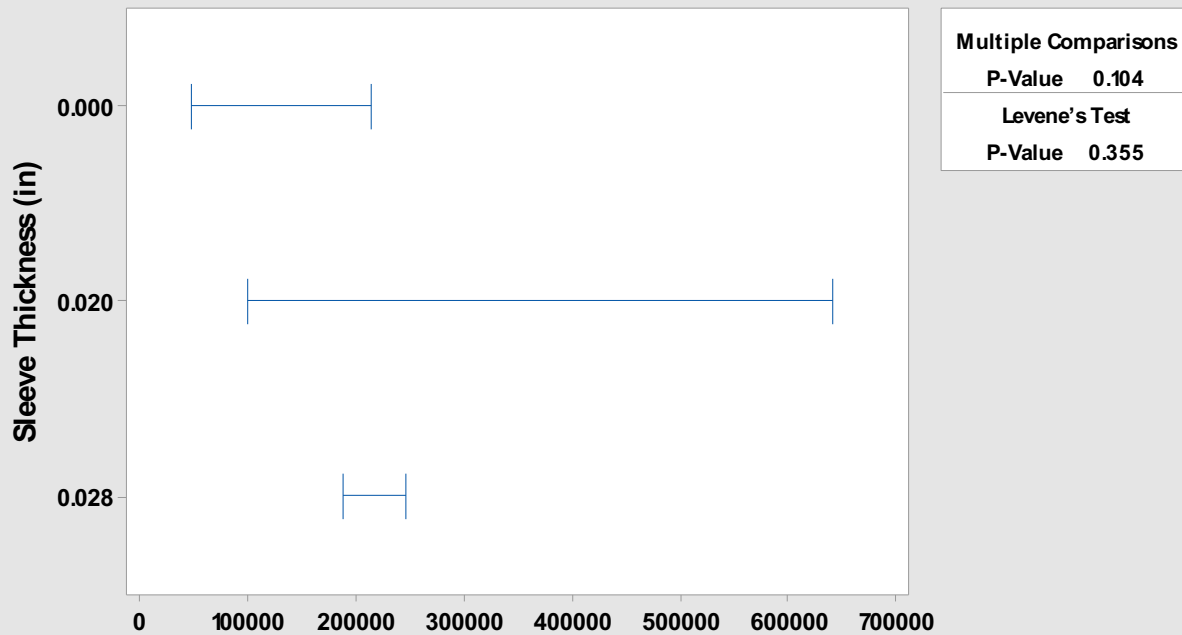


Figure 12.34: Bartlett's vs. sleeve thickness test for pre impact tension samples.

The Bartlett's test for equal variances showed a p-value of 0.095, greater than the  $\alpha$  of 0.05. Therefore, it was necessary to fail to reject the null hypothesis that the data has equal variance for this factor.

**Test for Equal Variances: Mean Effe. Tens. Modulus (psi) vs Sleeve Thickness (in)**  
**Multiple comparison intervals for the standard deviation,  $\alpha = 0.05$**



*If intervals do not overlap, the corresponding stdevs are significantly different.*

*Figure 12.35 Levene's vs. sleeve thickness test for pre impact tension samples.*

The Levene's test for equal variances showed a p-value of 0.355, greater than the  $\alpha$  of 0.05. Therefore, it was necessary to fail to reject the null hypothesis that the data has equal variance for this factor.

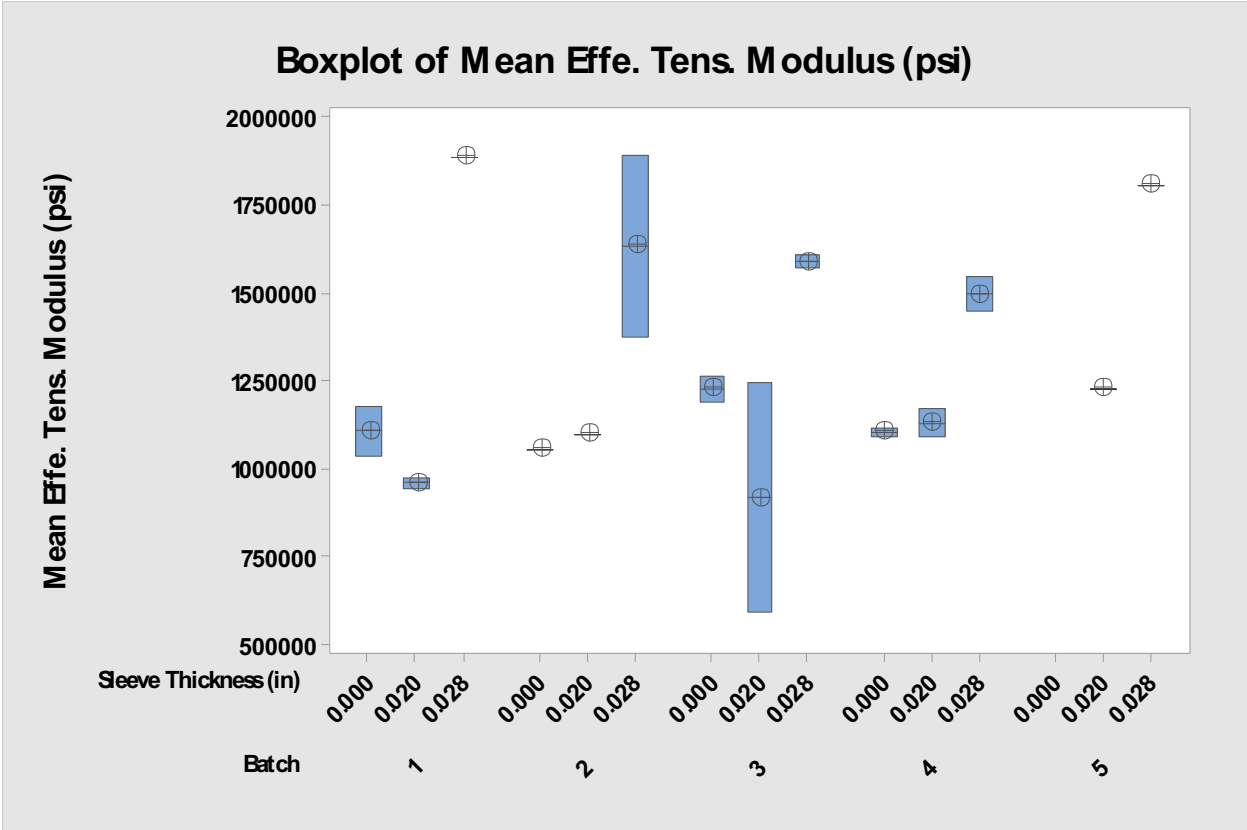


Figure 12.36: Boxplot of effective tensile modulus vs. batch and sieve thickness for pre impact tension samples.

Based on the plot of effective modulus vs. batch and sieve thickness, no higher level correlations could be determined. The batch factor was removed to help determine correlation, as it has been determined to not contribute to response variable variance.

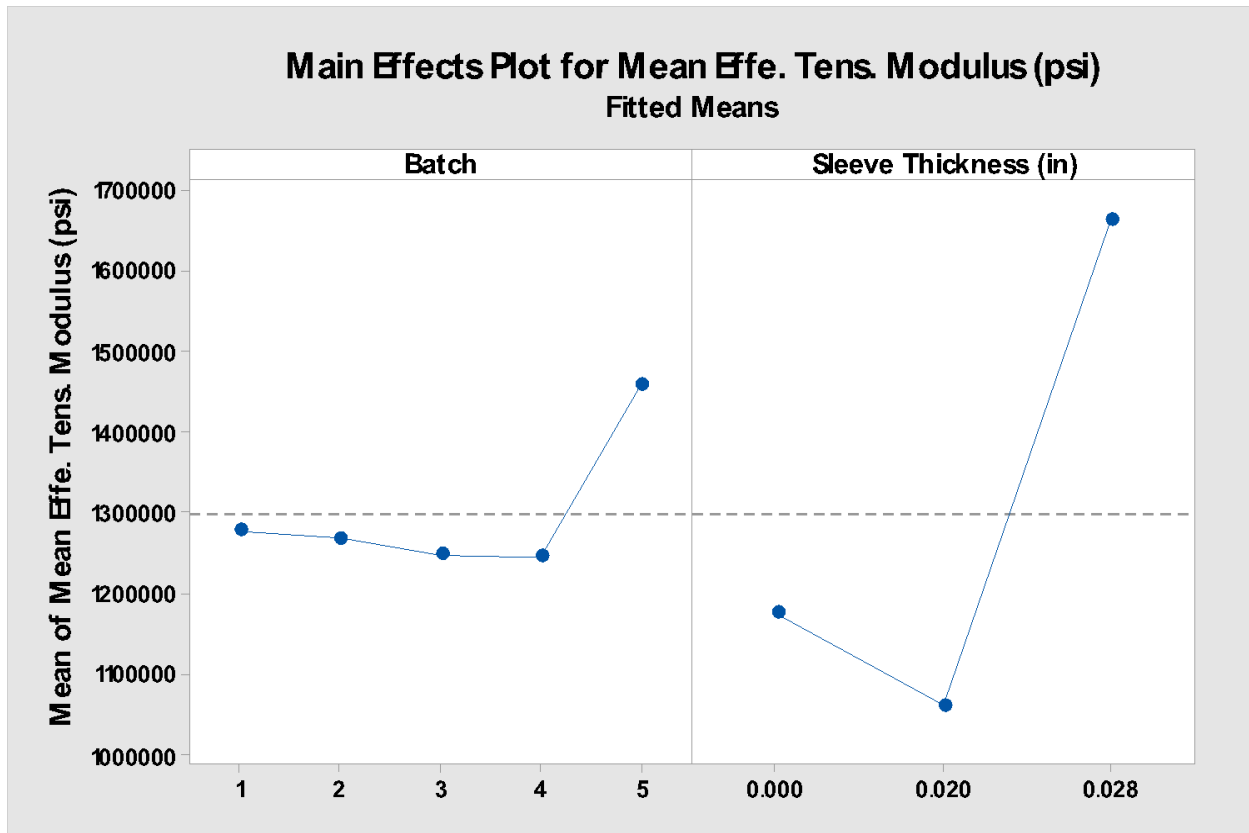


Figure 12.37 Main effects plot of effective tensile modulus for pre impact tension samples.

The main effects plot shows the batch factor levels as contributing the least to effective modulus response variance. Sleeve thickness factor levels contribute the greatest to effective modulus response variance. For the 0.000 and 0.020 sleeve thickness factor levels, the effective modulus was similar, and lower than the 0.028 sleeve thickness factor level.

## 12.5 Impact Data Analysis

### General Linear Model: Depression Depth (in) versus Batch, Sleeve Thickness (in)

The following terms cannot be estimated and were removed:

Batch\*Sleeve Thickness (in)

Method

Factor coding (-1, 0, +1)

Factor Information

Factor	Type	Levels	Values
Batch	Random	5	1, 2, 3, 4, 5
Sleeve Thickness (in)	Fixed	3	0.000, 0.020, 0.028

Analysis of Variance

Source	DF	Adj SS	Adj MS	F-Value	P-Value
Batch	4	0.002969	0.000742	0.92	0.477
Sleeve Thickness (in)	2	0.017774	0.008887	11.01	0.001
Error	16	0.012915	0.000807		
Lack-of-Fit	7	0.002158	0.000308	0.26	0.956
Pure Error	9	0.010757	0.001195		
Total	22	0.038918			

Model Summary

S	R-sq	R-sq(adj)	R-sq(pred)
0.0284110	66.81%	54.37%	32.42%

Figure 12.38: General linear model of depression depth for impacted samples.

Based on the analysis, the sleeve thickness factor appeared significant. The batch\*sleeve thickness interaction does not appear significant, and therefore was reduced.

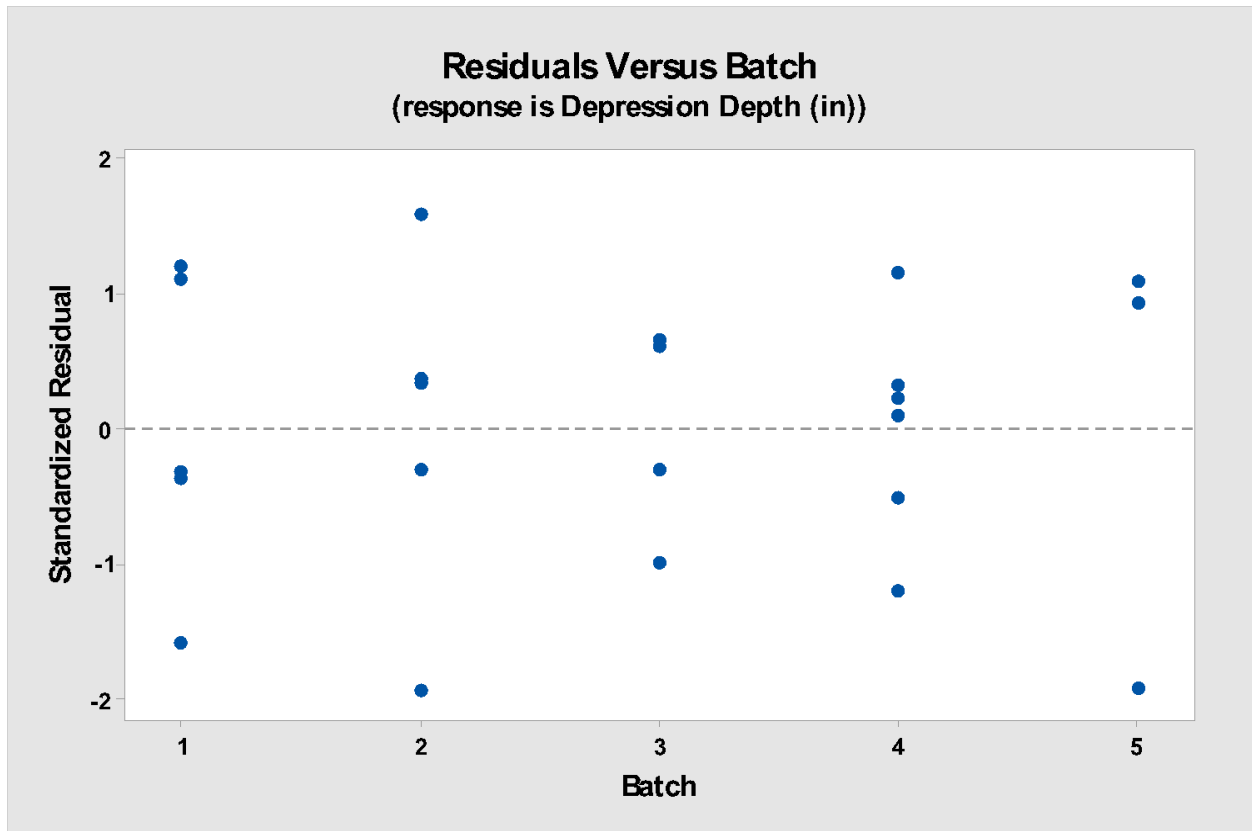


*Figure 12.39: Residuals vs. batch for impacted samples.*

Based on the residuals vs. batch plot, the data appeared to have equal variance.

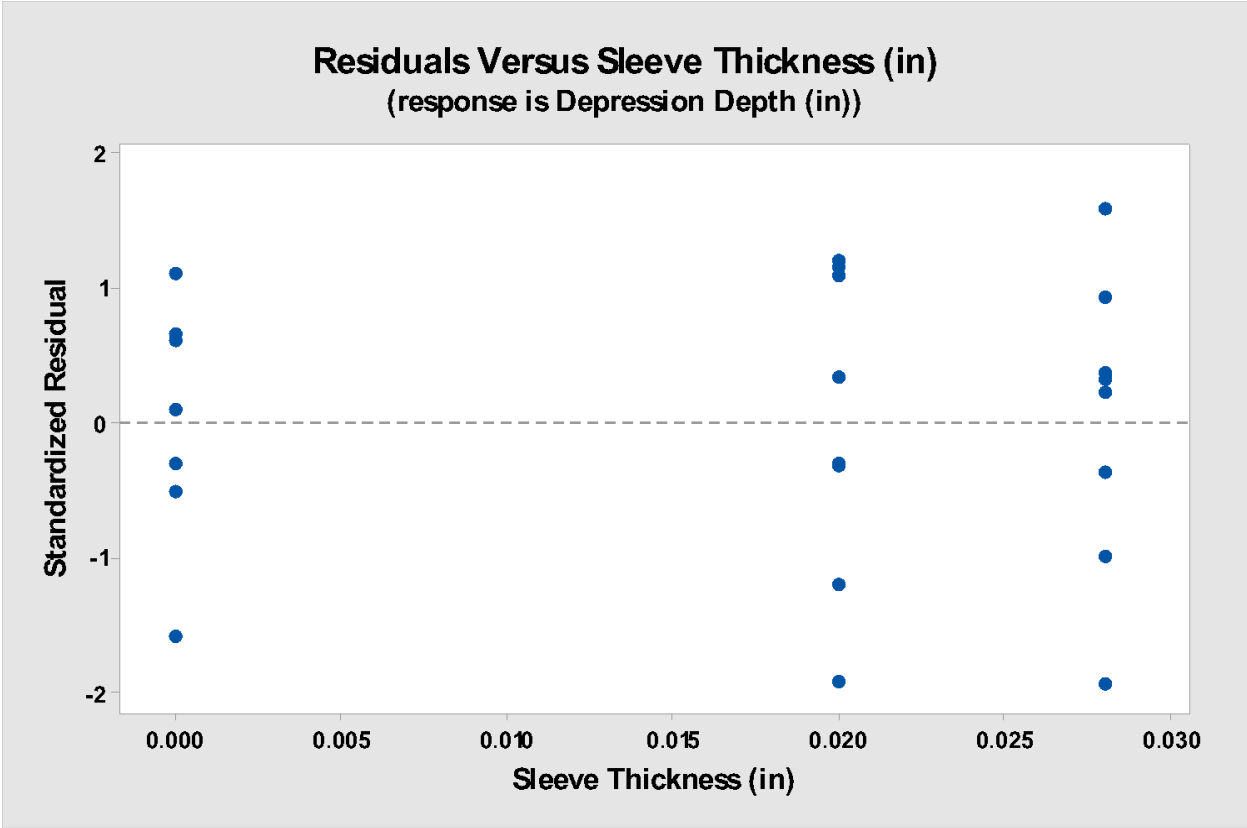


Figure 12.40: Residuals vs. sleeve thickness for impacted samples.

Based on the residuals vs. sleeve thickness plot, the data appeared to have equal variance.

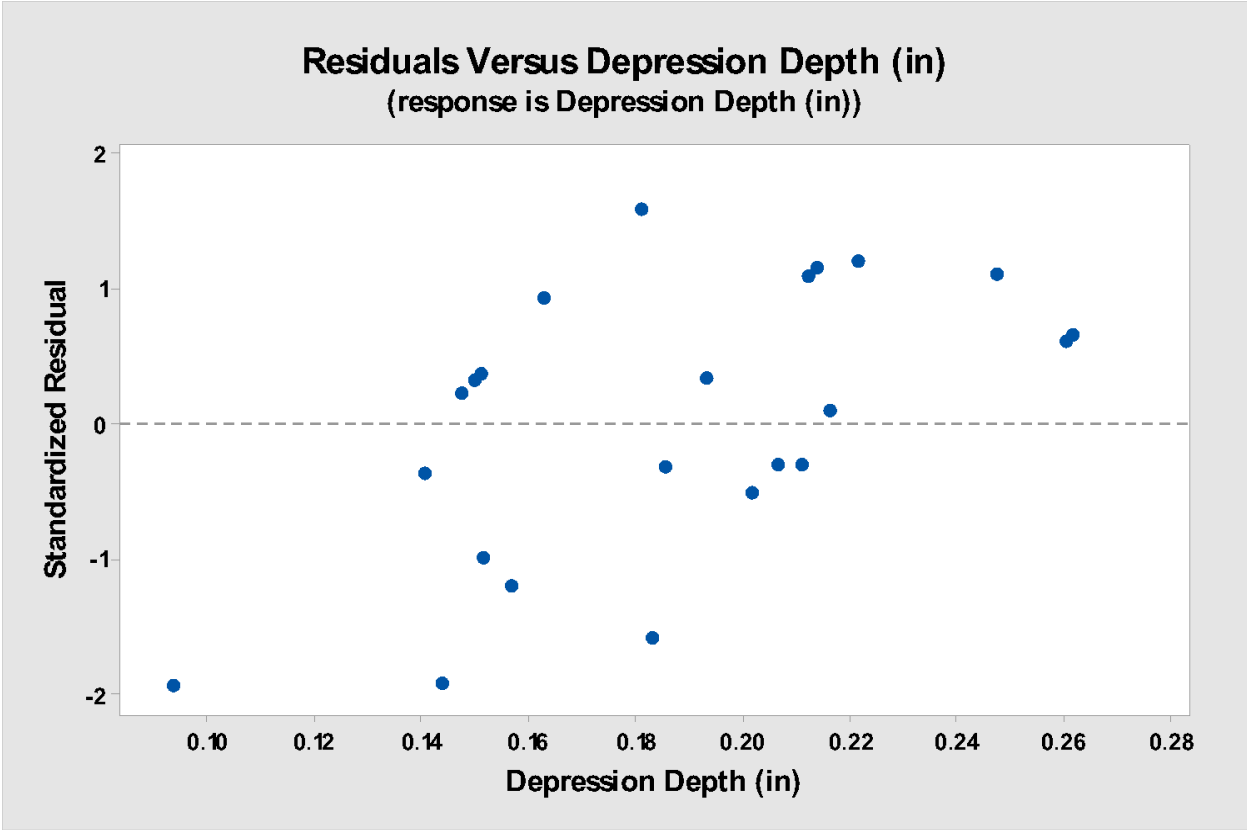
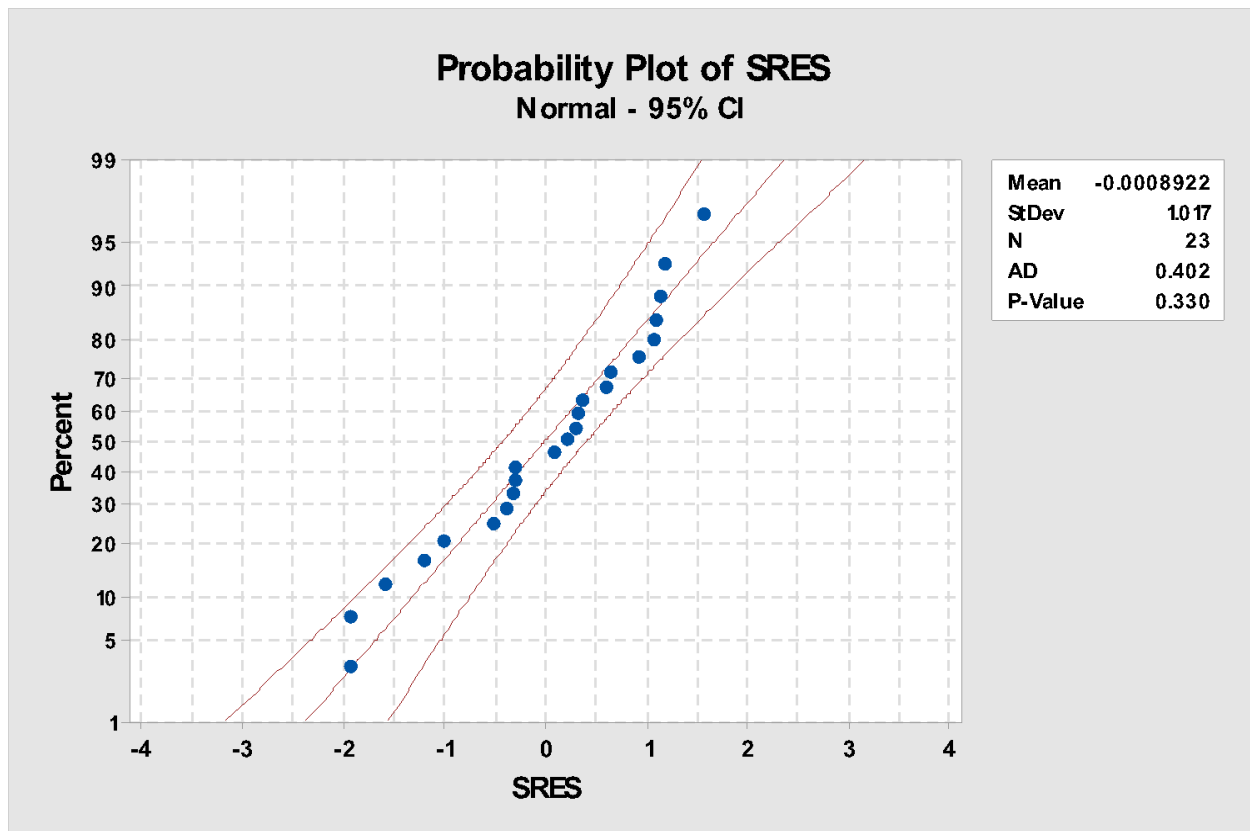


Figure 12.41: Residuals vs. depression depth for impacted samples.

Based on the residuals vs. Depression Depth plot, the data appeared to have equal variance.



*Figure 12.42: Normal probability plot for impacted samples.*

The normal probability plot of standardized residuals showed a p value of 0.330, greater than the  $\alpha$  of 0.05. Therefore, it was necessary to fail to reject the null hypothesis that the data comes from a normal population.

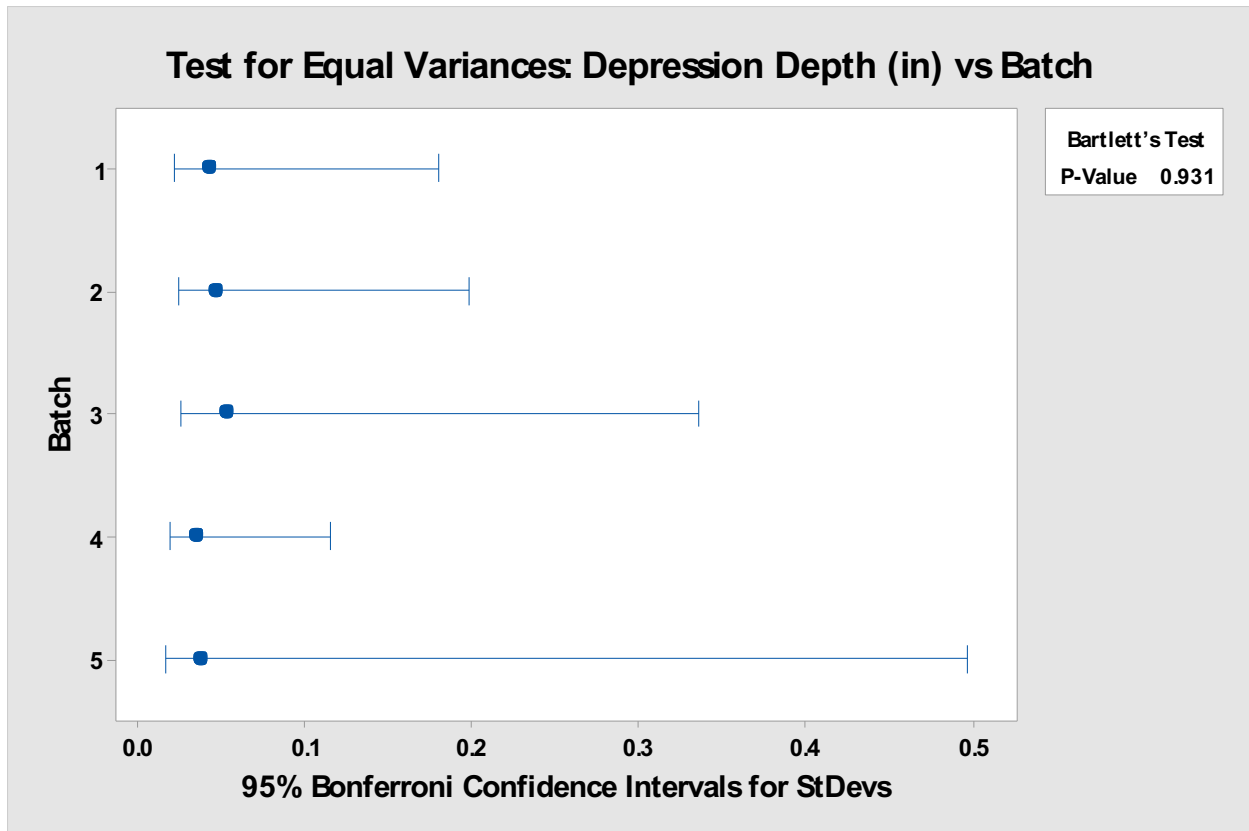
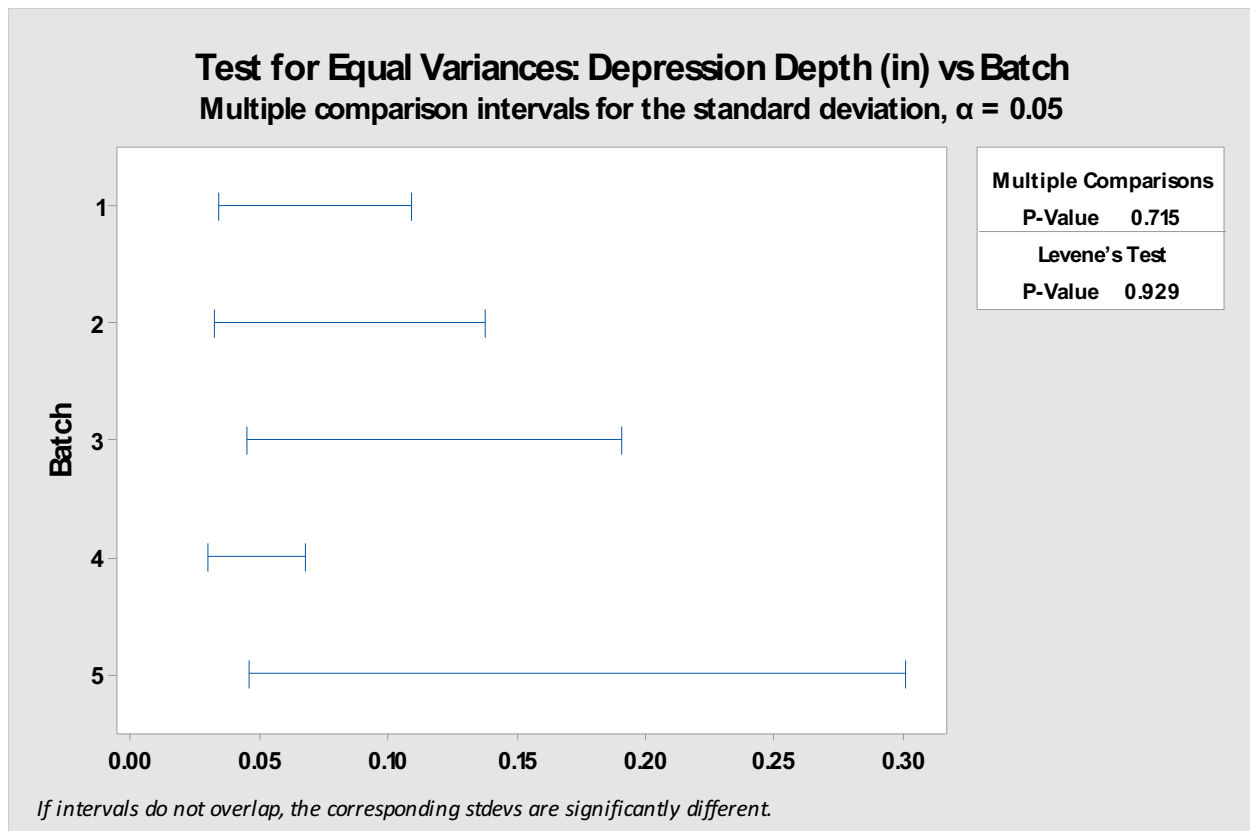


Figure 12.43: Bartlett's vs. batch test for impacted samples.

The Bartlett's test for equal variances showed a p-value of 0.931, greater than the  $\alpha$  of 0.05. Therefore, it was necessary to fail to reject the null hypothesis that the data has equal variance for this factor.



*Figure 12.44: Levene's vs. batch test for impacted samples.*

The Levene's test for equal variances showed a p-value of 0.929, greater than the  $\alpha$  of 0.05. Therefore, it was necessary to fail to reject the null hypothesis that the data has equal variance for this factor.

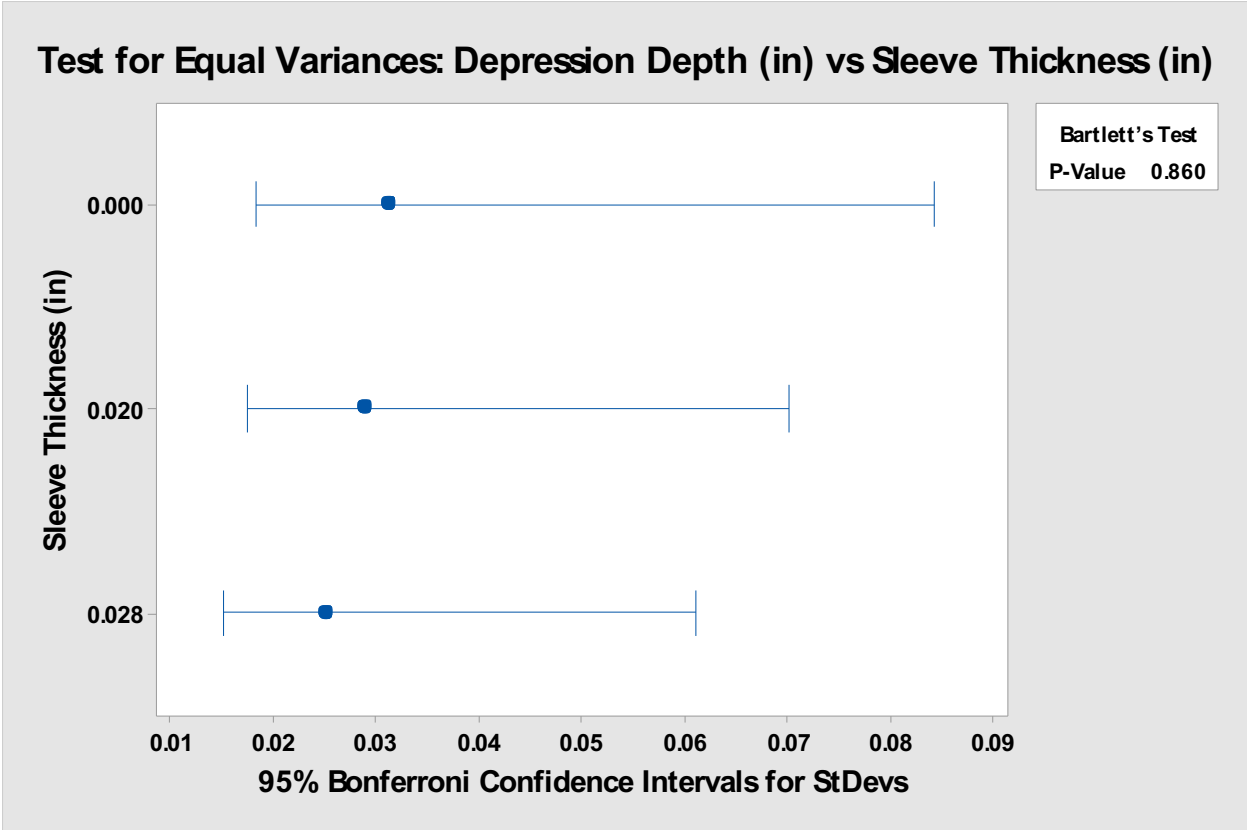
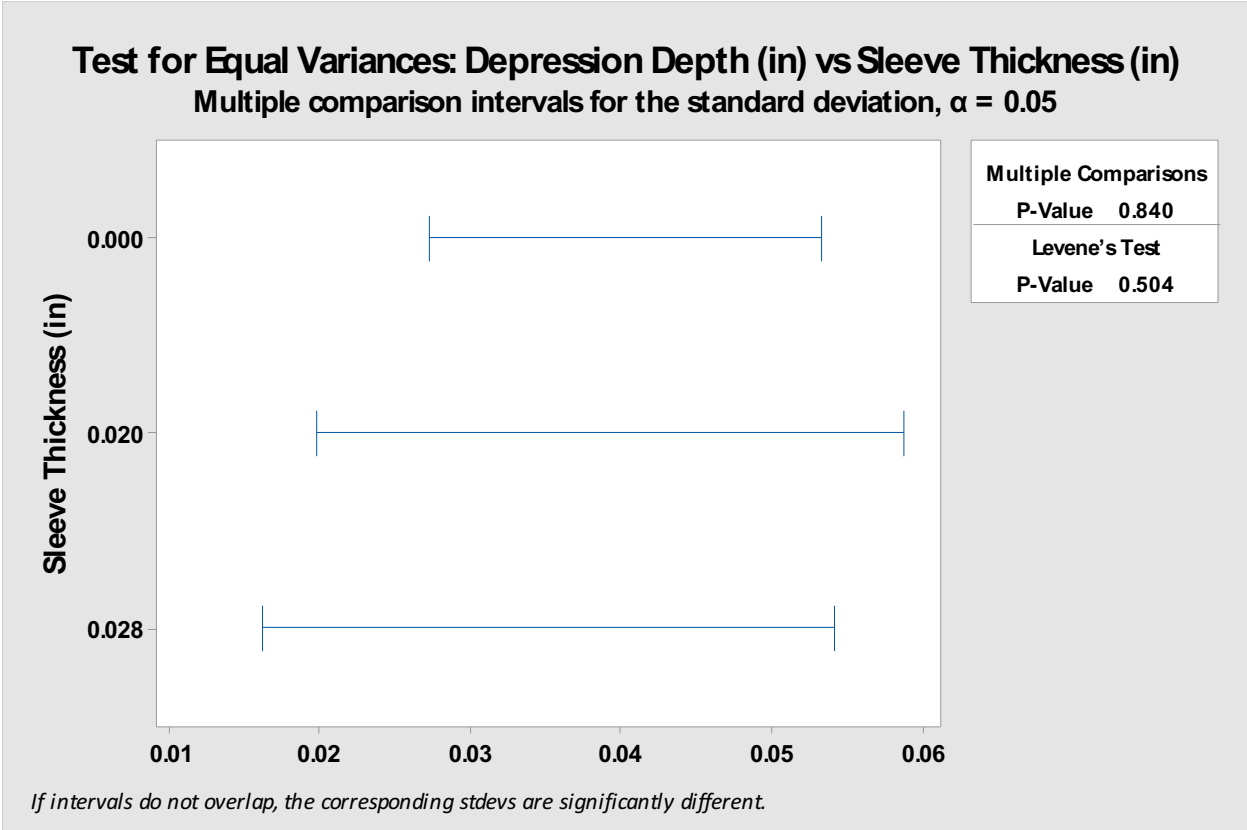


Figure 12.45: Bartlett's vs. sleeve thickness test for impacted samples.

The Bartlett's test for equal variances showed a p-value of 0.860, greater than the  $\alpha$  of 0.05. Therefore, it was necessary to fail to reject the null hypothesis that the data has equal variance for this factor.



*Figure 12.46: Levene's vs. sleeve thickness test for impacted samples.*

The Levene's test for equal variances showed a p-value of 0.504, greater than the  $\alpha$  of 0.05. Therefore, it was necessary to fail to reject the null hypothesis that the data has equal variance for this factor.

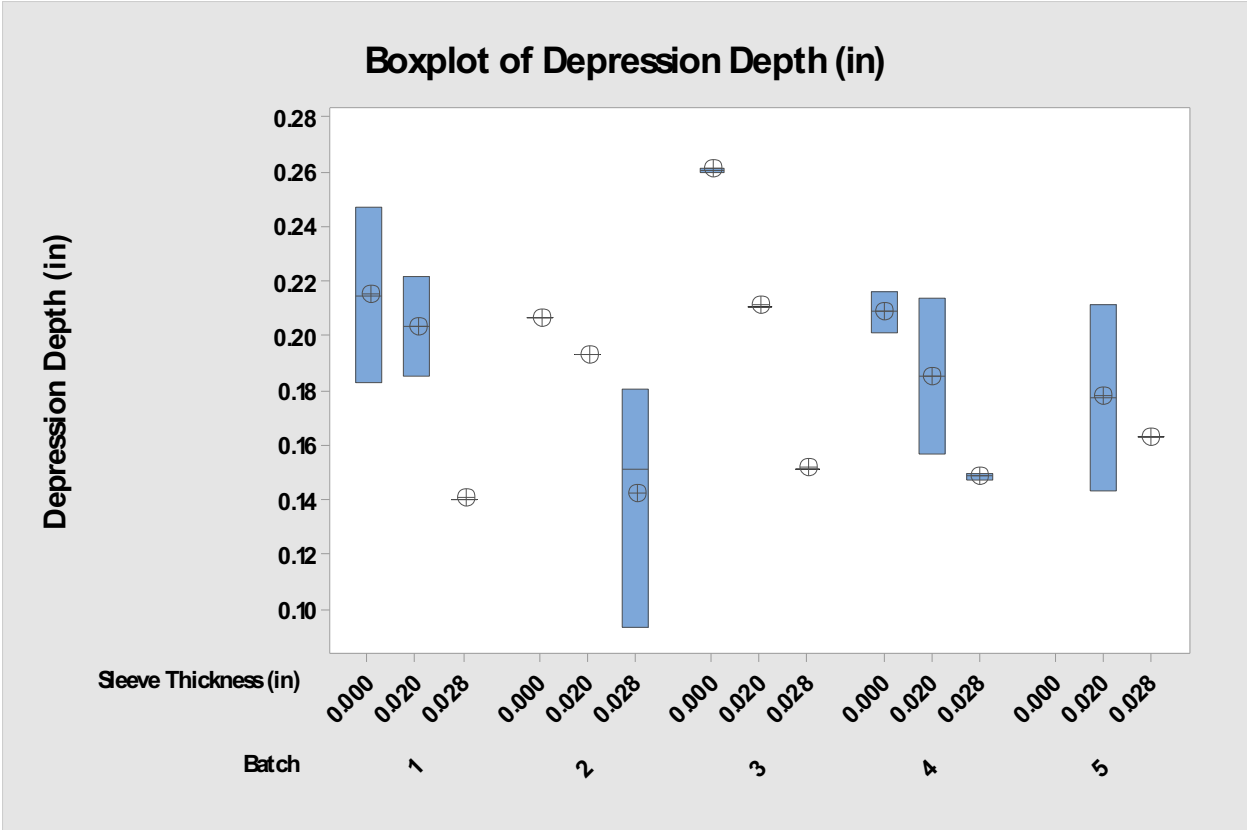


Figure 12.47: Boxplot of depression depth vs. batch and sleeve thickness for impacted samples.

Based on the plot of effective modulus vs. batch and sleeve thickness, no higher level correlations could be determined. The batch factor was removed to help determine correlation.

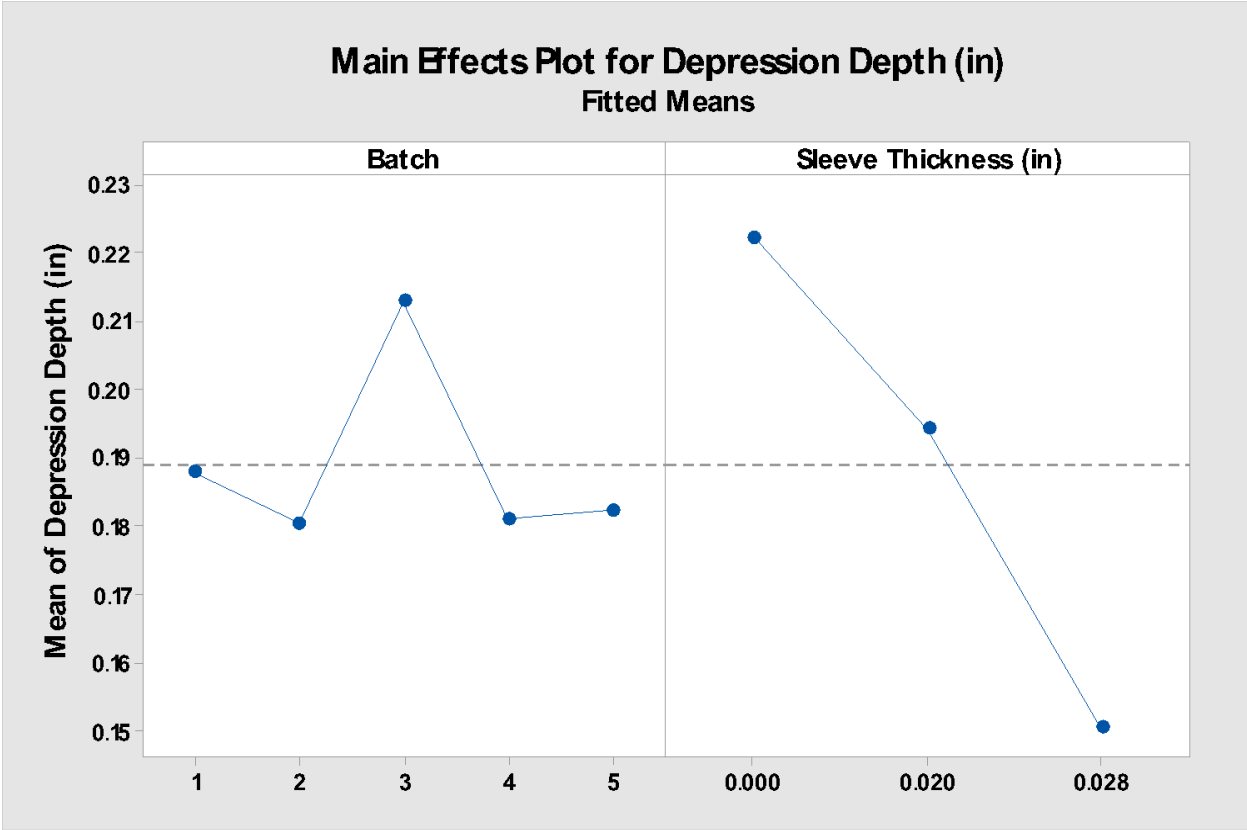


Figure 12.48: Main effects plot of depression depth for impacted samples.

The main effects plot shows the batch factor levels as contributing the least to Depression Depth response variance. Sleeve thickness factor levels contribute the greatest to Depression Depth response variance.

## 12.6 Post Impact Torsion Data Analysis

### General Linear Model: Mean Effe. Shear Modulus (psi) versus Batch, Sleeve Thickness (in)

The following terms cannot be estimated and were removed:

Batch\*Sleeve Thickness (in)

Method

Factor coding (-1, 0, +1)

Factor Information

Factor	Type	Levels	Values
Batch	Random	5	1, 2, 3, 4, 5
Sleeve Thickness (in)	Fixed	3	0.000, 0.020, 0.028

Analysis of Variance

Source	DF	Adj SS	Adj MS	F-Value	P-Value
Batch	4	96401247129	24100311782	0.23	0.920
Sleeve Thickness (in)	2	1.28394E+13	6.41969E+12	60.27	0.000
Error	16	1.70425E+12	1.06516E+11		
Lack-of-Fit	7	2.53237E+11	36176653084	0.22	0.969
Pure Error	9	1.45101E+12	1.61224E+11		
Total	22	1.68642E+13			

Model Summary

S	R-sq	R-sq(adj)	R-sq(pred)
326367	89.89%	86.10%	80.51%

*Figure 12.49: General linear model of effective shear modulus for post impact torsion samples.*

Based on the analysis, the sleeve thickness factor appeared significant. The batch\*sleeve thickness interaction does not appear significant, and therefore was reduced.

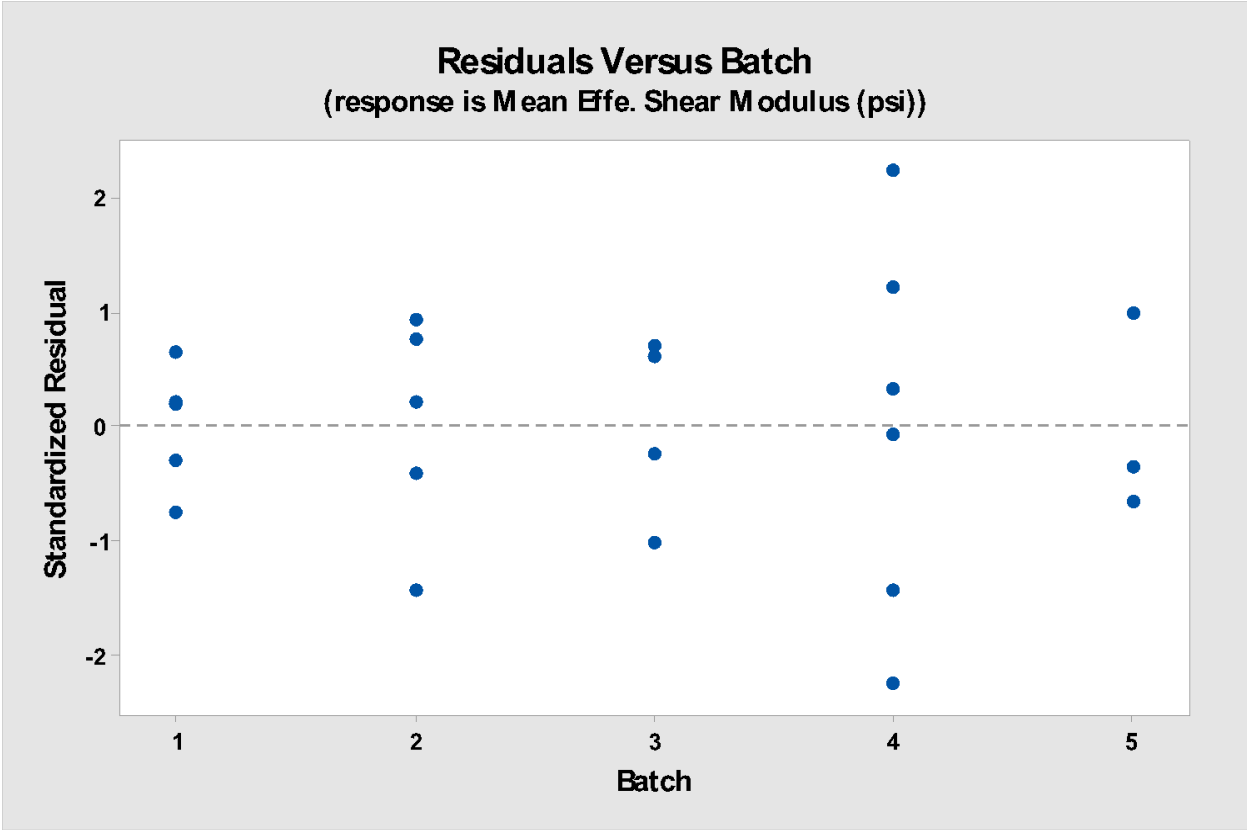


Figure 12.50: Residuals vs. batch for post impact torsion samples.

Based on the residuals vs. batch plot, the data appeared to have equal variance.

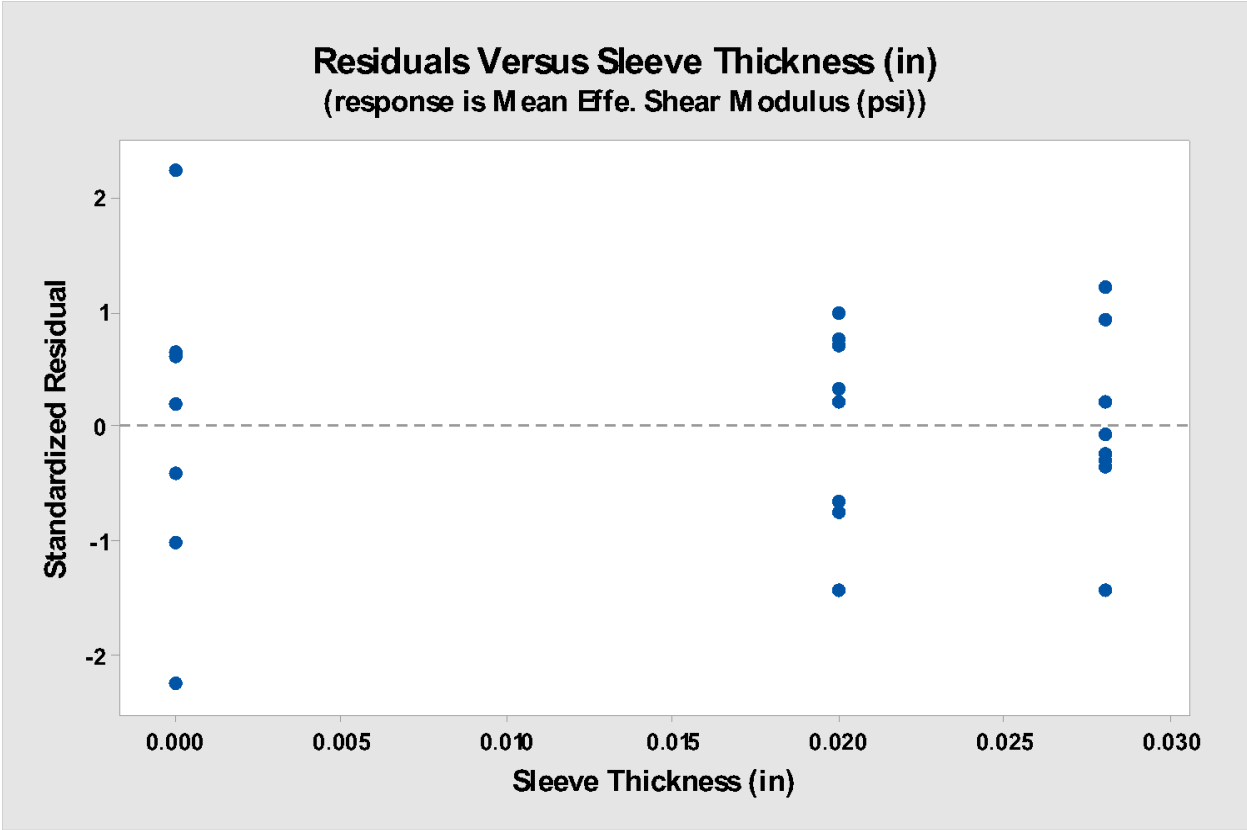


Figure 12.51: Residuals vs. sleeve thickness for post impact torsion samples.

Based on the residuals vs. sleeve thickness plot, the data appeared to have equal variance.

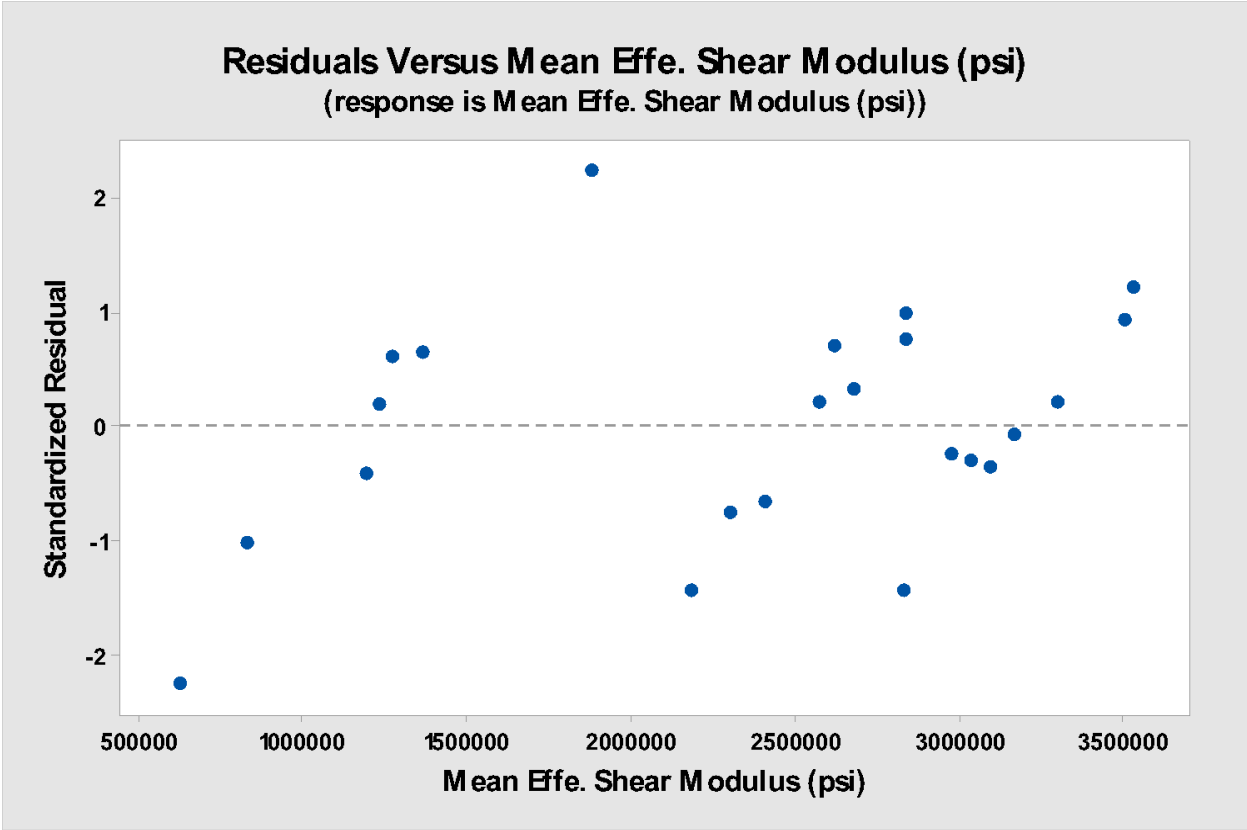
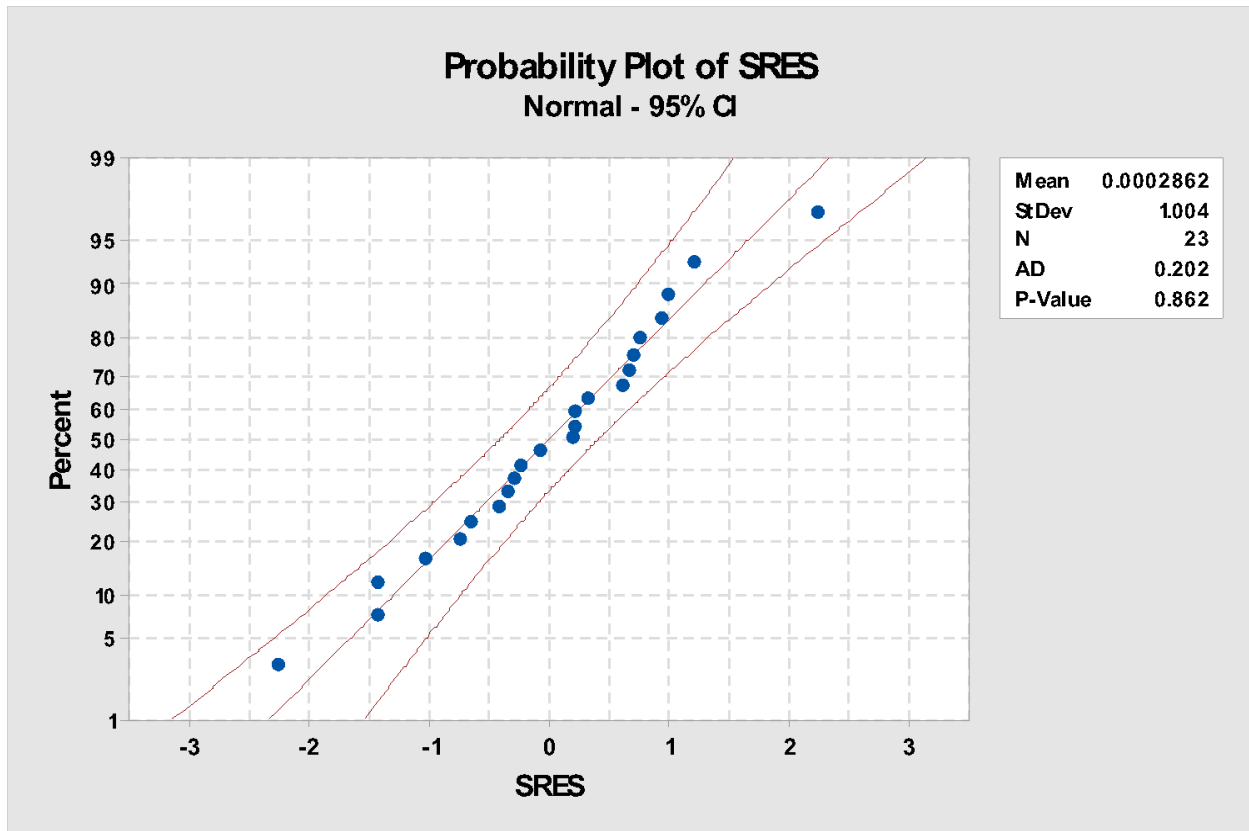


Figure 12.52: Residuals vs. effective shear modulus for post impact torsion samples.

Based on the residuals vs. effective modulus plot, the data appeared to have equal variance.



*Figure 12.53: Normal probability plot for post impact torsion samples.*

The normal probability plot of standardized residuals showed a p value of 0.862, greater than the  $\alpha$  of 0.05. Therefore, it was necessary to fail to reject the null hypothesis that the data comes from a normal population.

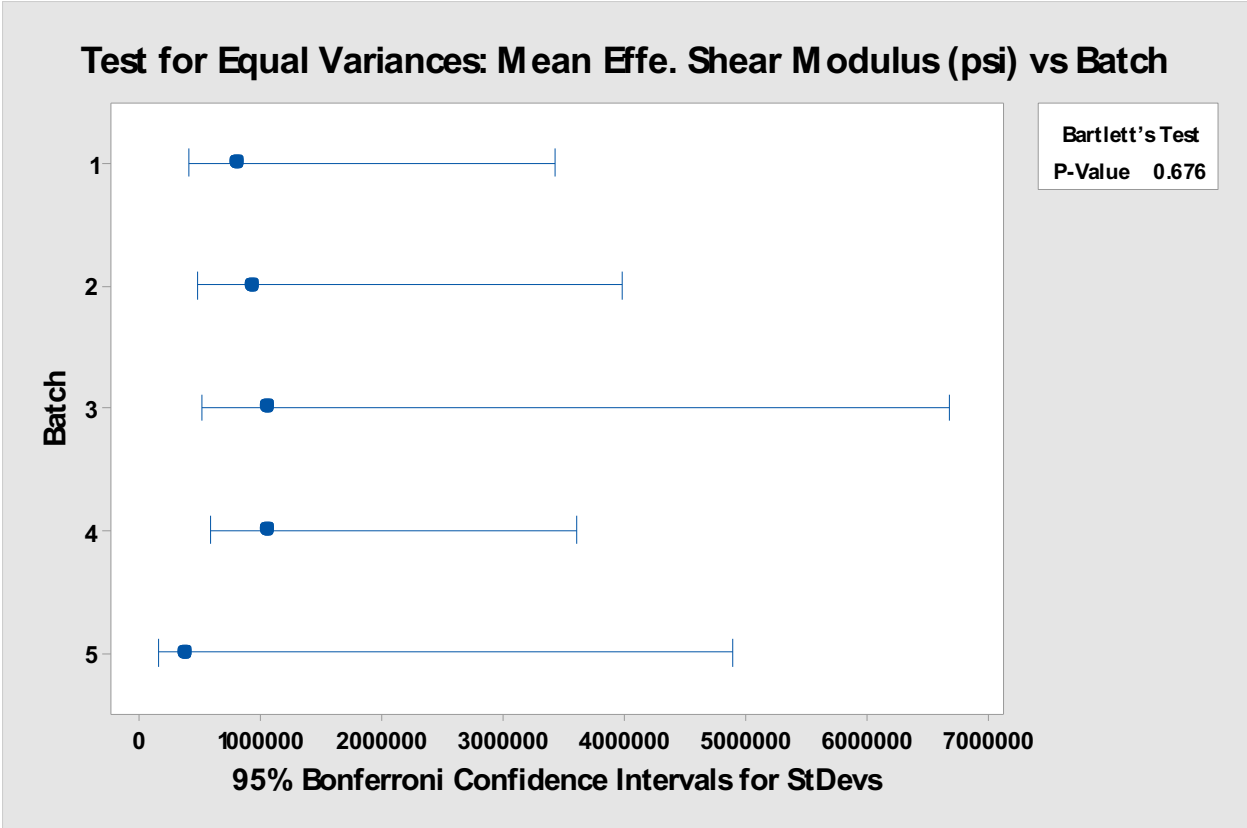
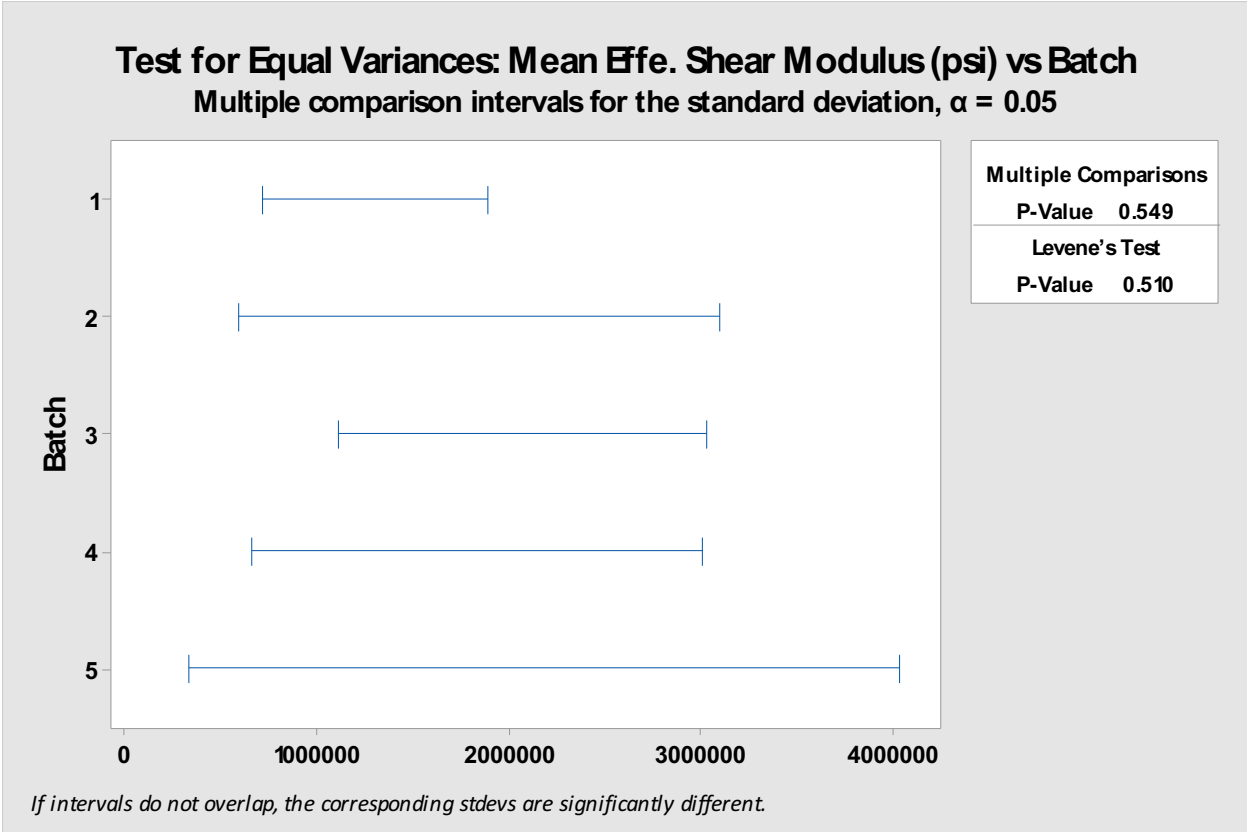


Figure 12.54: Bartlett's vs. batch test for post impact torsion samples.

The Bartlett's test for equal variances showed a p-value of 0.676, greater than the  $\alpha$  of 0.05. Therefore, it was necessary to fail to reject the null hypothesis that the data has equal variance for this factor.



*Figure 12.55: Levene's vs. batch test for post impact torsion samples.*

The Levene's test for equal variances showed a p-value of 0.510, greater than the  $\alpha$  of 0.05. Therefore, it was necessary to fail to reject the null hypothesis that the data has equal variance for this factor.

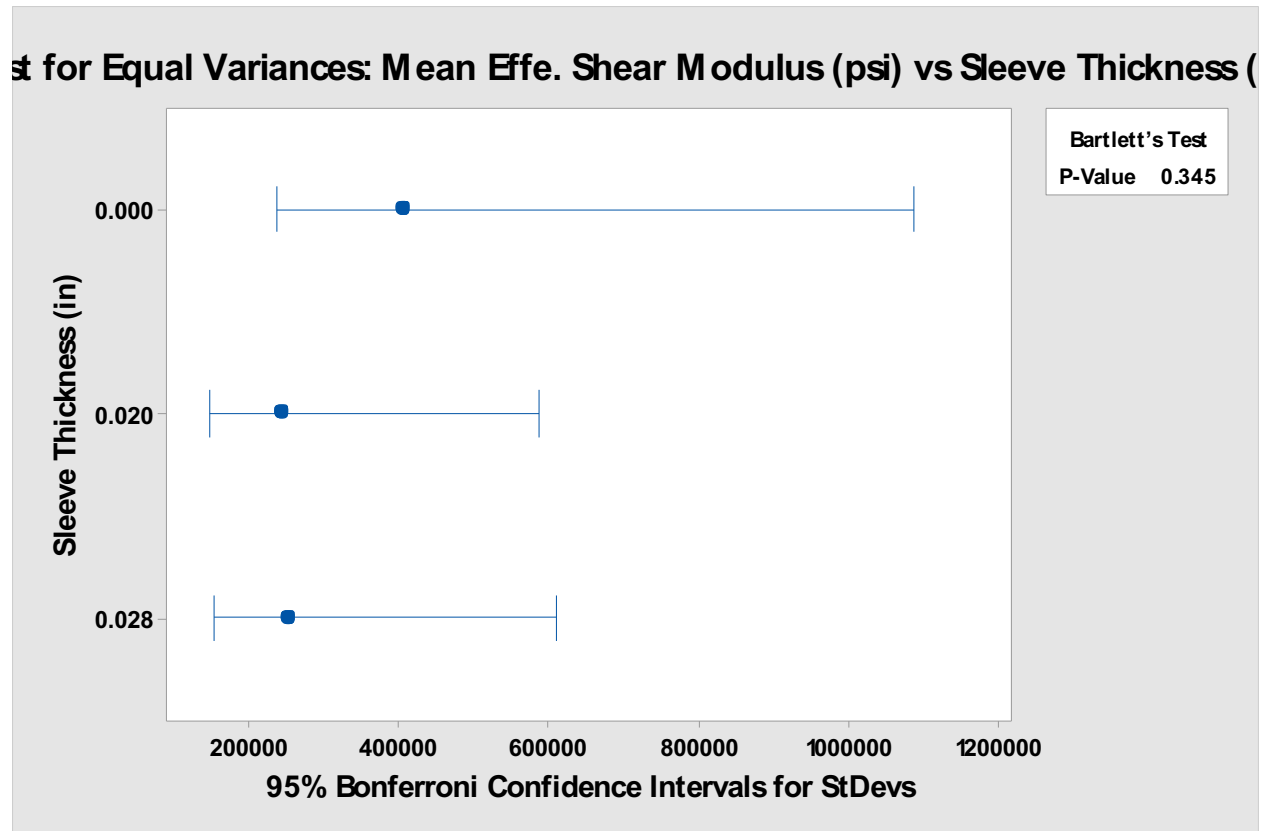
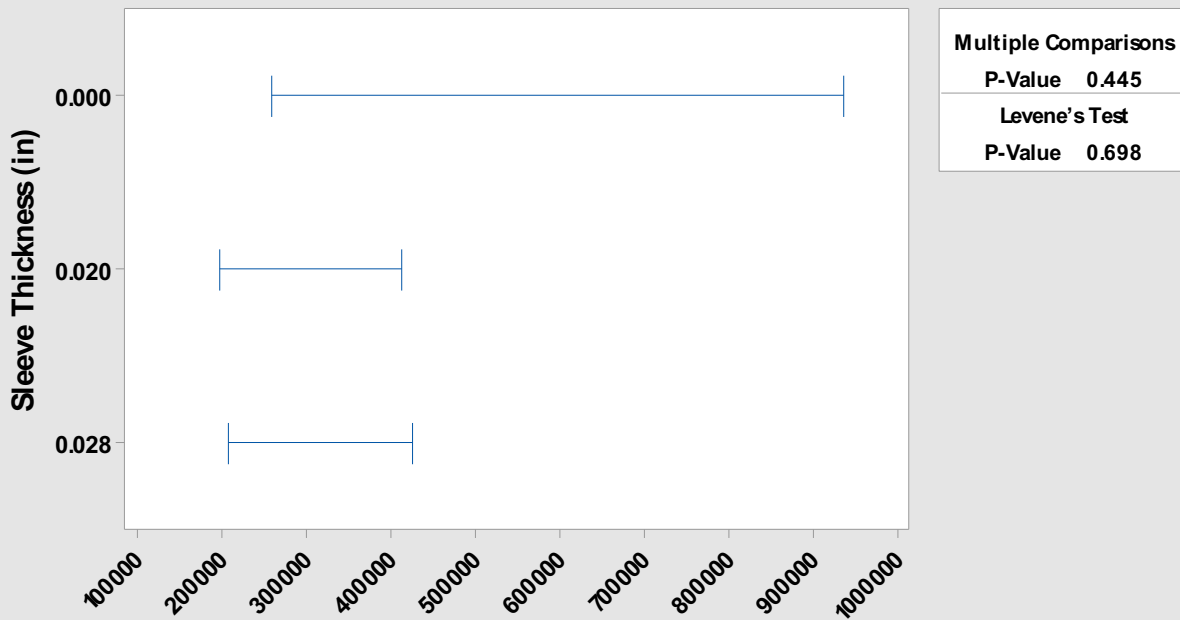


Figure 12.56: Bartlett' vs. sleeve thickness for post impact torsion samples.

The Bartlett's test for equal variances showed a p-value of 0.345, greater than the  $\alpha$  of 0.05. Therefore, it was necessary to fail to reject the null hypothesis that the data has equal variance for this factor.

**Test for Equal Variances: Mean Effe. Shear Modulus (psi) vs Sleeve Thickness (in)**  
 Multiple comparison intervals for the standard deviation,  $\alpha = 0.05$



*If intervals do not overlap, the corresponding stdevs are significantly different.*

*Figure 12.57: Levene's vs. sleeve thickness test for post impact torsion samples.*

The Levene's test for equal variances showed a p-value of 0.698, greater than the  $\alpha$  of 0.05. Therefore, it was necessary to fail to reject the null hypothesis that the data has equal variance for this factor.

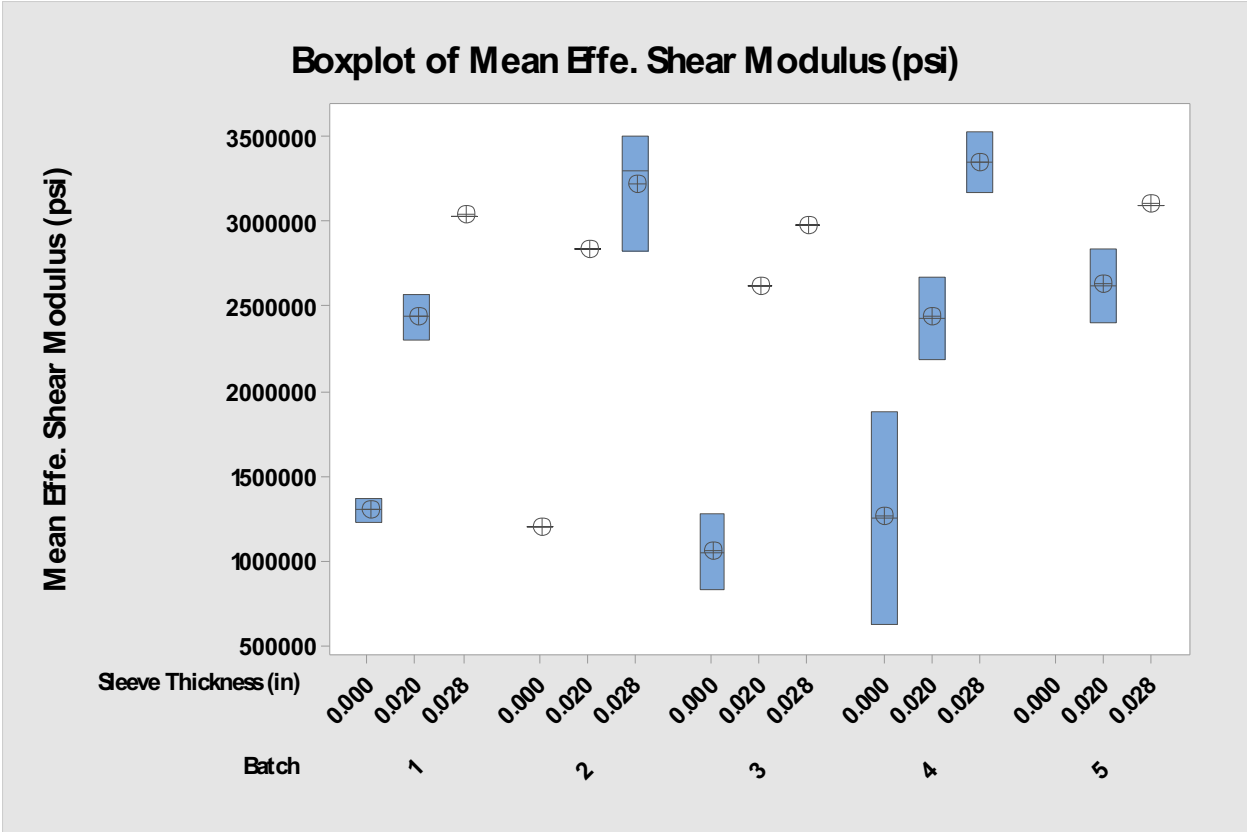


Figure 12.58: Boxplot of effective shear modulus vs. batch and sleeve thickness for post impact torsion samples.

Based on the plot of effective modulus vs. batch and sleeve thickness, no higher level correlations could be determined. The batch factor was removed to help determine correlation.

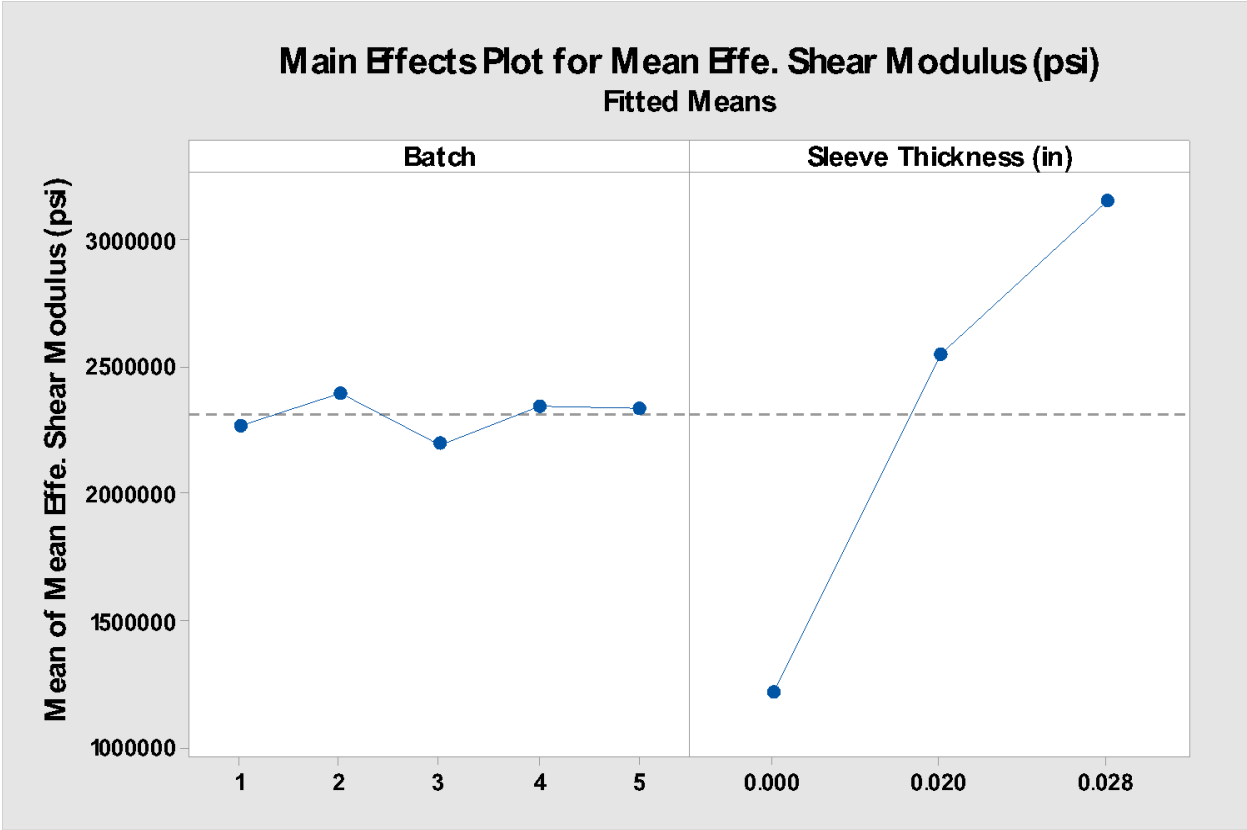


Figure 12.59: Main effects plot of effective shear modulus for post impact torsion samples.

The main effects plot shows the batch factor levels as contributing the least to effective modulus response variance. Sleeve thickness factor levels contribute the greatest to effective modulus response variance.

## 12.7 Post Impact Tension Data Analysis

### General Linear Model: Mean Effe. Tens. Modulus (psi) versus Batch, Sleeve Thickness (in)

The following terms cannot be estimated and were removed:

Batch\*Sleeve Thickness (in)

Method

Factor coding (-1, 0, +1)

Factor Information

Factor	Type	Levels	Values
Batch	Random	5	1, 2, 3, 4, 5
Sleeve Thickness (in)	Fixed	3	0.000, 0.020, 0.028

Analysis of Variance

Source	DF	Adj SS	Adj MS	F-Value	P-Value
Batch	4	7.36899E+11	1.84225E+11	1.50	0.262
Sleeve Thickness (in)	2	4.19486E+12	2.09743E+12	17.13	0.000
Error	12	1.46963E+12	1.22469E+11		
Lack-of-Fit	6	8.33134E+11	1.38856E+11	1.31	0.376
Pure Error	6	6.36492E+11	1.06082E+11		
Total	18	7.80320E+12			

Model Summary

S	R-sq	R-sq(adj)	R-sq(pred)
349956	81.17%	71.75%	44.61%

*Figure 12.60: General linear model output of effective tensile modulus for post impact tension samples.*

Based on the analysis, the sleeve thickness factor appeared significant. The batch\*sleeve thickness interaction could not be calculated, and therefore was reduced.

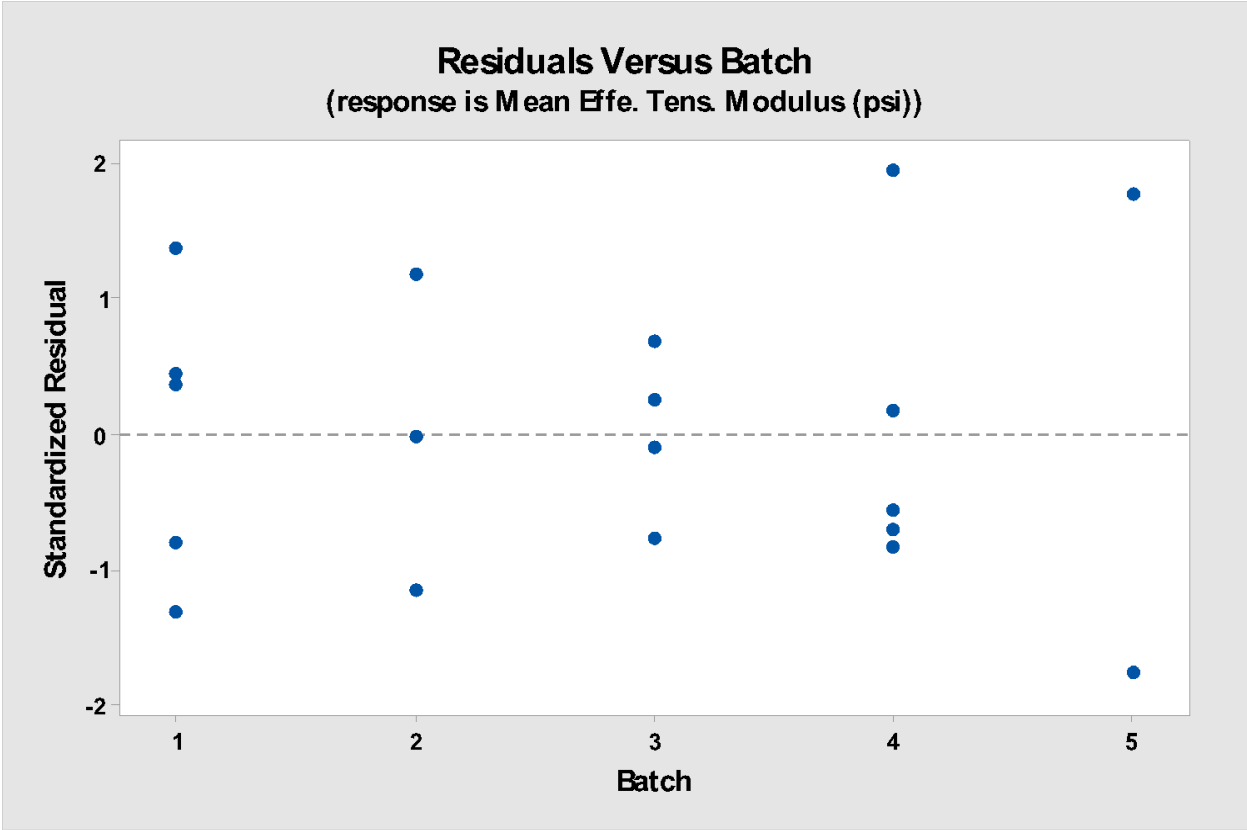


Figure 12.61: Residuals vs. batch for post impact tension samples.

Based on the residuals vs. batch plot, the data appeared to have equal variance.

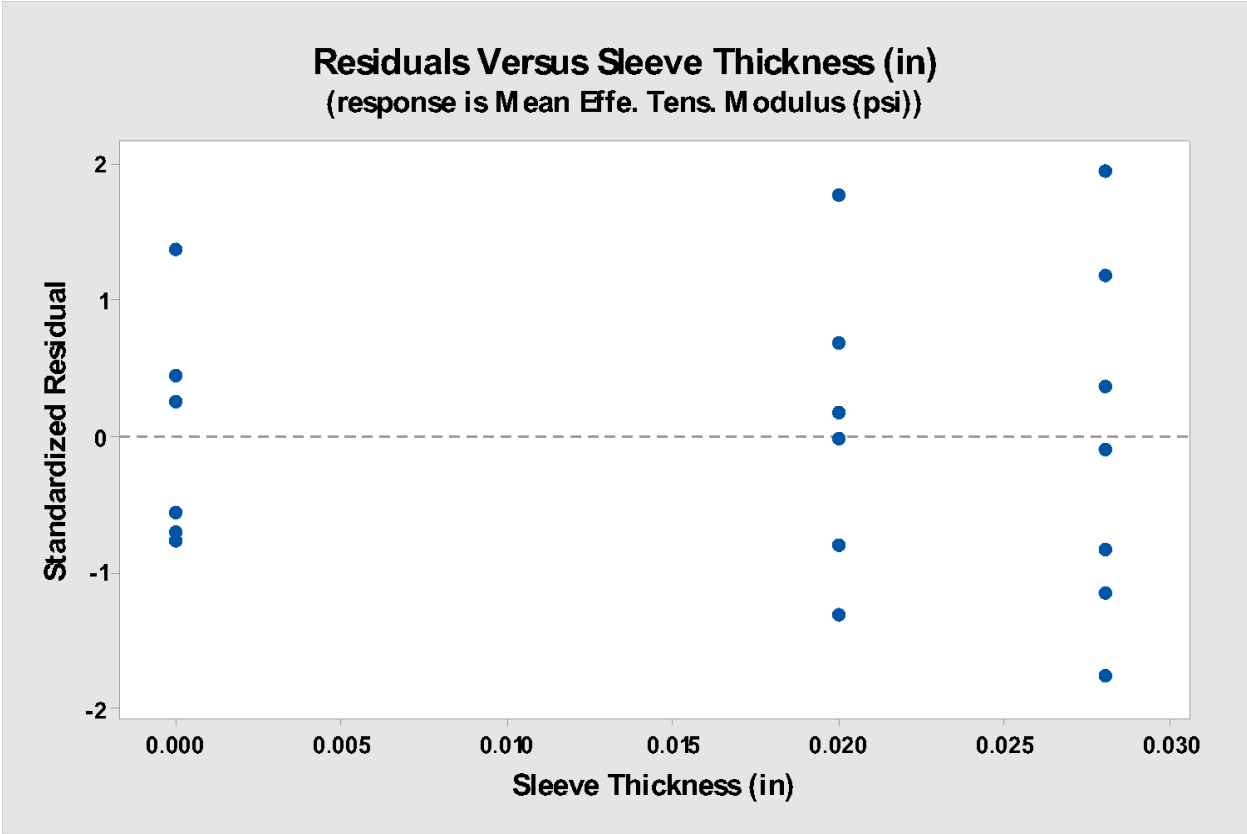


Figure 12.62: Residuals vs. sleeve thickness for post impact tension samples.

Based on the residuals vs. sleeve thickness plot, the data appeared to have equal variance.

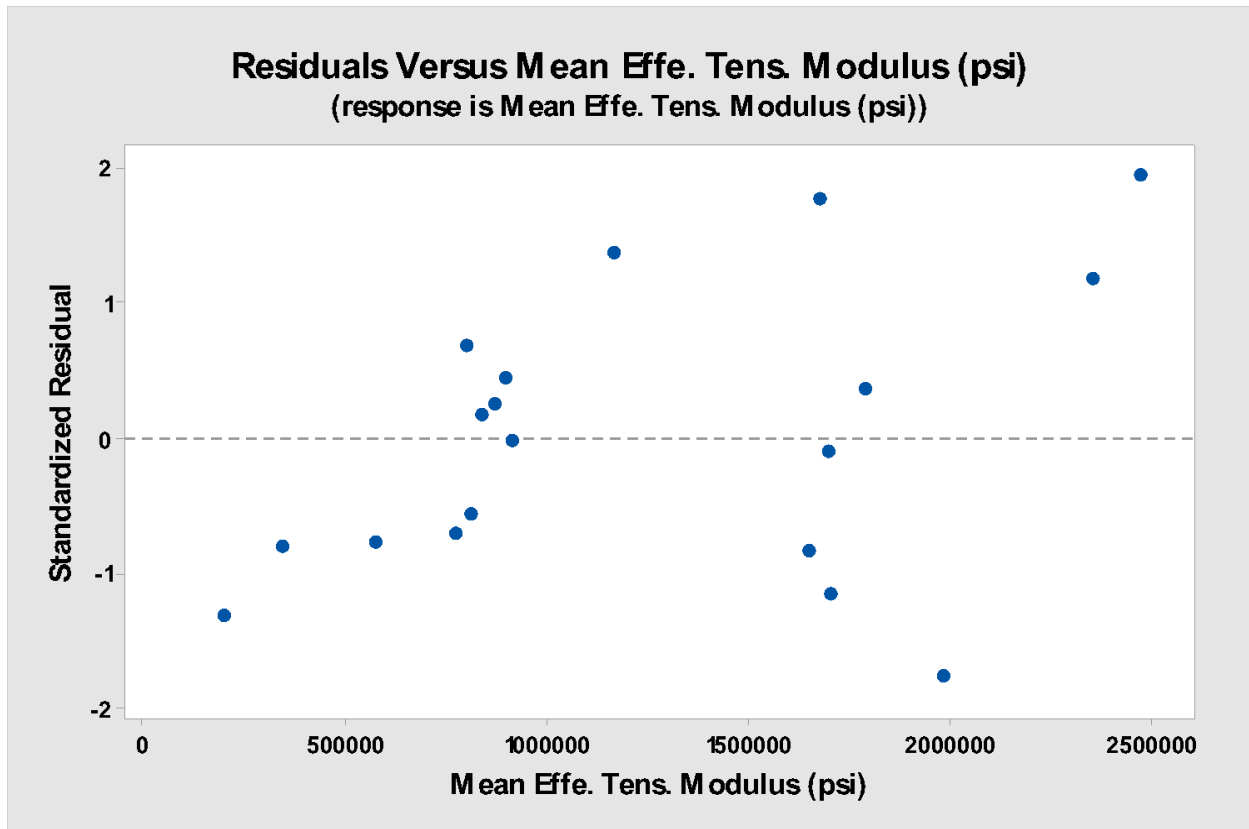


Figure 12.63: Residuals vs. effective tensile modulus for post impact tension samples.

Based on the residuals vs. effective modulus plot, the data appeared to have equal variance.

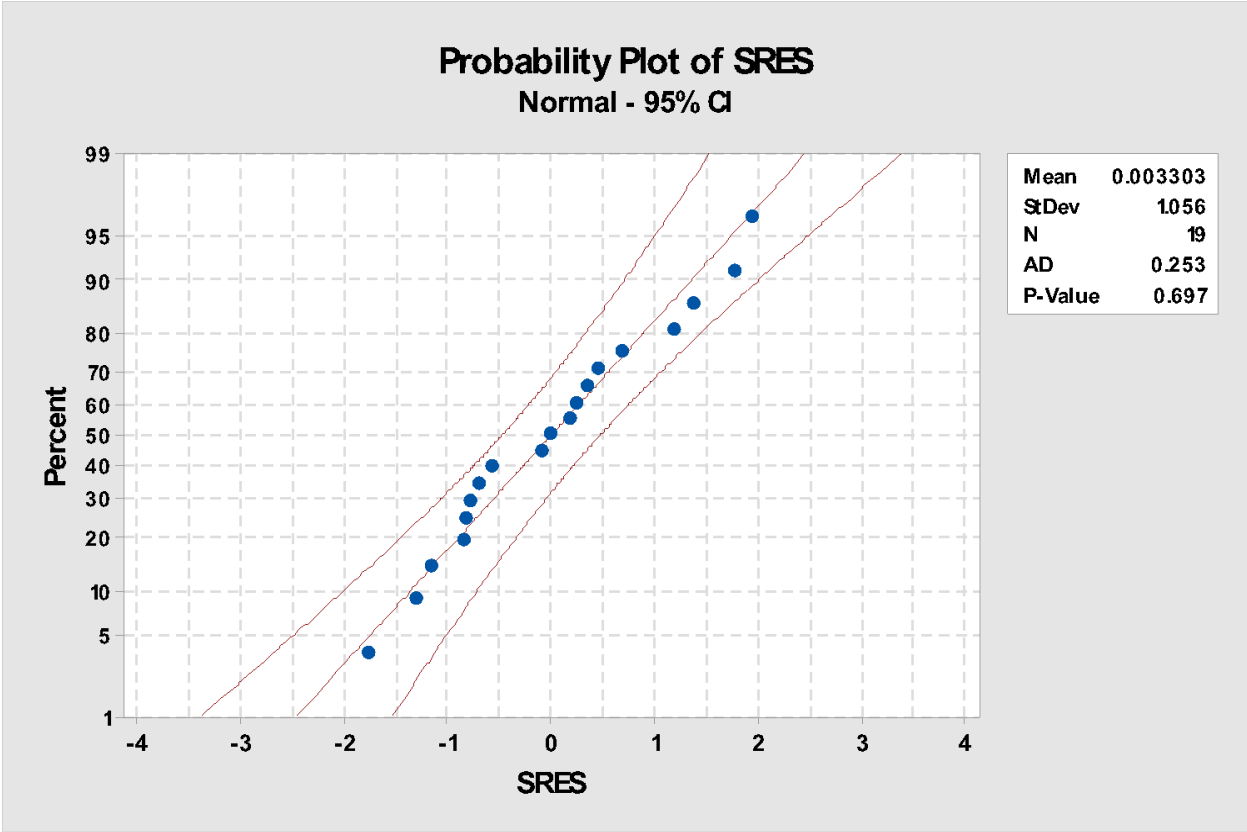


Figure 12.64: Normal probability plot for post impact tension samples.

The normal probability plot of standardized residuals showed a p value of 0.697, greater than the  $\alpha$  of 0.05. Therefore, it was necessary to fail to reject the null hypothesis that the data comes from a normal population.

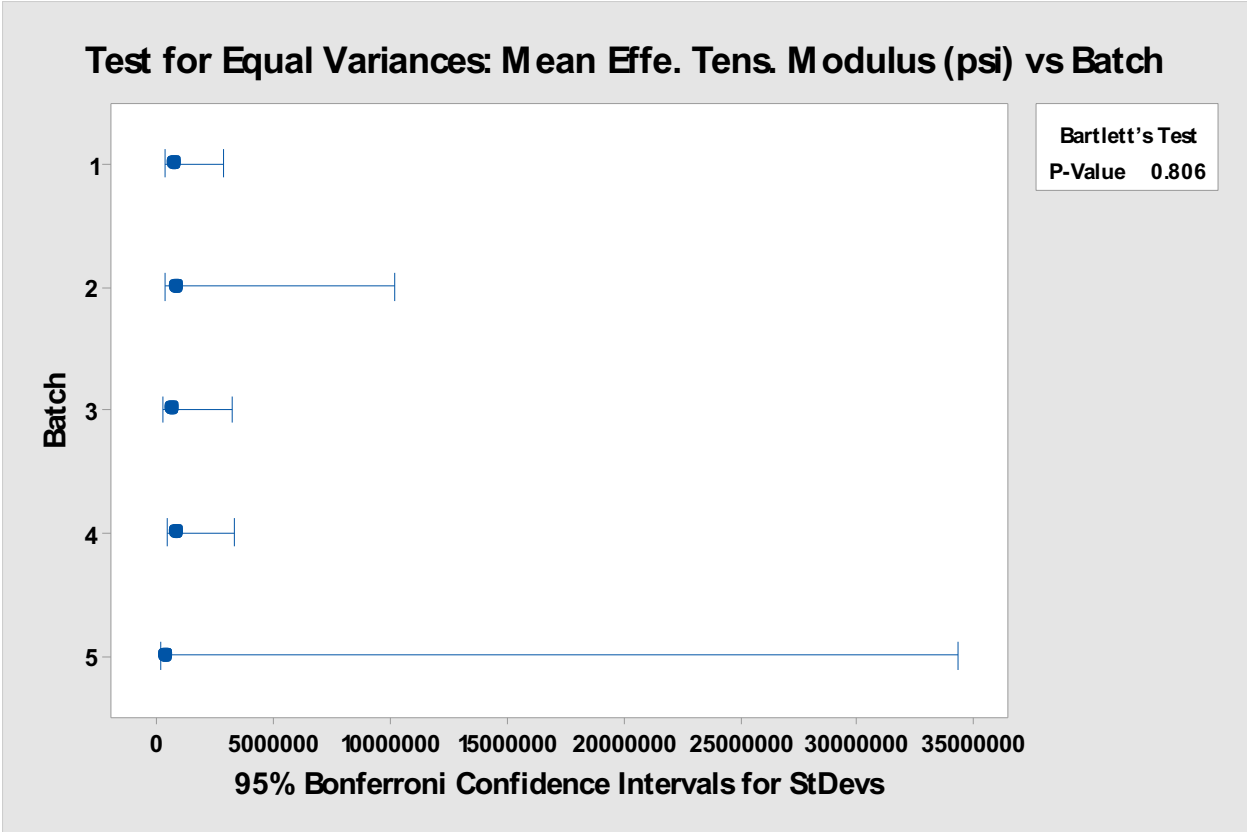


Figure 12.65: Bartlett's vs. batch test for post impact tension samples.

The Bartlett's test for equal variances showed a p-value of 0.806, greater than the  $\alpha$  of 0.05. Therefore, it was necessary to fail to reject the null hypothesis that the data has equal variance for this factor.

## Test for Equal Variances: Mean Effe. Tens. Modulus (psi) versus Batch

Method

Null hypothesis All variances are equal  
 Alternative hypothesis At least one variance is different  
 Significance level  $\alpha = 0.05$

95% Bonferroni Confidence Intervals for Standard Deviations

Batch	N	StDev	CI
1	5	643220	(192929, 4423118)
2	3	719680	( 718, 5103783314)
3	4	488515	( 44631, 15018065)
4	5	743523	(193888, 5880903)
5	2	215483	( *, *)

Individual confidence level = 99%

Tests

Method	Test	
	Statistic	P-Value
Multiple comparisons	-	0.841
Levene	0.28	0.883

\* NOTE \* The graphical summary cannot be displayed because the multiple comparison intervals cannot be calculated.

*Figure 12.66: Levene's vs. batch test for post impact tension samples.*

The Levene's test for equal showed a p-value of 0.883, greater than the  $\alpha$  of 0.05. Therefore, it was necessary to fail to reject the null hypothesis that the data has equal variance for this factor. Due to the nature of the multiple comparisons test, and since there were just two samples within the batch 5 factor level, a graphical summary could not be presented.

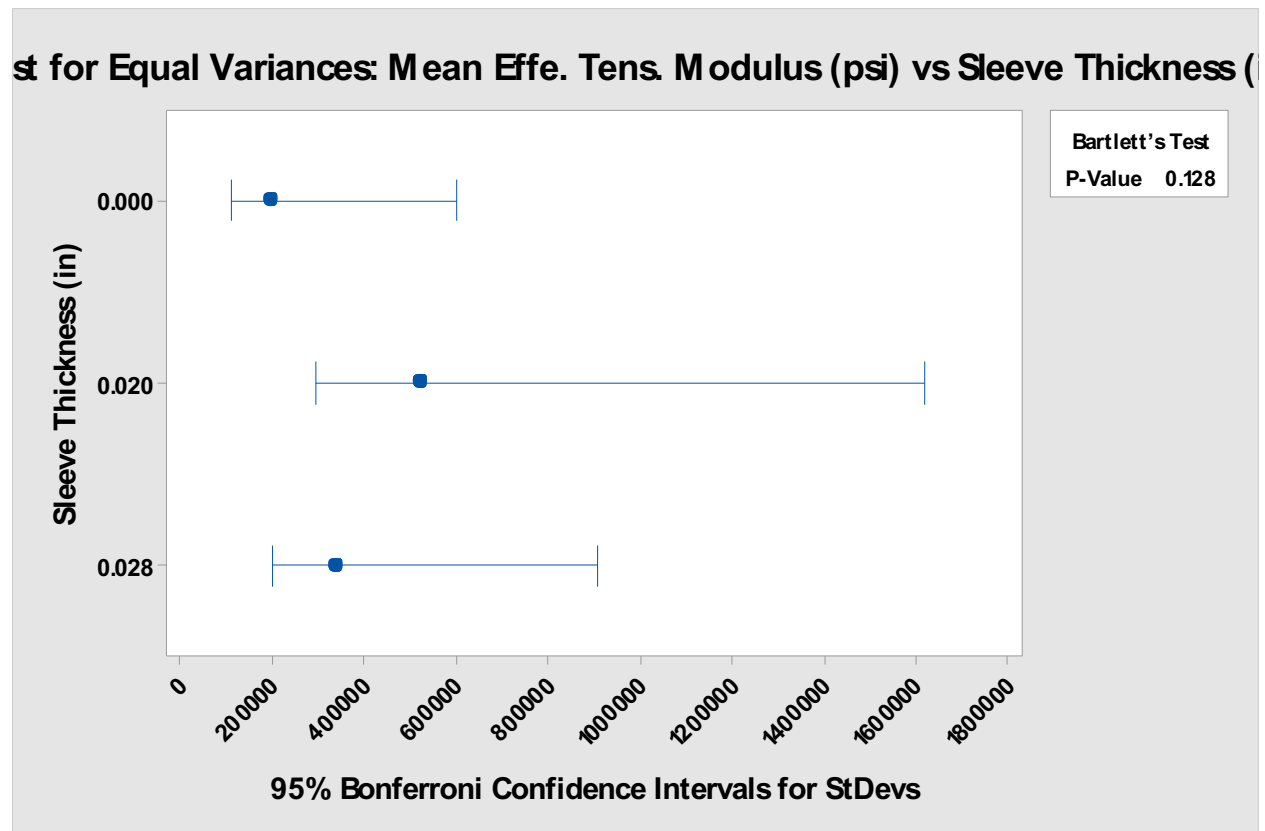
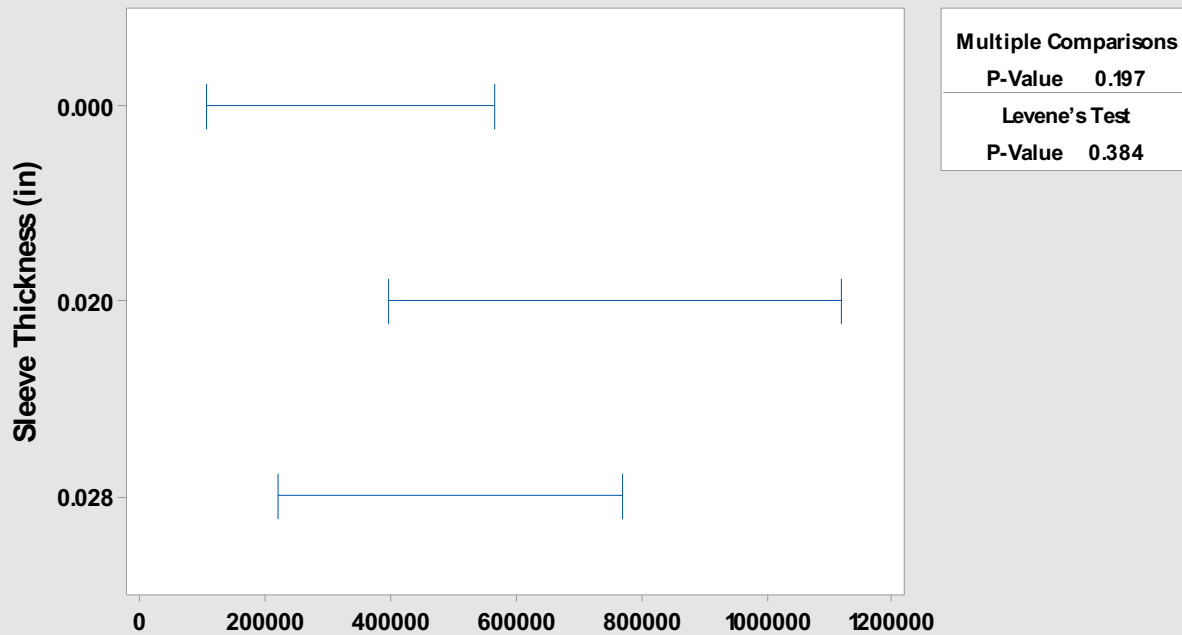


Figure 12.67: Bartlett's vs. sleeve thickness test for post impact tension samples.

The Bartlett's test for equal variances showed a p-value of 0.128, greater than the  $\alpha$  of 0.05. Therefore, it was necessary to fail to reject the null hypothesis that the data has equal variance for this factor.

**Test for Equal Variances: Mean Effe. Tens. Modulus (psi) vs Sleeve Thickness (in)**  
**Multiple comparison intervals for the standard deviation,  $\alpha = 0.05$**



*If intervals do not overlap, the corresponding stdevs are significantly different.*

*Figure 12.68: Levene's vs. sleeve thickness test for post impact tension samples.*

The Levene's test for equal variances showed a p-value of 0.384, greater than the  $\alpha$  of 0.05. Therefore, it was necessary to fail to reject the null hypothesis that the data has equal variance for this factor.

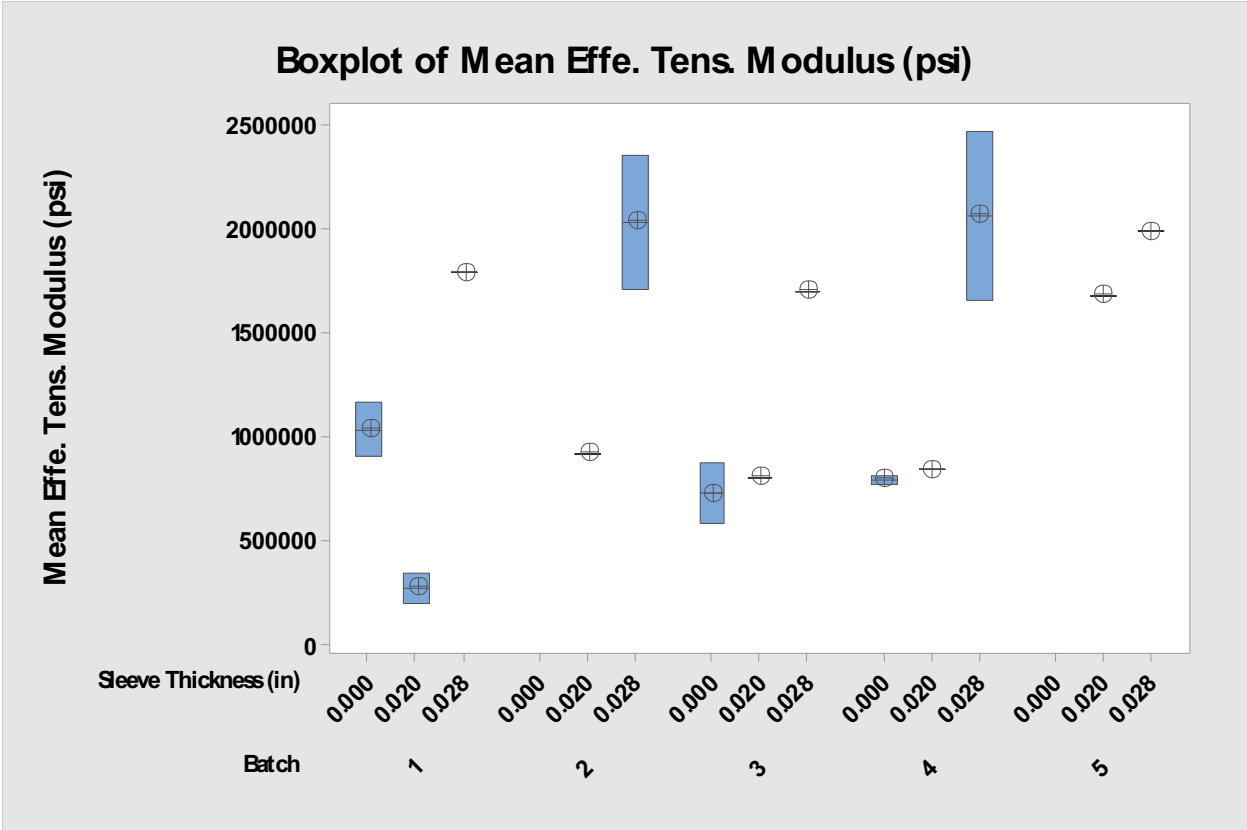


Figure 12.69: Boxplot of effective tensile modulus vs. batch and sieve thickness for post impact tension samples.

Based on the plot of effective modulus vs. batch and sieve thickness, no higher level correlations could be determined. The batch factor was removed to help determine correlation.

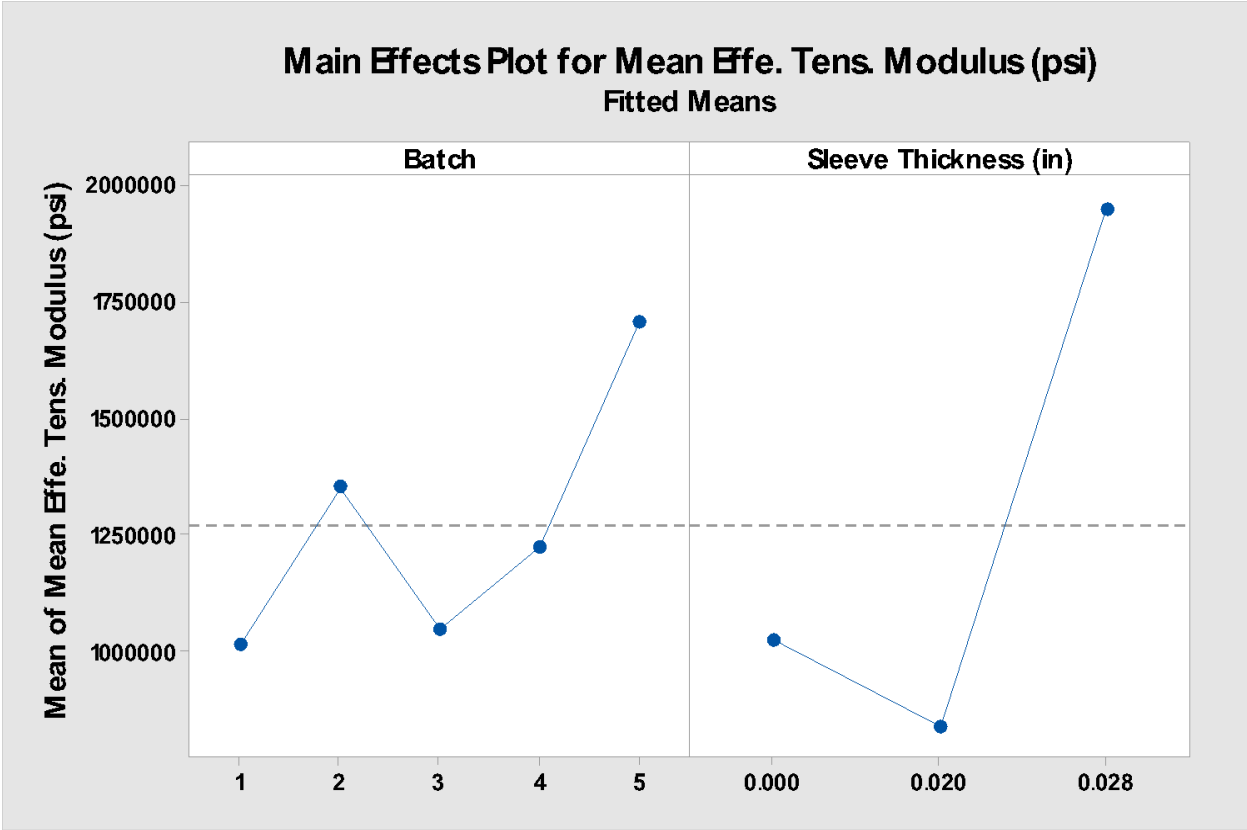


Figure 12.70: Main effects plot of effective tensile modulus for post impact tension samples.

The main effects plot shows the batch factor levels as contributing the least to effective modulus response variance. Sleeve thickness factor levels contribute the greatest to effective modulus response variance.

## 12.8 Post Impact Torsion Change Data Analysis

### General Linear Model: Mean Eff. Shear Mod. % Change versus Batch, Sleeve Thickness (in)

The following terms cannot be estimated and were removed:  
Batch\*Sleeve Thickness (in)

Method

Factor coding (-1, 0, +1)

|  
Factor Information

Factor	Type	Levels	Values
Batch	Random	5	1, 2, 3, 4, 5
Sleeve Thickness (in)	Fixed	3	0.000, 0.020, 0.028

Analysis of Variance

Source	DF	Adj SS	Adj MS	F-Value	P-Value
Batch	4	32.0	8.00	0.10	0.982
Sleeve Thickness (in)	2	13920.6	6960.32	84.04	0.000
Error	16	1325.2	82.82		
Lack-of-Fit	7	176.2	25.17	0.20	0.978
Pure Error	9	1149.0	127.67		
Total	22	17049.9			

Model Summary

S	R-sq	R-sq(adj)	R-sq(pred)
9.10066	92.23%	89.31%	85.05%

*Figure 12.71: General linear model of effective shear modulus change for torsion samples.*

Based on the analysis, the sleeve thickness factor appeared significant. The batch\*sleeve thickness interaction could not be estimated, and was therefore reduced.

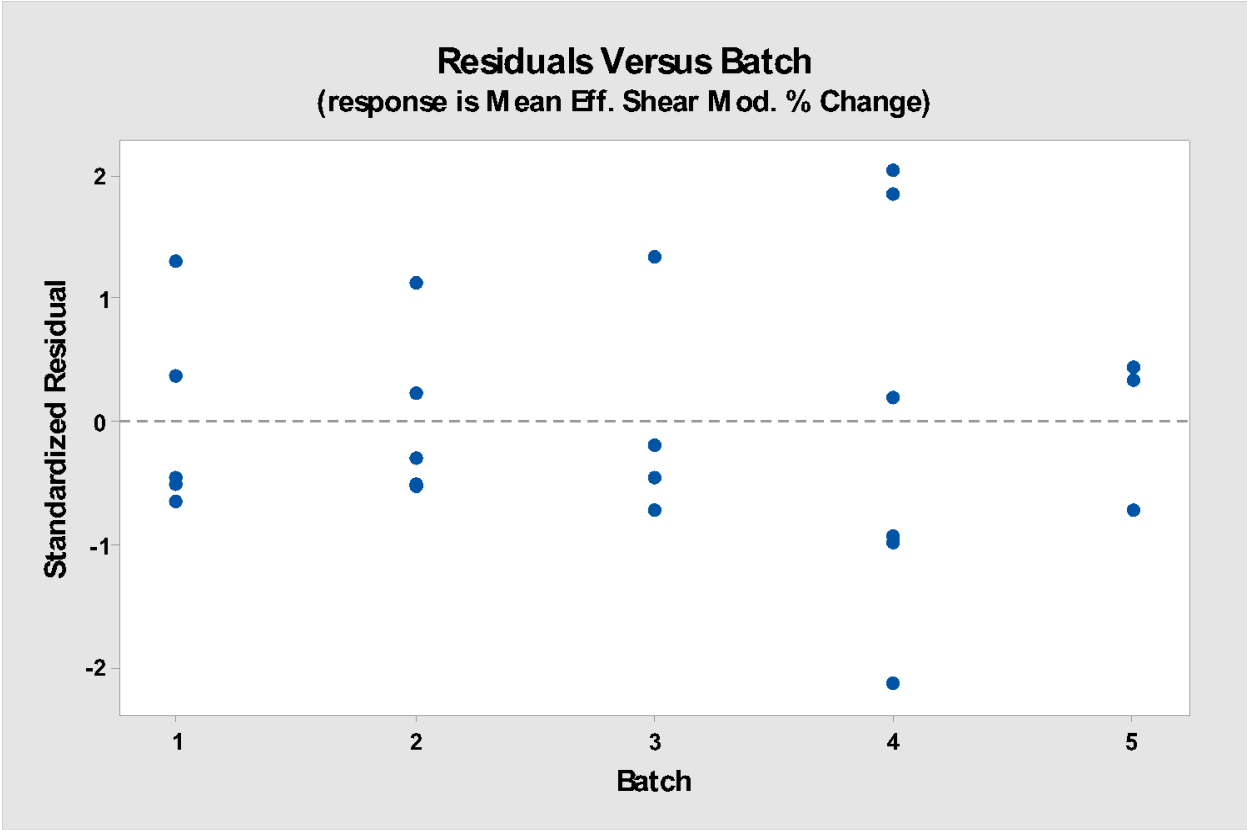


Figure 12.72: Residuals vs. batch for torsion samples.

Based on the residuals vs. batch plot, the data appeared to have equal variance.

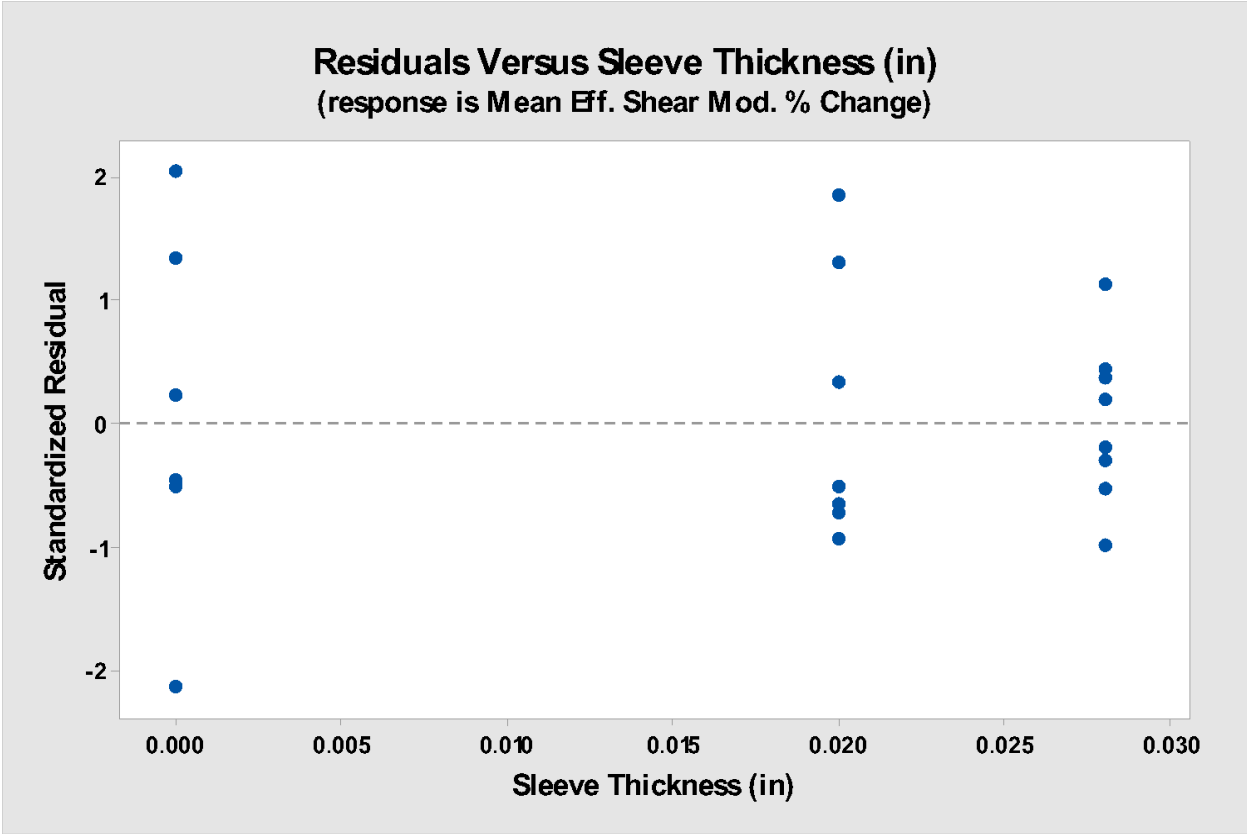


Figure 12.73: Residuals vs. sleeve thickness for torsion samples.

Based on the residuals vs. sleeve thickness plot, the data appeared to have equal variance.

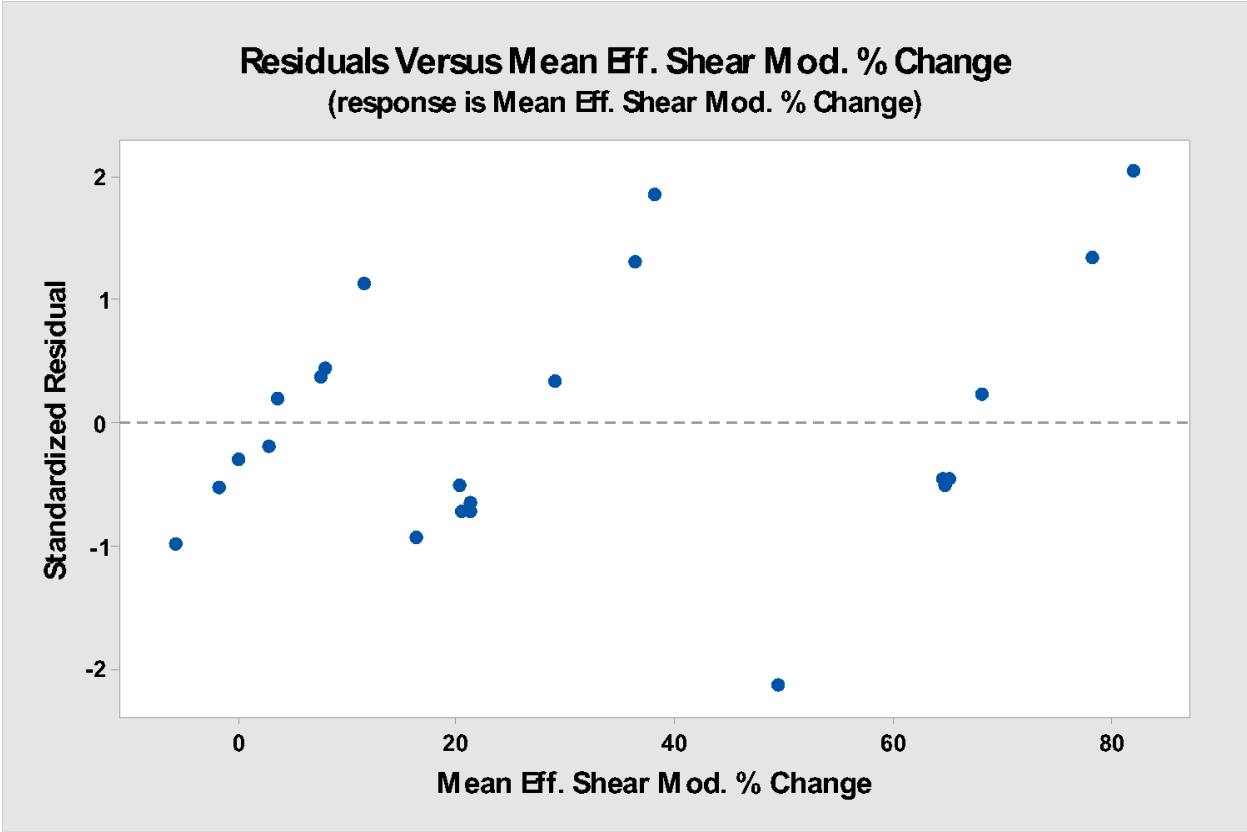
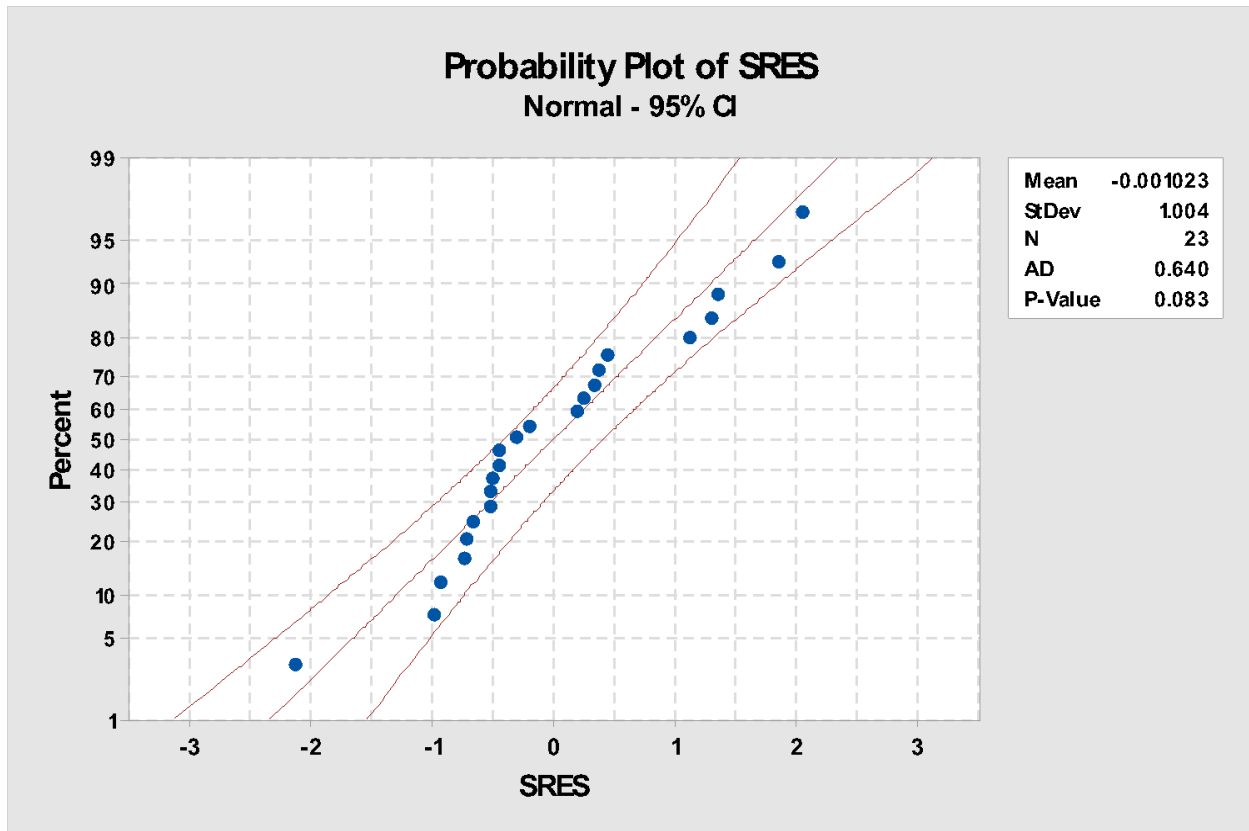


Figure 12.74: Residuals vs. effective shear modulus for torsion samples.

Based on the residuals vs. effective modulus change plot, the data appeared to have equal variance.



*Figure 12.75: Normal probability plot for torsion samples.*

The normal probability plot of standardized residuals showed a p-value of 0.083, greater than the  $\alpha$  of 0.05. Therefore, it was necessary to fail to reject the null hypothesis that the data comes from a normal population.

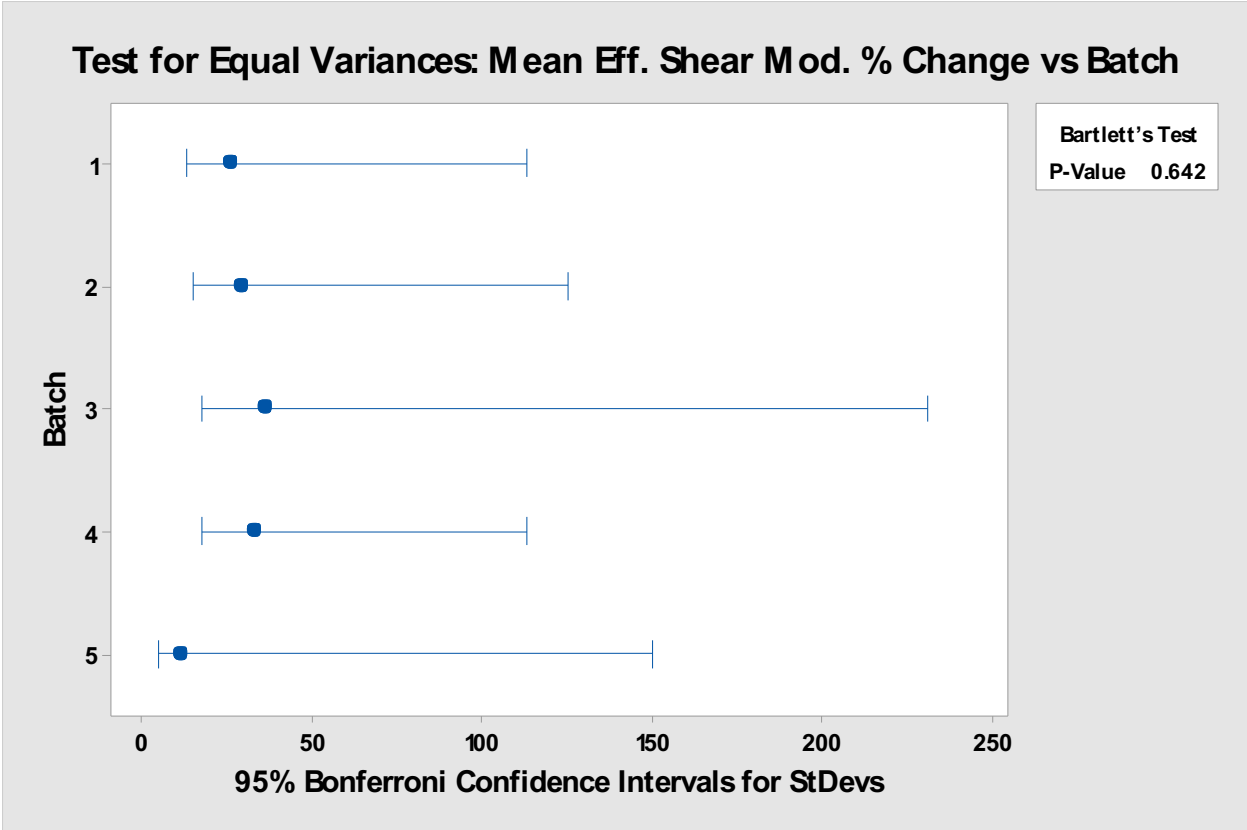


*Figure 12.76: Bartlett's vs. batch test for torsion samples.*

The Bartlett's test for equal variances showed a p-value of 0.642, greater than the  $\alpha$  of 0.05. Therefore, it was necessary to fail to reject the null hypothesis that the data has equal variance for this factor.

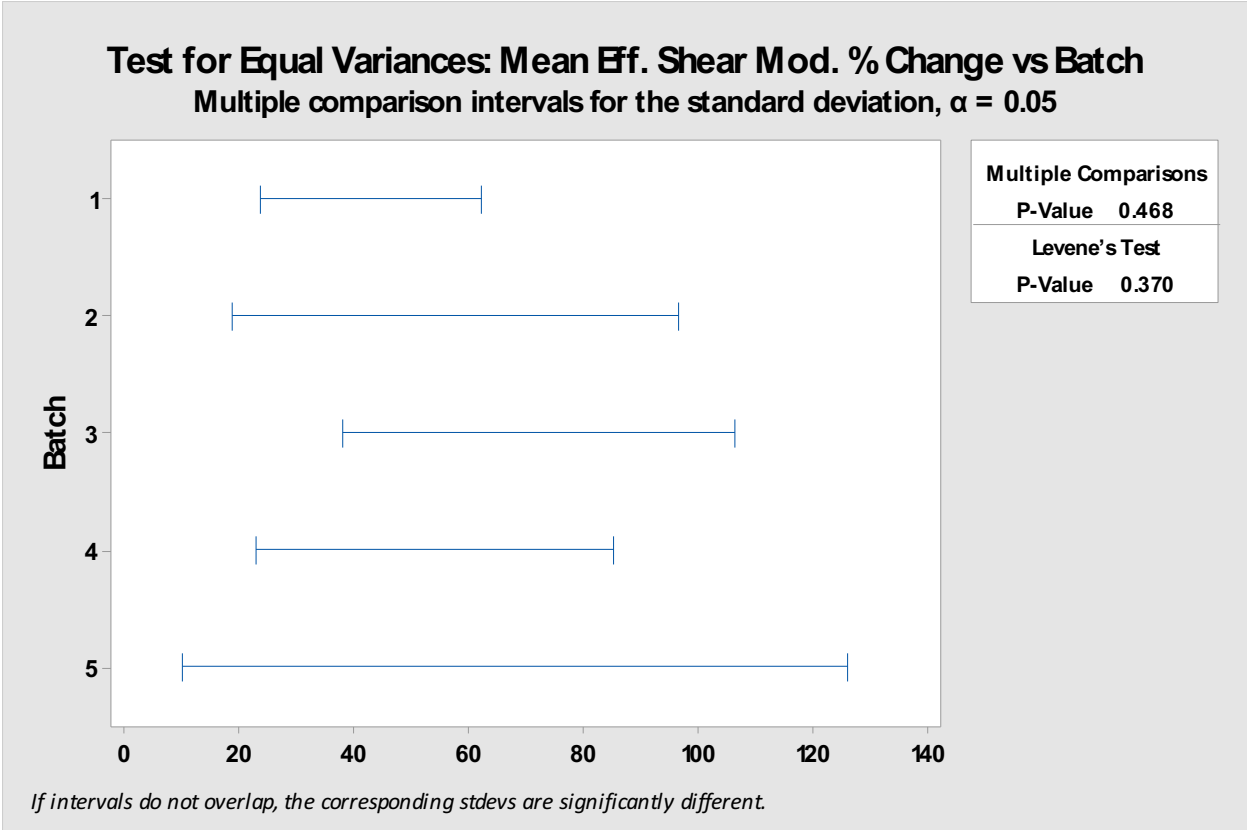


*Figure 12.77: Levene's vs. batch test for torsion samples.*

The Levene's test for equal variances showed a p-value of 0.370, greater than the  $\alpha$  of 0.05. Therefore, it was necessary to fail to reject the null hypothesis that the data has equal variance for this factor.

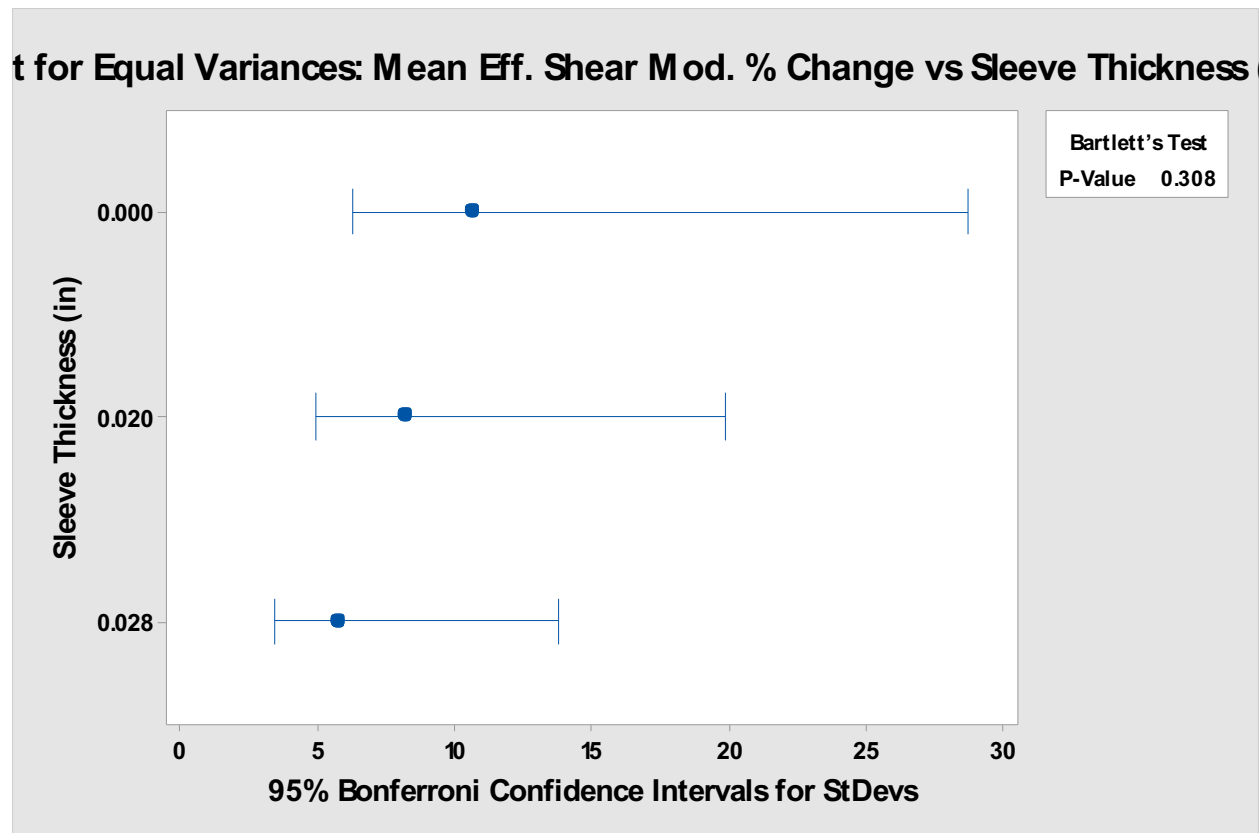
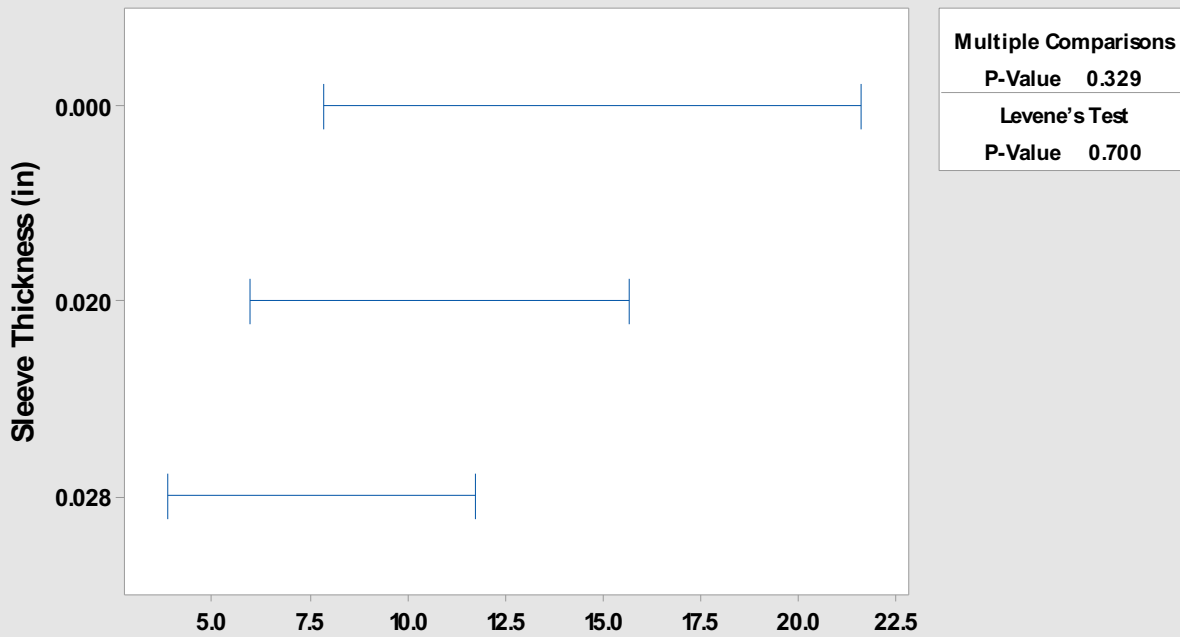


Figure 12.78: Bartlett's vs. sleeve thickness test for torsion samples.

The Bartlett's test for equal variances showed a p-value of 0.308, greater than the  $\alpha$  of 0.05. Therefore, it was necessary to fail to reject the null hypothesis that the data has equal variance for this factor.

**Test for Equal Variances: Mean Eff. Shear Mod. % Change vs Sleeve Thickness (in)**  
**Multiple comparison intervals for the standard deviation,  $\alpha = 0.05$**



*If intervals do not overlap, the corresponding stdevs are significantly different.*

*Figure 12.79: Levene's vs. sleeve thickness test for torsion samples.*

The Levene's test for equal variances showed a p-value of 0.700, greater than the  $\alpha$  of 0.05. Therefore, it was necessary to fail to reject the null hypothesis that the data has equal variance for this factor.

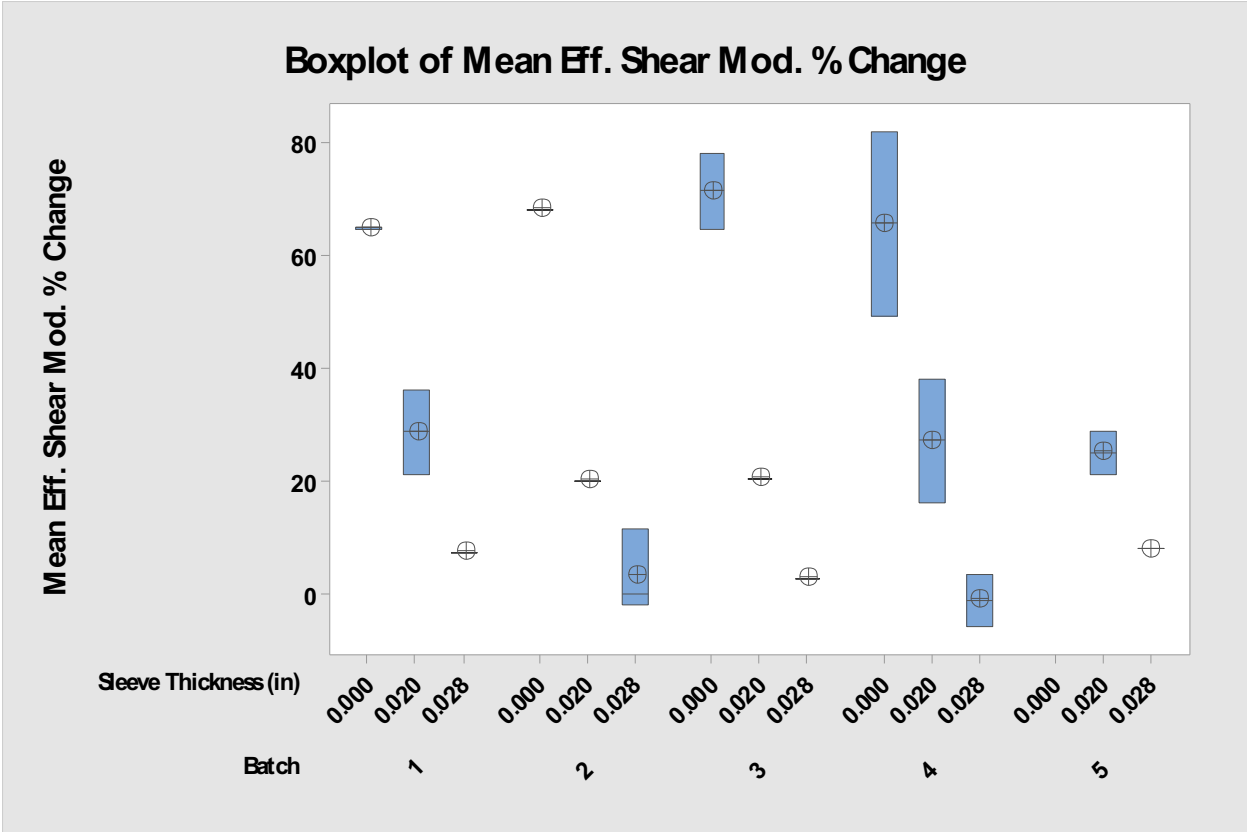


Figure 12.80: Boxplot of effective shear modulus change vs. batch and sleeve thickness for torsion samples.

Based on the plot of effective modulus change vs. batch and sleeve thickness, no higher level correlations could be determined. The batch factor was removed to help determine correlation.

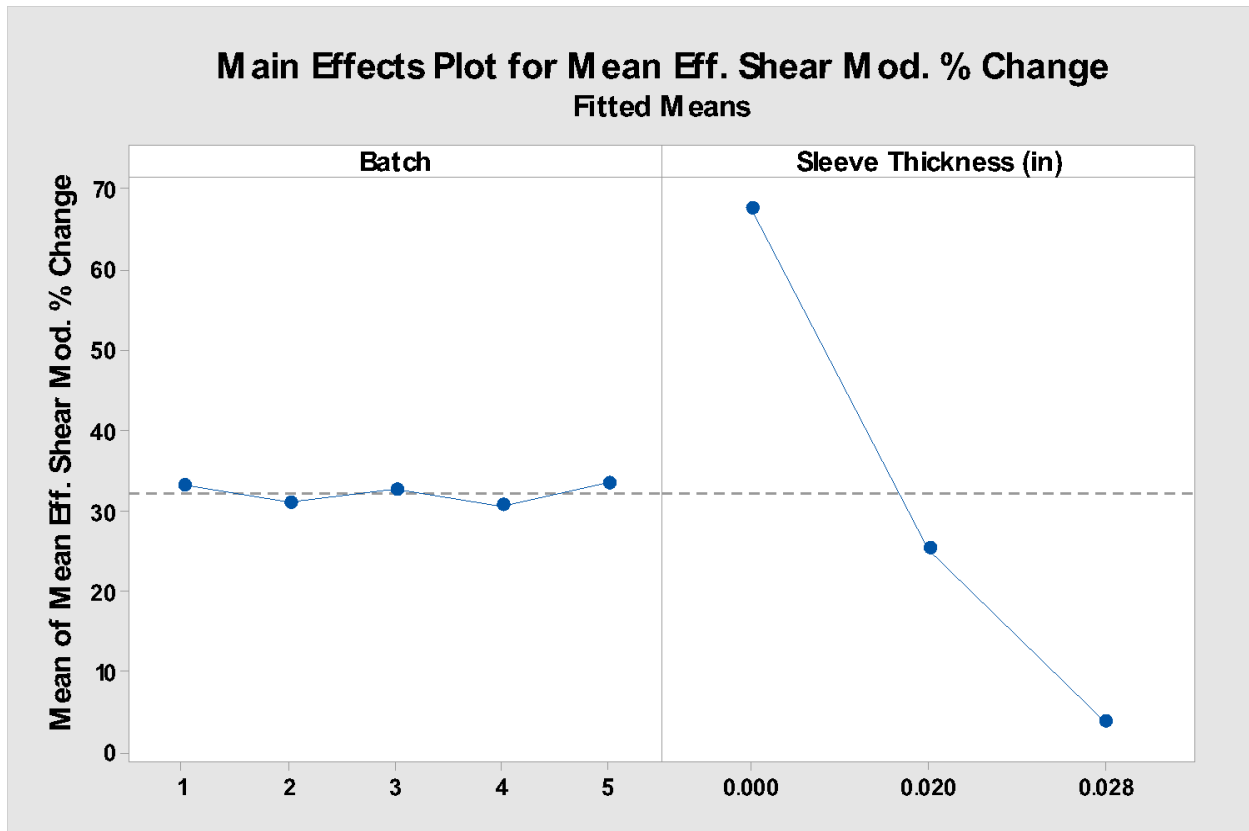


Figure 12.81: Main effects plot of effective shear modulus for torsion samples.

The main effects plot shows the batch factor levels as contributing the least to effective modulus change response variance. Sleeve thickness factor levels contribute the greatest to effective modulus change response variance.

## 12.9 Post Impact Tension Change Data Analysis

### General Linear Model: Mean Effe. Tens. Mod. % Change versus Batch, Sleeve Thickness (in)

The following terms cannot be estimated and were removed:

Batch\*Sleeve Thickness (in)

Method

Factor coding (-1, 0, +1)

|

Factor Information

Factor	Type	Levels	Values
Batch	Random	5	1, 2, 3, 4, 5
Sleeve Thickness (in)	Fixed	2	0.000, 0.028

Analysis of Variance

Source	DF	Adj SS	Adj MS	F-Value	P-Value
Batch	4	1526	381.6	0.50	0.739
Sleeve Thickness (in)	1	4141	4140.8	5.40	0.053
Error	7	5364	766.3		
Lack-of-Fit	2	1631	815.3	1.09	0.404
Pure Error	5	3734	746.7		
Total	12	14402			

Model Summary

S	R-sq	R-sq(adj)	R-sq(pred)
27.6820	62.75%	36.15%	*

Figure 12.82: General linear model of effective tensile modulus change for tension samples.

Based on the analysis, the no factors appear significant. The batch and sleeve thickness factors do not appear significant. The batch\*sleeve thickness interaction could not be estimated, and was therefore reduced.

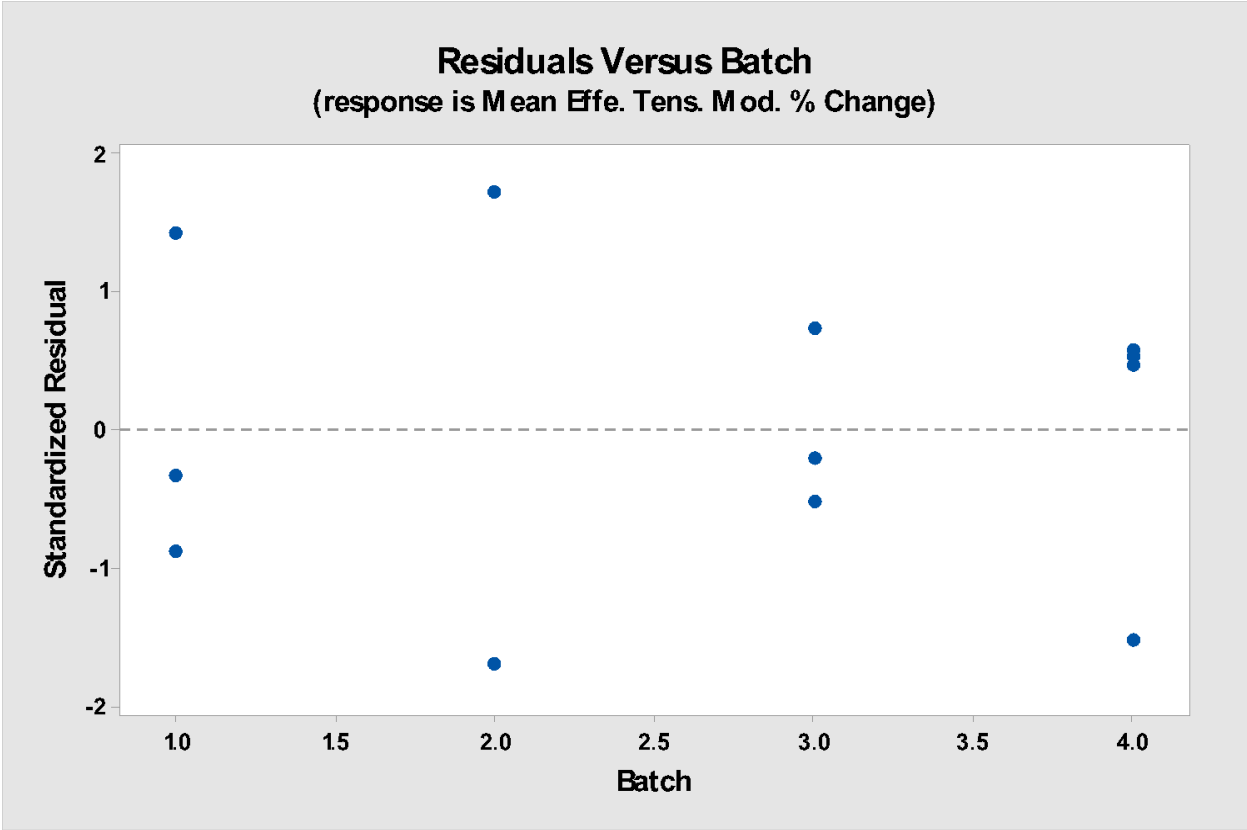


Figure 12.83: Residuals vs. batch for tension samples.

Based on the residuals vs. batch plot, the data appeared to have equal variance.

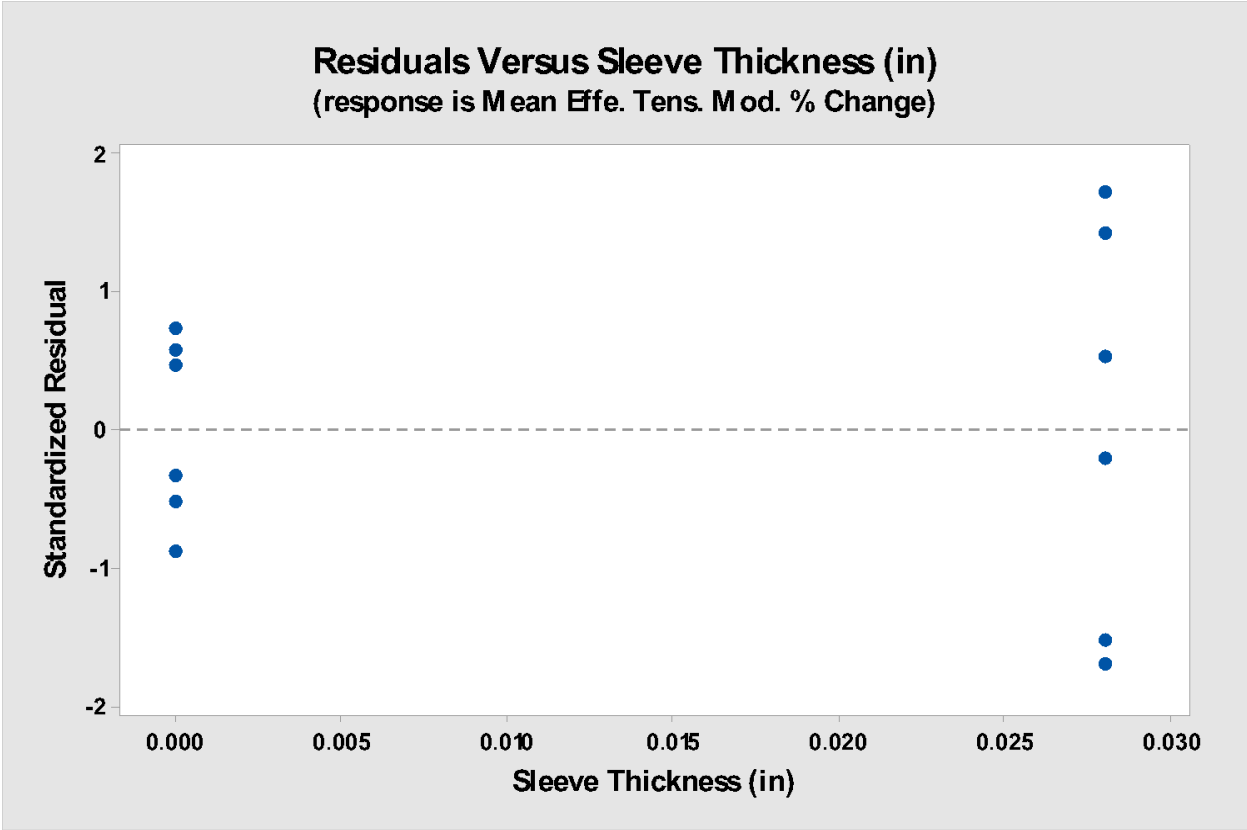


Figure 12.84: Residuals vs. sleeve thickness for tension samples.

Based on the residuals vs. sleeve thickness plot, the data appeared to have equal variance.

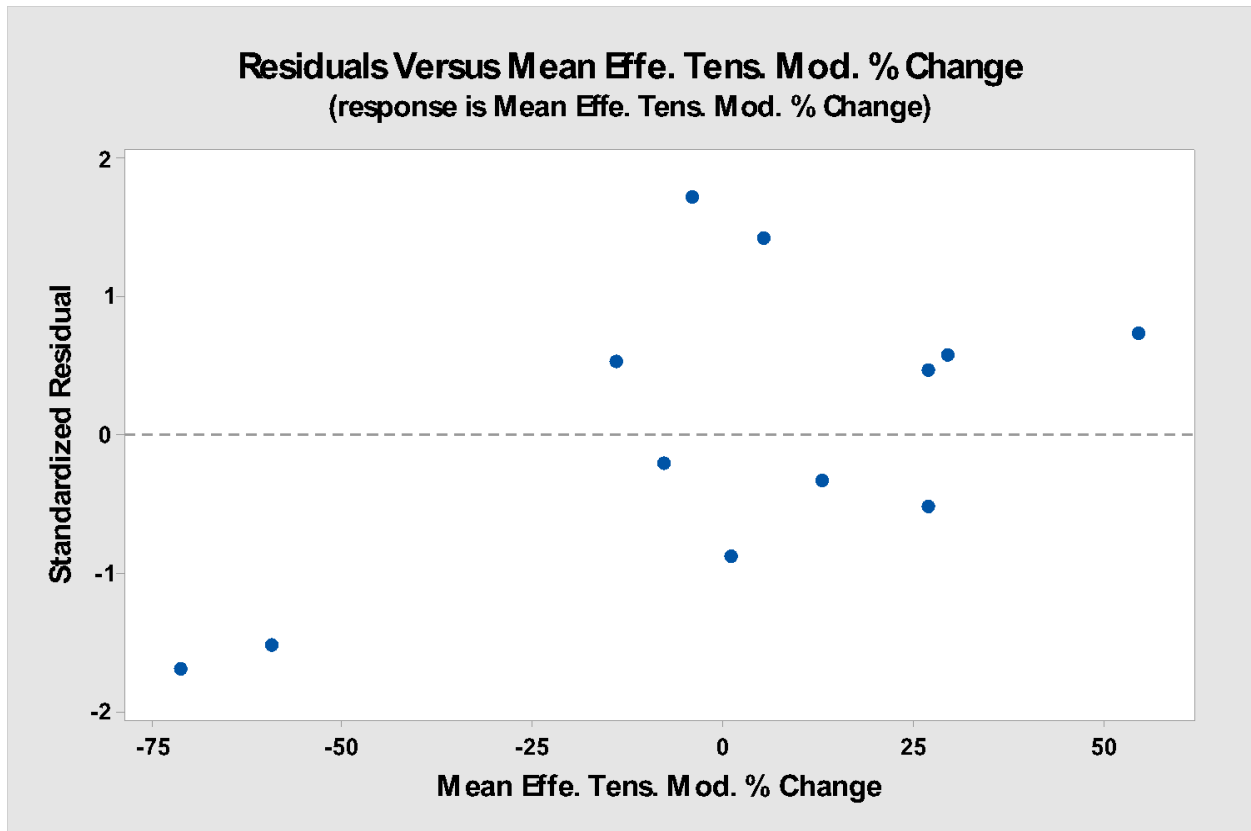
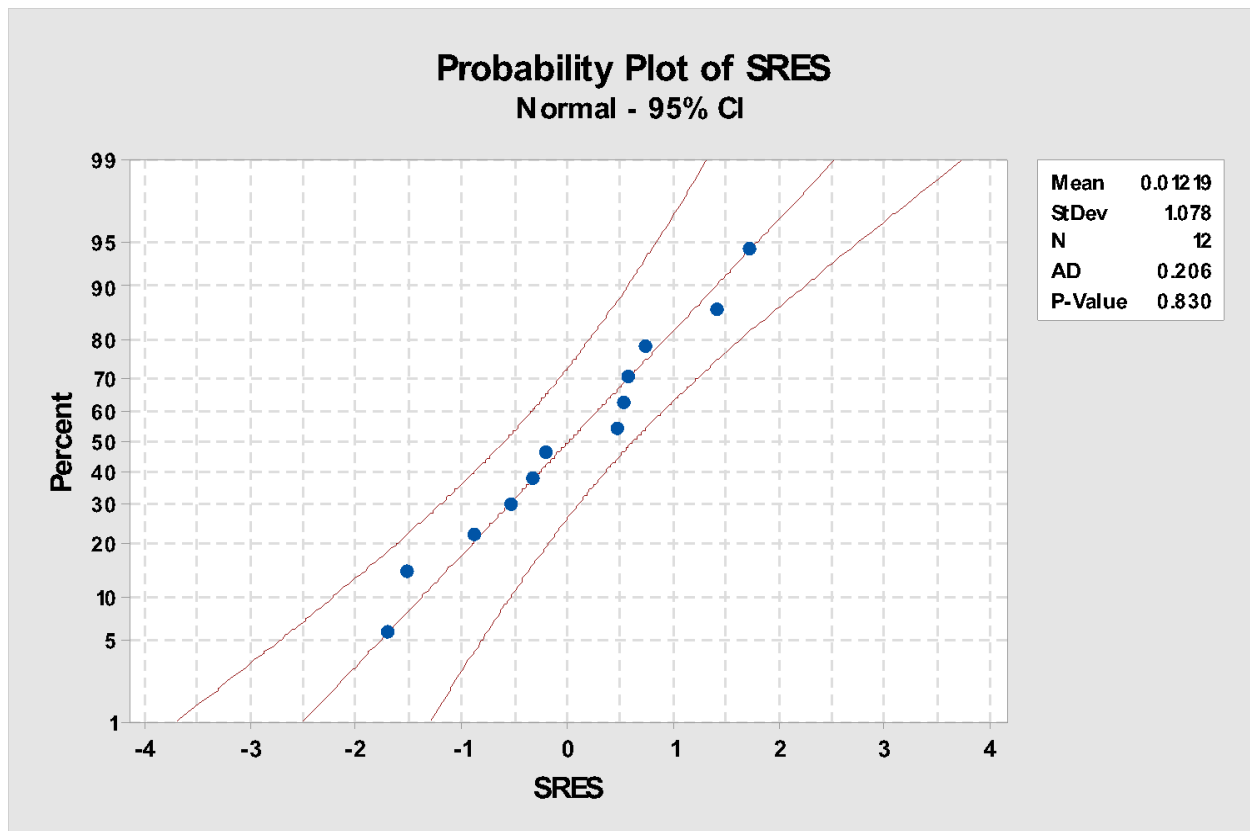


Figure 12.85: Residuals vs. effective tensile modulus for tension samples.

Based on the residuals vs. effective modulus change plot, the data appeared to have equal variance.



*Figure 12.86: Normal probability plot for tension samples.*

The normal probability plot of standardized residuals showed a p value of 0.830, greater than the  $\alpha$  of 0.05. Therefore, it was necessary to fail to reject the null hypothesis that the data comes from a normal population.

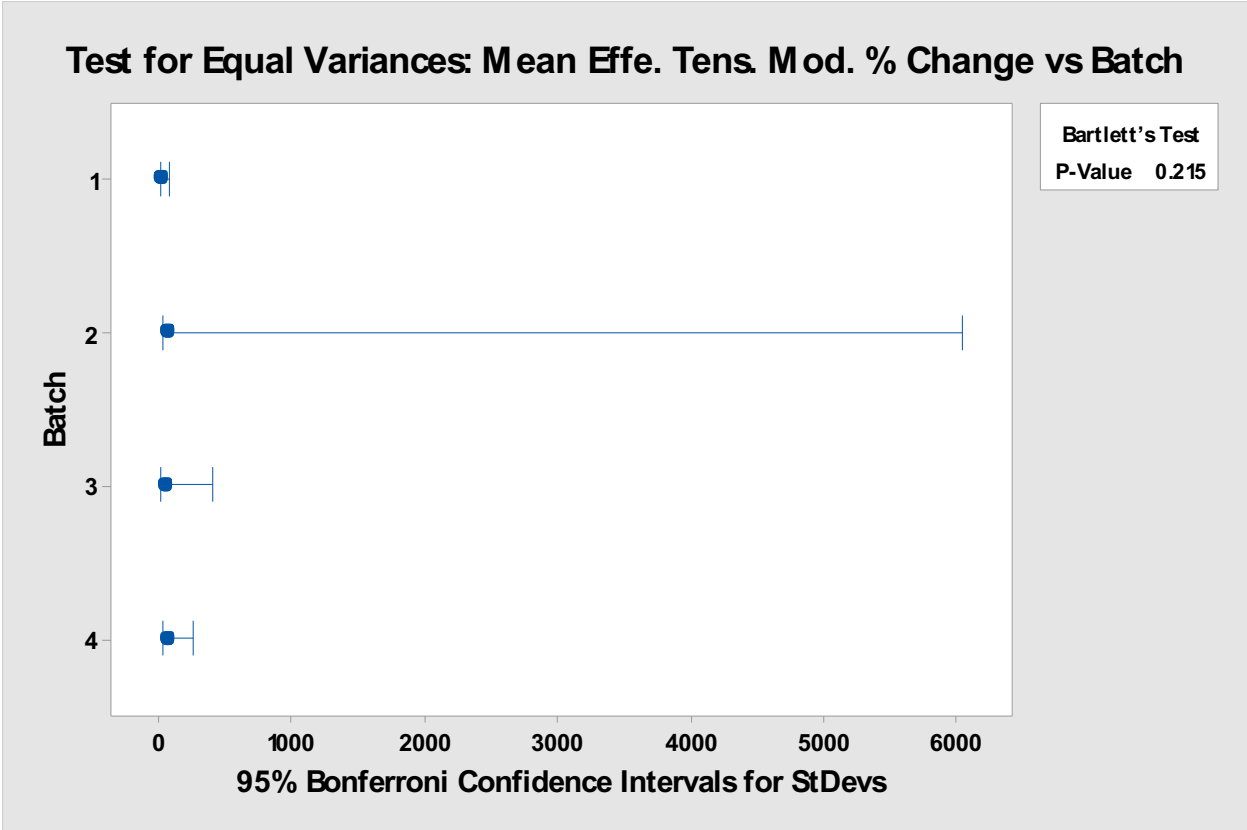


Figure 12.87: Bartlett's vs. batch test for tension samples.

The Bartlett's test for equal variances showed a p-value of 0.215, greater than the  $\alpha$  of 0.05. Therefore, it was necessary to fail to reject the null hypothesis that the data has equal variance for this factor.

## Test for Equal Variances: Mean Effe. Tens. Mod. % Change versus Batch

Method

Null hypothesis All variances are equal  
Alternative hypothesis At least one variance is different  
Significance level  $\alpha = 0.05$

95% Bonferroni Confidence Intervals for Standard Deviations

Batch	N	StDev	CI
1	3	6.0471	(0.02313, 9440.5)
2	2	47.4207	( *, *)
3	3	31.1524	(0.11918, 48633.5)
4	4	41.8015	(6.90807, 673.5)
5	1	*	( *, *)

Individual confidence level = 98.75%

Tests

Method	Test	
	Statistic	P-Value
Multiple comparisons	-	0.000
Levene	2.04	0.188

\* NOTE \* The graphical summary cannot be displayed because the multiple comparison intervals cannot be calculated.

*Figure 12.88: Levene's vs. batch test for tension samples.*

The Levene's test for equal variances showed a p-value of 0.188, greater than the  $\alpha$  of 0.05. Therefore, it was necessary to fail to reject the null hypothesis that the data has equal variance for this factor. Due to the nature of the multiple comparisons test, and since there were just two samples within the batch 2 factor level and just one sample within the batch 5 factor level, a graphical summary could not be presented.

t for Equal Variances: Mean Effe. Tens. Mod. % Change vs Sleeve Thickness

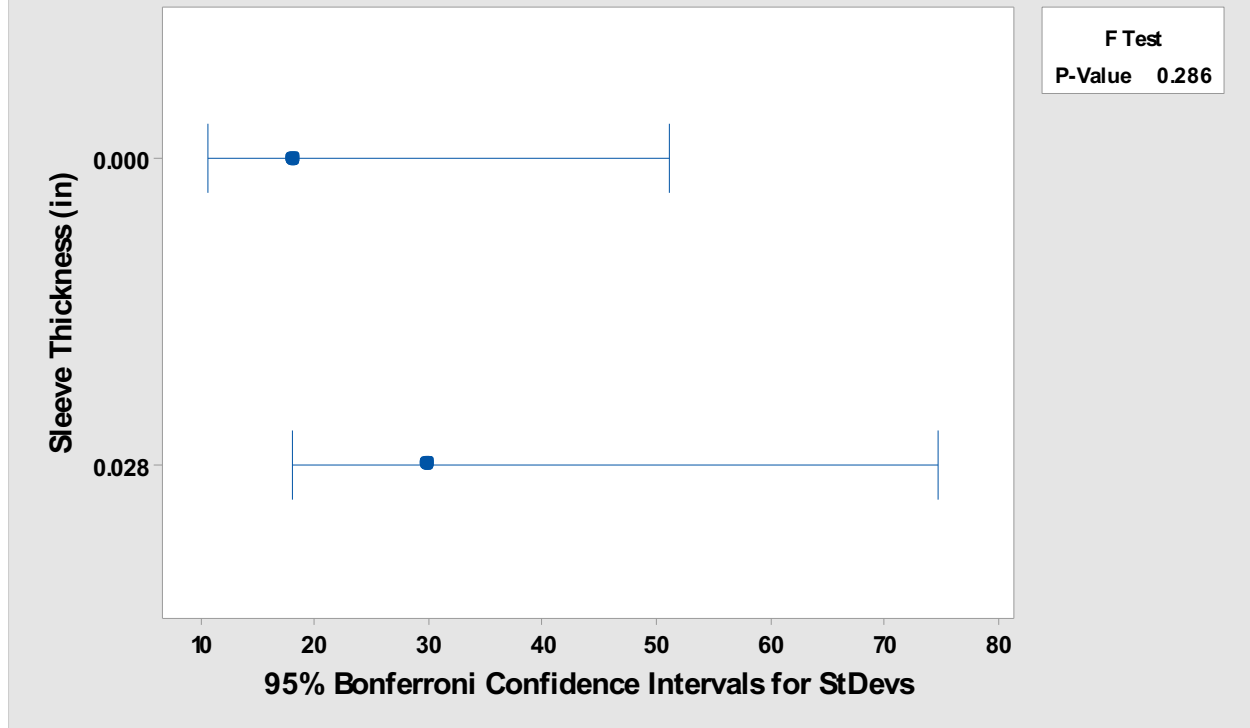
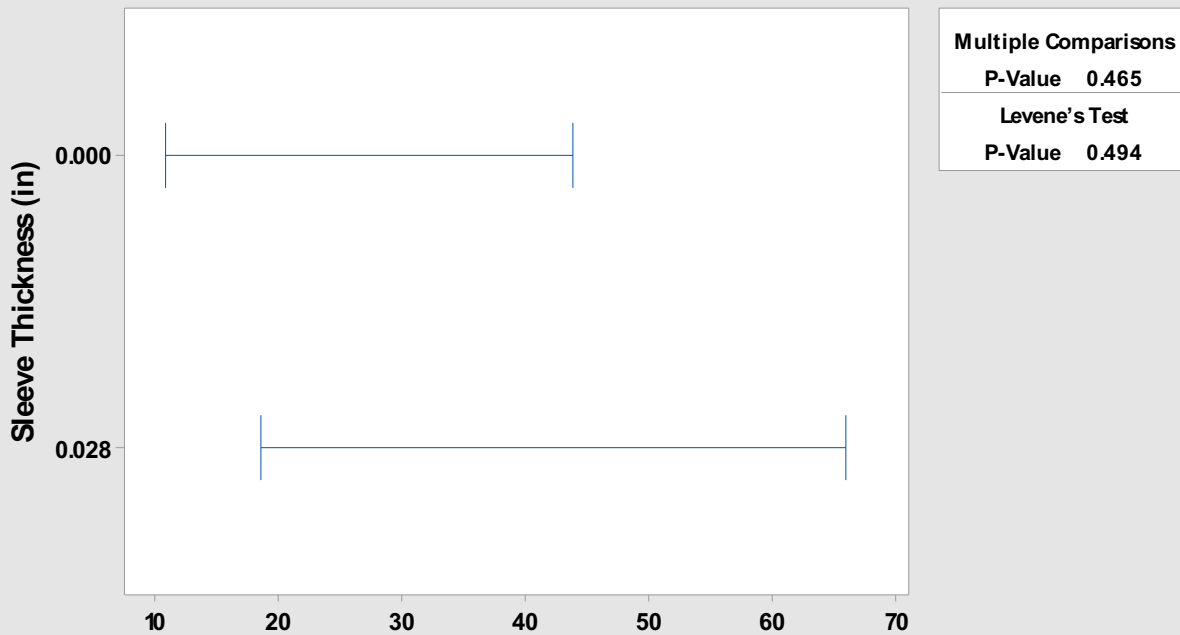


Figure 12.89: Bartlett's vs. sleeve thickness test for tension samples.

The Bartlett's test for equal variances showed a p-value of 0.286, greater than the  $\alpha$  of 0.05. Therefore, it was necessary to fail to reject the null hypothesis that the data has equal variance for this factor.

**est for Equal Variances: Mean Effe. Tens. Mod. % Change vs Sleeve Thickness (in)**  
**Multiple comparison intervals for the standard deviation,  $\alpha = 0.05$**



*If intervals do not overlap, the corresponding stdevs are significantly different.*

*Figure 12.90: Levene's vs. sleeve thickness test for tension samples.*

The Levene's test for equal variances showed a p-value of 0.494, greater than the  $\alpha$  of 0.05. Therefore, it was necessary to fail to reject the null hypothesis that the data has equal variance for this factor.

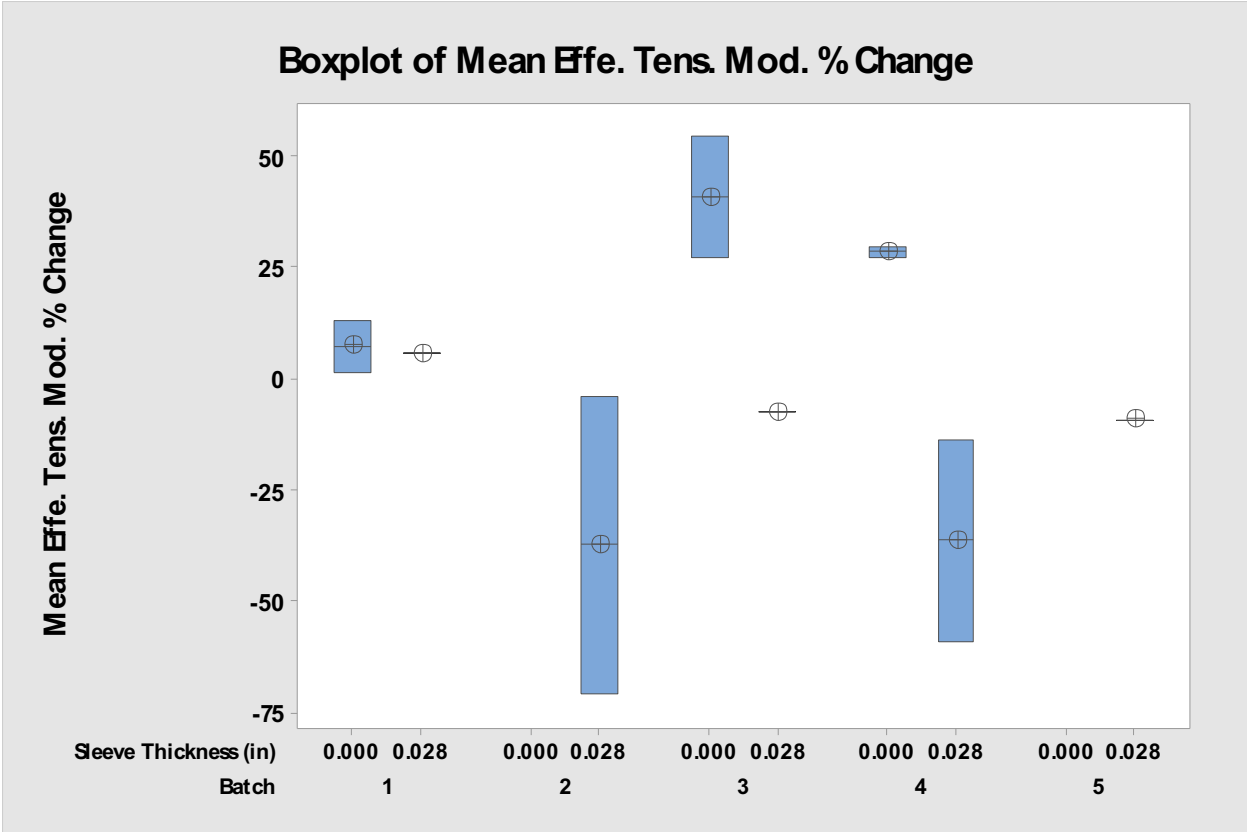


*Figure 12.91: Boxplot of effective tensile modulus change vs. batch and sleeve thickness for tension samples.*

Based on the plot of effective modulus change vs. batch and sleeve thickness, no higher order correlations could be determined. The batch factor was removed to help determine correlation.

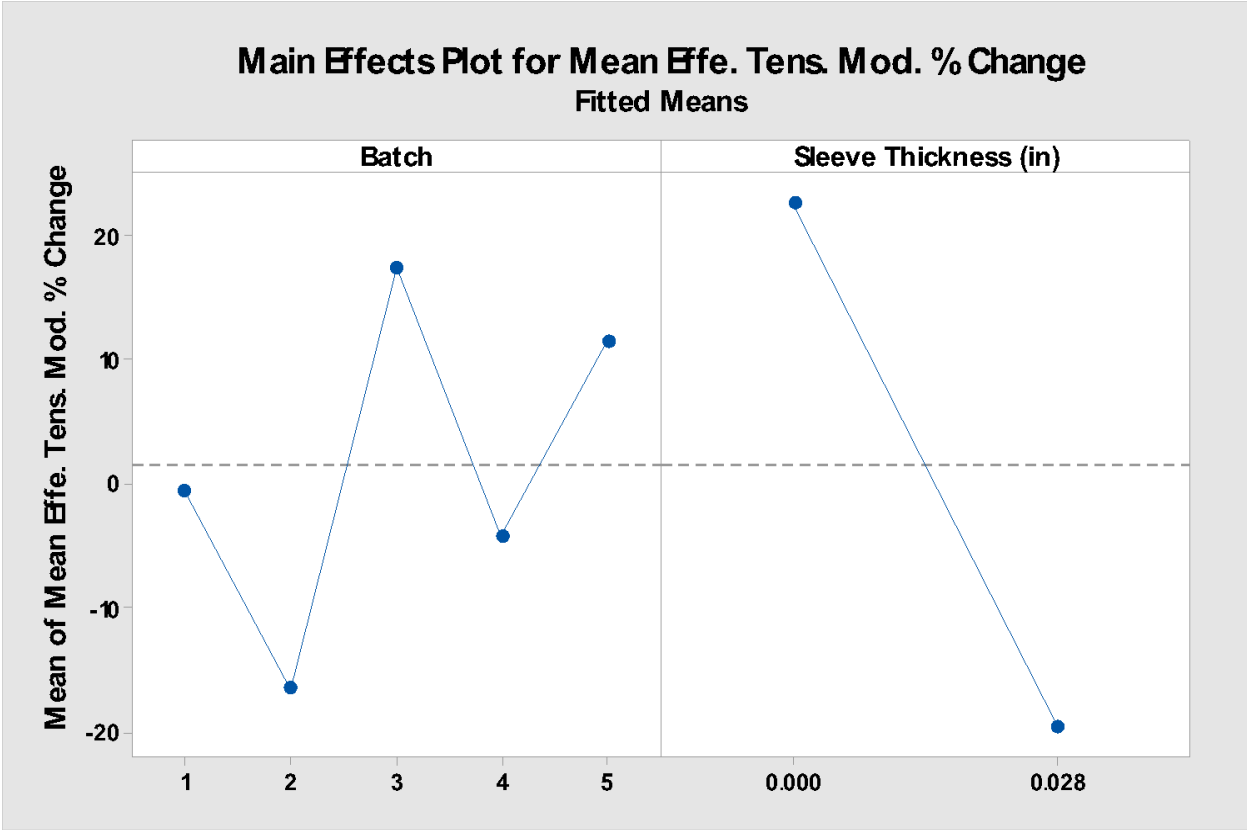
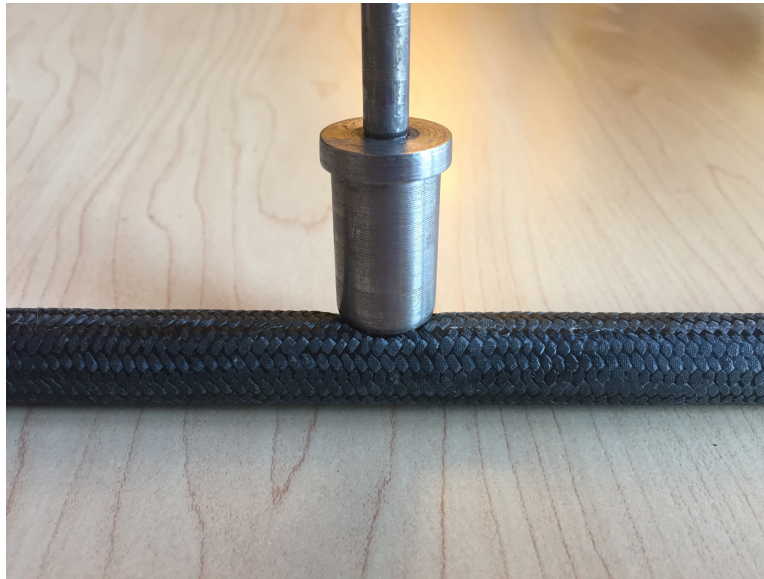


Figure 12.92: Main effects plot of effective tensile modulus change for tension samples.

The main effects plot shows the batch factor as contributing to a lesser degree than the sleeve thickness factor.

## 12.10 Observations



*Figure 12.93: Impactor overlap of a non sleeve (0.000 sleeve thickness factor level) post impact sample.*



*Figure 12.94: Profile of non sleeve post impact sample*

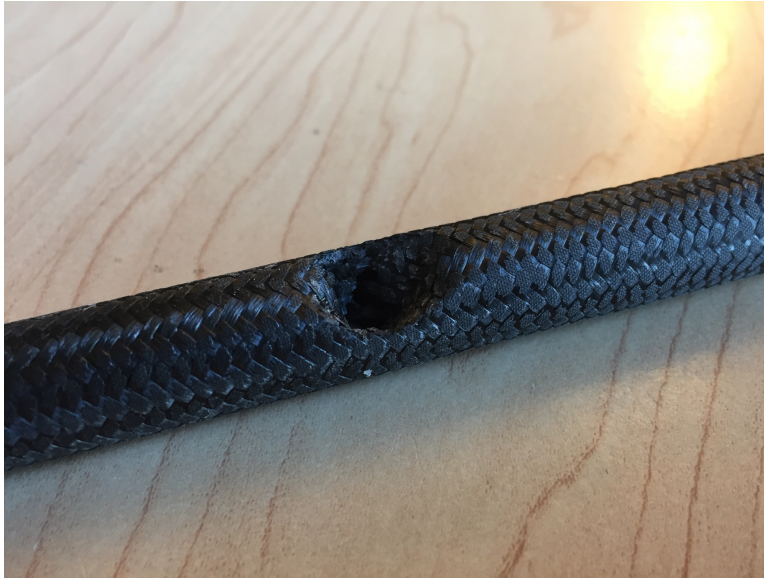


*Figure 12.95: Impact site of non sleeve post impact sample.*

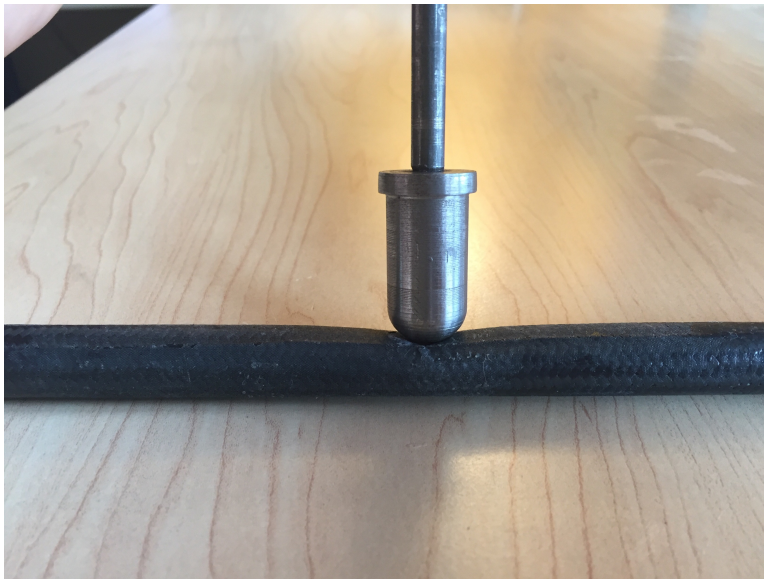


*Figure 12.96: Impactor overlap of 0.020 sleeve thickness post impact sample.*



*Figure 12.97: Profile of 0.020 sleeve thickness post impact sample.*



*Figure 12.98: Impact site of 0.020 sleeve thickness post impact sample.*



*Figure 12.99: Impactor overlap of 0.028 sleeve thickness post impact sample.*



*Figure 12.100: Profile of 0.028 sleeve thickness post impact sample.*



*Figure 12.101: Impact site of 0.028 sleeve thickness post impact sample.*